This document was too large to scan as a single document. It has been divided into smaller sections.

Section 4 of 4

Document Information			
Document #	**RPP-10098**	**Revision**	**1**
Title	FIELD INVESTIGATION REPORT FOR WASTE MGMT AREA B-BX-BY [VOL 2 APPENEDICES D-I]		
Date	**1/6/2003**		
Originator	**KNEPP AJ**	**Originator Co.**	**CH2M**
Recipient		**Recipient Co.**	
References	**EDT-630527**		
Keywords			
Projects	**TFARM**		
Other Information			

59677
4054

APPENDIX E

IMPACT ASSESSMENT APPROACH AND RESULTS

This page intentionally left blank.

CONTENTS

E.1.0 INTRODUCTION E-1

E.2.0 MODELING APPROACH E-2
E.2.1 NUMERICAL CASES CONSIDERED E-7
E.2.2 RECHARGE ESTIMATES AND VADOSE ZONE FLOW AND TRANSPORT PARAMETERS E-9
E.2.2.1 Recharge Estimates E-10
E.2.2.2 Vadose Zone Flow and Transport Parameters E-10
E.2.2.3 Stochastic Model for Macroscopic Anisotropy E-11
E.2.2.4 Effective Transport Parameters E-12
E.2.3 GROUNDWATER FLOW AND TRANSPORT E-14
E.2.4 CONTAMINANT INVENTORY E-16
E.2.4.1 Basis for Inventory Estimates E-16
E.2.4.2 Inventory Distributions E-17
E.2.4.3 Inventory Distribution Maps E-24

E.3.0 NUMERICAL SIMULATION RESULTS E-25
E.3.1 BASE CASE, NO ACTION ALTERNATIVE (CASE 1) E-25
E.3.2 BARRIER ALTERNATIVE AND NO WATER LINE LEAKS (CASE 2) E-27
E.3.3 NO INTERIM BARRIER AND WATER LINE LEAK OF 1 GPM FOR 20 YEARS (CASE 3) E-29
E.3.4 NO BARRIER AND WATER LINE LEAK OF 200,000 GALLONS OVER 5 DAYS (CASE 4) E-31
E.3.5 ALTERNATE INVENTORY DISTRIBUTION AND NO INTERIM BARRIER (CASE 5) E-33
E.3.6 ALTERNATE INVENTORY DISTRIBUTION WITH INTERIM BARRIER (CASE 6) E-35
E.3.7 BASE CASE WITH 50 MM/YR METEORIC RECHARGE (CASE 7) E-36
E.3.8 BASE CASE WITH 30 MM/YR METEORIC RECHARGE (CASE 8) E-38
E.3.9 BASE CASE WITH 10 MM/YR METEORIC RECHARGE (CASE 9) E-40
E.3.10 BASE CASE WITH KD = 0.1 ML/G FOR URANIUM-238 (CASE 10) E-42
E.3.11 BASE CASE WITH KD = 1.0 ML/G FOR URANIUM-238 (CASE 11) E-44
E.3.12 TRENCH B-38 WITH 55.4 MM/YR METEORIC RECHARGE (CASE 12) E-45
E.3.13 TRENCH B-38 WITH 100.0 MM/YR METEORIC RECHARGE (CASE 13) E-47
E.3.14 TRENCH B-38 WITH DELAYED CLOSURE BARRIER AND 100.0 MM/YR METEORIC RECHARGE E-49
E.3.15 SOLUTE MASS BALANCE E-51

E.4.0 HUMAN HEALTH RISK AND DOSE ESTIMATION APPROACH E-53
E.4.1 RECEPTOR SCENARIO RATIONALE E-56
E.4.1.1 Residential Exposure Scenario (MTCA Method B) E-56
E.4.1.2 Industrial Exposure Scenario (MTCA Method C) E-57

E.4.1.3 Industrial Worker Scenario E-57
E.4.1.4 Residential Farmer Scenario E-59
E.4.1.5 Recreational Shoreline User Scenario E-59
E.4.2 TANK WASTE CONSTITUENTS OF POTENTIAL CONCERN E-59
E.4.2.1 Rationale for Excluding Constituents of Potential Concern E-60
E.4.2.2 Contaminants of Potential Concern for Risk Assessment E-61
E.4.3 ESTIMATING TOTAL INCREMENTAL LIFETIME CANCER RISK AND HAZARD INDEX E-61
E.4.4 DOSE METHODOLOGY E-62

E.5.0 HUMAN HEALTH RISK AND DOSE RESULTS E-63
E.5.1 BASE CASE, NO ACTION ALTERNATIVE (CASE 1) E-63
E.5.2 BARRIER ALTERNATIVE AND NO WATER LINE LEAKS CASE (CASE 2) E-67
E.5.3 BASE CASE WITH 50 MM/YR METEORIC RECHARGE (CASE 7) E-70
E.5.4 BASE CASE WITH 30 MM/YR METEORIC RECHARGE (CASE 8) E-73

E.6.0 CONCLUSIONS OF RISK AND DOSE E-76

E.7.0 REFERENCES E-77

ATTACHMENTS

E1 BX TANK FARM SATURATION AND CONCENTRATION DISTRIBUTIONS ... E1-i

E2 TRENCH 216-B-38 SATURATION AND CONCENTRATION DISTRIBUTIONS. E2-i

E3 BX TANK FARM MASS FLUX AND BREAKTHROUGH CURVES E3-i

E4 TRENCH 216-B-38 MASS FLUX AND BREAKTHROUGH CURVES E4-i

E5 PEAK CONCENTRATIONS AND ARRIVAL TIMES E5-i

FIGURES

E.1. Location Map of Single-Shell Tanks in Waste Management Area B-BX-BY and Surrounding Facilities in the 200 East Area E-3
E.2. West to East Profile for Cross-Section through Tanks BX-111 to BX-102 (distance ~180 to 300 m) and Trench B-38 (distance ~20 to 70 m) E-4
E.3. Geologic Cross-Section through Tanks BX-102, BX-105, and BX-108 ..... E-5
E.4. Geologic Cross-Section through Trench B-38 ..... E-5
E.5. Uranium-238 Concentration Profile for Initial Conditions in STOMP and the Corresponding Reported Inventory E-18
E.6. Technetium-99 Concentration Profile for Initial Conditions in STOMP and the Corresponding Reported Inventory E-19
E.7. Nitrate Concentration Profile for Initial Conditions in STOMP and the Corresponding Reported Inventory E-19
E.8. Aqueous Uranium-238 Concentration E-21
E.9. Translation Geometry E-22
E.10. Hypothetical Receptor Locations for Risk Evaluation E-55
E.11. Case 1 Industrial Worker ILCR Versus Time at Calculation Points Between the BX Tank Farm East Fence Line Boundary and the Columbia River E-65
E.12. Case 2 Industrial Worker ILCR Versus Time at Calculation Points Between the BX Tank Farm East Fence Line Boundary and the Columbia River E-68
E.13. Case 7 Industrial Worker ILCR Versus Time at Calculation Points Between the BX Tank Farm Fence Line Boundary and the Columbia River E-71
E.14. Case 8 Industrial Worker ILCR Versus Time at Calculation Points Between the BX Tank Farm East Fence Line Boundary and the Columbia River E-74

TABLES

E.1. Timeline Estimates for Emplacement of Interim and Closure Barriers at the BX Tank Farm and Corresponding Recharge Estimates E-10
E.2. Composite van Genuchten-Mualem Parameters for Various Strata at the BX Tank Farm E-10
E.3. Macroscopic Anisotropy Parameters Based on Polmann (1990) Equations for Various Strata at WMA B-BX-BY E-12
E.4. Effective Parameter Estimates, $E[\rho_b K_d]$, for Uranium-238 for the Product of Bulk Density (g/cm^3) and K_d (cm^3/g) at Waste Management Area B-BX-BY E-13
E.5. Non-Reactive Macrodispersivity Estimates for Various Strata at Waste Management Area B-BX-BY E-13
E.6. Distance to Specified Boundary, Groundwater Velocity, and Travel Time from Waste Management Area B-BX-BY E-16
E.7. Transport Parameters for the Site-Wide Groundwater Model E-17
E.8. Unit Dose Factors for Uranium-238 and Technetium-99 ..... E-17
E.9. Calculated Plan View Areas of Different 2-Dimensional Plume Geometries for BX-108 to BX-102 Concentration Profiles and Inventory and Their Scale Factors Based on a Mean Inventory Diameter of 92 feet E-22
E.10. Concentration Scale Factors for the BX Tank Farm from BX-108 to BX-102 Cross-Section Concentrations E-23
E.11. Concentration Scale Factors for B Trenches from Unit Inventory Cross-Section Concentrations E-23
E.12. Trench B-38 Case Inventory Summary E-23
E.13. Initial Inventory Distribution Schedule E-24
E.14. Peak Concentrations and Arrival Times at the First Boundary for Case 1 ..... E-27
E.15. Peak Concentrations and Arrival Times at the First Boundary for Case 2 ..... E-29
E.16. Peak Concentrations and Arrival Times at the First Boundary for Case 3 ..... E-31
E.17. Peak Concentrations and Arrival Times at the First Boundary for Case 4 ..... E-33
E.18. Peak Concentrations and Arrival Times at the First Boundary for Case 5 ..... E-34
E.19. Peak Concentrations and Arrival Times at the First Boundary for Case 6 ..... E-36
E.20. Peak Concentrations and Arrival Times at the First Boundary for Case 7 ..... E-38
E.21. Peak Concentrations and Arrival Times at the First Boundary for Case 8 ..... E-40
E.22. Peak Concentrations and Arrival Times at the First Boundary for Case 9 ..... E-42
E.23. Peak Concentrations and Arrival Times at the First Boundary for Case 10 ..... E-43
E.24. Peak Concentrations and Arrival Times at the First Boundary for Case 11 ..... E-45
E.25. Peak Concentrations and Arrival Times at the First Boundary for Case 12 ..... E-47
E.26. Peak Concentrations and Arrival Times at the First Boundary for Case 13 ..... E-49
E.27. Peak Concentrations and Arrival Times at the First Boundary for Case 14 ..... E-50
E.28. STOMP Mass Balance for Uranium-238 ..... E-51
E.29. STOMP Mass Balance for Technetium-99 ..... E-52
E.30. STOMP Mass Balance for Nitrate E-52
E.31. Unit Risk Factors for the Industrial Worker, Residential Farmer, and Recreational Shoreline User Scenarios E-58
E.32. Basis for Scaled Groundwater Concentrations E-61
E.33. Industrial Worker Scenario Groundwater Unit Dose Factors E-62

E.34. Human Health Risk and Dose Assessment Cases E-63
E.35. Peak Long Term Human Health Impacts for Case 1 ..... E-66
E.36. Peak Long Term Human Health Impacts for Case 2 ..... E-69
E.37. Peak Long Term Human Health Impacts for Case 7 ..... E-72
E.38. Peak Long Term Human Health Impacts for Case 8 ..... E-75
E.39. Comparison of Peak Incremental Lifetime Cancer Risk, Hazard Index, and Dose for the Industrial Worker E-76

LIST OF TERMS

BTC	breakthrough curve
CERCLA	*Comprehensive Environmental Response, Compensation, and Liability Act*
CoPCs	constituents of potential concern
DOE	U.S. Department of Energy
Ecology	Washington State Department of Ecology
EDE	effective dose equivalent
EPA	U.S. Environmental Protection Agency
HSRAM	*Hanford Site Risk Assessment Methodology*
ILCR	incremental lifetime cancer risk
Kd	partition (distribution) coefficient
MTCA	"Model Toxics Control Act"
TWRS EIS	Tank Waste Remediation System Environmental Impact Statement
WMA	waste management area

E.1.0 INTRODUCTION

A series of numerical simulations were conducted to evaluate the performance of interim corrective measures such as surface barriers in reducing long-term human health risks from potential groundwater contamination at waste management area (WMA) B-BX-BY. The specific objectives of the numerical assessment were to: 1) quantify the risks posed by past tank releases to the groundwater if no interim corrective measures are implemented, and 2) determine to what degree implementation of selected interim corrective measures would decrease the risks posed by past tank releases. The assessments focus specifically on impacts to groundwater resources (i.e., the concentration of contaminants in groundwater) and long-term risk to human health (associated with groundwater use). The evaluations consider the extent of contamination presently within the vadose zone, contaminant movement through the vadose zone to the saturated zone (groundwater), contaminant movement in the groundwater to specified boundaries, and the types of assumed human receptor activities at those boundaries. The impact assessment results present several key evaluations for decision-maker input that may impact current operations and future decisions on tank retrieval and closure.

E.2.0 MODELING APPROACH

Both base case (existing tank farm conditions) and engineered alternatives for the interim corrective measures were considered. The focus for the contaminant transport modeling was chemicals (i.e., nitrate), moderately mobile radionuclides (i.e., uranium-238) and long-lived radionuclides (i.e., technetium-99) that are environmentally mobile. The postulated conceptual model utilized the recently collected data on technetium-99 and other constituents from a borehole near tank BX-102 and the MACTEC-ERS spectral gamma data (DOE-GJPO 1998). Losses from B tank farm (e.g., tank B-110) and BY tank farm were not considered because of the small releases and the short half-life of the contaminants. Limited attention was given to past practice sites (e.g., cribs and trenches) because they are the focus of the 200 Area Remediation Project.

For simulations with barriers in the BX tank farm, it was assumed that an interim barrier is in place by the year 2010. It was also assumed that for all simulations, as part of tank farm closure, a closure barrier is in place by the year 2040. Placing a barrier was expected to significantly reduce infiltration of meteoric water and therefore arrival of contaminants at the water table. The modeling considered the estimated inventories of contaminants within the vadose zone and calculated the associated risk (i.e., exceeding the drinking water standards [40 CFR 141] at a specified boundary). Inventory estimates were considered to be a critical factor in calculations, and uncertainties in inventories were considered. It was assumed that no tank leaks will occur in the future. It was also assumed that, as part of good housekeeping, water line leaks from existing piping will be addressed and resolved. However, as part of sensitivity analysis, simulations were run to evaluate long-term effects of water line leaks in the vicinity of tank BX-102. The umbrella structure of the tank and shedding of water were simulated. Sediments adjacent to the tanks attain elevated water content and, while remaining unsaturated, they develop moisture dependent anisotropy. Such effects were simulated in the model. Numerical results were obtained at the BX tank farm fence east line boundary, exclusion boundary beyond the 200 Areas, and the Columbia River. These boundaries are based on DOE-RL (2000), but in addition DOE-RL (2000) also includes the 200 Areas boundary. However, 200 Areas and the exclusion boundaries are relatively close. Streamtube/analytical models were used to route computed contaminant concentrations at the water table to other boundaries.

A location map of WMA B-BX-BY and the surrounding facilities is shown in Figure E.1. Two-dimensional cross-sectional models were used to model vadose zone flow and transport. A representative (west-east) cross-sectional model through tanks BX-108, BX-105, and BX-102 (Figure E.1) were considered. In addition to the row of tanks, two-dimensional flow and transport simulations were run for a (west-east) trench (i.e., 216-B-38) west of the BX tank farms (Figure E.1).

A west to east profile for the two modeled cross-sections, including trench B-38, is shown in Figure E.2.

Figure E.1. Location Map of Single-Shell Tanks in Waste Management Area B-BX-BY and Surrounding Facilities in the 200 East Area

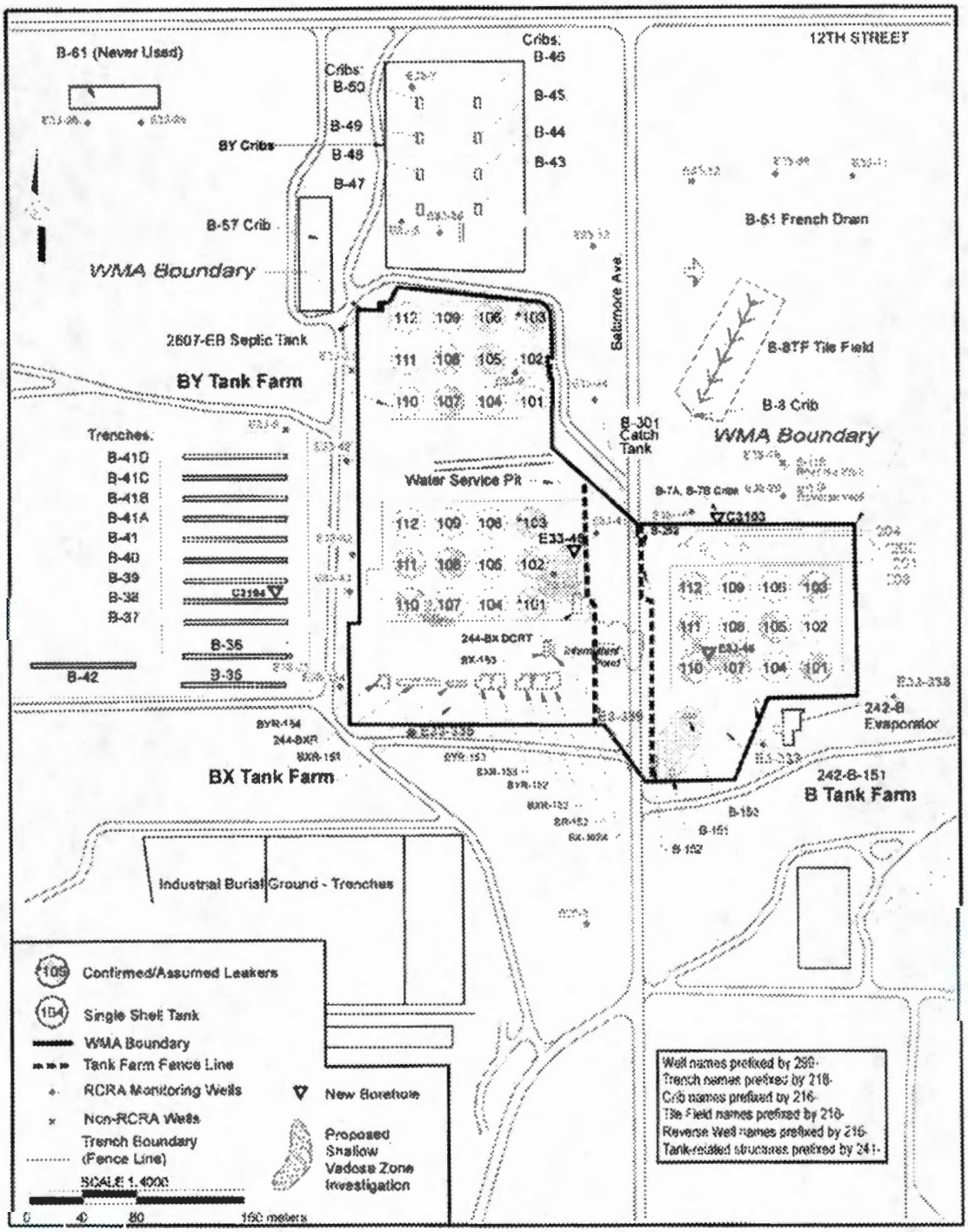

Note: All wells are preceded by 299-.

Note: The intermittent pond between the B and BX tank farms has been addressed by interim measures.

Figure E.2. West to East Profile for Cross-Section through Tanks BX-111 to BX-102 (distance ~180 to 300 m) and Trench B-38 (distance ~20 to 70 m)

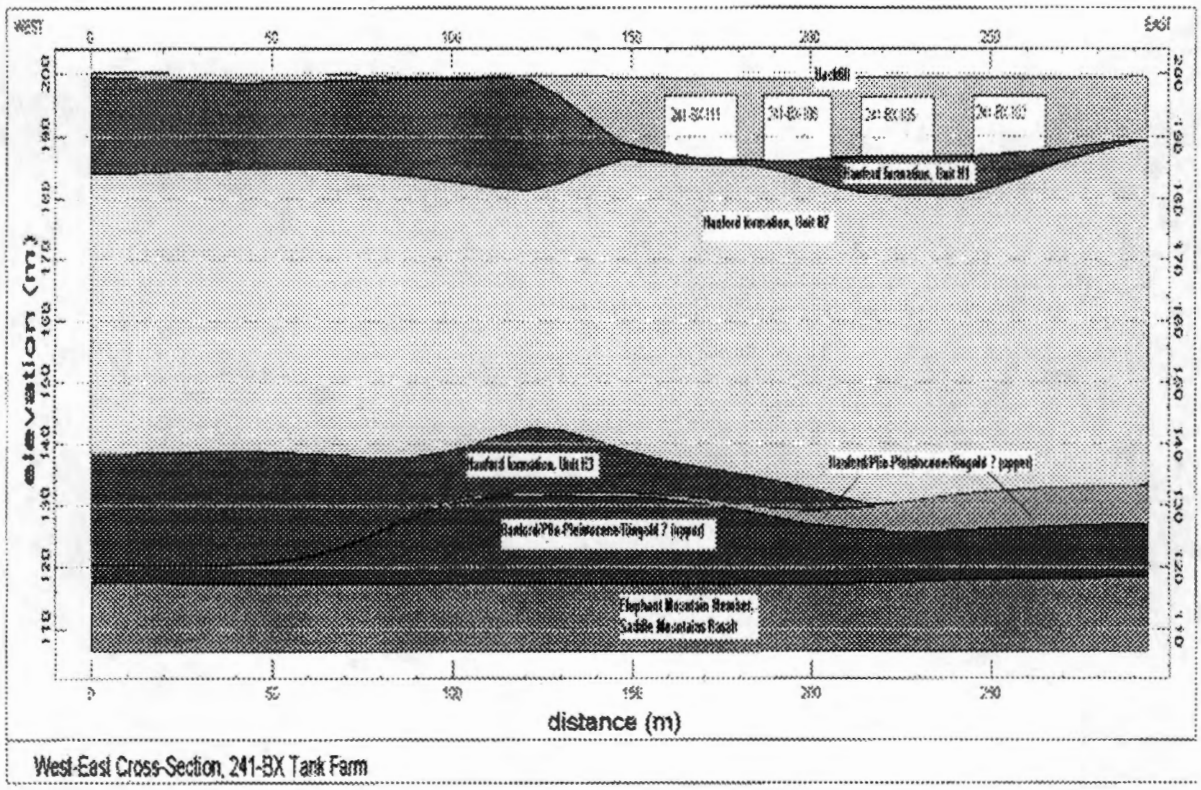

The cross-section containing tanks BX-108, BX-105 and BX-102 (Figure E.3) was modeled using a computation domain with a horizontal extent of 117.4 m (385.0 ft) and unit width. Because the inventory was emplaced at areas east of tank BX-108, the western-most tank, BX-111, was not included in the domain. To avoid boundary effects when the domain terminated at the east fence line, the geology shown at the eastern edge of the BX cross-section was extended by 15 feet.

The region west of tank BX-111 was used to model flow and transport for trench B-38. The horizontal extent of the trench B-38 cross-section was 109.9 m (306.5 ft) and the width was 10 ft (Figure E.4). Note that, in this appendix and in Section 4.0, the cross-section containing the row of tanks BX-108, BX-105, and BX-102 is also labeled as cross-section BX-HH'. Also, the trench cross-section is often labeled as B-38.

Simulation of flow and transport through each cross-section generates a breakthrough curve (BTC) at the water table. The temporal and spatial distribution for each of these BTCs is recognized and the principle of superposition is used to generate a composite BTC. An analytical/streamline approach is used to route the BTCs through the unconfined aquifer to the remote boundaries. The BTCs are converted into dose estimates using appropriate factors.

Figure E.3. Geologic Cross-Section through Tanks BX-102, BX-105, and BX-108

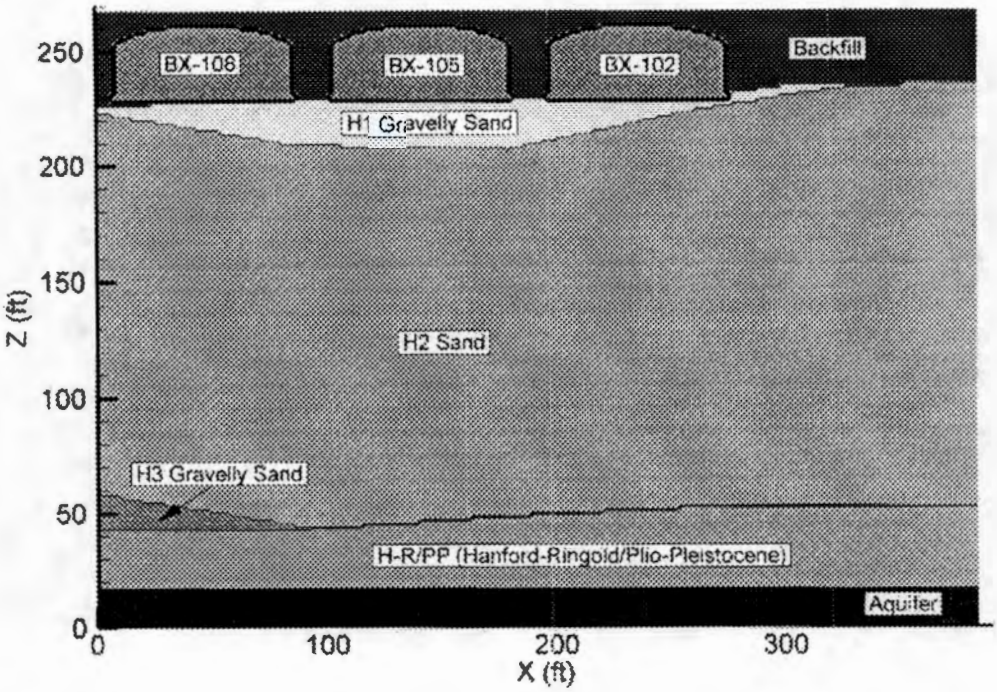

Figure E.4. Geologic Cross-Section through Trench B-38

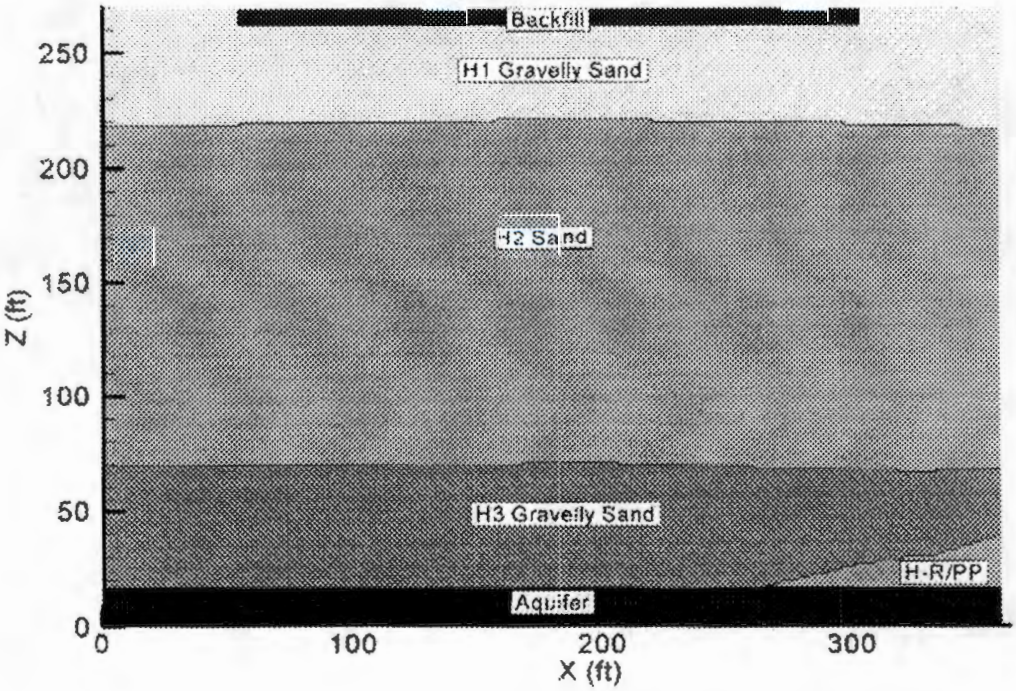

Fluid flow within the vadose zone is described by Richards' equation (Domenico and Schwartz 1990), whereas the contaminant transport is described by the conventional advective-dispersive transport equation with an equilibrium linear sorption coefficient (Kd) formulation. Detailed stratigraphic cross-sectional model data are based on information in Lindsey et al. (2001). The model includes the effects of dipping strata. The enhanced spreading at the fine-grained /coarse-grained interfaces and the increased downdip movement of the plume along these interfaces are included in the model.

Data on laboratory measurements for moisture retention, particle-size distribution, saturated and unsaturated hydraulic conductivity, and bulk density for individual stratum are based on data on 200 East and 200 West Area soils (Khaleel et al. 2001). For each stratum defined by the stratigraphic cross-sectional model, the small-scale laboratory measurements are upscaled to obtain equivalent horizontal and vertical unsaturated hydraulic conductivities as a function of mean tension (Khaleel et al. 2001). Upscaling (Khaleel et al. 2002a, b) of unsaturated hydraulic conductivities (Ks) leads to development of macroscopic anisotropies (as a function of mean tension) for each layer. An averaging of van Genuchten parameters (θ_r, θ_s, α, and n) (van Genuchten 1980) is used to define a moisture retention curve for each stratum.

In case multiple samples were not available for each stratum, data from other sites in the 200 Areas were used (Khaleel and Relyea 2001). Attempts were made to use hydraulic properties that were obtained using both laboratory-measured moisture retention and unsaturated hydraulic conductivity. This was primarily to avoid extrapolating the unsaturated conductivities (van Genuchten 1980; Mualem 1976) to the dry end, based on saturated conductivity estimate (Khaleel et al. 1995). Also, to reflect field conditions, the laboratory data were corrected for the presence of any gravel fraction in the sediment samples (Khaleel and Relyea 1997). As with flow modeling, each stratum was modeled with different transport parameters (i.e., bulk density, diffusivity, and dispersivity).

Initial Conditions

Initial conditions are needed for moisture content (or pressure head) and contaminant concentration. For simulations not considering a barrier, initial conditions for pressure head (and moisture content) are established by allowing the vadose zone to equilibrate with an infiltration rate representative of natural infiltration for tank farm conditions. The data on infiltration rates with and without barriers are included in Section E.2.2.1. Initial conditions for contaminant concentration are provided as part of inventory estimates for uranium-238, technetium-99, and nitrate.

Model Setup and Boundary Conditions

A two-dimensional (west-east) vertical (x-z) slice of the flow domain was used for modeling flow and transport. The simulation domain extends horizontally to include the fence line boundary and the water table, which is located about 77.4 m (254 ft) below ground surface. The geologic strata are assumed continuous but not of constant thickness. Sloped interfaces for geologic units are included.

For flow modeling, Neumann boundary conditions were prescribed at the surface with the flux equal to the recharge rate estimate. For transport modeling, a zero flux boundary was prescribed at the surface for technetium-99, nitrate, and uranium. The western and eastern boundaries were assigned no-flux boundaries for both flow and transport. The water table boundary was prescribed by water table elevations and the unconfined aquifer hydraulic gradient. No-flux boundaries were used for the lower boundary. Detailed inputs for various flow and transport parameters are presented later.

E.2.1 NUMERICAL CASES CONSIDERED

All simulations reported were performed using the STOMP simulator (White and Oostrom 2000a, b). The flow and solute transport simulation cases were specified in the modeling data package (Khaleel et al. 2001). The suite of simulations investigated the need for interim corrective measures (e.g., surface barriers) and the sensitivity of water line leaks, recharge, sorption, and initial inventory placement on solute transport. Two-dimensional cross-sections, representing west to east transects through the BX tank farms and B trenches were used for the computational domains. For the BX tank farm, the following simulations were conducted for cross-section BX-108, BX-105 and BX-102:

- Inventory distribution east of tank BX-102 (cases 1 through 4 and 7 through 11)
- Inventory distribution centered between tanks BX-105 and BX-102 (cases 5 and 6)
- Interim barriers (cases 2 and 6)
- Water line leaks (cases 3 and 4)
- Variations in recharge rates (cases 7, 8, and 9)
- Variations in uranium-238 Kd (cases 10 and 11).

For the B trench simulations, the following simulations were conducted for the B-38 cross-section west of the BX tank farm:

- Variations in recharge rates (cases 12 and 13)
- Closure barrier schedule analogous to the one used for the BX tank farm cases (case 14).

Simulations were run for 1000 years. The individual cases are summarized below.

- **Case 1: Base Case, No Action Alternative.** This scenario involves simulating flow and transport for the cross-section through tanks BX-108, BX-105, and BX-102, considering an initial recharge rate of 100 mm/yr, no water line leak, no interim barrier, a closure barrier at year 2040, a partitioning coefficient (Kd) of 0.6 mL/g for uranium-238, and an inventory distribution that extends east of tank BX-102 to the BX tank farm east fence line boundary.

- **Case 2: Barrier Alternative and No Water Line Leak.** This scenario involves simulating flow and transport for the cross-section through tanks BX-108, BX-105, and BX-102, considering initial recharge rate of 100 mm/yr, placement of an interim barrier by 2010, a closure barrier at year 2040 (i.e., the interim barrier replaced by the closure barrier), no water line leak, a Kd of 0.6 mL/g for uranium-238, and an inventory distribution that extends east of tank BX-102 to the BX tank farm east fence line boundary.

- **Case 3: No Interim Barrier and Water Line Leak (1 gpm for 20 years).** This scenario involves simulating flow and transport for the cross-section through tanks BX-108, BX-105, and BX-102, considering initial recharge rate of 100 mm/yr, water line leak (1 gpm for 20 years) for BX-102 only, no interim barrier until closure at year 2040, a Kd of 0.6 mL/g for uranium-238, and an inventory distribution that extends east of tank BX-102 to the BX tank farm east fence line boundary. The water line leak occurs east of tank BX-102 over a 15-foot radius at the elevation of the top of the tank dome.
- **Case 4: No Interim Barrier and Water Line Leak (200,000 gallons over 5 days).** This scenario involves simulating flow and transport for the cross-section through tanks BX-108, BX-105, and BX-102, considering initial recharge rate of 100 mm/yr, water line leak (200,000 gallons in 5 days) for BX-102 only, no interim barrier until closure at year 2040, a Kd of 0.6 mL/g for uranium-238, and an inventory distribution that extends east of tank BX-102 to the BX tank farm east fence line boundary. The water line leak occurs east of tank BX-102 over a 15-foot radius at the elevation of the top of the tank dome.
- **Case 5: Alternate Inventory Distribution and No Interim Barrier.** This scenario involves simulating flow and transport for the cross-section through tanks BX-108, BX-105, and BX-102, considering initial recharge rate of 100 mm/yr, no water line leak, no interim barrier until closure at year 2040, a Kd of 0.6 mL/g for uranium-238, and an inventory distribution that is centered between tanks BX-105 and BX-102.
- **Case 6: Alternate Inventory Distribution with Interim Barrier.** This scenario involves simulating flow and transport for the cross-section through tanks BX-108, BX-105, and BX-102, considering initial recharge rate of 100 mm/yr, placement of an interim barrier at year 2010, a closure barrier at year 2040 (i.e., the interim barrier replaced by the closure barrier), no water line leak, a Kd of 0.6 mL/g for uranium-238, and an inventory distribution that is centered between tanks BX-105 and BX-102.
- **Case 7: Base Case with 50 mm/yr Meteoric Recharge.** This scenario involves simulating flow and transport for the cross-section through tanks BX-108, BX-105, and BX-102, considering initial recharge rate of 50 mm/yr, no water line leak, no interim barrier until a closure at year 2040, a Kd of 0.6 mL/g for uranium-238, and an inventory distribution that extends east of tank BX-102 to the BX tank farm east fence line boundary.
- **Case 8: Base Case with 30 mm/yr Meteoric Recharge.** This scenario involves simulating flow and transport for the cross-section through tanks BX-108, BX-105, and BX-102, considering initial recharge rate of 30 mm/yr, no water line leak, no interim barrier until closure at year 2040, a Kd of 0.6 mL/g for uranium-238, and an inventory distribution that extends east of tank BX-102 to the BX tank farm east fence line boundary.
- **Case 9: Base Case with 10 mm/yr Meteoric Recharge.** This scenario involves simulating flow and transport for the cross-section through tanks BX-108, BX-105, and BX-102, considering initial recharge rate of 10 mm/yr, no water line leak, no interim barrier until closure at year 2040, a Kd of 0.6 mL/g for uranium-238, and an inventory distribution that extends east of tank BX-102 to the BX tank farm east fence line boundary.

- **Case 10: Base Case with Kd = 0.1 ml/g for Uranium-238.** This scenario involves simulating flow and transport for the cross-section through tanks BX-108, BX-105, and BX-102, considering initial recharge rate of 100 mm/yr, no interim barrier until closure at year 2040, a partition coefficient (Kd) of 0.1 mL/g for uranium-238, and an inventory distribution that extends east of tank BX-102 to the BX tank farm east fence line boundary.
- **Case 11: Base Case with Kd = 1.0 ml/g for Uranium-238.** This scenario involves simulating flow and transport for the cross-section through tanks BX-108, BX-105, and BX-102, considering initial recharge rate of 100 mm/yr, no interim barrier until closure at year 2040, a Kd of 1.0 mL/g for uranium-238, and an inventory distribution that extends east of tank BX-102 to the BX tank farm east fence line boundary.
- **Case 12: Trench B-38 with 55.4 mm/yr Meteoric Recharge.** This scenario involves simulating flow and transport for a cross-section west of tank BX-111, considering initial recharge rate of 55.4 mm/yr, a 378,000-gallon leak in 1954, no water line leak, no interim barrier until closure at year 2010, and a unit inventory distribution for a sorbed species (i.e., uranium-238, Kd = 0.6 mL/g) and a non-sorbing species (i.e., technetium-99 and nitrate). The unit inventory results are also scaled to the uranium-238, technetium-99, and nitrate inventory estimates for trench B-38 and all of the B trenches.
- **Case 13: Trench B-38 with 100.0 mm/yr Meteoric Recharge.** This scenario involves simulating flow and transport for a cross-section west of tank BX-111, considering initial recharge rate of 100 mm/yr, a 378,000-gallon leak in 1954, no interim barrier until closure at year 2010, and a unit inventory distribution for a sorbed species (i.e., uranium-238, Kd = 0.6 mL/g) and a non-sorbing species (i.e., technetium-99 and nitrate). The unit inventory results are also scaled to the uranium-238, technetium-99, and nitrate inventory estimates for trench B-38 and all of the B trenches.
- **Case 14: Trench B-38 with Delayed Closure Barrier with 100.0 mm/yr Meteoric Recharge.** This scenario involves simulating flow and transport for a cross-section west of tank BX-111, considering initial recharge rate of 100 mm/yr, a 378,000-gallon leak in 1954, no interim barrier until closure at year 2040, and a unit inventory distribution for a sorbed species (i.e., uranium-238, Kd = 0.6 mL/g) and a non-sorbing species (i.e., technetium-99 and nitrate). The unit inventory results are also scaled to the uranium-238, technetium-99, and nitrate inventory estimates for trench B-38 and all of the B trenches.

E.2.2 RECHARGE ESTIMATES AND VADOSE ZONE FLOW AND TRANSPORT PARAMETERS

Modeling inputs for recharge estimates and effective (upscaled) flow and transport parameters are presented in this section. The effective parameters are based on laboratory measurements of moisture retention, saturated and unsaturated hydraulic conductivity, and bulk density for sediment samples in the 200 Areas.

E.2.2.1 Recharge Estimates

The tank farm surfaces are covered with gravel to prevent vegetation growth and provide radiation shielding for site workers. Bare gravel surfaces, however, enhance net infiltration of meteoric water compared to undisturbed naturally vegetated surfaces. Infiltration is further enhanced in the tank farms by the effect of percolating water being diverted by an impermeable, sloping surface of the tank domes. The basis for recharge estimates (Table E.1) for the field investigation report modeling is presented in Section 3.2.1. Recharge estimates for the trench simulations are presented in Table 4.1 in Section 4.1.

Table E.1. Timeline Estimates for Emplacement of Interim and Closure Barriers at the BX Tank Farm and Corresponding Recharge Estimates

Condition Simulated	Recharge Estimate (mm/yr)
No barrier (2000 to 2010)	100
Interim barrier (2010 to 2040)	0.5
Closure barrier (first 500 yrs) (2040 to 2540)	0.1
Degraded closure barrier (post 500 yrs) (2540 to 3000)	3.5

E.2.2.2 Vadose Zone Flow and Transport Parameters

This section provides effective (upscaled) values of flow and transport parameters for the vadose zone. Specific flow parameters include moisture retention and saturated and unsaturated hydraulic conductivity. Transport parameters include bulk density, diffusivity, sorption coefficients, and macrodispersivity. Details on deriving the effective (upscaled) parameters are addressed in *Modeling Data Package for B-BX-BY Field Investigation Report (FIR)* (Khaleel et al. 2001).

Table E.2 lists composite, fitted van Genuchten-Mualem (van Genuchten 1980; van Genuchten et al. 1991) parameters for various strata at the BX tank farm. Estimates for the equivalent horizontal and vertical hydraulic conductivities are presented in Section E.2.2.3.

Table E.2. Composite van Genuchten-Mualem Parameters for Various Strata at the BX Tank Farm

Strata/Material Type	Number of Samples	θs	θr	α (1/cm)	n	ℓ	Fitted Ks (cm/s)
Backfill	10	0.1380	0.0100	0.0210	1.3740	0.5	5.60E-04
Sand H2	12	0.3819	0.0443	0.0117	1.6162	0.5	9.88E-05
Gravelly sand H1	11	0.2126	0.0032	0.0141	1.3730	0.5	2.62E-04
Gravelly Sand H3	8	0.2688	0.0151	0.0197	1.4194	0.5	5.15E-04
Plio-Pleistocene	4	0.4349	0.0665	0.0085	1.8512	0.5	2.40E-04
Aquifer/Sandy gravel	8	0.2688	0.0151	0.0197	1.4194	0.5	1.87E-01

Source: Khaleel et al. (2001)

E.2.2.3 Stochastic Model for Macroscopic Anisotropy

Variable, tension-dependent anisotropy provides a framework for upscaling small scale, laboratory measurements to the effective (upscaled) properties for the large scale tank farm vadose zone. A stochastic model (Polmann 1990) is used to evaluate tension-dependent anisotropy for sediments at the WMA; details are in Appendix C of Khaleel et al. (2001). The following is a brief description of the variable anisotropy model used in the field investigation report modeling.

Yeh et al. (1985) analyze steady unsaturated flow through heterogeneous porous media using a stochastic model; parameters such as hydraulic conductivity are treated as random variables rather than as deterministic quantities. The Gardner (1958) relationship is used in Yeh et al. (1985) to describe unsaturated hydraulic conductivity (K) as a function of saturated hydraulic conductivity (K_s) and tension (ψ), that is,

$$K(\psi) = K_s \exp(-\beta\psi) \tag{E.1}$$

where:

β = fitting parameter.

Equation E.1 can be written as

$$\ln K(\psi) = LnK_s - \beta\psi \tag{E.2}$$

Equation E.2 is referred to as the log-linear model, because *LnK* is linearly related to ψ through the constant slope β. However, such a constant slope is often inadequate in describing $LnK(\psi)$ over ranges of tension of practical interest for field applications. As an alternative, the slope β can be approximated locally by straight lines over a fixed range of tension. The *LnKs* in Equation E.2 can then be derived by extrapolating the local slopes back to zero tension.

Using a linear correlation model between the log-conductivity zero-tension intercept and β, Polmann (1990) presents a generalized model that accounts for the cross-correlation of the local soil property (i.e., LnK_s and β) residual fluctuations. Compared to uncorrelated LnK_s and β model, partial correlation of the properties is shown to have a significant impact on the magnitude of the effective parameters derived from the stochastic theory. The Polmann (1990) equations for deriving the effective parameters are as follows.

$$\begin{aligned}
&< LnK > = < LnK_s > - A < \psi > - \sigma^2_{LnKs}\lambda[p - p^2 < \psi > - \zeta^2 < \psi >]/(1 + A\lambda) \\
&\sigma^2_{LnK} = \sigma^2_{LnKs}[(1 - p < \psi >)^2 + \zeta^2 < \psi >^2]/(1 + A\lambda) \\
&K_h^{eq} = \exp[< LnK > + (\sigma^2_{LnK}/2)] \\
&K_v^{eq} = \exp[< LnK > - (\sigma^2_{LnK}/2)]
\end{aligned} \tag{E.3}$$

where:

σ^2_{LnK} = variance of log unsaturated conductivity (which depends on mean tension)

$<\psi>$ = mean tension

σ^2_{LnKs} = variance of LnK_s
$<LnK_s>$ = mean of LnK_s
p = slope of the β versus LnK_s regression line
ζ = $\sigma_\delta/\sigma_{LnKs}$
σ_δ = standard deviation of the residuals in the β versus LnK_s regression
A = mean slope, β, for LnK_s vs. ψ
λ = vertical correlation lengths for LnK_s (assumed to be same as that of β)
K_h^{eq} = equivalent unsaturated horizontal conductivity
K_v^{eq} = equivalent unsaturated vertical conductivity.

E.2.2.3.1 Macroscopic Anisotropy Parameters. Table E.3 lists the variable, macroscopic anisotropy parameter estimates for various strata at WMA B-BX-BY. Details on derivation of the parameter estimates are included in Appendix C of Khaleel et al. (2001)

Table E.3. Macroscopic Anisotropy Parameters Based on Polmann (1990) Equations for Various Strata at WMA B-BX-BY

Strata/Material Type	Number of Samples	$<LnK_s>$	$\sigma^2_{LnK_s}$	p	ζ	λ (cm)	A
Backfill	10	-15.76	3.56	-1.1E-4	1.84E-4	30	0.00371
Sand H2	12	-14.60	1.50	-7.2E-4	6.55E-4	50	0.00620
Gravelly Sand H1	11	-14.85	1.94	-2.6E-4	2.50E-4	30	0.00368
Gravelly Sand H3	8	-15.30	1.83	-5.6E-4	5.16E-4	50	0.00415
Plio-Pleistocene	4	-10.43	1.01	-2.4E-3	9.34E-4	50	0.0104

E.2.2.4 Effective Transport Parameters

Effective transport parameter (bulk density, diffusivity, and dispersivity) estimates are presented in this section. Because of natural variability, the transport parameters are all spatially variable. Similar to the flow parameters, the purpose is to evaluate the effect of such variability on the large-scale transport process.

E.2.2.4.1 Bulk Density and Sorption Coefficient. Both bulk density (ρ_b) and sorption coefficient estimates are needed to calculate retardation factors for different species. The effective, large-scale estimate for the product [$\rho_b K_d$] is the average of the product of small-scale laboratory measurements for bulk density and sorption coefficient (Gelhar 1993). Table E.4 provides the effective, large-scale estimates for uranium-238. The average ρ_b, E[ρ_b] (Table E.4) estimates are based on data in Khaleel et al. (2001) for the five strata. The sorption coefficient estimates (Table E.4) for uranium-238 are based on data from *Geochemical Data Package for the Immobilized Low-Activity Waste Performance Assessment* (Kaplan and Serne 1999) for undisturbed sediments. No other species are included, because the sorption coefficients for technetium-99 and nitrate are estimated to be zero. Calculations for E[ρ_b] and E[$\rho_b K_d$] include correction for the gravel fraction (Table E.4).

Table E.4. Effective Parameter Estimates, $E[\rho_b K_d]$, for Uranium-238 for the Product of Bulk Density (g/cm^3) and K_d (cm^3/g) at Waste Management Area B-BX-BY

Strata/Material Type	Kd	E[ρb]	E[ρbKd]
Backfill	0.6	1.94	0.59
Sand H2	0.6	1.76	1.04
Gravelly sand H1	0.6	2.07	1.24
Gravelly sand H3	0.6	1.94	1.17
Plio-Pleistocene	0.6	1.65	0.98

Source: Khaleel et al. (2001)

E.2.2.4.2 Diffusivity. It is assumed that the effective, large-scale diffusion coefficients for all strata at the BX tank farm are a function of volumetric moisture content (θ) and can be expressed using the empirical relation from "Permeability of Porous Solids" (Millington and Quirk 1961):

$$D_e(\theta) = D_0 \frac{\theta^{10/3}}{\theta_s^2} \tag{E.4}$$

where:

$D_e(\theta)$ = effective diffusion coefficient of an ionic species
D_0 = effective diffusion coefficient for the same species in free water.

The molecular diffusion coefficient for all species in porewater is assumed to be 2.5×10^{-5} cm^2/s (Kincaid et al.1995).

E.2.2.4.3 Macrodispersivity. An extended review is provided in Appendix C of Khaleel et al. (2001) on the rationale for vadose zone macrodispersivity estimates. Macrodispersivity estimates are needed for both reactive (uranium-238) and non-reactive (i.e., technetium-99 and nitrate) species.

Macrodispersivity Estimates for Non-Reactive Species. Macrodispersivity estimates for non-reactive species (i.e., technetium-99 and nitrate) are listed in Table E.5. Details on the basis for the estimates are provided in Appendix C of Khaleel et al. (2001).

Table E.5. Non-Reactive Macrodispersivity Estimates for Various Strata at Waste Management Area B-BX-BY

Strata/Material Type	AL (cm)	AT (cm)
Backfill	~150	15
Sand H2	~150	15
Gravelly sand H1	~100	10
Gravelly sand H3	~100	10
Plio-Pleistocene	~50	5

E.2.2.4.4 Heterogeneous Sorption Enhanced Macrodispersivities for the Reactive Species. The net effect of sorption is to retard the velocity of the contaminant. Because sorption for specific contaminants may be a function of soil properties, as the soil properties experience spatial variability, the sorption also varies (Gelhar 1993; Talbott and Gelhar 1994).

Stochastic analysis results for macrodispersivity enhancement for various strata are presented in Table C-7 of Khaleel et al. (2001) for the reactive species (i.e., uranium-238). Note that the unsaturated conductivities were evaluated at -100 cm via the fitted van Genuchten-Mualem relation. The macrodispersivity enhancement ranged from about 1.06 for backfill sediments to about 2.24 for Plio-Pleistocene (silty) sediments.

E.2.3 GROUNDWATER FLOW AND TRANSPORT

This section provides flow and transport parameters for the unconfined aquifer including the unit dose conversion factors. The preceding section provides vadose zone flow and transport parameters.

Instead of the Hanford Site-wide groundwater model, an analytical/streamtube approach was used to model groundwater flow and transport. Flow and transport information needed for the analytical/streamtube model is based on the VAM3D site-wide groundwater model (Law et al. 1996). Details are included in Appendix C of Khaleel et al. (2001).

An instantaneous point source model was used to calculate the concentration of contaminant species originating at the BX tank farm fence line and monitored in the model at two remote boundaries along the groundwater flow path. The two boundaries are the 200 Area exclusion boundary (~1.25 Km east of the 200 East Area) and the Columbia River (Table E.6). The distance to each boundary along the groundwater flow path was based on streamlines derived from the VAM3D site-wide groundwater models of Law et al. (1996) and Lu (1996). Steady-flow conditions, water table maps, and streamlines generated from the VAM3D simulation are reported by Khaleel et al. (2001). The analytical groundwater model assumes transport from a point source from a series of solute slugs and considers longitudinal and horizontal transverse dispersion, molecular diffusion, and first order decay. The method of superposition was used to integrate the individual slug sources. The instantaneous point source model for a three-dimensional space, as reported by Domenico and Schwartz (1990), is shown in Equation (E.5):

$$C(x,y,z,t) = \left[\frac{C_0 V_0}{\left(8(\pi t)^{3/2}\left(D_x D_y D_z\right)^{1/2}\right)}\right] \exp\left[-\frac{(x-vt)^2}{4D_x t} - \frac{y^2}{4D_y t} - \frac{z^2}{4D_z t} - \lambda t\right] \qquad \text{(E.5)}$$

where:

$C(x,y,z,t)$	= solute concentration as a function of position and time (pCi/L or μg/L)
$C_0 V_0$	= instantaneous source of solute mass (pCi or μg)
D_x, D_y, D_z	= coefficients of hydrodynamic dispersion (m^2/yr)
x, y, z	= spatial distances from the solute source (m)

t	= time (yr)
λ	= solute species radioactive decay constant (1/yr)
v	= porewater velocity (m/yr).

The hydrodynamic dispersion coefficients include dispersive and diffusive components, according to Equation (E.6)

$$D_i = \alpha_i v + D_m \quad for \ i = x, y, z \qquad (E.6)$$

where, α_i is the dispersivity (m), and D_m is the molecular diffusion coefficient (m^2/yr).

Material property maps for the three elemental layers of the VAM3D site-wide groundwater model are reported in Khaleel et al. (2001). Hydraulic properties for each of the 18 soil zones identified in the VAM3D site-wide groundwater model, including hydraulic conductivity in the north-south, east-west, and vertical directions, specific storage, and porosity are additionally reported in Khaleel et al. (2001). The VAM3D site-wide groundwater model assumed equal hydraulic conductivities for the horizontal directions and a vertical conductivity one order of magnitude less than the horizontal components. Specific storage was assumed constant across the site at 1×10^{-6} 1/m and porosities were either 0.10 or 0.25.

Distances and travel times from WMA B-BX-BY to the two specified boundaries were derived from streamline results from steady-state VAM3D unconfined aquifer flow simulations of the Hanford Site (Lu 1996). The simulation results were based on post-Hanford conditions representing the water table at the site without the impact of unconfined aquifer discharges from Hanford activities. Results of the VAM3D simulated hydraulic heads and streamlines are shown in Figures 15 and 19 in Lu (1996). Two streamlines are analyzed from Figure 19 (Lu 1996) starting at WMA B-BX-BY to determine the unconfined aquifer path length to the Columbia River. Travel markers indicating twenty-year intervals on the streamlines were used to estimate the travel time to the Columbia River from WMA B-BX-BY. One streamline initially goes north from WMA B-BX-BY through the gap between Gable Mountain and Gable Butte and then travels east to the Columbia River. The second (and shorter) streamline goes directly east to the Columbia River south of Gable Mountain. Since these had dramatically different lengths and travel times to the specified boundaries, only values for the second (shorter) streamline were used in this analytical streamtube analysis (Table E.6). Other groundwater flow simulations of the Hanford Site and Hanford Site monitoring data have shown the potential for groundwater flow that goes northward through the Gable Mountain/Gable Butte gap. These pathlines were not considered in this analysis and may be transient in nature from the extensive artificial recharge on the Hanford Site. Results from the shorter path length provide conservative estimates.

The concentration at the two remote boundaries is calculated by a FORTRAN code that implements the instantaneous pulse equation. Input to the model is read from two separate input files. The distance from the source zone to each boundary in the longitudinal (x) direction and groundwater velocity for each successive interval are listed in Table E.6. The distances reported in Table E.6 represent the longitudinal distance x of Equations (E.5) and (E.6). Values for the y and z directions are assigned values of zero signifying that the point of observation was along the longitudinal centerline.

Table E.6. Distance to Specified Boundary, Groundwater Velocity, and Travel Time from Waste Management Area B-BX-BY

Boundary	Distance m	Velocity m/yr	Time yr
Exclusion Boundary	4,600	115	40
Columbia River	16,000	61.5	260

The second input file provided solute mass flux across WMA B-BX-BY as a function of time for the three species (i.e., uranium-238, technetium-99, and nitrate). The concentration at each boundary was calculated for a time series of solute release events using linear superposition of Equation (E.5) for each release event. The 1000-year period between years 2000 and 3000 was modeled using 1000 uniformly spaced solute release events. Radiological decay of the non-radioactive species (i.e., nitrate) was neglected.

Other parameters needed for groundwater transport modeling are listed in Table E.7. Note that a small vertical macrodispersivity of 10 mm is used based on the limited vertical mixing observed in stratified aquifers such as those in the 200 Areas (van der Kamp et al. 1994). The other macrodispersivities are the same as those used in the site-wide model (Law et al. 1996).

E.2.4 CONTAMINANT INVENTORY

This section provides details on the basis for vadose zone contaminant inventory estimates and their distributions. Also included are details on how various inventory distributions are implemented in the numerical model.

E.2.4.1 Basis for Inventory Estimates

B, BX, BY tank farms vadose zone inventory estimates for the three species (i.e., technetium-99, uranium-238, and nitrate) are primarily based on soil samples collected from borehole 299-E33-45 located near tank BX-102 as reported in Khaleel et al. (2001). The extent of contamination within the tank farm is based on the MACTEC-ERS spectral gamma plume maps (DOE-GJPO 1998).

For the trench B-38 simulations, only uranium-238 and technetium-99 were included in the STOMP simulations, as nitrate was scaled from the non-sorbing technetium-99 results. In contrast to the BX tank farm simulations, the trench B-38 simulations assumed no inventory was initially present in the subsurface. Instead, these contaminants were simulated as discrete sources of unit inventory discharged to the trench at the beginning of the simulation in 1954. The results of these simulations were scaled to the trench B-38 inventory and the inventory of all the trenches.

Table E.7. Transport Parameters for the Site-Wide Groundwater Model

Parameter	Estimate
Longitudinal macrodispersivity, cm	3050
Lateral macrodispersivity, cm	305
Vertical macrodispersivity, mm	10
Diffusion coefficient, cm^2/s	2.5×10^{-5}
Cs-137 sorption coefficient, cm^3/g	500
Cs-137 decay coefficient, 1/yr	0.0231

Table E.8. Unit Dose Factors for Uranium-238 and Technetium-99

Radionuclide	Dose factor [a]
Uranium-238	0.196
Technetium-99	0.00107

[a] Units are mrem per pCi/L of concentration in the groundwater.
Source: Rittmann (1999)

E.2.4.2 Inventory Distributions

Because of uncertainty with inventory estimates, two different distributions were considered in the BX tank farm. The same mass inventory (i.e., total Ci or Kg) was maintained for each species, but it was placed in two different locations in the subsurface. For the base case and its variants, the inventory profile was located east of tank BX-102 and extended to the east fence line. Such a distribution is consistent with the MACTEC-ERS spectral gamma data (DOE-GJPO 1998). In the alternate inventory scenario, the inventory profile was centered in the tank umbrella region between tanks BX-105 and BX-102. For both inventory placements, the inventory distribution was assumed to be laterally uniform and extended over the same distance of 91.5 ft, which is the distance between tank BX-102 and the east fence line.

Because the borehole concentrations for technetium-99 and nitrate were low relative to the total estimated leak inventory, these concentrations were scaled according to the method outlined in this section to maintain a plume extent similar to uranium-238. Initial inventory distributions used in the STOMP numerical simulations were scaled concentrations. However, the inventory distribution honors the concentration per gram of soil by depth reported in the modeling data package (Appendix D of Khaleel et al. 2001). Thus, the data presented in this section represent the unscaled initial inventory distributions for both technetium-99 and nitrate.

To determine the inventory profiles, concentrations measured at discrete depths were assigned to nodes in the computation domain corresponding to the midpoint of the sample interval. Since the sampling intervals for technetium-99 and nitrate were larger than the distance between nodes in the computational domain, nodes that did not correspond to a sample depth were assigned interpolated values of concentration. These concentrations were determined with a linear interpolation scheme, using the nearest measured concentrations above and below nodes not

corresponding to a measurement depth. For example, the vertical distance between nodes in the computational node was 1.5 ft, whereas the largest distance between samples for technetium-99 was 32.7 ft. Instead of assigning zero concentrations to nodes falling within the 32.7 ft interval, these nodes were assigned interpolated values of concentration.

By contrast, the sampling interval for uranium-238 was more frequent, and in many instances, smaller than the vertical distance between nodes (e.g., 0.5 ft). Laboratory analyses reported several soil samples with uranium-238 concentrations below the minimum detection level. When this occurred, a zero concentration was assigned at the corresponding depth. Thus, the uranium-238 profile differed from those of the technetium-99 and nitrate inventories in that it contained zero values of concentrations throughout its profile. However, similar to the estimates for the technetium-99 and nitrate inventories, concentrations of uranium-238 were interpolated when the distance between nodes was smaller than the sampling interval.

Figures E.5 through E.7 demonstrate how the reported inventories from the laboratory analyses translated to the computational grid for a one-dimensional slice through the domain. The solid line in Figure E.5 traces the initial inventory in STOMP for species uranium-238. The reported inventories are shown with a solid marker. Several areas of the plot show that markers lie between the reported inventory symbols, indicating regions of interpolated concentrations. By contrast, Figure E.5 shows areas where the reported inventory sampling intervals were smaller than the node spacing. For example, concentrations were measured at 98.2 and 99.6 ft. Because the elevation at the node was closer to 98.2 ft than 99.6 ft, the concentration assigned to this node corresponded to measurements at 98.2 ft (113.26 pCi/g), rather than 99.6 ft (211.59 pCi/g).

Figure E.5. Uranium-238 Concentration Profile for Initial Conditions in STOMP and the Corresponding Reported Inventory

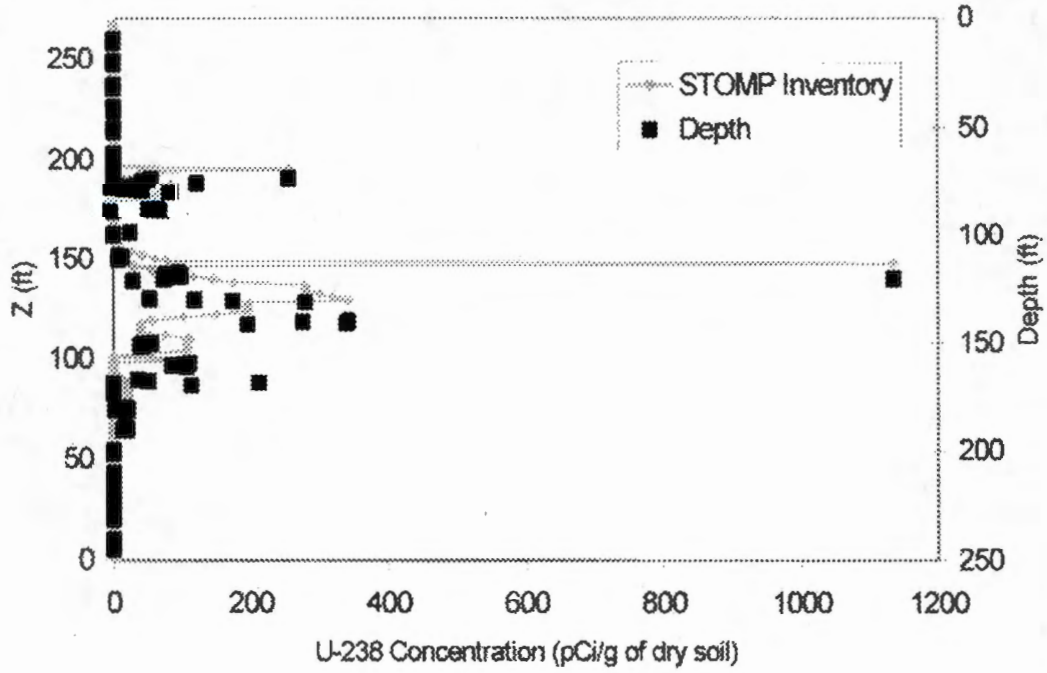

Figure E.5 also demonstrates a correlation between reported uranium-238 concentrations that were less than the minimum detection level and the zero concentrations assigned to nodes in the STOMP computational domain. This differs from the technetium-99 and nitrate concentration profiles in Figures E.6 and E.7, in which zero concentrations are only assigned to nodes at the endpoints of the plume. Similar to the uranium-238 profile, areas of the plots for technetium-99 and nitrate also illustrate interpolated concentration values. These appear in regions where markers on the solid lines lie between the values indicated for the reported inventory.

Figure E.6. Technetium-99 Concentration Profile for Initial Conditions in STOMP and the Corresponding Reported Inventory

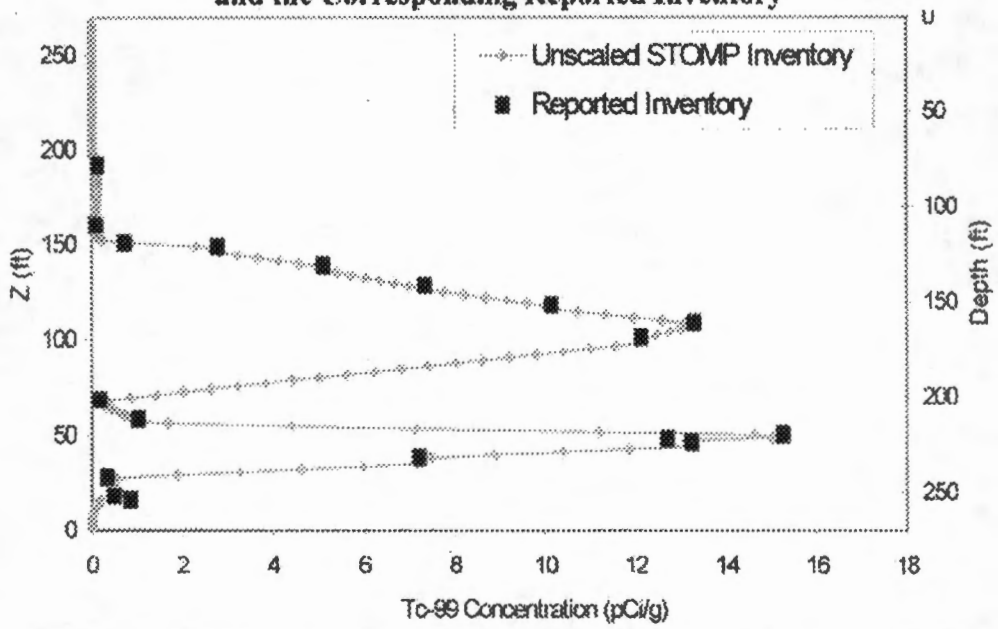

Figure E.7. Nitrate Concentration Profile for Initial Conditions in STOMP and the Corresponding Reported Inventory

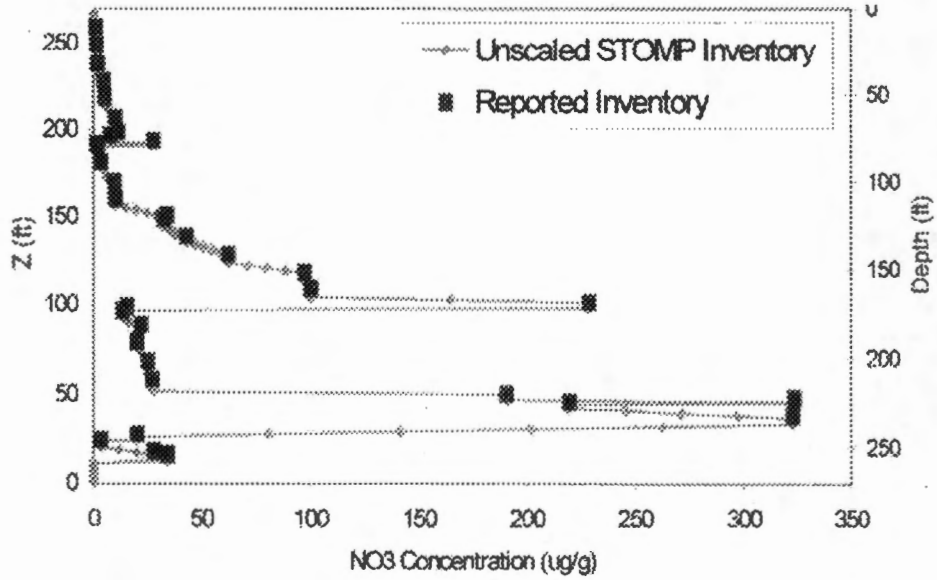

The solute concentrations for the three species were measured in terms of soil concentration (e.g., µg/g soil, pCi/g soil). These concentrations were converted to aqueous-phase concentrations based on the soil bulk density (i.e., from grain density and porosity) and the initial saturation. Initial saturations were determined using the steady-state saturation distribution simulated in STOMP for different recharge rates. The aqueous concentrations are calculated as

$$C_\ell = \frac{C_s \rho_s (1 - n_T) y_\ell}{s_\ell n_D} \tag{E.7}$$

where:

C_ℓ = the aqueous-phase concentration
C_s = the soil concentration
ρ_s = the soil grain density
n_T = the total porosity
s_ℓ = the aqueous-phase saturation
n_D = the diffusive porosity.

The product of s_ℓ and n_D represents the moisture content. It was assumed that diffusive porosities were equal to the total porosities of the media. In Equation E.7, y_ℓ represents the equilibrium fraction of solute in the aqueous phase, and is given by

$$y_\ell = \frac{s_\ell n_D}{s_\ell \rho_s K_d (1 - n_T) + s_\ell n_D} \tag{E.8}$$

where K_d is the partition coefficient. Thus, for the non-sorbed technetium-99 and nitrate species, y_ℓ is equal to one because the first term in the denominator is equal to zero (i.e. $K_d = 0$). By contrast, for uranium-238 (e.g. $K_d = 0.6$ mL/g), y_ℓ has a value between zero and one because it represents the fraction of the contaminant in the aqueous phase over the total amount in both the aqueous and sorbed phases.

The effect of partitioning is shown in Figure E.8, which reports the uranium-238 inventory in concentration per liter for the aqueous phase. This profile represents the initial concentration distribution for the base case scenario, where the value of the partition coefficient is 0.6 mL/g. Because these plots illustrate the effect of partitioning on the initial inventory distribution, the shape of the profile is identical to the uranium-238 total concentration presented in Figure E.5.

Figure E.8. Aqueous Uranium-238 Concentration

a)

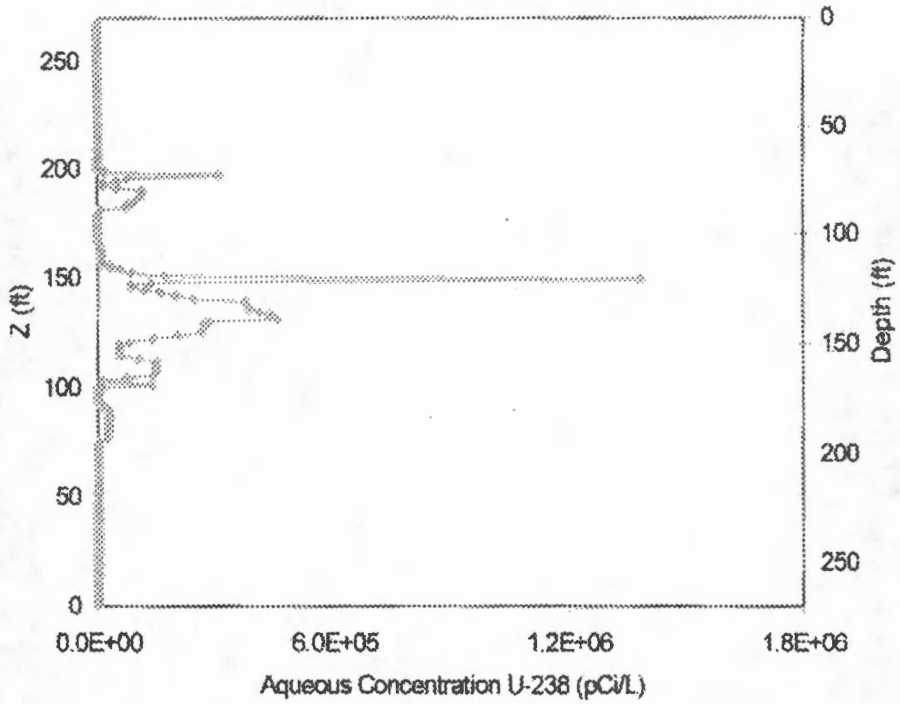

The concentration profiles presented in Figures E.5 through E.7 represent the total inventories at each node for a one-dimensional column. The total inventory (kg for nitrate and Ci for uranium-238 and technetium-99) for the tank farm is obtained by integrating the one-dimensional profiles over the area of the tank farm and the soil bulk density. For technetium-99 and nitrate, however, the computed integrated mass did not compare well the estimated inventory for the two species from tank leaks (i.e., borehole concentrations are very low relative to the inventory estimate).

To reconcile these differences in the borehole data and the estimated leak inventories, the borehole concentration data for technetium-99 and nitrate were scaled based on an inventory diameter of 92 ft (Figure E.9) that is based on the spectral gamma data. Scaling factors were calculated and are shown in Table E.9. These scaling factors are consistent with the estimated inventories (Table E.9) for the three species. It should also be noted that the uranium-238 data from the borehole measurements were already scaled in the modeling data package by a factor of 2 based on spectral gamma measurements in the BX drywells. No additional scaling of the borehole concentration data for uranium-238 was performed.

Figure E.9. Translation Geometry

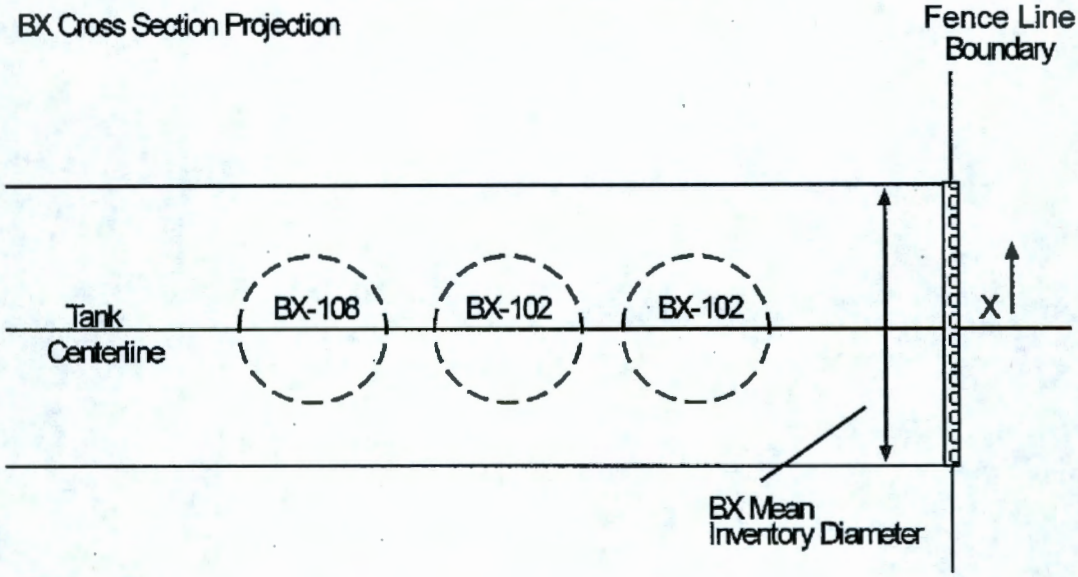

Table E.9. Calculated Plan View Areas of Different 2-Dimensional Plume Geometries for BX-108 to BX-102 Concentration Profiles and Inventory and Their Scale Factors Based on a Mean Inventory Diameter of 92 feet

Solute	Reported Leak Inventory	Unscaled Inventory per Unit Area (ft^2) (plan view)	Unscaled Circular Plume Diameter (plan view)	Cross-Section Concentration Scale Factors	Scaled Circular Plume Diameter (plan view)
Uranium-238	3.15 Ci	4.47E-04 Ci	92 ft	1	92 ft
Technetium-99	4.37 Ci	3.96E-05 Ci	375 ft	16.66	92 ft
Nitrate	13,100 kg	5.32E-01 kg	177 ft	3.66	92 ft

The aquifer water flux is upscaled from the cross-section for use in calculating the average solute concentrations. The cross-section water flux (per unit width) is multiplied by the fence line length to calculate the aquifer water flux for the tank farm. The scaled solute flux is divided by the scaled water flux to yield the average aqueous solute concentration for each species. This calculation is based on aqueous concentration scaling. The average tank farm is calculated by:

$$C_{tf} = C_{xsect} \frac{I_{tf}/I_{xsect}}{W_{fence\ line}/W_{xsect}} \tag{E.9}$$

where:

C_{tf} = the average tank farm aqueous concentration (pCi/L or ug/L)
C_{xsect} = the cross-section aqueous concentration (pCi/L or ug/L)
I_{tf} = the estimated total tank farm leak inventory (Ci or kg)
I_{xsect} = the cross-section inventory (Ci or kg)
$W_{fence\ line}$ = the fence line width (ft or m)
W_{xsect} = the cross-section width (ft or m).

The resulting concentration scale factors for the BX cross-section results are shown in Table E.10. Because the cross-section concentrations were scaled to the same mean inventory diameter, the tank farm concentration scale factor is the same for all three solutes.

Table E.10. Concentration Scale Factors for the BX Tank Farm from BX-108 to BX-102 Cross-Section Concentrations

Solute	Tank Farm Concentration Scale Factor
Uranium-238	0.122
Technetium-99	0.122
Nitrate	0.122

Although unit inventories were assumed for the B trenches, the trench mass fluxes and concentrations were determined by the same method. For the mass flux, the cross-section mass flux was multiplied by the inventory for each case. Similarly, the trench cross-section concentrations were determined by multiplying the cross-section concentrations by the inventory of the case. To calculate the average trench concentrations, the scaled mass fluxes were divided by the aquifer water flux at the trench fence line (650 ft long). Note that for aquifer water flux scaling, the width (y-dimension) of the STOMP trench cross-section was 10 feet, whereas the width of the BX-108 to BX-102 cross-section was 1 foot. The resulting concentration scale factors for the B trench cross-section are shown in Table E.11. Inventories for the trench B-38 and all eight trenches are summarized in Table E.12.

Table E.11. Concentration Scale Factors for B Trenches from Unit Inventory Cross-Section Concentrations

Solute	Unit Trench	Trench B-38	All Trenches (8)
Uranium-238	1.54×10^{-2}	2.43×10^{-4}	2.29×10^{-2}
Technetium-99	1.54×10^{-2}	2.83×10^{-4}	1.28×10^{-1}
Nitrate	1.54×10^{-2}	2.03×10^{3}	2.97×10^{4}

Table E.12. Trench B-38 Case Inventory Summary

	Uranium-238 Ci	Technetium-99 Ci	Nitrate kg
Unit Inventory	1.0	1.0	1.0
Trench B-38	1.58×10^{-2}	1.84×10^{-2}	1.32×10^{5}
All B Trenches (8)	1.49	8.31	1.93×10^{6}

E.2.4.3 Inventory Distribution Maps

Color-scaled images of the initial inventories are shown in Attachment E1 for tanks and Attachment E2 for trenches. For the inventory east of tank BX-102, the initial inventory distributions are shown in Attachment E1 Figures E1.2(a) for aqueous phase uranium-238, E1.3(a) for technetium-99, and E1.4 (a) for nitrate. For the alternate inventory distribution centered between tanks BX-105 and BX-102, the initial concentration distributions are shown in Figures E1.14 (a) for aqueous phase uranium-238, E1.15(a) for technetium-99, and E1.16(a) for nitrate. For trench B-38, the inventory distributions, after one year of simulation, are shown in color-scaled images in Attachment E2 Figures E2.3(a), E2.4(a), E2.9(a), and E2.10(a). The relationship between initial inventory distribution and simulation cases is shown in Table E.13.

Table E.13. Initial Inventory Distribution Schedule

Simulation Case	Inventory Distribution	Attachment E1 and E2 Figures
1. Base Case (No Action Alternative)	East of BX-102 to East Fence Line	Figs. E1.2(a), E1.3(a), and E1.4(a)
2. Interim Barrier	East of BX-102 to East Fence Line	Figs. E1.2(a), E1.3(a), and E1.4(a)
3. Water Line Leak (1 gpm for 20 yrs)	East of BX-102 to East Fence Line	Figs. E1.2(a), E1.3(a), and E1.4(a)
4. Water Line Leak (200,000 gal in 5 days)	East of BX-102 to East Fence Line	Figs. E1.2(a), E1.3(a), and E1.4(a)
5. Alternate Inventory Distribution and No Interim Barrier	Centered between BX-102 and BX-102	Figs. E1.14(a), E1.15(a), and E1.16(a)
6. Alternate Inventory Distribution and Interim Barrier	Centered between BX-102 and BX-102	Figs. E1.14(a), E1.15(a), and E1.16(a)
7. Base Case (50 mm/yr)	East of BX-102 to East Fence Line	Figs. E1.2(a), E1.3(a), and E1.4(a)
8. Base Case (30 mm/yr)	East of BX-102 to East Fence Line	Figs. E1.2(a), E1.3(a), and E1.4(a)
9. Base Case (10 mm/yr)	East of BX-102 to East Fence Line	Figs. E1.2(a), E1.3(a), and E1.4(a)
10. Base Case [Kd(Uranium-238) = 0.1 mL/g]	East of BX-102 to East Fence Line	Figs. E1.28(a), E1.3(a) and E1.4(a)
11. Base Case [Kd(Uranium-238) = 1.0 mL/g]	East of BX-102 to East Fence Line	Figs. E1.29(a), E1.3(a) and E1.4(a)
12. Trench (55.4 mm/yr)	Unit Inventory (uranium-238 and technetium-99)	Figs. E2.3(a) and E2.4(a)
13. Trench (100 mm/yr)	Unit Inventory (uranium-238 and technetium-99)	Figs. E2.9(a) and E2.10(a)
14. Trench (100 mm/yr) with delayed closure barrier	Unit Inventory (uranium-238 and technetium-99)	Figs. E2.9(a) and E2.10(a)

E.3.0 NUMERICAL SIMULATION RESULTS

All simulations reported herein were performed using the STOMP simulator (White and Oostrom 2000a, b). Detailed discussion on the numerical implementation for STOMP and simulation results are presented in *FY02 Initial Assessments for B-BX-BY Field Investigation Report (FIR): Numerical Simulations* (Freedman et al. 2002). Results presented in the following sections are essentially based on Freedman et al. (2002).

In this section, the simulated peak aqueous concentration, time to peak concentration, and the maximum aqueous initial concentration values for various cases are summarized. The maximum aqueous initial concentration values (based on the inventory estimates in Section E.2.4.3) are presented for comparison with the simulated peak aqueous concentration.

Saturations and inventory profiles for the tank cross-section (tanks BX-108 to BX-102) are shown in Attachment E1, and their breakthrough curves for the various cases are presented in Attachment E3. Saturations and inventory profiles for the B trench simulations are presented in Attachment E2, and their breakthrough curves in Attachment E4. Results of translation of the breakthrough curves to the down-gradient boundaries via streamtube modeling are presented in Attachment E5. Note that the tank cross-section is often labeled as BX-HH'. The trench cross-section is often labeled as B-38.

E.3.1 BASE CASE, NO ACTION ALTERNATIVE (CASE 1)

The base case (case 1) simulation investigated solute transport through WMA B-BX-BY considering natural surface infiltration, with no water line leaks and no interim surface barriers, but with a closure barrier at year 2040. The closure barrier degrades after 500 years. (Table E.1 shows recharge rates used in these simulations). This simulation was initialized using a steady-flow solution defined by the upper surface recharge rate of 100 mm/yr and a specified flux in the unconfined aquifer. Ambient flow in the saturated zone was from west to east. For uranium-238, the value of the partition coefficient (Kd) was 0.6 ml/g, and was used to determine the partitioning between the solid (sorbed) and aqueous phases for uranium-238. Inventories of the three species were initialized using a laterally uniform distribution pattern. Plot-file output for this simulation were generated at years 2000, 2010, 2040, 2100, 2200, 2300, 2400, 2540, 2600, 2800, and 3000 and include values for the saturation (i.e., θ/θ_s, where θ is the moisture content and θ_s is the saturated moisture content), aqueous pressure head, moisture content, and concentrations for the three solute species. The moisture field for these simulations remains unchanged from the initial steady-flow field until the year 2040, when the closure barrier becomes effective.

The saturation field is dependent on the surface recharge, hydrologic parameters, soil distribution, and impermeable structures (e.g., single-shell tanks). The saturation fields for the BX-108 to BX-102 cross-section with 100 mm/yr of meteoric recharge are shown in Figure E1.1, Attachment E1. In Figure E1.1 (a), the initial saturation field shows the impacts of the tanks on the moisture content distribution in the subsurface. For example, higher than ambient saturations occur above and between the tanks and lower than ambient saturations occur just below the tanks. In 2040, a closure barrier was assumed to be active, which lowered the meteoric recharge from 100 mm/yr to 0.1 mm/yr. In 2540, assuming some degradation in the closure barrier, the

meteoric recharge was increased to 3.5 mm/yr. The final saturation field at 3000 years is shown in Figure E1.1(b). Due to the reduction in surface recharge, the saturation field dried and the impact of the impermeable tanks on the saturation was reduced. The regions directly beneath the tanks showed lower variability in saturation. The variations in surface recharge had the greatest impact on saturations in the region between tanks within the backfill material and the soils immediately below the bottom level of the tanks. The Plio-Pleistocene unit showed the least amount of change in saturation with the variation in surface recharge, and the water table level showed little variation with the rate of surface recharge.

Color-scaled images of the initial and final solute concentrations for the three mobile species (uranium-238, technetium-99 and nitrate) are shown in Figures E1.2 through E1.4. A comparison of the inventory profiles for aqueous uranium-238 shows that the downward migration of uranium-238 in the subsurface is limited by sorption to the solid phase. Peak concentrations differ by approximately 15% between the initial and final profiles, and are still confined within the vadose zone. By contrast, the technetium-99 and nitrate inventory profiles show significant downward movement. In both contaminant profiles, the initial vertical distributions show multiple peaks, whereas their final distributions show only a single peak. A comparison of peak concentrations and mass balances between initial and final time steps show a reduction of approximately 97% from their initial values for both technetium-99 and nitrate.

Solute mass flux and aqueous concentration breakthrough curves are shown in Attachment E3 for the three solute species (uranium-238, technetium-99, and nitrate). Peak arrival times and peak aqueous concentrations at the first boundary (i.e., cross-section) are summarized in Table E.14. Attachment E5, Tables E5.1 through E5.3 summarize the peak arrival times and peak aqueous concentrations for the BX tank farm east fence line boundary as well as for the two other boundaries (i.e., exclusion boundary and Columbia River) based on the results of the analytical aquifer streamtube mode. See Section E.2.3 for description. The mass flux results and aqueous concentration breakthrough curve results are discussed below for each species.

For the base case, only a small portion (~ 0.2 %) of the uranium-238 inventory has migrated from the vadose zone by the end of the simulation at year 3000. As shown in Attachment E3 Figure E3.1(a), the cumulative uranium-238 inventory that has left the BX tank farm fence line is 6.5×10^9 pCi, compared to an initial inventory of 3.15×10^{12} pCi. Aqueous uranium-238 concentrations are also very low (< 1pCi/L). The initial arrival of low concentrations of uranium-238 at the tank farm boundary does not occur until year 2050 with the peak predicted concentration occurring about 50 years later. The predicted uranium-238 concentrations remain relatively close to the peak concentration for the remainder of the simulation with a slight decreasing trend.

Technetium-99 mass flux and aqueous concentration breakthrough curves are shown in Figure E3.2 in Appendix E3 for the base case. Arrival of the technetium-99 at the BX tank farm fence line occurs shortly after the simulation start due to the location of the initial concentration profile in the vadose zone and simulated non-sorbing behavior of the solute. Almost the entire technetium-99 inventory has migrated from the vadose zone at year 2200, with only residual amounts remaining afterwards. The peak mass flux and concentrations also occurs shortly after the beginning of the simulation. These breakthrough curves have a distinct trimodal shape of

approximately the same magnitude, which is caused by low concentration gap in the initial technetium-99 vadose zone distribution [Figure E1.3 (a)]. Note that the initial spike in the breakthrough curve occurs at year 2000 and is not easily discerned in Figure E3.2.

Nitrate mass flux and aqueous concentration breakthrough curves are shown in Figure E3.3 for the base case. Similar to the predicted technetium-99, the predicted nitrate also arrives quickly at the boundary from the start of the simulation and most of the mass has migrated from the vadose zone by the year 2200. The nitrate breakthrough curves are also trimodal, but the last peak is only about 1/3 the size of the initial peak value. This is also caused by the initial vertical distribution of nitrate in the vadose zone [Figure E1.4 (a)]. Similar to Figure E3.2, the initial spike in the breakthrough curve occurs at year 2000 and is not easily discerned in Figure E3.3.

Table E.14. Peak Concentrations and Arrival Times at the First Boundary for Case 1

Parameter	BX-HH'
Technetium-99	
Arrival Time	Year 2048
Peak Concentration	6.65×10^3 pCi/L
Maximum Initial Concentration [a]	1.92×10^5 pCi/L
Uranium-238	
Arrival Time	Year 2149
Peak Concentration	0.85 μg/L
Maximum Initial Concentration	1.4×10^6 μg/L
Nitrate	
Arrival Time	Year 2012
Peak Concentration	3.69×10^4 μg/L
Maximum Initial Concentration	8.92×10^6 μg/L

[a] Maximum initial concentration is based on inventory data (Section E.2.4.3) and listed for comparison with the simulated peak concentration at the boundary.

E.3.2 BARRIER ALTERNATIVE AND NO WATER LINE LEAKS (CASE 2)

The barrier alternative and no water line leaks (case 2) simulation investigated solute transport through the BX tank farms considering natural surface infiltration, with no water line leaks and closure barrier at year 2040. This simulation differs from the base case simulation in that an interim surface barrier was implemented between the years 2010 and 2040. This simulation was initialized using a steady-flow solution defined by the upper surface recharge rate of 100 mm/yr and a specified flux in the unconfined aquifer. Inventories of the three contaminant species were initialized using the laterally uniform distribution pattern as in the base case scenario. Plot-file output for this simulation were generated for the same output times as the base case and include the same variables. The initial moisture field for these simulations remained unchanged from the initial steady-flow until the year 2010, when the interim barrier becomes effective.

The steady-flow saturation field for the BX-108 to BX-102 tank cross-section with 100 mm/yr of meteoric recharge and interim barrier is shown in Figure E1.1. In Attachment E1 Figure E1.5, the final saturation field shows that the interim barrier has a similar moisture content distribution [Figure E1.1(b)] as in the base case.

The aqueous concentration distributions for all three contaminant species are shown in Figures E1.6 and E1.7. Changes in the vertical migration are similar for all of the solutes. At year 3000, the vertical movement is approximately 10 feet smaller than shown by the inventory profiles of the base case scenario.

Predicted solute mass flux and aqueous concentration breakthrough curves are shown for case 2 in Figures E3.4 through E3.6 for uranium-238, technetium-99, and nitrate. While the initial arrival of all of the solutes in case 2 are similar to the base case until about 2050, the reduced recharge from the interim barrier has a significant impact on the solute mass flux and aqueous concentrations after this time. The cumulative mass of uranium-238 that has left the vadose zone is approximately one order of magnitude less than the base case by the end of the simulation (although the amount is very low in both cases). The uranium-238 concentrations, while low in this case, show a continuous increase throughout the entire simulation period with the peak concentration occurring at the end.

The peak arrival times and concentrations for technetium-99 and nitrate are earlier and lower in the interim barrier case relative to the base case. This is due to the initial inventory distribution, which shows high concentrations of both technetium-99 and nitrate near the water table. The barrier has little effect on the initial breakthrough because the contaminants have already migrated to the water table before the lower infiltration rates have become effective at that depth. For the inventory present in the upper part of the vadose zone, the interim barrier has a significant impact on contaminant transport. While both the technetium-99 and nitrate breakthrough curves were distinctly trimodal in the base case, the reduced recharge caused by the interim barrier has eliminated the third, slightly higher peak.

Peak arrival times and peak aqueous concentrations at the first boundary (i.e., cross-section) are summarized in Table E.15. Attachment E5 Tables E5.1 through E5.3 summarize the peak arrival times and peak aqueous concentrations for the BX tank farm east fence line boundary as well as for the two other boundaries (i.e., exclusion boundary and Columbia River). It should noted that a cursory glace at Table E.16 may be deceptive in assessing the impact of the interim barrier on technetium-99 concentrations given the earlier arrival time and with a similar concentration compared to the base case (Table E.14). Both simulations yield very similar results up to about year 2025. Afterwards, the base case then has an additional, slightly higher technetium-99 peak at 2048. The reduced recharge of the interim barrier case eliminated the last peak.

Table E.15. Peak Concentrations and Arrival Times at the First Boundary for Case 2

Parameter	BX-HH'
Technetium-99	
Arrival Time	Year 2015
Peak Concentration	6.58×10^3 pCi/L
Maximum Initial Concentration [a]	1.92×10^5 pCi/L
Uranium-238	
Arrival Time	Year 2999
Peak Concentration	9.96E-02 µg/L
Maximum. Initial Concentration	1.4×10^6 µg/L
Nitrate	
Arrival Time	Year 2012
Peak Concentration	3.69×10^4 µg/L
Maximum Initial Concentration	8.92×10^6 µg/L

[a] Maximum initial concentration is based on inventory data (Section E.2.4.3) and listed for comparison with the simulated peak concentration at the boundary.

E.3.3 NO INTERIM BARRIER AND WATER LINE LEAK OF 1 GPM FOR 20 YEARS (CASE 3)

The no barrier and water line leak (case 3) simulation investigated solute transport through the BX tank farm cross-section considering natural surface infiltration and a closure barrier at year 2040. This simulation differs from the base case simulation in that a water line leak occurs east of tank BX-102 at the level of the top surface of the tank. The water line leak was modeled as a point source (1 gallon per minute over a 20 year period) spread over a 9.15-m (30-ft) diameter. This simulation was initialized using a steady-flow solution defined by the upper surface recharge rate of 100 mm/yr and a specified flux in the unconfined aquifer. Inventories of the three species were initialized using the laterally uniform distribution pattern. Plot-file output for these simulations were generated at years 2000, 2010, 2020, 2030, 2040, 2100, 2200, 2300, 2400, 2540, 2600, 2800, and 3000, and include values for the saturation, aqueous pressure head, moisture content, and concentrations for the three solute species.

Preliminary simulations showed that the water line leak caused a rapid migration of contaminants. Hence, the domain for this simulation was extended 30.5 m (100 ft) (Figures E1.8 through E1.10). In this way, the contaminants were able to migrate laterally without coming into contact with the boundary.

The flow environment following the leak event is shown in Figure E1.8 (a) at year 2020, and the final saturation distribution is shown in Figure E1.8 (b), year 3000. After 20 years, Figure E1.8 (a) demonstrates a significantly higher saturation distribution relative to the base case. The region to the east of tank BX-102 and the area beneath it, are nearly fully saturated.

An increase in saturation is also noted between the tanks, with larger areas of higher saturations relative to the base case. This indicates that flow from the water line leak has also migrated to the drier areas beneath the tanks. However, after 1000 years, Figure E1.8 (b) shows that despite the fact that the leaked water has descended into the domain, the final saturation distribution is similar to that of the base case shown in Figure E1.1 (b).

Significant differences in the inventory profiles relative to the base case are noted in the color-scaled images of the final solute concentrations for uranium-238, technetium-99, and nitrate (Figures E1.9 and E1.10). The most notable effect of the water line leak is in the location of all three contaminant species. For example, Figure E1.9, shows that uranium-238 is concentrated near 122 m (400 ft), showing significantly more lateral movement relative to the base case. Both technetium-99 and nitrate (Figure E1.10) show similar migration patterns, and have migrated even further than uranium-238.

The transport of the mobile species in the upper region of the vadose zone out of the model domain is delayed because of the shift in the hydraulic gradient that pushes the plumes upgradient of the exit boundary. For the mobile species located in the lower region of the vadose zone, their transport is accelerated relative to the base case due to increased saturations. Because uranium-238 sorbs to subsurface materials, it is less affected by the shift in hydraulic gradient.

Peak arrival times and peak aqueous concentrations at the first boundary (i.e., cross-section) are summarized in Table E.16. Attachment E5 Tables E5.1 through E5.3 summarize the peak arrival times and peak aqueous concentrations for the BX tank farm east fence line boundary as well as for the two other boundaries (i.e., exclusion boundary and Columbia River).

Predicted solute mass flux and aqueous concentration breakthrough curves are shown for case 3 in Figures E3.7 through E3.9 for uranium-238, technetium-99, and nitrate. The large volume of water discharged in this simulation resulted in this case having the highest solute mass flux and concentrations than any of the other cases. The peak concentrations were also much earlier, even for uranium-238. Peak concentrations for uranium-238 were in excess of four orders of magnitude greater than for the base case and occurred earlier in the simulation. Additionally, more than 85% of the uranium-238 inventory had migrated from the vadose zone at year 2030. For technetium-99, the peak concentrations were 20 times greater than for the base case and occurred within the first few years of the simulation. Similarly for nitrate, peak concentrations occurred within a few years of the start of the simulation and were 14 times greater than for the base case.

Table E.16. Peak Concentrations and Arrival Times at the First Boundary for Case 3

Parameter	BX-HH'
Technetium-99	
Arrival Time	Year 2002
Peak Concentration	1.40×10^5 pCi/L
Maximum Initial Concentration [(a)]	1.92×10^5 pCi/L
Uranium-238	
Arrival Time	Year 2008
Peak Concentration	2.31×10^4 µg/L
Maximum Initial Concentration	1.4×10^6 µg/L
Nitrate	
Arrival Time	Year 2002
Peak Concentration	5.06×10^5 µg/L
Maximum Initial Concentration	8.92×10^6 µg/L

[(a)] Maximum initial concentration is based on inventory data (Section E.2.4.3) and listed for comparison with the simulated peak concentration at the boundary.

E.3.4 NO BARRIER AND WATER LINE LEAK OF 200,000 GALLONS OVER 5 DAYS (CASE 4)

The no barrier and water line leak (case 4) simulation investigated solute transport through the BX tank farm cross-section considering natural surface infiltration and a closure barrier at year 2040. Although a larger leak rate occurs in case 4 than in the case 3 water line leak scenario, the quantity of water entering the domain is higher in case 3 (1.05×10^7 gallons over a 20-year period) than in case 4 (2×10^5 gallons over a 5-day period). Similar to case 3, the leak occurs east of tank BX-102, at the level of the top surface of the tank and extended over a 30-foot diameter. This simulation was also initialized using a steady-flow solution defined by the upper surface recharge rate of 100 mm/yr and a specified flux in the unconfined aquifer. Inventories of the three species were initialized using the laterally uniform distribution pattern. Plot-file output for these simulations were generated at years 2000, 2000.01389, 2010, 2020, 2030, 2040, 2100, 2200, 2300, 2400, 2540, 2600, 2800, and 3000, and include values for the saturation, aqueous pressure head, moisture content, and concentrations for the three solute species.

The flow environment following the leak event is shown in Figure E1.11 (a) at year 2000 plus 5 days, and the final saturation distribution is shown in Figure E1.11 (b) at year 3000. After 5 days of simulation, the region east of tank BX-102 is fully saturated, as well as the region above the leak and to the west. This saturation distribution demonstrates that the release of a large volume of water in a short time period can cause ponding to occur, which corresponded to very high values of pressure head. Although ponding may occur with a large water line leak, the lack of drainage permitted by the selected soil properties in this simulation may have caused an

inadequate migration of the excess leak water. Because water ponded up against the upper boundary of the domain, it migrated in a westwardly direction above the tank domains. Contrary to the 1 gpm leak case over a 20-year time period (case 3), a shift in hydraulic gradient did not occur in the region beneath the tank bottoms.

After 1000 years of simulation, Figure E1.8 (b) and Figure E1.11 (b) show that the region beneath tank BX-102 and to the east the saturations are nearly identical to the final saturation distribution for the base case. Although a large volume of water was input into the system, it occurred over a relatively short time period, and with time, drained from the system.

The shape of the final concentration distributions for each of the contaminants shown in Figures E1.12, E1.13(a), and E1.13(b) is similar to those for the base case [Figures E1.2(b), E1.3(b), and E1.4(b)]. However, increase in saturations has caused a slightly accelerated transport out of the domain. For example, in the year 3000, peak nitrate concentrations decrease by nearly 50%, whereas the peak technetium-99 concentrations decrease by 60%. The leak water effect on uranium-238 is less notable because of its sorption to the sediments.

Peak arrival times and peak aqueous concentrations at the first boundary (i.e., cross-section) are summarized in Table E.17. Attachment E5 Tables E5.1 through E5.3 summarize the peak arrival times and peak aqueous concentrations for the BX tank farm east fence line boundary as well as for the two other boundaries (i.e., exclusion boundary and Columbia River).

Predicted solute mass flux and aqueous concentration breakthrough curves are shown for case 4 in Figures E3.10 through E3.12 for uranium-238, technetium-99, and nitrate. The simulated pressure heads for water line leak scenarios were large due to the high water flux rate specified resulting in a complete saturation of the upper zone and an extensive lateral spreading. While the peak concentrations for all three solutes are greater than those for the base case, they are still significantly smaller than the values predicted for the other water leak case (i.e., case 3).

For uranium-238 in case 4, the peak concentrations are 3.5 times the base case, but the percentage of uranium-238 inventory that has migrated from the vadose zone is still very low (less than 0.5% of the initial specified value). The technetium-99 and nitrate peaks are also trimodal, but for both solutes, the second peak is narrower and about 2.5 times higher than for the base case. The final technetium-99 and nitrate peaks are about the same value as in the base case.

Table E.17. Peak Concentrations and Arrival Times at the First Boundary for Case 4

Parameter	BX-HH'
Technetium-99	
Arrival Time	Year 2007
Peak Concentration	1.67×10^4 pCi/L
Maximum Initial Concentration [a]	1.92×10^5 pCi/L
Uranium-238	
Arrival Time	Year 2075
Peak Concentration	2.99 μg/L
Maximum. Initial Concentration	1.4×10^6 μg/L
Nitrate	
Arrival Time	Year 2006
Peak Concentration	1.05×10^5 μg/L
Maximum Initial Concentration	8.92×10^6 μg/L

[a]Maximum initial concentration is based on inventory data (Section E.2.4.3) and listed for comparison with the simulated peak concentration at the boundary.

E.3.5 ALTERNATE INVENTORY DISTRIBUTION AND NO INTERIM BARRIER (CASE 5)

The alternate inventory distribution and no barrier (case 5) simulation investigated solute transport through the BX tank farm considering natural surface infiltration, with no water line leaks, and a closure barrier at year 2040. This simulation differs from the base case simulation in that the initial concentration distribution was shifted so that it was centered between tanks BX-105 and BX-102. This simulation was initialized using a steady-flow solution defined by the upper surface recharge rate of 100 mm/yr and a specified flux in the unconfined aquifer. Plot-file output for these simulations were generated at years 2000, 2010, 2040, 2100, 2200, 2300, 2400, 2540, 2600, 2800, and 3000, and include values for the saturation, aqueous pressure head, moisture content, and concentrations for the three solute species. The moisture field for these simulations remains unchanged from the initial steady-flow field until the year 2040, when the closure barrier becomes effective.

In general, the saturations immediately beneath the tanks are lower than the saturations in the region east of tank BX-102, whereas the saturations between the tanks are generally higher as shown in the initial saturation field in Figure E1.1 (a). However, the depth of the saturation increases is limited, and thus has only a minor effect on the concentration profiles shown in Figures E1.14 through E1.16. For all three contaminants, the shape of the contaminant plumes in the year 3000 differs from those of the base case due to the differences in the saturation distributions. Peak concentrations also differ between the two cases due to dilution effects. For uranium-238, the effect is most pronounced, whereas for technetium-99 and nitrate the impact is not as great because they are distributed at a greater depth in the subsurface.

Peak arrival times and peak aqueous concentrations at the first boundary (i.e., cross-section) are summarized in Table E.18. Attachment E5 Tables E5.1 through E5.3 summarize the peak arrival times and peak aqueous concentrations for the BX tank farm east fence line boundary as well as for the two other boundaries (i.e., exclusion boundary and Columbia River).

Predicted solute mass flux and aqueous concentration breakthrough curves are shown for case 5 in Figures E3.13 through E3.15 for uranium-238, technetium-99, and nitrate. For case 5, the uranium-238 peak concentration was approximately half of the base case and the initial arrival time was similar. Peak concentrations for technetium-99 and nitrate were about 10% lower than for the base case with similar shapes and arrival times. The technetium-99 and nitrate pulses had slightly longer tailing.

Based solely on distance to various boundaries, it was expected that the arrival times for all three contaminants would be longer than those of the base case. However, the areas beneath the tank farm in the alternate concentration profile and the base case profile differ in their initial saturation distribution. As shown in Figure E1.1(a), saturations are higher between tanks BX-105 and BX-102 than the area east of tank BX-102. This causes greater mobility of the contaminants and a similarity in the initial breakthrough times relative to the base case. Because of shadowing beneath the tanks, the saturations are lower in these regions, which decreases contaminant mobility. Thus, tailing is longer for the mobile species relative to the base case.

Table E.18. Peak Concentrations and Arrival Times at the First Boundary for Case 5

Parameter	BX-HH'
Technetium-99	
Arrival Time	Year 2017
Peak Concentration	5.79×10^3 pCi/L
Maximum Initial Concentration [a]	2.209×10^5 pCi/L
Uranium-238	
Arrival Time	Year 2284
Peak Concentration	0.422 µg/L
Maximum Initial Concentration	1.42×10^6 µg/L
Nitrate	
Arrival Time	Year 2000
Peak Concentration	3.46×10^4 µg/L
Maximum Initial Concentration	9.33×10^6 µg/L

[a]Maximum initial concentration is based on inventory data (Section E.2.4.3) and listed for comparison with the simulated peak concentration at the boundary.

E.3.6 ALTERNATE INVENTORY DISTRIBUTION WITH INTERIM BARRIER (CASE 6)

The alternate inventory distribution and barrier (case 6) simulation investigated solute transport through the BX tank farms considering natural surface infiltration, an interim barrier, with no water line leaks, and a closure barrier at year 2040. This simulation differs from the base case simulation in that an interim surface barrier was implemented between the years 2010 and 2400, and a shifted distribution was used for the initial inventory. Similar to case 5, the alternate inventory distribution shifted the initial inventory of the base case so that it was centered between tanks BX-105 and BX-102. This simulation was initialized using a steady-flow solution defined by the upper surface recharge rate of 100 mm/yr and a specified flux in the unconfined aquifer. Plot-file output for this simulation were generated at years 2000, 2010, 2040, 2100, 2300, 2400, 2540, 2600, 2800, and 3000, and include values for the saturation, aqueous pressure head, moisture content, concentrations for the three solute species. The moisture field for these simulations remains unchanged from the initial steady-flow field until the year 2010, when the interim barrier becomes effective.

The steady-flow saturation field for the BX-108 to BX-102 cross-section with 100 mm/yr of meteoric recharge and interim barrier is the same as case 2 and is shown in Figure E1.6. As previously discussed, the final saturation field in Figure E1.6 shows the saturation distribution is similar to that for the base case. For all three contaminants, shown in Figures E1.17 and E1.18, the concentrations are higher than in case 5 (alternate inventory, no interim barrier). For example, peak aqueous concentration for uranium-238 is increased by 12% relative to that for case 5, whereas a two-fold increase in peak concentration occurs for nitrate, and a greater than three-fold increase for technetium-99. These differences in peaks occur because the interim barrier has caused a reduction in the water flux through the vadose zone. Contrary to case 2 results, the depth at which the mobile species are present at year 3000 is similar to the case with no interim barriers. For relatively immobile phases, however, there is a delay in the vertical migration of sorbed uranium-238 (Figure E1.17) by approximately 10 feet.

Peak arrival times and peak aqueous concentrations at the first boundary (i.e., cross-section) are summarized in Table E.19. Attachment E5 Tables E5.1 through E5.3 summarize the peak arrival times and peak aqueous concentrations for the BX tank farm east fence line boundary as well as for the two other boundaries (i.e., exclusion boundary and Columbia River).

Predicted solute mass flux and aqueous concentration breakthrough curves are shown for case 6 in Figures E3.17 through E3.18 for uranium-238, technetium-99, and nitrate. For case 6, the uranium-238 peak concentration and mass flux were more than an order of magnitude lower than for the base case. Technetium-99 and nitrate peak concentrations were about 10% less than for the base case. The third peaks noticeable in the base case were not present for the mobile solutes and the second pulse had longer tailing. The remaining inventory at the end of the simulation was about 10% of the initial inventory for technetium-99, and about 15% for nitrate.

Similar to case 2, the interim barrier has little affect on the initial breakthrough because the contaminants have already entered the water table before the reduced recharge rate has impacted their transport. While the initial arrival times and shapes of the breakthrough curves for the solutes for case 6 were similar to case 2, the predicted concentrations were lower. This occurs

because the higher saturations between tanks BX-105 and BX-102 dilute the contaminant concentrations more than in the area east of tank BX-102. Concentrations were about 10% lower than in case 2 for technetium-99 and nitrate, and approximately 33% lower for uranium-238.

Table E.19. Peak Concentrations and Arrival Times at the First Boundary for Case 6

Parameter	BX-HH'
Technetium-99	
Arrival Time	Year 2017
Peak Concentration	5.78×10^3 pCi/L
Maximum Initial Concentration [(a)]	1.42×10^6 pCi/L
Uranium-238	
Arrival Time	Year 2999
Peak Concentration	0.06 µg/L
Maximum Initial Concentration	1.089×10^5 µg/L
Nitrate	
Arrival Time	Year 2000
Peak Concentration	2.46×10^4 µg/L
Maximum Initial Concentration	9.62×10^6 µg/L

[(a)]Maximum initial concentration is based on inventory data (Section E.2.4.3) and listed for comparison with the simulated peak concentration at the boundary.

E.3.7 BASE CASE WITH 50 MM/YR METEORIC RECHARGE (CASE 7)

The base case with 50 mm/yr meteoric recharge simulation investigated solute transport through the BX cross-section considering natural surface infiltration, with no water line leaks and no interim surface barriers, but with a closure barrier at year 2040. This simulation, along with cases 1, 8, and 9, form a sensitivity study on the effect of the initial meteoric recharge rate on the migration of solutes to various boundaries. The simulation in this case was initialized using a steady-flow solution defined by the upper surface recharge rate of 50 mm/yr and a specified flux in the unconfined aquifer. Inventories of the three species were initialized using the same laterally uniform distribution pattern as in the base case. Plot-file output for these simulations were generated at years 2000, 2010, 2040, 2100, 2300, 2400, 2540, 2600, 2800, and 3000, and include values for the saturation, aqueous pressure head, moisture content, and concentrations for the three solute species. The moisture field for these simulations remains unchanged from the initial steady-flow field until the year 2040, when the closure barrier becomes effective.

The steady-flow saturation field for the BX-108 to BX-102 cross-section with 50 mm/yr of meteoric recharge is shown in Figure E1.19(a). The saturation field shows a significant variation from that of the 100 mm/yr meteoric recharge case [Figure E1.1 (a)]. The most notable impact is in the region beneath the tanks, in the H1 gravelly sand, where on average, the saturations are

5 to 10% lower than in the base case. There is also a reduction in saturation in the H2 sand unit just beneath the tanks, although to a lesser extent. The saturation distribution shown in Figure E1.19(b) after 1000 years is similar to the base case (Figure E1.1 (b)).

Peak arrival times and peak aqueous concentrations at the first boundary (i.e., cross-section) are summarized in Table E.20. Attachment E5 Tables E5.1 through E5.3 summarize the peak arrival times and peak aqueous concentrations for the BX tank farm east fence line boundary as well as for the two other boundaries (i.e., exclusion boundary and Columbia River).

Changes in the peak initial concentrations (Table E.20) are a result of the lower initial moisture content. Significant changes in the final peak concentrations are apparent in Figures E1.20 and E1.21. The peak technetium-99 and nitrate concentrations were increased four fold and two fold, respectively, whereas uranium-238 peak solute concentrations increased by 8%. The corresponding change in the total uranium-238 peak concentration profile was 13%, because when lower saturations occur in the subsurface, the greater the partitioning onto the sorbed phase, which retards even further the vertical migration of the uranium-238 plume.

Predicted solute mass flux and aqueous concentration breakthrough curves are shown for case 7 in Figures E3.19 through E3.21 for uranium-238, technetium-99, and nitrate. Peak concentrations and mass fluxes for uranium-238 are approximately an order of magnitude lower than for the base case due to the reduced recharge rate. The initial arrival of uranium-238 also occurred at a slightly later time. The predicted peak concentrations for the cross-section and fence line average concentrations for technetium-99 and nitrate (Tables E5.2 and E5.3, Attachment E5) occur during the first year of the simulation. This is due to the initial inventory distribution, which contained high concentrations of both technetium-99 and nitrate in the vadose zone and near the water table. These values are only about 10% less than the peak concentrations reported for the base case, and corresponded to the initial spike at year 2000 in the breakthrough curves.

A comparison of the breakthrough curves for this simulation with the base case shows that reducing the recharge rate has a significant impact on the last peak of the curves but little effect on the first peak. For example, in the base case, the first peak that occurs in year 2000 is lower than the two subsequent peaks. In case 7, however, the peak concentrations for technetium-99 and nitrate are significantly reduced (by approximately half of the value of the base case) after the initial peak value occurs in year 2000. Although the breakthrough curve for the nitrate base case was trimodal, the third peak for nitrate is absent in this simulation. Because the effect of the reduced recharge rate is only seen at later times due to the initial contaminant distribution in the vadose zone, only the second peaks of the breakthrough curves are reported in Attachment E5 Tables E5.2 and E5.3 so that the effect of reduced meteoric recharge can be made. For both technetium-99 and nitrate, a greater inventory remained within the domain at the end of the simulation (< 10% for technetium-99 and 5% for nitrate).

Table E.20. Peak Concentrations and Arrival Times at the First Boundary for Case 7

Parameter	BX-HH'
Technetium-99	
Arrival Time	Year 2028
Peak Concentration	3.59×10^3 pCi/L
Maximum Initial Concentration [a]	2.11×10^6 pCi/L
Uranium-238	
Arrival Time	Year 2999
Peak Concentration	0.11 μg/L
Maximum Initial Concentration	1.49×10^6 μg/L
Nitrate	
Arrival Time	Year 2023
Peak Concentration	2.01×10^4 μg/L
Maximum Initial Concentration	8.92×10^6 μg/L

[a] Maximum initial concentration is based on inventory data (Section E.2.4.3) and listed for comparison with the simulated peak concentration at the boundary.

E.3.8 BASE CASE WITH 30 MM/YR METEORIC RECHARGE (CASE 8)

The base case with 30 mm/yr meteoric recharge simulation investigated solute transport through the BX tank cross-section considering natural surface infiltration, with no water line leaks and no interim surface barriers, but with a closure barrier at year 2040. These simulations, along with those from cases 1, 7, and 9, form a sensitivity study on the effect of meteoric recharge on the migration of solutes to various boundaries. The simulations in this case were initialized using a steady-flow solution defined by the upper surface recharge rate of 30 mm/yr and a specified flux in the unconfined aquifer. Inventories of the three species were initialized using the laterally uniform distribution pattern from the base case scenario. Plot-file output for these simulations were generated at years 2000, 2010, 2040, 2100, 2300, 2400, 2540, 2600, 2800, and 3000, and include values for the saturation, aqueous pressure head, moisture content, and concentrations for the three solute species. The moisture field for these simulations remains unchanged from the initial steady-flow field until the year 2040, when the closure barrier becomes effective.

The steady-flow saturation field for the BX-108 to BX-102 cross-section with 30 mm/yr of meteoric recharge is shown in Figure E1.22 (a). Again, the saturation field shows a significant variation from that of the 100 mm/yr meteoric recharge case [Figure E1.1 (a)]. Most notable is the overall reduction in saturation and the increase in shadowing beneath the tanks. Lowering the initial meteoric recharge to 30 mm/yr resulted in a continuation of the trend established in lowering the recharge from 100 to 50 mm/yr. For example, peak initial concentrations (Tables E.16 and E.17) show that a decrease in saturation increases the initial aqueous concentrations. As expected, the plume movement is retarded with respect to the 100 mm/yr and 50 mm/yr recharge cases.

Peak arrival times and peak aqueous concentrations at the first boundary (i.e., cross-section) are summarized in Table E. 21. Attachment E5 Tables E5.1 through E5.3 summarize the peak arrival times and peak aqueous concentrations for the BX tank farm east fence line boundary as well as for the two other boundaries (i.e., exclusion boundary and Columbia River).

Predicted solute mass flux and aqueous concentration breakthrough curves are shown for case 8 in Figures E3.22 through E3.24 for uranium-238, technetium-99, and nitrate. Peak concentrations and mass fluxes for uranium-238 are approximately 1.5 orders of magnitude lower than the base case due to the reduced recharge rate. The initial arrival of uranium-238 was slightly later with the peak concentration occurring at the end of the simulation. The estimated peak cross-section and fence line average concentrations for technetium-99 and nitrate (Tables E5.2 and E5.3) occur during the first year of the simulation. This is due to the initial inventory distribution, which contained high concentrations of both technetium-99 and nitrate in the vadose zone near the water table. These values are only about 10% less than the peak concentrations reported for the base case, and correspond to the initial spike at year 2000 in the breakthrough curves.

A comparison of the breakthrough curves for this simulation with the base case shows that reducing the recharge rate even further has a significant impact on the last peak of the curves. Similar to the other reduced recharge cases, the peak concentrations for technetium-99 and nitrate are significantly reduced after the initial peak value occurs in year 2000. For example, these pulses occur later and are of a longer duration. Peak concentrations for technetium-99 and nitrate were about one third of their initial values and arrived much later than the base case. Whereas a 50% reduction in recharge was sufficient to eliminate the last peak for only nitrate in case 7, the 70% reduction in recharge in this simulation also eliminated the final peak for technetium-99. Because the effect of the reduced recharge rate is only seen at later times due to the initial contaminant distribution in the vadose zone, only the second peaks of the breakthrough curves are reported in Attachment E5 Tables E5.2 and E5.3 so that the effect of reduced meteoric recharge can be seen. For both solutes, these later pulses were more spread out in time, and a substantial quantity of technetium-99 and nitrate inventory remained at the end of the simulation (18% for technetium-99 and 15% for nitrate).

Table E.21. Peak Concentrations and Arrival Times at the First Boundary for Case 8

Parameter	BX-HH'
Technetium-99	
Arrival Time	Year 2043
Peak Concentration	2.27×10^3 pCi/L
Maximum Initial Concentration [a]	2.24×10^6 pCi/L
Uranium-238	
Arrival Time	Year 2999
Peak Concentration	0.025 µg/L
Maximum Initial Concentration	1.54×10^6 µg/L
Nitrate	
Arrival Time	Year 2036
Peak Concentration	1.26×10^4 µg/L
Maximum Initial Concentration	1.02×10^7 µg/L

[a]Maximum initial concentration is based on inventory data (Section E.2.4.3) and listed for comparison with the simulated peak concentration at the boundary.

E.3.9 BASE CASE WITH 10 MM/YR METEORIC RECHARGE (CASE 9)

The base case with 10 mm/yr meteoric recharge simulation investigated solute transport through the BX-108 to BX-102 tank cross-section considering natural surface infiltration, with no water line leaks and no interim surface barriers, but with a closure barrier at year 2040. This simulation, in conjunction with cases 1, 7, and 8, form a sensitivity study on the effect of meteoric recharge on the migration of solutes to various boundaries. The simulations in this case were initialized using a steady-flow solution defined by the upper surface recharge rate of 10 mm/yr and a specified flux in the unconfined aquifer. Inventories of the three species were initialized using the same laterally uniform distribution pattern used in the base case. Plot-file output for these simulations were generated at years 2000, 2010, 2040, 2100, 2300, 2400, 2540, 2600, 2800, and 3000, and include values for the saturation, aqueous pressure head, moisture content, and concentrations for the three solute species. The moisture field for these simulations remains unchanged from the initial steady-flow field until the year 2040, when the closure barrier becomes effective.

The steady-flow saturation field for the BX cross-section with 10 mm/yr of meteoric recharge is shown in Figure E1.25 (a). Compared to the steady-flow saturation fields for 100, 50, and 30 mm/yr [Figures E1.1 (a), E1.19 (a), and E1.22 (a)], the saturation field at 10 mm/yr shows only a small amount of shadowing from the tanks and only a slight moisture increase between the tanks. As in the other reduced recharge cases, the saturation distribution at 3000 years [Figure E1.25 (b)] is similar to that for the base case.

Peak arrival times and peak aqueous concentrations at the first boundary (i.e., cross-section) are summarized in Table E.22. Attachment E5 Tables E5.1 through E5.3 summarize the peak arrival times and peak aqueous concentrations for the BX tank farm east fence line boundary as well as for the two other boundaries (i.e., exclusion boundary and Columbia River).

Peak inventory concentrations in Tables E.20 and E.21 show that a decrease in saturation increases aqueous concentrations. However, for case 9, contrary to the other reduced recharge cases, the plumes are more elongated and the delay in vertical movement more pronounced even for the mobile contaminants. For the sorbed uranium-238, the vertical migration of the plume is delayed even more than in the other reduced recharge cases.

Predicted solute mass flux and aqueous concentration breakthrough curves are shown for case 9 in Figures E3.25 through E3.27 for uranium-238, technetium-99, and nitrate. For this very low initial recharge case, the predicted uranium-238 mass flux and concentrations were more than three orders of magnitude lower than for the base case. Initial uranium-238 arrivals were much later than for the base case and the peak concentration occurred toward the end of the simulation. This is due to the initial inventory distribution, which contained high concentrations of both technetium-99 and nitrate in the vadose zone near the water table. These values are only about 10% less than the peak concentrations reported for the base case, and corresponded to the initial spike at year 2000 in the breakthrough curves.

Similar to the other reduced recharge cases, the peak concentrations for technetium-99 and nitrate are significantly reduced after the initial peak value occurs in year 2000. A comparison of the breakthrough curves for this simulation with the base case and the other reduced recharge cases (cases 7 and 8) shows that arrival times are delayed and longer tailing results with a further reduction in recharge. Excluding the initial spike of contaminant that occurs due to the high concentration zone near the water table, the peak concentrations of technetium-99 and nitrate were about 10% of the values for the base case. Because the effect of the reduced recharge rate is only seen at later times due to the initial contaminant distribution in the vadose zone, only the second peaks of the breakthrough curves are reported in Attachment E5 Tables E5.2 and E5.3 so that the effect of reduced meteoric recharge can be seen. A substantial quantity of technetium-99 and nitrate inventory also remained in the vadose zone at the end of the simulation (50% for technetium-99 and 30% for nitrate).

Table E.22. Peak Concentrations and Arrival Times at the First Boundary for Case 9

Parameter	BX-HH'
Technetium-99	
Arrival Time	Year 2109
Peak Concentration	8.33×10^2 pCi/L
Maximum Initial Concentration [a]	2.52×10^6 pCi/L
Uranium-238	
Arrival Time	Year 2999
Peak Concentration	3.72×10^{-4} µg/L
Maximum Initial Concentration	1.61×10^6 µg/L
Nitrate	
Arrival Time	Year 2091
Peak Concentration	4.65×10^3 µg/L
Maximum Initial Concentration	1.16×10^7 µg/L

[a] Maximum initial concentration is based on inventory data (Section E.2.4.3) and listed for comparison with the simulated peak concentration at the boundary.

E.3.10 BASE CASE WITH Kd = 0.1 mL/g FOR URANIUM-238 (CASE 10)

The base case with a Kd = 0.6 ml/g for uranium-238 investigated solute transport through the BX-108 to BX-102 tank cross-section considering natural surface infiltration, with no water line leaks and no interim surface barriers, but with a closure barrier at year 2040. This simulation, in conjunction with cases 1 and 11, form a sensitivity study on the effect of the magnitude of the partitioning coefficient on the migration of uranium-238 to various boundaries. The simulations in this case were initialized using a steady-flow solution defined by the upper surface recharge rate of 100 mm/yr and a specified flux in the unconfined aquifer. Inventories of the three species were initialized using the same laterally uniform distribution pattern used in the base case. Plot-file output for these simulations were generated at years 2000, 2010, 2040, 2100, 2300, 2400, 2540, 2600, 2800, and 3000, and include values for the saturation, aqueous pressure head, moisture content, and concentrations for the three solute species. The moisture field for these simulations remains unchanged from the initial steady-flow field until the year 2040, when the closure barrier becomes effective.

Color-scaled images of the initial and final aqueous concentrations for uranium-238 are shown in Figure E1.28. As expected, a comparison of the inventory profiles shows that when the Kd value is reduced from 0.6 to 0.1 ml/g, the downward migration of uranium-238 in the subsurface is accelerated. Initial aqueous phase uranium-238 concentrations are higher than those in the base case. With less uranium-238 present in the sorbed phase, the aqueous concentrations of uranium-238 increase. For example, peak aqueous phase uranium-238 concentrations differ by approximately 200% relative to the base case. The increased mobility of uranium-238 with a lower Kd results in uranium-238 exiting the modeled domain at a faster rate.

Peak arrival times and peak aqueous concentrations at the first boundary (i.e., cross-section) are summarized in Table E.23. Attachment E5 Tables E5.1 through E5.3 summarize the peak arrival times and peak aqueous concentrations for the BX tank farm east fence line boundary as well as for the two other boundaries (i.e., exclusion boundary and Columbia River).

Predicted solute mass flux and aqueous concentration breakthrough curves are shown for case 10 in Figure E3.28 for uranium-238. The lower Kd value for uranium-238 in case 10 results in much more uranium-238 migrating from the vadose zone to the aquifer. While the initial arrival of uranium-238 occurs at about the same time as in the base case, the magnitude of the mass flux and peak concentrations are about 650 times greater in case 10 due to the increased mobility. The predicted breakthrough curves for uranium-238 show a single peak with very long tailing up to the end of the simulation. While there is still a substantial amount of uranium-238 inventory in the vadose zone at the end of the simulation, the simulation predicted that about one-third of the inventory has migrated into the aquifer based on the cumulative mass flux. For both technetium-99 and nitrate, the breakthrough curves were identical to the base case, which is the expected result.

Table E.23. Peak Concentrations and Arrival Times at the First Boundary for Case 10

Parameter	BX-HH'
Technetium-99	
Arrival Time	Year 2048
Peak Concentration	6.65×10^3 pCi/L
Maximum Initial Concentration [(a)]	1.92×10^5 pCi/L
Uranium-238	
Arrival Time	Year 2063
Peak Concentration	544 µg/L
Maximum Initial Concentration	1.42×10^6 µg/L
Nitrate	
Arrival Time	Year 2012
Peak Concentration	3.69×10^4 µg/L
Maximum Initial Concentration	8.92×10^6 µg/L

[(a)] Maximum initial concentration is based on inventory data (Section E.2.4.3) and listed for comparison with the simulated peak concentration at the boundary.

E.3.11 BASE CASE WITH Kd = 1.0 ML/G FOR URANIUM-238 (CASE 11)

The base case with a Kd = 0.6 ml/g for uranium-238 investigated solute transport through the BX-108 to BX-102 tank cross-section considering natural surface infiltration, with no water line leaks and no interim surface barriers, but with a closure barrier at year 2040. This simulation, in conjunction with cases 1 and 10, form a sensitivity study on the effect of the magnitude of the partitioning coefficient on the migration of uranium-238 to various boundaries. The simulations in this case were initialized using a steady-flow solution defined by the upper surface recharge rate of 100 mm/yr and a specified flux in the unconfined aquifer. Inventories of the three species were initialized using the same laterally uniform distribution pattern used in the base case. Plot-file output for these simulations were generated at years 2000, 2010, 2040, 2100, 2300, 2400, 2540, 2600, 2800, and 3000, and include values for the saturation, aqueous pressure head, moisture content, and concentrations for the three solute species. The moisture field for these simulations remains unchanged from the initial steady-flow field until the year 2040, when the closure barrier becomes effective.

Peak arrival times and peak aqueous concentrations at the first boundary (i.e., cross-section) are summarized in Table E.24. Attachment E5 Tables E5.1 through E5.3 summarize the peak arrival times and peak aqueous concentrations for the BX tank farm east fence line boundary as well as for the two other boundaries (i.e., exclusion boundary and Columbia River).

Color-scaled images of the initial and final aqueous concentrations for uranium-238 are shown in Figure E1.29. Again as expected, a comparison of the inventory profiles for uranium-238 shows that when the Kd value is increased from 0.6 to 1.0 ml/g, the downward migration of uranium-238 in the subsurface is retarded. Initial peak aqueous concentrations are lower than in the base case due to a greater partitioning. As expected, peak concentrations of uranium-238 are much lower (Table E.20) than for the base case (Table E.10) due to the slower rate of migration.

Predicted solute mass flux and aqueous concentration breakthrough curves are shown for case 11 in Figure E3.29 for uranium-238. The larger Kd for uranium-238 significantly reduces the amount of uranium-238 migrating from the vadose zone to the aquifer. The initial arrival time of uranium-238 is about the same as in the base case and the concentration increases throughout the simulation. Peak uranium-238 concentrations (Table E.20) are about one-half the peak concentrations predicted for the base case (Table E.10) and occur at the end of the simulation. For both technetium-99 and nitrate, the breakthrough curves were identical to those for the base case, as expected.

Table E.24. Peak Concentrations and Arrival Times at the First Boundary for Case 11

Parameter	BX-HH[a]
Technetium-99	
Arrival Time	Year 2048
Peak Concentration	6.65×10^3 pCi/L
Maximum Initial Concentration [a]	1.92×10^5 pCi/L
Uranium-238	
Arrival Time	Year 2999
Peak Concentration	0.044 µg/L
Maximum Initial Concentration	9.38×10^5 µg/L
Nitrate	
Arrival Time	Year 2012
Peak Concentration	3.69×10^4 µg/L
Maximum Initial Concentration	8.92×10^6 µg/L

[a] Maximum initial concentration is based on inventory data (Section E.2.4.3) and listed for comparison with the simulated peak concentration at the boundary.

E.3.12 TRENCH B-38 WITH 55.4 MM/YR METEORIC RECHARGE (CASE 12)

The trench B-38 simulation investigated solute transport through a cross-section west of tank BX-111, considering natural infiltration only at 55.4 mm/yr, no interim barrier, and a closure barrier by 2010. A 378,000-gal discharge containing a unit inventory distribution for uranium-238 and technetium-99 occurred over the entire width of the trench in 1954. This simulation, in conjunction with case 12, form a sensitivity study on the effect of meteoric recharge on the migration of solutes to the trench fence line. This simulation was initialized using a steady-flow solution defined by the upper surface recharge rate of 55.4 mm/yr and a specified flux in the unconfined aquifer. Ambient flow in the saturated zone was from west to east in the domain. The value of the partition coefficient (Kd) was 0.6 ml/g, and was used to determine the partitioning between the solid (sorbed) and aqueous phases for uranium-238. Plot-file output for these simulations were generated at years 1954, 1955, 2000, 2010, 2110, 2210, 2310, 2410, 2510, 2700, and 3000 and include values for the saturation, aqueous pressure, moisture content, and concentrations for the three solute species.

The saturation field is dependent on the surface recharge, hydrologic parameters, and soil distribution. The steady-flow saturation field in 1954 for the trench B-38 cross-section with 55.4 mm/yr of meteoric recharge is shown in Figure E2.1, Attachment E2. In Figure E2.1, the initial saturation field shows the impacts of the trench structure on the moisture content distribution in the subsurface, as lower than ambient saturations occur at the corners of the trench. In the year 2010, a closure barrier was assumed to be active, which lowered the meteoric

recharge from 100 mm/yr to 0.1 mm/yr. In 2510, assuming some degradation in the closure barrier, the meteoric recharge was increased to 3.5 mm/yr.

The saturation field in year 1955 is shown in Figure E2.2 (a), one year after the 378,000-gal discharge into the trench. Flow from the discharge has migrated nearly 150 feet into the subsurface, as noted by the elevated saturations (> 0.80) in the region beneath the trench. This saturation field contrasts sharply with the final saturation field at year 3000 shown in Figure E2.2 (b). Due to the drainage of the initial discharge, and the reduction in surface recharge caused by the closure barrier, the saturation field has dried. The region directly beneath the trench shows lower variability in saturation.

Color-scaled images of the initial and final solute concentrations for the two species (uranium-238 and technetium–99) are shown in Figures E2.3 through E2.6. The aqueous concentration distribution for uranium-238 (Figure E2.3) show that the vertical migration of uranium-238 is limited significantly by both sorption to the subsurface materials, as well as the closure barrier in 2010. In fact, the majority of the uranium-238 plume is concentrated in the H2 sand and backfill units, and none of the uranium-238 has exited the domain. By contrast, the technetium-99 concentration profiles in Figures E2.4 through E2.6 show that technetium-99 does enter the ground water and migrate from the domain. However, the closure barrier has had a profound effect on technetium-99 migration. As noted in Figure E2.4, the technetium-99 plume is largely concentrated in the H1 gravelly sand unit, and has quickly migrated through the H2 sand unit immediately beneath the trench. With the closure barrier becoming effective in year 2010, Figure E2.5 shows that the technetium-99 transport has been considerably delayed, even at year 2210. At year 3000, much of the technetium-99 is still present in the vadose zone (Figure E2.6).

Peak arrival times and peak aqueous concentrations at the first boundary (i.e., cross-section) are summarized in Table E.25. Attachment E5 Tables E5.1 through E5.3 summarize the peak arrival times and peak aqueous concentrations for the BX tank farm east fence line boundary as well as for the two other boundaries (i.e., exclusion boundary and Columbia River).

Predicted solute mass flux and aqueous concentration breakthrough curves are shown for case 12 in Figures E4.1 and E4.2 for technetium-99 and nitrate. Since this simulation did not predict any uranium-238 migration from the vadose zone for the time period that was simulated, the mass flux and concentration figures for uranium-238 were omitted. For technetium-99 and nitrate, scaled results using the inventories for trench B-38 are shown in Figures E4.3 and E4.4 and scaled results using the inventories for all eight trenches are shown in Figures E4.5 and E4.6.

As noted in Section E2.4, both technetium-99 and nitrate results were scaled from the unit inventory release of a non-sorbing solute. Therefore, the breakthrough curves and relative results for technetium-99 and nitrate are identical. The technetium 99 and nitrate mass flux and concentration breakthrough curves have single peaks at year 2050 and long tails that extend the duration of the simulation (year 3000). The simulation predicted about 40% of the inventory migrated from the vadose zone by the end of the time period.

Table E.25. Peak Concentrations and Arrival Times at the First Boundary for Case 12

Parameter	Trench B-38
Technetium-99	
Arrival Time	Year 2036
Peak Concentration	24.1 pCi/L
Maximum Initial Concentration [a]	5.074×10^6 pCi/L
Uranium-238	
Arrival Time	—
Peak Concentration	—
Maximum Initial Concentration	1.089×10^5 μg/L
Nitrate	
Arrival Time	Year 2036
Peak Concentration	1.73×10^5 μg/L
Maximum Initial Concentration	3.616×10^7 μg/L

[a]Maximum initial concentration is based on inventory data (Section E.2.4.3) and listed for comparison with the simulated peak concentration at the boundary.

E.3.13 TRENCH B-38 WITH 100.0 MM/YR METEORIC RECHARGE (CASE 13)

The second trench B-38 simulation investigated solute transport through a cross-section west of tank BX-111, considering natural infiltration only at 100 mm/yr and no interim barrier, and a closure barrier in 2010. Like the previous trench simulation (case 12), a 378,000-gal leak containing a unit inventory distribution for uranium-238 and technetium-99 occurred over the entire width of the trench in 1954. With the exception of the recharge, all other conditions were the same as in case 12. Plot-file output for this simulation were generated at years 1954, 1955, 2000, 2010, 2110, 2210, 2310, 2410, 2510, 2700, and 3000 and include values for the saturation, aqueous pressure head, moisture content, and concentrations for the three solute species.

The steady-flow saturation field in 1954 for the trench B-38 cross-section with 100 mm/yr of meteoric recharge is shown in Figure E2.7, Attachment E2. Relative to case 12 (55.4 mm/yr meteoric recharge), the increase in meteoric recharge has caused an increase in saturations within all of the geologic units, though there are no significant differences in the water table elevation. Saturations are significantly higher so that the impact of the trench on the moisture content is not noticeable in the saturation distribution. Similar to case 12, the 378,000-gal release in 1954 had a significant impact on the saturation distribution [Figure E2.8 (a), year 1955] by increasing the saturations beneath the trench to greater than 80%. Like case 12, this saturation field contrasts sharply with the final saturation field at year 3000 shown in Figure E2.8 (b). Due to the drainage of the initial discharge and the reduction in surface recharge caused by the closure barrier, the saturation field has dried and shows little variability in saturation.

Peak arrival times and peak aqueous concentrations at the first boundary (i.e., cross-section) are summarized in Table E.26. Attachment E5 Tables E5.1 through E5.3 summarize the peak arrival times and peak aqueous concentrations for the BX tank farm east fence line boundary as well as for the two other boundaries (i.e., exclusion boundary and Columbia River).

Only small differences in the uranium-238 aqueous concentration distribution (Figures E2.9) are noted relative to case 12. Peak concentrations are lower due to dilution, and the increased recharge has caused a subsequent acceleration in uranium-238 transport. However, the vertical migration of uranium-238 is still severely limited and largely confined to the H2 sand unit, even at year 3000.

The technetium-99 concentration profiles shown in Figures E2.10 through E2.12 show a similar pattern to the lower recharge scenario presented in case 12. The implementation of the closure barrier in 2010 significantly delays technetium-99 transport. Relative to case 12, peak concentrations are lower. Transport out of the system is also accelerated due to the increased saturations of the domain.

Predicted solute mass flux and aqueous concentration breakthrough curves are shown for case 13 in Attachment E4 Figures E4.7 and E4.8 for technetium-99 and nitrate. Since this simulation did not predict any uranium-238 migration from the vadose zone for the time period simulated, the mass flux and concentration figures for uranium-238 were omitted. For technetium-99 and nitrate, scaled results using the inventories for trench B-38 are shown in Figures E4.9 and E4.10. Scaled results using the inventories for all eight trenches are shown in Figures E4.11 and E4.12.

As noted in Section E2.4, both technetium-99 and nitrate results were scaled from the unit inventory release of a non-sorbing solute. Therefore, the breakthrough curves and relative results for technetium-99 and nitrate are identical. Due to the increase in recharge, the technetium-99 and nitrate mass flux and concentration breakthrough curves had single peaks that were slightly earlier than those in case 12, and peak concentrations that were more than three times higher. They also had long tailings that extended the duration of the simulation until year 3000. The simulation predicted about 70% of the technetium-99 and nitrate inventory migrated from the vadose zone by the end of the simulation time.

Table E.26. Peak Concentrations and Arrival Times at the First Boundary for Case 13

Parameter	Trench B-38
Technetium-99	
Arrival Time	Year 2025
Peak Concentration	80.8 pCi/L
Maximum Initial Concentration [a]	5.074×10^6 pCi/L
Uranium-238	
Arrival Time	—
Peak Concentration	—
Maximum Initial Concentration	1.089×10^5 µg/L
Nitrate	
Arrival Time	Year 2025
Peak Concentration	5.79×10^5 µg/L
Maximum Initial Concentration	3.616×10^7 µg/L

[a] Maximum initial concentration is based on inventory data (Section E.2.4.3) and listed for comparison with the simulated peak concentration at the boundary.

E.3.14 TRENCH B-38 WITH DELAYED CLOSURE BARRIER AND 100.0 MM/YR METEORIC RECHARGE

The third trench B-38 simulation investigated solute transport through a cross-section west of tank BX-111, considering natural infiltration at 100 mm/yr, no interim barrier, and a closure barrier in the year 2040. In this simulation, the year the closure barrier is emplaced is the same as in BX tank simulations (cases 1 through11). Like the previous trench simulations (cases 12 and 13), a 378,000-gal discharge containing a unit inventory distribution for uranium-238 and technetium-99 occurred over the entire width of the trench in the year 1954. With the exception of the closure barrier implementation in 2040, all other conditions were the same as in case 13. Plot-file output for this simulation were generated at years 1954, 1955, 2000, 2010, 2110, 2210, 2310, 2410, 2510, 2700, and 3000 and include values for the saturation, aqueous pressure head, moisture content, and concentrations for the three solute species.

The final saturation distribution for the trench B-38 cross-section with 100 mm/yr of meteoric recharge and the delayed closure barrier is shown in Figure E2.13. Relative to case 13 (100 mm/yr meteoric recharge and a closure barrier in 2010), the delay in the closure barrier has not had a significant impact on the moisture content distribution. However, the delay has had an effect on solute concentrations and transport. For example, relative to case 13, the uranium-238 plume is more diffuse and has migrated a few feet deeper into the profile as shown in Figure E2.14 for year 3000. For the mobile species such as technetium-99, the effect is more pronounced. Figures E2.15 and E2.16 show that the delay in the closure barrier has accelerated the transport of technetium-99 to the water table. For example, in year 2110 [Figure E2.15 (a)],

the upper boundary of the technetium-99 plume is approximately 160 ft above the water table, whereas in case 13, it is at approximately 180 ft. The effect of the closure barrier, however, is noticeable in both simulations. The upper boundary of the plume in year 3000 for both the delayed closure barrier and case 13 is at 150 ft.

Peak arrival times and peak aqueous concentrations at the first boundary (i.e., cross-section) are summarized in Table E.27. Attachment E5 Tables E5.1 through E5.3 summarize the peak arrival times and peak aqueous concentrations for the BX tank farm east fence line boundary as well as for the two other boundaries (i.e., exclusion boundary and Columbia River).

Predicted solute mass flux and aqueous concentration breakthrough curves are shown for case 14 in Figures E4.13 and E4.14 for technetium-99 and nitrate. Since this simulation did not predict any uranium-238 migration from the vadose zone for the time period simulated, the mass flux and concentration figures for uranium-238 were omitted. Again, for technetium-99 and nitrate, scaled results using the inventories for trench B-38 are shown in Figures E4.15 and E4.16. Scaled results using the inventories for all eight trenches are shown in Figures E4.17 and E4.18.

As noted in Section E2.4, both technetium-99 and nitrate results were scaled from the unit inventory release of a non-sorbing solute. Therefore, the breakthrough curves and relative results for technetium-99 and nitrate are identical. Due to the increase in recharge from the delay in implementation of the closure barrier, the technetium-99 and nitrate mass flux and concentration breakthrough curves had peak concentrations that were more than six times higher than the base case (case 12) and 1.8 times higher than for case 13. This simulation predicted about 92% of the technetium-99 and nitrate inventory migrated from the vadose zone by the end of the simulation period.

Table E.27. Peak Concentrations and Arrival Times at the First Boundary for Case 14

Parameter	Trench B-38
Technetium-99	
Arrival Time	Year 2052
Peak Concentration	149 pCi/L
Maximum Initial Concentration [a]	5.074×10^6 pCi/L
Uranium-238	
Arrival Time	—
Peak Concentration	—
Maximum Initial Concentration	1.089×10^5 µg/L
Nitrate	
Arrival Time	Year 2052
Peak Concentration	1.07×10^6 µg/L
Maximum Initial Concentration	3.616×10^7 µg/L

[a]Maximum initial concentration is based on inventory data (Section E.2.4.3) and listed for comparison with the simulated peak concentration at the boundary.

E.3.15 SOLUTE MASS BALANCE

Mass balance checks were performed on the three solutes (uranium-238, technetium-99, and nitrate) for each simulation case, using the expression shown in Equation (E.10)

$$m_{error} = \frac{m_{initial} - m_{final} - m_{exiting}}{m_{initial}} \qquad \text{(E.10)}$$

where:

m_{error} = the mass balance error, expressed in percent

$m_{initial}$ = the initial solute inventory computed from the STOMP plot-file output at year 2000

m_{final} = the final solute inventory computed from the STOMP plot-file output at year 3000

$m_{exiting}$ = the integrated solute inventory leaving the computation domain, computed from the STOMP surface-flux output.

The initial solute masses were computed by STOMP by integrating the solute concentrations over the flow domain. The solute mass leaving the computational domain through the aquifer was determined using surface-flux output on the eastern side of the domain. The surface-flux output provided both the solute-flux rate and integral. Other than solving the solute mass conservation equations, the STOMP simulator contains no algorithms for correcting local or global mass. Therefore mass balance errors represent the actual mass balance errors from the conservation equations. Mass balance errors, expressed as percent error, were small as shown in Tables E.28, E.29, and E.30 for uranium-238, technetium-99, and nitrate, respectively.

Table E.28. STOMP Mass Balance for Uranium-238

Uranium-238 (pCi) Case	Initial	Final	Exit	% Error
1	4.311E+10	4.302E+10	8.661E+07	2.2E-04
2	4.311E+10	4.310E+10	9.105E+06	2.2E-04
3	4.311E+10	2.089E+08	4.292E+10	-5.0E-02
4	4.311E+10	4.291E+10	1.984E+08	6.3E-05
5	4.311E+10	4.306E+10	4.804E+07	1.3E-04
6	4.311E+10	4.311E+10	4.966E+06	7.9E-05
7	4.311E+10	4.310E+10	9.497E+06	6.6E-06
8	4.311E+10	4.311E+10	1.474E+06	6.0E-05
9	4.311E+10	4.311E+10	1.044E+04	2.1E-04
10	4.311E+10	2.768E+10	1.543E+10	-1.9E-03
11	4.311E+10	4.311E+10	4.416E+06	2.0E-04
12	1.000E+12	1.000E+12	0.000E+00	0.00E+00
13	1.000E+12	1.000E+12	0.000E+00	0.00E+00
14	1.000E+12	1.000E+12	0.000E+00	0.00E+00

Table E.29. STOMP Mass Balance for Technetium-99

Technetium-99 (pCi) Case	Initial	Final	Exit	% Error
1	6.013E+10	8.726E+08	5.926E+10	-5.85E-03
2	6.013E+10	6.167E+09	5.396E+10	3.33E-05
3	6.013E+10	2.235E+03	5.988E+10	4.15E-01
4	6.013E+10	3.394E+08	5.979E+10	1.00E-02
5	6.045E+10	1.683E+09	5.878E+10	-2.39E-02
6	6.045E+10	8.623E+09	5.183E+10	-1.93E-02
7	6.013E+10	4.805E+09	5.533E+10	1.96E-03
8	6.013E+10	1.060E+10	4.953E+10	4.99E-05
9	6.013E+10	2.719E+10	3.294E+10	9.98E-05
10	6.013E+10	8.726E+08	5.926E+10	-5.85E-03
11	6.013E+10	8.726E+08	5.926E+10	-5.85E-03
12	1.000E+12	6.026E+11	3.979E+11	-3.00E-05
13	1.000E+12	3.012E+11	6.993E+11	3.00E-05
14	1.000E+12	8.450E+10	9.160E+11	-2.00E-05

Table E.30. STOMP Mass Balance for Nitrate

Nitrate (μg) Case	Initial	Final	Exit	% Error
1	1.790E+11	6.473E+09	1.722E+11	1.40E-01
2	1.790E+11	2.172E+10	1.571E+11	9.64E-02
3	1.790E+11	1.599E+06	1.773E+11	9.55E-01
4	1.790E+11	3.418E+09	1.754E+11	6.08E-02
5	1.795E+11	9.172E+09	1.704E+11	-1.65E-02
6	1.795E+11	2.678E+10	1.528E+11	-5.31E-02
7	1.790E+11	1.821E+10	1.605E+11	1.46E-01
8	1.790E+11	3.118E+10	1.478E+11	6.70E-04
9	1.790E+11	6.313E+10	1.158E+11	2.23E-04
10	1.790E+11	6.473E+09	1.722E+11	1.40E-01
11	1.790E+11	6.473E+09	1.722E+11	1.40E-01
12	1.000E+09	6.026E+08	3.979E+08	-3.00E-05
13	1.000E+09	3.012E+08	6.993E+08	3.00E-05
14	1.000E+09	8.450E+07	9.160E+08	-2.00E-05

E.4.0 HUMAN HEALTH RISK AND DOSE ESTIMATION APPROACH

This section presents the approach used to estimate human health risk (risk) and dose associated with exposure to contaminants of concern from past waste releases from WMA B-BX-BY.

Risk is used herein to refer to the following:

- Incremental lifetime cancer risk (ILCR), which can occur from exposure to carcinogenic chemicals and radionuclides
- Hazard index, which is a measure of the potential for toxic health effects from exposure to noncarcinogenic chemicals.

Dose is the measure of radioactivity potentially received in a human body.

The interim measures under consideration for WMA B-BX-BY address mitigation of groundwater impacts. The exposure pathways for this risk and dose assessment therefore are based on the groundwater exposure medium. The exposure scenarios used for this assessment are as follows:

- Industrial
- Residential
- Industrial worker
- Residential farmer
- Recreational shoreline user.

Risk and dose associated with the use of groundwater from a hypothetical water supply well was estimated at several downgradient locations over a 1,000-year timeframe. Groundwater contaminant concentration estimates were based on the results of the contaminant transport analysis presented in Section E.3.0.

The risk assessment for this WMA B-BX-BY field investigation report is qualitative at this stage in the corrective action process even though substantial site-specific data have been generated. Qualitative WMA risk evaluations have been performed at the Hanford Site using historical process and characterization data (DOE-RL 1995c; DOE-RL 1996). These qualitative risk evaluations have been used to initially evaluate the applicability and relative effectiveness of interim measures (e.g., eliminate leaking water lines and replace well caps). The risk and dose assessment presented herein also relies on historical process and characterization data but is supplemented with additional site-specific data collected under the *Resource Conservation and Recovery Act of 1976* corrective action program as described in Appendices A and B. The results of this risk and dose assessment are used to support evaluation of potential interim measures or interim corrective measures and to determine the need for additional WMA-specific characterization data.

Procedures for the approach and assumptions necessary to calculate human health risk and dose are described in the following:

- "The Model Toxics Control Act Cleanup Regulation" (WAC 173-340), which implements "Model Toxics Control Act" (MTCA) requirements

- *Hanford Site Risk Assessment Methodology* (HSRAM) (DOE-RL 1995b), which is the risk and dose assessment methodology that the U.S. Department of Energy (DOE), Washington State Department of Ecology (Ecology), and the U.S. Environmental Protection Agency (EPA) have agreed to use to support Hanford Site cleanup decisions.

The WAC 173-340 implementing regulations define exposure scenarios and input parameters for two types of site uses: unrestricted (MTCA Method B) and industrial (MTCA Method C). Both the Method B and C exposure scenarios include potential consumption of groundwater. The Method B exposure scenario essentially assumes residential use; the scenario has been used in risk assessments of the Hanford Site 100 Areas to represent unrestricted land use (DOE-RL 1995a). The Method C exposure scenario has been applied for site-specific decisions at the Hanford Site in the 300 Area (Ecology 2001).

Under MTCA, risk assessment requirements for nonradioactive contaminants stipulate that carcinogenic risks shall be less than 1.0×10^{-6} (1.0×10^{-5} for multiple contaminants) for Method B and 1.0×10^{-5} for Method C. Also, concentrations of individual noncarcinogenic contaminants that pose acute or chronic toxic effects to human health shall not exceed a hazard quotient of 1.0. The MTCA risk criteria apply only to nonradioactive contaminants. The EPA guidance indicates that action is generally warranted when the cumulative carcinogenic risk is greater than 1×10^{-4} or the cumulative noncarcinogenic hazard index exceeds 1.0. Carcinogenic risks below 1×10^{-6} or hazard indices less than 1.0 are regarded as 'points of departure' below which no action is required. DOE orders require that groundwater protection standards be consistent with federal and Washington State requirements (i.e., EPA and Ecology requirements).

Dose assessments are based on HSRAM (DOE-RL 1995b). Four exposure scenarios are defined by the HSRAM to estimate radiation doses to hypothetical future members of the public: agricultural, residential, industrial, and recreational. The four HSRAM exposure scenarios were developed for the Hanford Site to facilitate evaluation of risk related to *Comprehensive Environmental Response, Compensation, and Liability Act of 1980* (CERCLA) remedial investigations and *Resource Conservation Recovery Act* (RCRA) facility investigations. Groundwater transport was the primary exposure pathway considered in this analysis.

The primary dose limit specified by DOE Order 435.1 includes the DOE primary dose limit of 100 mrem effective dose equivalent (EDE) in a year applied to a hypothetical future member of the public. This all-pathways dose to the maximally exposed offsite individual is calculated for 1000 years at points on the Hanford Site that a future member of the public could access. The point of access nearest the waste disposal sites in the future is defined by the boundary (Figure E.10). The dose constraint is defined as 30 mrem EDE in a year to the maximally exposed offsite individual for 1000 years in DOE Order 435.1 and ensures that no single source, practice, or pathway accounts for an extraordinary portion of the primary dose limit.

Figure E.10. Hypothetical Receptor Locations for Risk Evaluation

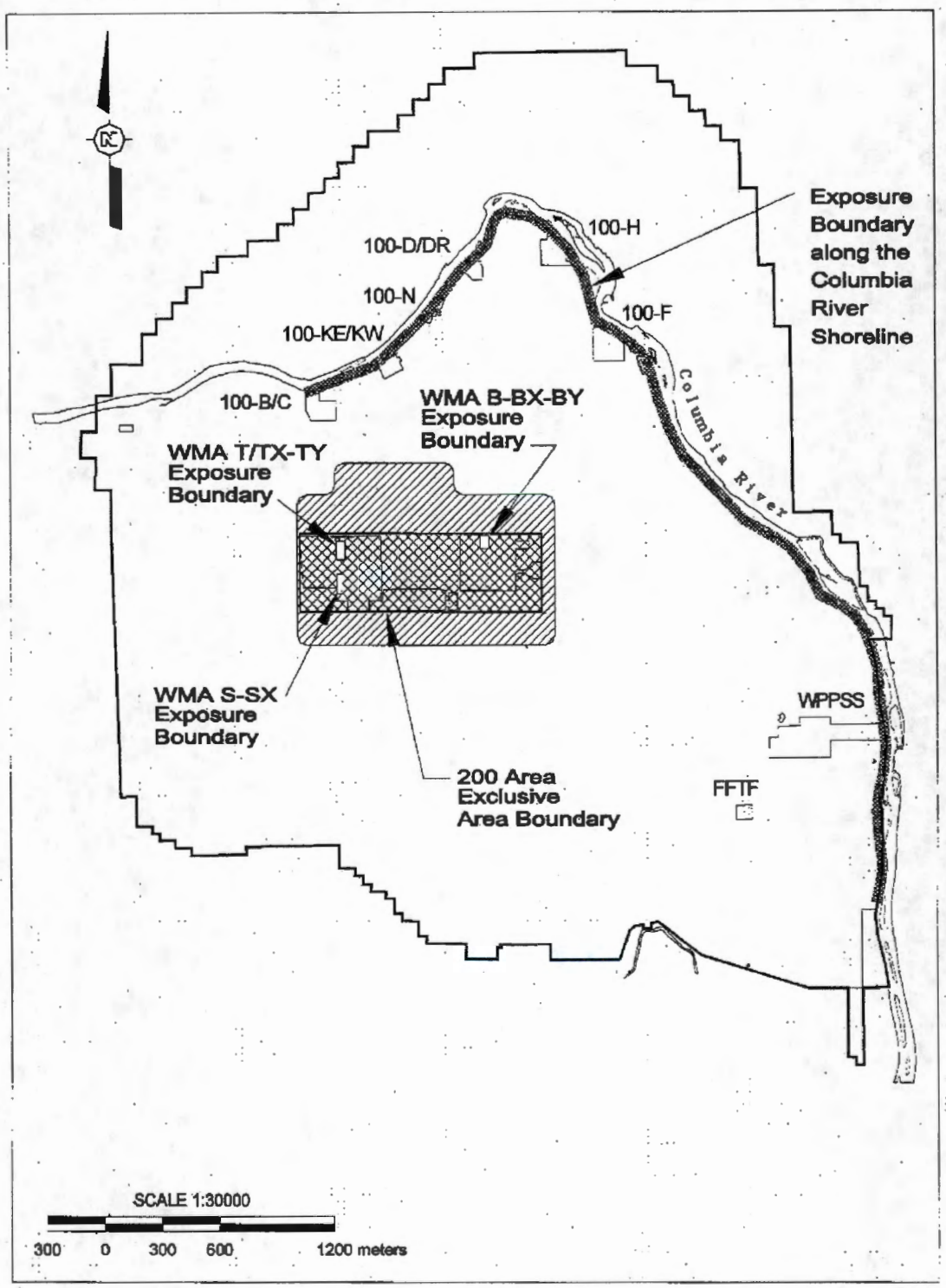

E.4.1 RECEPTOR SCENARIO RATIONALE

Current land use planning assumptions are documented in *Final Hanford Comprehensive Land-Use Plan Environmental Impact Statement* (DOE 1999), which provides an evaluation of several land uses for the Hanford Site for the next 50 years. That environmental impact statement and associated "Hanford Comprehensive Land-Use Plan Environmental Impact Statement (HCP EIS), Hanford Site, Richland, Washington; Record of Decision (ROD)" (64 FR 61615) identify 'industrial-exclusive use' as the planned use for the 200 Areas Central Plateau, an area that encompasses the 200 East and 200 West Areas. Ecology is evaluating how the DOE land use planning efforts fit within the Ecology cleanup framework. Ecology has not yet agreed to an industrial use scenario. Therefore, multiple exposure scenarios are considered in the WMA B-BX-BY risk assessment to account for the uncertainty of long-term Hanford Site land use.

As shown in *Phase 1 RCRA Facility Investigation/Corrective Measures Study Work Plan for Single-Shell Tank Waste Management Areas* (DOE-RL 2000), DOE and Ecology have agreed to use MTCA Methods B and C in the corrective action program. MTCA Methods B and C risks are calculated based on equations and parameters specified in the MTCA protocol for establishing groundwater cleanup levels (WAC 173-340-720). Risk is calculated for the residential farmer, industrial worker, and recreational shoreline user exposure scenarios based on the HSRAM. Estimates of risk based on the three HSRAM exposure scenarios are provided in this assessment to allow for comparison to risks cited in *Tank Waste Remediation System, Hanford Site, Richland, Washington, Final Environmental Impact Statement* (TWRS EIS) (DOE and Ecology 1996), *Retrieval Performance Evaluation Methodology for the AX Tank Farm* (DOE-RL 1999), and *Field Investigation Report for Waste Management Area S-SX* (Knepp 2002). Risk calculations for the three HSRAM-based scenarios use groundwater pathway unit risk factors adapted without modification directly from the TWRS EIS.

Three hypothetical receptor locations identified by DOE and Ecology (DOE-RL 2000) as the locations for which potential risk and dose will be calculated are as follows:

- Downgradient at the BX tank farm east fence line boundary
- Downgradient at the boundary of the 200 Area exclusion zone as defined by the Hanford Future Site Uses Working Group (FSUWG 1992)
- Downgradient at the Columbia River shoreline.

E.4.1.1 Residential Exposure Scenario (MTCA Method B)

The MTCA cleanup standards are applicable only to nonradioactive constituents. Under the Method B groundwater cleanup level protocol, exposure to hazardous and carcinogenic chemicals is based solely on ingestion of drinking water (with an inhalation correction factor used for volatile chemicals). Method B exposures for noncarcinogenic health effects are based on a drinking water intake rate of 1 L/day (0.2 gal/day) and an average body weight of 16 kg (35 lb) (WAC 173-340-720(3)(a)(ii)(A)). Method B exposures for carcinogenic health effects are based on a drinking water intake rate of 2 L/day (0.5 gal/day), an average body weight of 70 kg (150 lb), an exposure duration of 30 years, and a lifetime of 75 years

(WAC 173-340-720(3)(a)(ii)(B)). Oral reference doses (mg/kg-day) and oral slope factors (kg-day/mg) developed by the EPA are applied to convert the exposures to the health effect appropriate for each constituent.

For the BX tank farm boundary, risk is calculated at one location axis corresponding to the cross-section through tanks BX-108 to BX-102 considered in the contaminant transport analysis. Method B risk is calculated at all locations as defined in Section E.4.1.

E.4.1.2 Industrial Exposure Scenario (MTCA Method C)

As in the MTCA Method B residential exposure scenario, the MTCA Method C industrial exposure scenario is applicable only to nonradioactive constituents. Under the Method C groundwater cleanup level protocol, exposure to hazardous and carcinogenic chemicals is based solely on ingestion of drinking water (with an inhalation correction factor used for volatile chemicals). Method C exposures for noncarcinogenic health effects are based on a drinking water intake rate of 2 L/day (0.5 gal/day) and an average body weight of 70 kg (150 lb) (WAC 173-340-720(4)(b)(ii)(A)). Method C exposures for carcinogenic health effects are based on a drinking water intake rate of 2 L/day (0.5 gal/day), an average body weight of 70 kg (150 lb), an exposure duration of 30 years, and a lifetime of 75 years (WAC 173-340-720(4)(b)(ii)(B)). Oral reference doses (mg/kg-day) and oral slope factors (kg-day/mg) developed by the EPA are applied to convert the exposures to the health effect appropriate for each constituent.

Method C risk is calculated for the same three locations as defined in Section E.4.1.

E.4.1.3 Industrial Worker Scenario

An industrial worker scenario consistent with the scenario described in HSRAM (DOE-RL 1995b) is used to represent potential exposure to workers in a commercial or industrial setting. The receptors are adult employees assumed to work at a location for 20 years. A body weight of 70 kg (150 lb) and a lifetime of 70 years are assumed. The scenario involves mainly indoor activities, although outdoor activities (e.g., soil contact) also are included. The groundwater exposure pathways for this scenario include drinking water ingestion (1 L/day [0.2 gal/day]), dermal absorption during showering, shower water ingestion, and inhalation. These exposures would not be continuous because the worker would go home at the end of each workday (i.e., after 8 hours). The scenario is intended to represent nonremediation workers who are assumed to wear no protective clothing.

Industrial worker risk is evaluated using a unit risk factor approach consistent with that used for the TWRS EIS (DOE and Ecology 1996), DOE-RL (1999) and Knepp (2002) analyses. This approach involves calculating risk as the product of the groundwater concentration and the unit risk factor. The basic expression for risk using a unit risk factor approach is:

$$R_{x,y,t} = \sum C^{i}_{x,y,t} \cdot URF^{i}_{S} \qquad \text{(E.11)}$$

Where:

$R_{x,y,t}$ = risk at point of calculation x,y,t

$C^i_{x,y,t}$ = groundwater concentration at point of calculation x,y,t for contaminant i
URF^i_S = groundwater unit risk factor for contaminant i and receptor scenario S
x,y = horizontal location coordinates
t = time.

The summation in Equation E.11 represents addition of the contributions from all constituents. The unit risk factors used for the three HSRAM-based exposure scenarios are shown in Table E.31. These unit risk factors are for the groundwater pathway and are taken from the risk analysis presented in the TWRS EIS. These unit risk factors were also used in DOE-RL (1999) and Knepp (2002).

Industrial worker risk is calculated for the same three locations as defined in Section E.4.1.

Table E.31. Unit Risk Factors for the Industrial Worker, Residential Farmer, and Recreational Shoreline User Scenarios

Contaminant of Concern	Units	Industrial Worker[a]	Residential Farmer[b]	Recreational Shoreline User[c]
C-14	ILCR per Ci/mL	5.23E+06	6.06E+08	8.70E+05
Se-79	ILCR per Ci/mL	3.22E+07	2.87E+08	5.36E+06
Tc-99	ILCR per Ci/mL	7.11E+06	2.61E+08	1.18E+06
I-129	ILCR per Ci/mL	9.33E+08	1.29E+10	1.55E+08
U-232	ILCR per Ci/mL	7.83E+08	3.00E+09	9.98E+07
U-233	ILCR per Ci/mL	3.03E+08	1.38E+09	4.42E+07
U-234	ILCR per Ci/mL	3.00E+08	1.34E+09	4.38E+07
U-235	ILCR per Ci/mL	2.98E+08	1.37E+09	4.40E+07
U-236	ILCR per Ci/mL	2.85E+08	1.27E+09	4.15E+07
U-238	ILCR per Ci/mL	2.84E+08	1.28E+09	4.18E+07
Cr	HQ per g/mL	3.31E+06	1.14E+07	3.47E+05
F	HQ per g/mL	1.65E+05	1.61E+06	2.27E+04
Hg	HQ per g/mL	3.85E+07	8.36E+08	4.85E+06
NO_3	HQ per g/mL	6.20E+03	7.59E+06	8.52E+02
NO_2	HQ per g/mL	9.92E+03	3.73E+04	1.36E+03
U (Total)	HQ per g/mL	3.52E+06	1.41E+07	4.66E+05
EDTA	HQ per g/Ml	7.61E+06	1.47E+09	1.05E+06

[a] Source = TWRS EIS, Appendix D, Tables D.2.1.21 and D.2.1.23 (groundwater pathway)
[b] Source = TWRS EIS, Appendix D, Tables D.2.1.18 and D.2.1.20 (groundwater pathway)
[c] Source = TWRS EIS, Appendix D, Tables D.2.1.24 and D.2.1.26 (groundwater pathway)
ILCR = incremental lifetime cancer risk
HQ = hazard quotient

E.4.1.4 Residential Farmer Scenario

A residential farmer scenario is used to represent exposures associated with the use of the land for residential and agricultural purposes. This scenario is a slight modification to the residential scenario described in HSRAM (DOE-RL 1995b); it includes all of the exposure pathways for the residential scenario plus most of the food ingestion pathways described in the HSRAM agricultural scenario. The residential farmer scenario includes using groundwater for drinking water (ingestion rate of 2 L/day [0.5 gal/day]) and other domestic uses as well as for irrigation to produce and consume animals, vegetables, and fruit products. The exposures are assumed to be continuous and include occasional shoreline related recreational activities, which includes contact with surface water sediments. A composite adult is used as the receptor for some of the exposure pathways. The composite adult is evaluated using child parameters for 6 years and adult parameters for 24 years, with total exposure duration of 30 years. Body weights of 16 kg (35 lb) for a child and 70 kg (150 lb) for an adult and a lifetime of 70 years are assumed.

Residential farmer risk is evaluated using a unit risk factor approach as discussed for the industrial worker scenario in Section E.3.1.3. The unit risk factors used are shown in Table E.31.

Residential farmer risks are calculated for the same three locations as defined in Section E.4.1.

E.4.1.5 Recreational Shoreline User Scenario

A recreational shoreline user scenario consistent with the scenario described in the HSRAM is used to represent exposure to contamination in groundwater seeps along the Columbia River shoreline from recreational swimming, boating, and other shoreline activities. The scenario involves outdoor activities and occurs only in an area within 400 m (0.25 mi) of the river shoreline. These exposures would not be continuous but would occur for 14 days a year for 30 years. Exposure to both adults and children are taken into account using the same composite adult as described in the residential farmer scenario in Section E.4.1.4.

Recreational shoreline user risk is evaluated using a unit risk factor approach as described in the industrial worker scenario in Section E.4.1.3. The unit risk factors used are shown in Table E.31. Recreational shoreline user risks are calculated only at the downgradient Columbia River shoreline location that is defined in Section E.4.1.

The recreational land user scenario is not included in the WMA B-BX-BY risk assessment because this receptor does not have access to the groundwater pathways.

E.4.2 TANK WASTE CONSTITUENTS OF POTENTIAL CONCERN

Determination of the constituents of potential concern (CoPCs) to be used in the WMA B-BX-BY risk assessment starts with the estimated inventory released from the tank farm system to the environment. That estimated inventory is provided in *Preliminary Inventory Estimates for Single-Shell Tank Leaks in B, BX, and BY Tank Farms* (Jones et al. 2001). The CoPCs listed in Jones et al. (2001) include the analytes listed in the model cited in *Hanford Defined Wastes: Chemical and Radionuclide Compositions* (Agnew 1997). The following sections provide the rationale used to exclude some of these CoPCs from calculations of human health risk and dose in the WMA B-BX-BY risk assessment. Because not all of the constituents associated with the

released tank waste will migrate to the groundwater, the constituents of concern in a groundwater pathway must be selected. The rationale for making this constituents selection is provided in the following sections.

E.4.2.1 Rationale for Excluding Constituents of Potential Concern

Following are the criteria used to exclude CoPCs from consideration in the WMA B-BX-BY risk assessment.

- **Constituents having distribution coefficients (Kd) equal or greater than 0.6.** *Composite Analysis for Low-Level Waste Disposal in the 200 Area Plateau of the Hanford Site* (Kincaid et al. 1998) provides reference to distribution coefficient selection used in previous studies and for past tank leaks. *Hanford Immobilized Low-Activity Tank Waste Disposal Performance Assessment: 2001 Version* (Mann et al. 2001), along with Kincaid et al. (1998), provide rationale for selection of CoPCs for risk calculations. Numerical modeling results provided in the TWRS EIS indicate that constituents with distribution coefficients equal to or greater than 1.0 take over 1,000 years to reach the vadose zone/saturated zone interface. Numerical modeling of past tank leaks for S tank farm retrieval performance evaluation (Crass 2001) and for DOE-RL (1999) indicate that within 1,000 years, constituents with distribution coefficients equal to or greater than 0.6 would not reach the underlying aquifer or would reach the underlying aquifer at very low concentrations (less than 3.0×10^{-2} pCi/L) that would not contribute to significant human health risks (less than 4.0×10^{-8} ILCR for the residential farmer scenario) using base case recharge estimates as shown in Table E.1.

  CoPCs eliminated because of the distribution coefficient criterion are: aluminum, iron, bismuth, lanthanum, zirconium, lead, nickel, manganese, plutonium (total), nickel-59, nickel-63, cobalt-60, strontium-90, yttrium-90, zirconium-93, niobium-93m, cadmium-113m, tin-126, cesium-134, cesium-137, barium-137, samarium-151, europium-152, europium-154, europium-155, radium-226, radium-228, plutonium series, americium series, curium series, and thorium-232.

- **Low-activity radionuclides that are present in low concentrations and with short half-lives if they have decayed for at least five half-lives.** A decay time of 5 half-lives is sufficient for decay of 96.9% of the radionuclide activity and results in a reduced level of potential risk (EPA 1995). Based on numerical modeling results provided in the TWRS EIS, constituents with distribution coefficients of 0 take 150 years to reach the vadose zone/saturated zone interface under normal recharge.

  Additional CoPCs eliminated because of the half-life criterion are ruthenium-106, antimony-125, and tritium.

- **Constituents that have no documented human health risk or toxicity factors.** The basis for these factors is documented in the *Integrated Risk Information System* (EPA 2002a) or the *User's Guide: Radionuclide Carcinogenicity* (EPA 2002b) databases. A constituent lacking a toxicity reference dose or a carcinogenic slope factor is eliminated.

CoPCs eliminated because of the health effects criterion are: carbonate, chloride, calcium, hydroxide, potassium, phosphate, strontium, sulfate, silica, and sodium.

Although several organic chemicals are listed in the Agnew (1997) model, only EDTA (ethylene-diamine-tetraacetic acid) was carried forward because it is the only constituent that has a reference dose. All others were not listed in the Integrated Risk Information System (EPA 2002a).

E.4.2.2 Contaminants of Potential Concern for Risk Assessment

The CoPCs to be used in the WMA B-BX-BY risk assessment after applying the exclusion criteria described in Section E.4.2.1 are:

- Chemicals: chromium, fluoride, mercury, nitrate, nitrite, uranium (total), and EDTA
- Radionuclides: carbon-14, selenium-79, technetium-99, iodine-129, and uranium series.

E.4.3 ESTIMATING TOTAL INCREMENTAL LIFETIME CANCER RISK AND HAZARD INDEX

The total ILCR for a particular receptor scenario at a particular point in time and space is expressed as the sum of the ILCR calculated for the individual carcinogenic chemical and radionuclide CoPCs. Note that because none of the chemical CoPCs identified in Section E.4.2.2 is classified as carcinogenic, ILCR values for this assessment are based only on radionuclide exposures. Although hexavalent chromium is classified as carcinogenic by inhalation, carcinogenic impacts from hexavalent chromium would apply only for airborne releases from a facility, or for suspension of surface contamination. Because groundwater is the only exposure medium considered in this assessment, neither of these exposure routes applies and hexavalent chromium is treated as an ingestion toxicant. As for the total ILCR, the total hazard index is expressed as the sum of the hazard quotients calculated for the individual noncarcinogenic chemical CoPCs. Total ILCR and hazard index values are calculated for each receptor scenario and point of calculation for the 1,000-year period of analysis used in the contaminant transport simulations.

Risks for CoPCs included in the contaminant transport analysis (i.e., technetium-99, uranium-238, and nitrate) are based on the modeled groundwater concentrations. Risks for CoPCs not included in the contaminant transport analysis are based on scaled groundwater concentrations. Scaling is performed by multiplying the non-modeled CoPC source inventories (as reported in Jones et al. 2001) by the ratio of the modeled groundwater concentration to source inventory for one of the modeled CoPCs. The basis for the scaling calculations is shown in Table E.32.

Table E.32. Basis for Scaled Groundwater Concentrations

Simulated CoPC	Non-simulated CoPC Ratioed from Simulated CoPC
Tc-99	C-14, Se-79, I-129
U-238	U-232, U-233, U-234, U-235, U-236, U (Total), Cr
NO_3	NO_2, Hg, F, EDTA

E.4.4 DOSE METHODOLOGY

Radionuclide doses are calculated as the product of the groundwater concentration and a unit dose factor. The unit dose factors used are groundwater pathway unit dose factors provided in Kincaid et al. (1998) and Knepp (2002). Unit dose factors are shown in Table E.33. Dose calculations are performed only for the industrial worker exposure scenario. Exposure pathways and parameters associated with this scenario are described in Section E.4.1.3.

Table E.33. Industrial Worker Scenario Groundwater Unit Dose Factors

Constituent	Unit	Unit Dose Factor
C-14	(mrem/yr)/(pCi/L)	5.22E-04
Se-79	(mrem/yr)/(pCi/L)	2.17E-03
Tc-99	(mrem/yr)/(pCi/L)	3.65E-04
I-129	(mrem/yr)/(pCi/L)	6.90E-02
U (Total)	(mrem/yr)/(ug/L)	5.27E-02

Source = Kincaid et al. (1998)

Industrial worker dose is calculated at the three locations as defined in Section E.4.1.

E.5.0 HUMAN HEALTH RISK AND DOSE RESULTS

This section presents the results of the human health risk and dose assessment. The risk and dose values presented are based on the groundwater concentrations generated through contaminant transport modeling (Sections E.2.0 and E.3.0) and were calculated using the approach described in Section E.4.0. Groundwater concentration values from the cross-section at the BX tank farm east fence line boundary used Equation E.9 in Section E.3.0 to calculate the risk and dose values with the methodology described in Section E.4.0. Note that risk and dose results are presented only for a select group of simulation cases (Table E.34). Results for these cases are representative of the larger set of cases considered in the contaminant transport analysis and include information on the impacts associated with existing conditions (case 1), interim barrier use (case 2), and variable meteoric recharge rates (cases 7 and 8).

Table E.34. Human Health Risk and Dose Assessment Cases

Case	Description	Rationale
1	Base case (no action alternative)	Reference case. Estimation of impacts from past contaminant releases at WMA B-BX-BY if no interim measures or interim corrective measures were implemented.
2	Barrier alternative and no water line leaks	Interim corrective measure case. Estimation of degree to which implementation of an interim surface barrier would decrease impacts from past contaminant releases at WMA B-BX-BY.
7	Base case with 50 mm/yr meteoric recharge	Meteoric recharge sensitivity cases. Estimation of degree to which meteoric recharge modeling assumptions affect estimated base case impacts from past contaminant releases at WMA B-BX-BY.
8	Base case with 30 mm/yr meteoric recharge	

Section E.5.5 presents the conclusions of risk and dose results. Risk and dose results for the four cases shown in Table E.34 are presented individually in Sections E.5.1 through E.5.4. As discussed in Section E.4.1, multiple exposure scenarios are considered in this assessment to account for the uncertainty of long-term Hanford Site land use. To simplify the presentation, the individual case discussions focus on the results for the industrial worker scenario. Results for all the receptor scenarios are provided in table format for each case; however, for comparison purposes, a single scenario is sufficient because the relationship between the receptor scenarios remains relatively consistent within each case. For example, regardless of the case or calculation point, the peak residential farmer ILCR is always approximately 34 times higher than the peak industrial worker ILCR, and the MTCA Method B peak hazard index is always approximately 2.2 times higher than the MTCA Method C peak hazard index. Conclusions of the risk and dose calculations are presented in Section E.6.0.

E.5.1 BASE CASE, NO ACTION ALTERNATIVE (CASE 1)

Results for the base case (case 1) are summarized in Table E.35. Results for case 1 reveal two general trends that are also evident in the results for the other cases considered (cases 2, 7, 8). First, peak human health risk values for the cross-section at the BX tank farm east fence line

boundary exceed the peak values for the other two downgradient boundaries. Second, peak values at the last downgradient boundary (i.e., the Columbia River shoreline) are generally two to three orders of magnitude lower than the peak values at the BX tank farm east fence line boundary.

Peak values for case 1 are the highest of the four cases considered. Between the BX tank farm east fence line boundary and the Columbia River shoreline, the peak industrial worker ILCR ranges from 5.39×10^{-5} to 2.34×10^{-7}. Peak ILCR values are driven by technetium-99. The peak industrial worker hazard index ranges from 1.98×10^{-1} to 4.88×10^{-4}. Peak hazard index values are driven by nitrate. The peak dose ranges from 3.18 mrem/yr to 1.38×10^{-2} mrem/yr. Peak dose values are driven by technetium-99.

Temporal variations in ILCR for case 1 are shown in Figure E.11 for calculation locations between the BX tank farm east fence line boundary and the Columbia River shoreline. Temporal variations in hazard index and dose for case 1 are similar to those shown for ILCR. The results for the BX tank farm east fence line boundary and 200 Area exclusion boundary, display a bimodal character in the vicinity of the peak. In both cases, the maximum peak occurs in the second of the two high points. The peak at the BX tank farm east fence line boundary occurs in the year 2048 and the peaks for the 200 Area exclusion boundary and Columbia River shoreline calculation locations arrive after approximately 40 and 250 years, respectively (i.e., years 2098 and 2298).

Figure E.11. Case 1 Industrial Worker ILCR Versus Time at Calculation Points Between the BX Tank Farm East Fence Line Boundary and the Columbia River

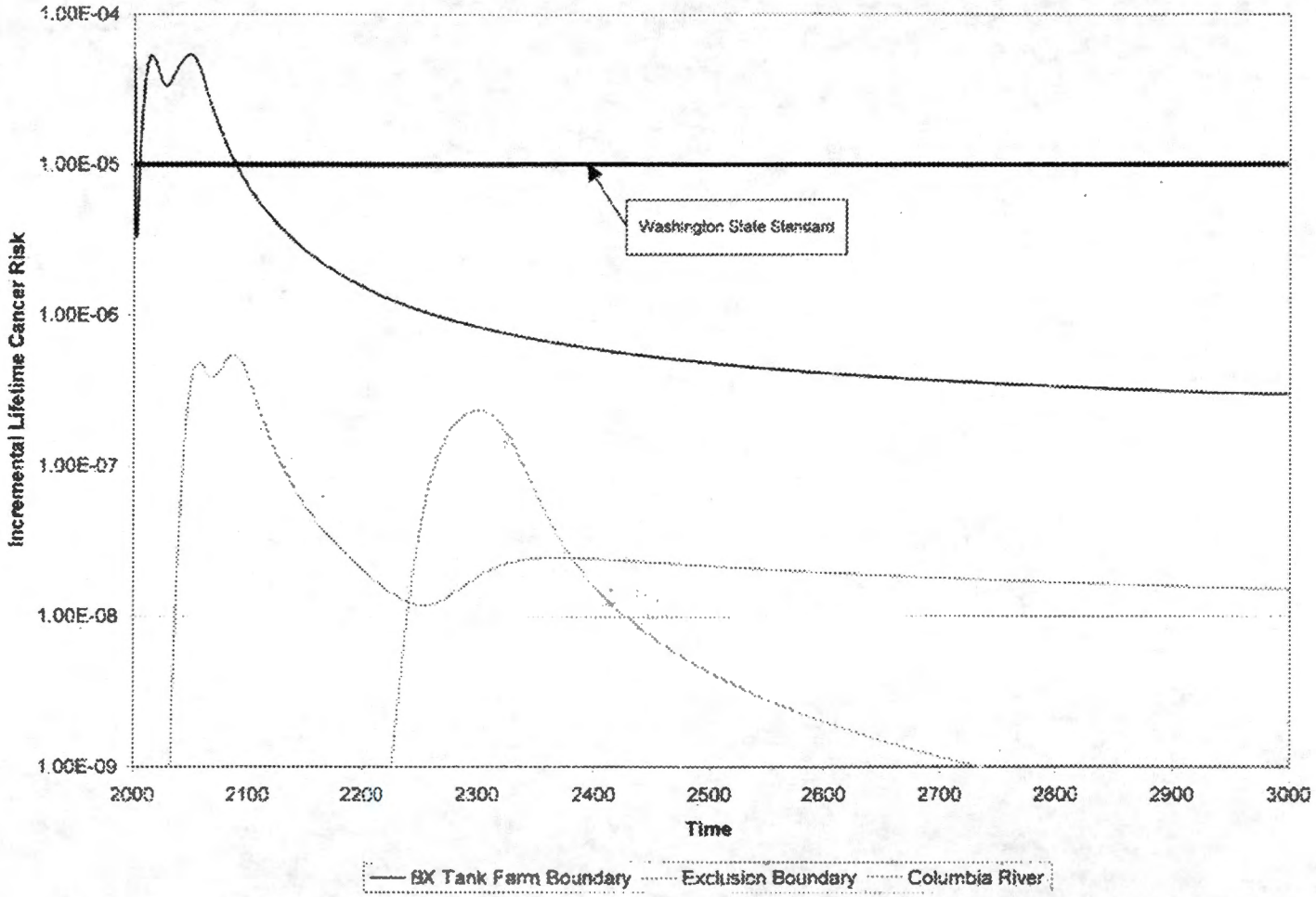

Table E.35. Peak Long Term Human Health Impacts for Case 1

Calculation Point	Residential Farmer		Industrial Worker		Recreational Shoreline User[a]		MTCA Method B[b]		MTCA Method C[b]		Dose to Worker
	ILCR	HI	ILCR	HI	ILCR	HI	ILCR	HI	ILCR	HI	mrem/yr
BX Tank Farm Fence Line	1.83E-03	2.20E+02	5.39E-05	1.98E-01	NA	NA	NA	2.30E+00	NA	1.05E+00	3.18E+00
200 Area Exclusion Boundary	1.86E-05	1.93E+00	5.48E-07	1.74E-03	NA	NA	NA	2.02E-02	NA	9.22E-03	3.23E-02
Columbia River Shoreline	7.94E-06	5.42E-01	2.34E-07	4.88E-04	3.89E-08	6.71E-05	NA	5.67E-03	NA	2.59E-03	1.38E-02

[a] Exposures defined to occur only within 400 m (1,300 ft) of the Columbia River shoreline.

[b] Cancer risks not shown because MTCA addresses only nonradioactive contaminants and no nonradioactive carcinogenic chemicals were identified as contaminants of concern for WMA B-BX-BY.

HI = hazard index
ILCR = incremental lifetime cancer risk
MTC = Model Toxics Control Act
NA = not applicable

E.5.2 BARRIER ALTERNATIVE AND NO WATER LINE LEAKS CASE (CASE 2)

Results for case 2, barrier alternative and no water line leaks, are summarized in Table E.36. Results for case 2 show the same general trends regarding the calculation points as discussed above for case 1. Peak values for case 2 are slightly lower than the corresponding values for case 1. Between the BX tank farm east fence line boundary and the Columbia River shoreline, the peak industrial worker ILCR ranges from 5.34×10^{-5} to 1.54×10^{-7}. Peak ILCR values are driven by technetium-99. The peak industrial worker hazard index ranges from 1.98×10^{-1} to 4.54×10^{-4}. Peak hazard index values are driven by nitrate. The peak dose ranges from 3.15 mrem/yr to 9.07×10^{-3} mrem/yr. Peak dose values are driven by technetium-99.

Temporal variations in ILCR for case 2 are shown in Figure E.12 for calculation locations between the BX tank farm east fence line boundary and the Columbia River shoreline. Temporal variations in hazard index and dose for case 2 are similar to those shown for ILCR. The peaks at the BX tank farm east fence line boundary and 200 Area exclusion boundary occur in the years 2015 and 2056, respectively. In both cases, the peak arrival time is the same year and approximate peak value as the first of the two peaks in the bimodal results found in case 1. The peak at the Columbia River shoreline calculation location arrives approximately 270 years (i.e., year 2285) after the peak at the BX tank farm east fence line boundary (i.e., year 2015).

Figure E.12. Case 2 Industrial Worker ILCR Versus Time at Calculation Points Between the BX Tank Farm East Fence Line Boundary and the Columbia River

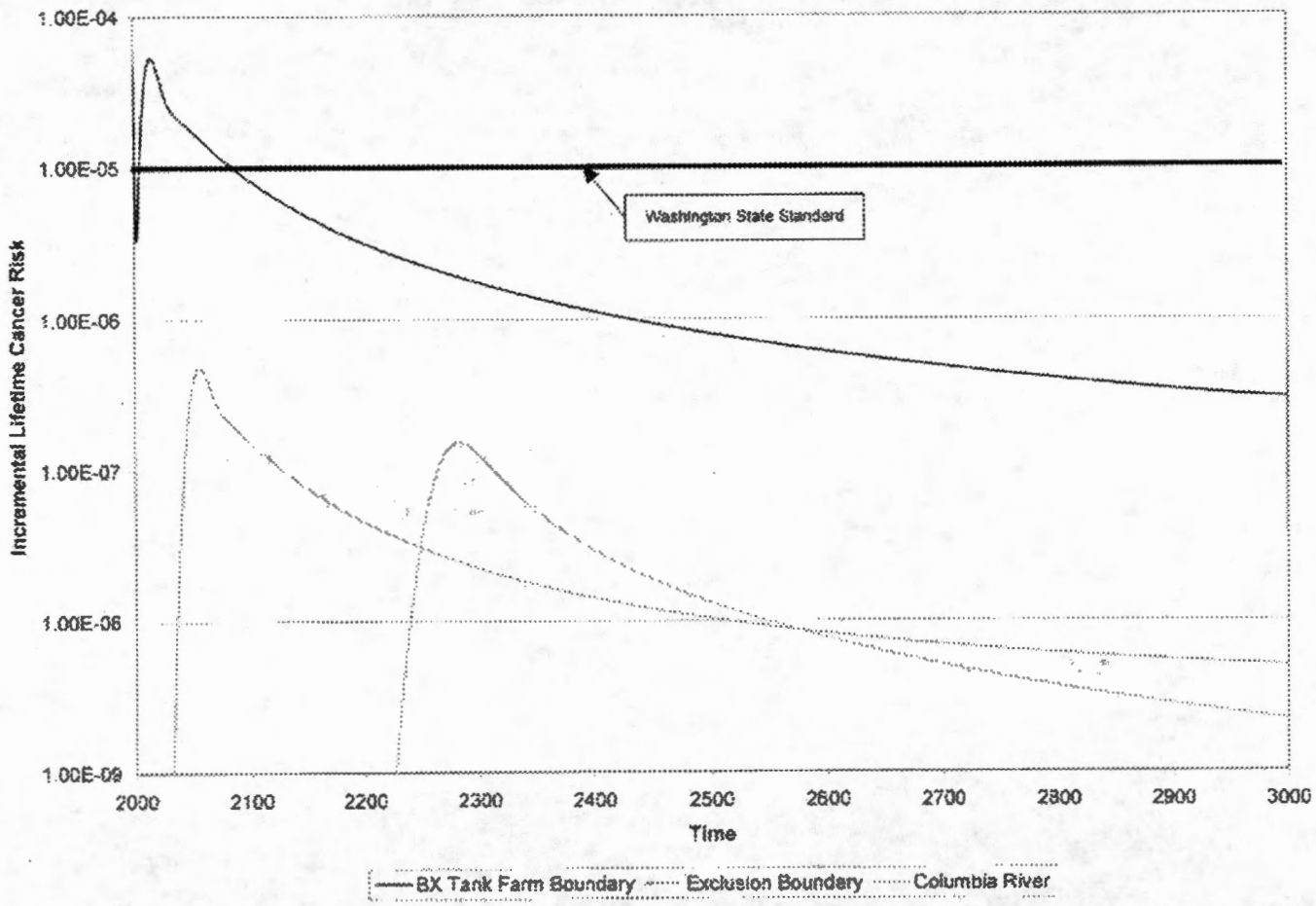

Table E.36. Peak Long Term Human Health Impacts for Case 2

Calculation Point	Residential Farmer		Industrial Worker		Recreational Shoreline User[a]		MTCA Method B[b]		MTCA Method C[b]		Dose to Worker
	ILCR	HI	ILCR	HI	ILCR	HI	ILCR	HI	ILCR	HI	mrem/yr
BX Tank Farm Fence Line	1.81E-03	2.20E+02	5.34E-05	1.98E-01	NA	NA	NA	2.30E+00	NA	1.05E+00	3.15E+00
200 Area Exclusion Boundary	1.63E-05	1.92E+00	4.82E-07	1.73E-03	NA	NA	NA	2.01E-02	NA	9.18E-03	2.84E-02
Columbia River Shoreline	5.21E-06	5.03E-01	1.54E-07	4.54E-04	2.56E-08	6.23E-05	NA	5.27E-03	NA	2.41E-03	9.07E-03

[a] Exposures defined to occur only within 400 m (1,300 ft) of the Columbia River shoreline.

[b] Cancer risks not shown because MTCA addresses only nonradioactive contaminants and no nonradioactive carcinogenic chemicals were identified as contaminants of concern for WMA B-BX-BY.

HI = hazard index

ILCR = incremental lifetime cancer risk

MTCA = Model Toxics Control Act

NA = not applicable

E.5.3 BASE CASE WITH 50 MM/YR METEORIC RECHARGE (CASE 7)

Results for case 7, base case with 50 mm/yr meteoric recharge, are summarized in Table E.37. Results for case 7 show the same general trends regarding the calculation points as discussed above for case 1. Peak values for case 7 generally range from slightly lower to a factor of 2 lower than the corresponding values for case 1. Between the BX tank farm east fence line boundary and the Columbia River shoreline, the peak industrial worker ILCR ranges from 4.85×10^{-5} to 1.19×10^{-7}. Peak ILCR values are driven by technetium-99. The peak industrial worker hazard index ranges from 1.77×10^{-1} to 3.72×10^{-4}. Peak hazard index values are driven by nitrate. The peak dose ranges from 2.86 mrem/yr to 7.00×10^{-3} mrem/yr. Peak dose values are driven by technetium-99.

Temporal variations in ILCR for case 7 are shown in Figure E.13 for calculation locations between the BX tank farm east fence line boundary and the Columbia River. Temporal variations in hazard index and dose for case 7 are similar to those shown for ILCR. Overall, the temporal variations for case 7 most closely resemble those for case 1, in that the predictions for the BX tank farm east fence line boundary and 200 Area exclusion boundary display a bimodal character. The peak at the BX tank farm east fence line boundary occurs in the year 2000 and the peaks for the 200 Area exclusion boundary and Columbia River shoreline calculation locations arrive after approximately 70 and 300 years, respectively (i.e., years 2070 and 2300).

Figure E.13. Case 7 Industrial Worker ILCR Versus Time at Calculation Points Between the BX Tank Farm Fence Line Boundary and the Columbia River

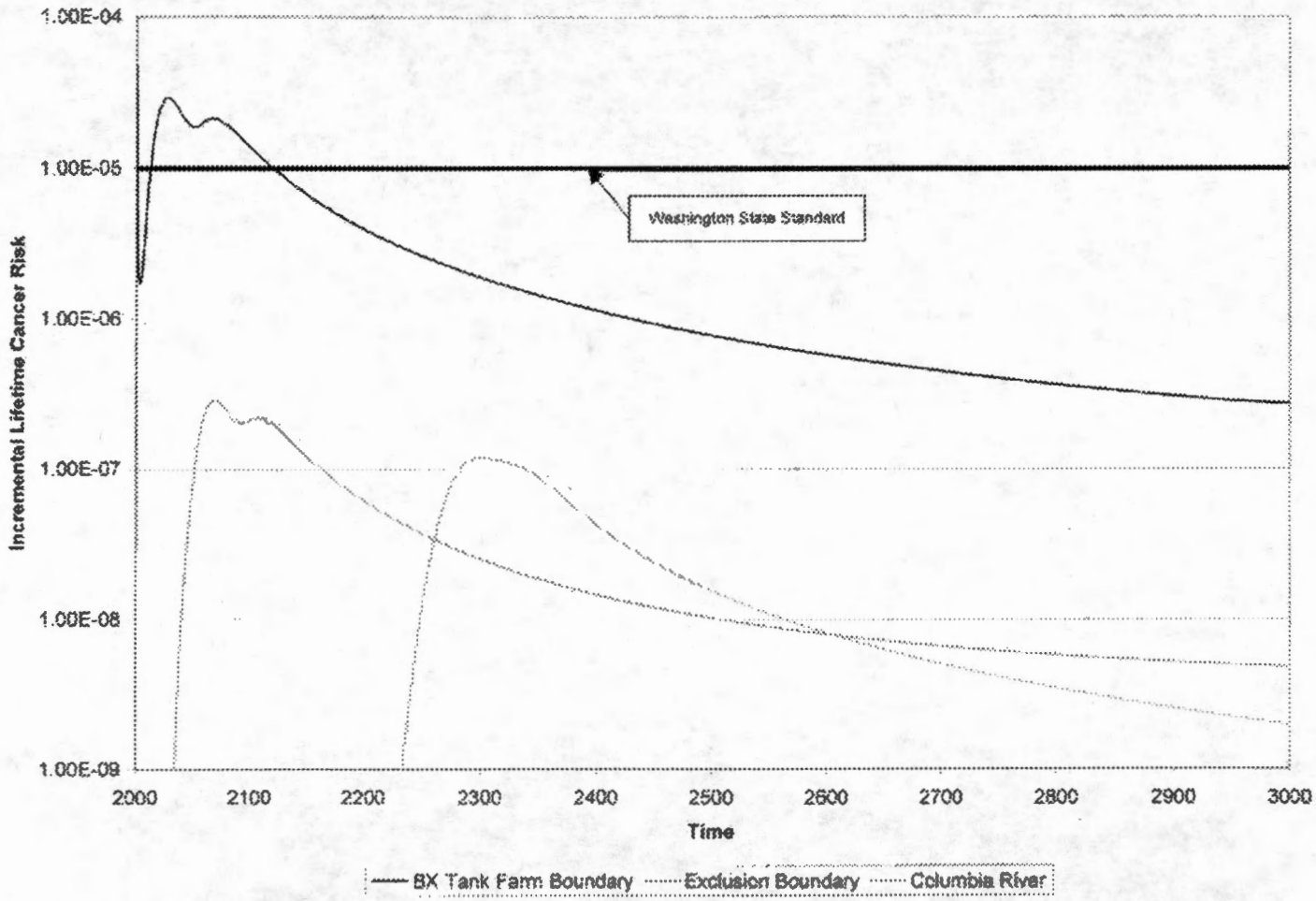

Table B.37. Peak Long Term Human Health Impacts for Case 7

Calculation Point	Residential Farmer		Industrial Worker		Recreational Shoreline User[a]		MTCA Method B[b]		MTCA Method C[b]	
	ILCR	HI	ILCR	HI	ILCR	HI	ILCR	HI	ILCR	HI
BX Tank Farm Fence Line	1.64E-03	1.97E+02	4.85E-05	1.77E-01	NA	NA	NA	2.06E+00	NA	9.40E-01
200 Area Exclusion Boundary	9.80E-06	1.18E+00	2.89E-07	1.07E-03	NA	NA	NA	1.24E-02	NA	5.66E-03
Columbia River Shoreline	4.02E-06	4.13E-01	1.19E-07	3.72E-04	NA	5.11E-05	NA	4.32E-03	NA	1.97E-03

[a] Exposures defined to occur only within 400 m (1,300 ft) of the Columbia River shoreline.

[b] Cancer risks not shown because MTCA addresses only nonradioactive contaminants and no nonradioactive carcinogenic chemicals were identified as contaminants of concern for WMA B-BX-BY.

HI = hazard index
ILCR = incremental lifetime cancer risk
MTCA = Model Toxics Control Act
NA = not applicable

E.5.4 BASE CASE WITH 30 MM/YR METEORIC RECHARGE (CASE 8)

Results for case 8, base case with 30 mm/yr meteoric recharge, are summarized in Table E.38. Results for case 8 show the same general trends regarding the calculation locations as discussed above for case 1. Peak values for case 8 generally range from slightly lower to a factor of 2 lower than the corresponding values for case 1. Between the BX tank farm east fence line boundary and the Columbia River shoreline, the peak industrial worker ILCR ranges from 4.83×10^{-5} to 8.27×10^{-8}. Peak ILCR values are driven by technetium-99. The peak industrial worker hazard index ranges from 1.97×10^{-1} to 2.89×10^{-4}. Peak hazard index values are driven by nitrate. The peak dose ranges from 2.85 mrem/yr to 4.88×10^{-3} mrem/yr. Peak dose values are driven by technetium-99.

Temporal variations in ILCR for case 8 are shown in Figure E.14 for calculation points between the BX tank farm east fence line boundary and the Columbia River. Temporal variations in hazard index and dose for case 8 are similar to those shown for ILCR. The peak at the BX tank farm east fence line boundary occurs in the year 2000, and the peaks at the 200 Area exclusion boundary and Columbia River shoreline calculation locations arrive after approximately 80 and 310 years, respectively (i.e., years 2080 and 2310).

Figure E.14. Case 8 Industrial Worker ILCR Versus Time at Calculation Points Between the BX Tank Farm East Fence Line Boundary and the Columbia River

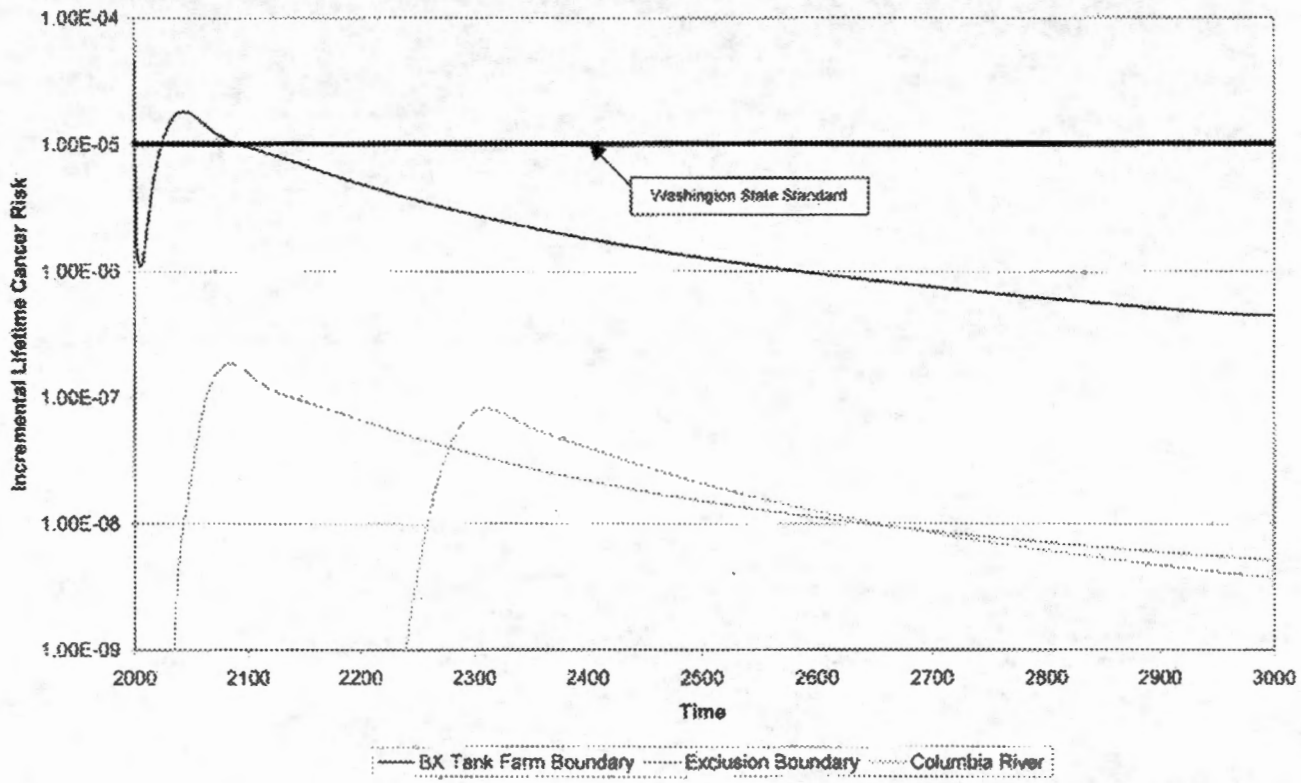

Table E.38. Peak Long Term Human Health Impacts for Case 8

Calculation Point	Residential Farmer		Industrial Worker		Recreational Shoreline User[a]		MTCA Method B[b]		MTCA Method C[b]		Dose to Worker
	ILCR	HI	ILCR	HI	ILCR	HI	ILCR	HI	ILCR	HI	mrem/yr
BX Tank Farm Fence Line	1.64E-03	2.19E+02	4.83E-05	1.97E-01	NA	NA	NA	2.29E+00	NA	1.05E+00	2.85E+00
200 Area Exclusion Boundary	6.37E-06	7.67E-01	1.88E-07	6.91E-04	NA	NA	NA	8.02E-03	NA	3.67E-03	1.11E-02
Columbia River Shoreline	2.80E-06	3.21E-01	8.27E-08	2.89E-04	1.37E-08	3.98E-05	NA	3.36E-03	NA	1.54E-03	4.88E-03

[a] Exposures defined to occur only within 400 m (1,300 ft) of the Columbia River shoreline.

[b] Cancer risks not shown because MTCA addresses only nonradioactive contaminants and no nonradioactive carcinogenic chemicals were identified as contaminants of concern for WMA B-BX-BY.

HI = hazard index
ILCR = incremental lifetime cancer risk
MTCA = Model Toxics Control Act
NA = not applicable

E.6.0 CONCLUSIONS OF RISK AND DOSE

Table E.39 presents the peak ILCR, hazard index, and dose for the industrial worker scenario for the four cases analyzed. This comparison indicates the following ranking from the highest risk to lowest risk:

- Case 1 (no action alternative)
- Case 2 (barrier case with no water line breaks)
- Case 7 (base case with 50 mm/yr meteoric recharge)
- Case 8 (base case with 30 mm/yr meteoric recharge).

Table E.39. Comparison of Peak Incremental Lifetime Cancer Risk, Hazard Index, and Dose for the Industrial Worker

Case	BX Tank Farm Fence Line Boundary	200 Area Exclusion Boundary	Columbia River Shoreline
Industrial Worker Peak Incremental Lifetime Cancer Risk			
1	5.39E-05	5.48E-07	2.34E-07
2	5.34E-05	4.82E-07	1.54E-07
7	4.85E-05	2.89E-07	1.19E-07
8	4.83E-05	1.88E-07	8.27E-08
Industrial Worker Peak Hazard Index			
1	1.98E-01	1.74E-03	4.88E-04
2	1.98E-01	1.73E-03	4.54E-04
7	1.77E-01	1.07E-03	3.72E-04
8	1.97E-01	6.91E-04	2.89E-04
Industrial Worker Peak Dose (mrem/yr)			
1	3.18E+00	3.23E-02	1.38E-02
2	3.15E+00	2.84E-02	9.07E-03
7	2.86E+00	1.71E-02	7.00E-03
8	2.85E+00	1.11E-02	4.88E-03

Rankings by calculation points indicate the following ranking usually occurs (from highest to lowest risk):

- BX tank farm east fence line boundary
- 200 Area exclusion boundary
- Columbia River shoreline.

The CoC driver for risk and dose is technetium-99. For the hazard index, the principal CoC driver is nitrate.

E.7.0 REFERENCES

40 CFR 141, "National Primary Drinking Water Regulations," *Code of Federal Regulations*, as amended.

64 FR 61615, 1999, "Record of Decision: Hanford Comprehensive Land-Use Plan Environmental Impact Statement (HCP EIS)," *Federal Register*, Vol. 64, No. 218, pp. 61615, November 12.

Agnew, S. F., 1997, *Hanford Tank Chemical and Radionuclide Inventories: HDW Model Rev. 4*, LA-UR-96-3860, Los Alamos National Laboratory, Los Alamos, New Mexico.

Crass, D. W., 2001, *Single-Shell Tank S-112 Full Scale Saltcake Waste Retrieval Technology Demonstration Functions and Requirements*, RPP-7825, Rev. 0A, CH2M HILL Hanford Group, Inc., Richland, Washington.

DOE, 1999, *Final Hanford Comprehensive Land-Use Plan Environmental Impact Statement*, DOE/EIS-0222F, U.S. Department of Energy, Washington, D.C.

DOE, 2001, *Radioactive Waste Management*, DOE O 435.1, U.S. Department of Energy, Washington, D. C.

DOE and Ecology, 1996, *Tank Waste Remediation System, Hanford Site, Richland, Washington, Final Environmental Impact Statement*, DOE/EIS-0189, U.S. Department of Energy, Washington, D.C., and Washington State Department of Ecology, Olympia, Washington.

DOE-GJPO, 1998, *Hanford Tank Farms Vadose Zone: BX Tank Farm Report*, GJO-98-40-TAR, GJO-HAN-19, U.S. Department of Energy, Grand Junction Project Office, Grand Junction, Colorado.

DOE-RL, 1995a, *Corrective Measures Study for the 100-NR-1 and 100-NR-2 Operable Units*, DOE/RL-95-111, Rev. 0, U.S. Department of Energy, Richland Operations Office, Richland, Washington.

DOE-RL, 1995b, *Hanford Site Risk Assessment Methodology*, DOE/RL-91-45, Rev. 3, U.S. Department of Energy, Richland Operations Office, Richland, Washington.

DOE-RL, 1995c, *Limited Field Investigation for the 200-UP-2 Operable Unit*, DOE/RL-95-13, Rev. 0, U.S. Department of Energy, Richland Operations Office, Richland, Washington.

DOE-RL, 1996, *Programmatic Agreement Among the U.S. Department of Energy, Richland Operations Office, the Advisory Council on Historic Preservation, and the Washington State Historic Preservation Office for the Maintenance, Deactivation, Alteration, and Demolition of the Built Environment on the Hanford Site, Washington*, DOE/RL-96-77, Rev. 0, U.S. Department of Energy, Richland Operations Office, Richland, Washington.

DOE-RL, 1999, *Retrieval Performance Evaluation Methodology for the AX Tank Farm*, DOE/RL-98-72, U.S. Department of Energy, Richland Operations Office, Richland, Washington.

DOE-RL, 2000, *Phase 1 RCRA Facility Investigation/Corrective Measures Study Work Plan for Single-Shell Tank Waste Management Areas*, DOE/RL-99-36, Rev. 1, U.S. Department of Energy, Richland Operations Office, Richland, Washington.

Domenico, P. A. and F. W. Schwartz, 1990, *Physical and Chemical Hydrogeology*, John Wiley & Sons, New York, New York.

Ecology, 2001, *Dangerous Waste Portion of the Resource Conservation and Recovery Act Permit for the Treatment, Storage, and Disposal of Dangerous Waste*, Rev. 7, Permit 7890008967, Washington State Department of Ecology, Olympia, Washington.

EPA, 1995, *Record of Decision for the 100-BC-1, 100-DR-1, and 100-HR-1 Operable Units*, U.S. Environmental Protection Agency, Washington, D.C.

EPA, 2002a, *Integrated Risk Information System*, at http://www.epa.gov/iriswebp/iris/index.htm as of September 5, U.S. Environmental Protection Agency, Washington, D.C.

EPA, 2002b, *User's Guide: Radionuclide Carcinogenicity*, at http://www.epa.gov/radiation/heast/userguid.htm as of September 5, U.S. Environmental Protection Agency, Washington, D.C.

Freedman, V. L, M. D. Williams, C. R. Cole, M. D. White, and M. P. Bergeron, 2002, 2002 *Initial Assessments for B-BX-BY Field Investigation Report (FIR): Numerical Simulations*, PNNL-13949, Pacific Northwest National Laboratory, Richland, Washington.

FSUWG, 1992, *The Future for Hanford: Uses and Cleanup, The Final Report of the Hanford Future Site Uses Working Group*, Hanford Future Site Uses Working Group, Westinghouse Hanford Company, Richland, Washington.

Gardner, W. R., 1958, "Some Steady-State Solutions of the Unsaturated Moisture Flow Equation with Application to Evaporation from a Water Table," *Soil Sci.* 85:228-232.

Gelhar, L. W., 1993, *Stochastic Subsurface Hydrology*, Prentice Hall, New York.

Jones, T. E., B. C. Simpson, M. I. Wood, and R. A. Corbin, 2001, *Preliminary Inventory Estimates for Single-Shell Tank Leaks in B, BX, and BY Tank Farms*, RPP-7389, CH2M HILL Hanford Group, Inc., Richland, Washington.

Kaplan, D. I., and R. J. Serne, 1999, *Geochemical Data Package For the Hanford Immobilized Low-Activity Tank Waste Performance Assessment (ILAW-PA), HNF-5636, Ref:* PNNL-13037, Rev. 0, Pacific Northwest National Laboratory, Richland, Washington.

Khaleel, R., J. F. Relyea, and J. L. Conca, 1995, "Evaluation of van Genuchten-Mualem relationships to estimate unsaturated conductivity at low water contents," *Water Resources Research*, Vol. 31, No. 11, pp 2659-2668.

Khaleel, R. and J. F. Relyea, 1997, "Correcting laboratory-measured moisture retention data for gravels," *Water Resources Research*, 33:1875-1878.

Khaleel, R., and J. F. Relyea, 2001, "Variability of Gardner's α for coarse-textured sediments," *Water Resources Research*, Vol. 37, No. 6, pp 1567-1575.

Khaleel, R., T. E. Jones, A. J. Knepp, F. M. Mann, D. A. Myers, and M. I. Wood, 2001, *Modeling Data Package for B-BX-BY Field Investigation Report (FIR)*, RPP-9223, Rev. 0, CH2M HILL Hanford Group, Inc., Richland, Washington.

Khaleel, R., T. -C. J. Yeh, and Z. Lu, 2002a, "Upscaled flow and transport properties for heterogeneous unsaturated media" *Water Resources Research*, Vol. 38, No. 5, 10.1029/2000WR000072.

Khaleel, R., T. -C. J. Yeh, Z. Lu, 2002b, "Effective hydraulic conductivity and macrodispersivity estimates for heterogeneous unsaturated media", In *Computational Methods in Water Resources*, Eds. S. M. Hassanizadeh, R. J. Schotting, W. G. Gray, and G. F. Pinder, Proceedings of the XIVth International Conference on Computational Methods in Water Resources, Delft, The Netherlands.

Knepp, A. J., 2002, *Field Investigation Report for Waste Management Area S-SX*, RPP-7884, Rev. 0. CH2M HILL Hanford Group, Inc., Richland, Washington.

Kincaid, C. T., J. W. Shade, G. A. Whyatt, M. G. Piepho, K. Rhoads, J. A. Voogd, J. H. Westsik, Jr., M. D. Freshley, K. A. Blanchard, and B. G. Lauzon, 1995, *Volume 1: Performance Assessment of Grouted Double-Shell Tank Waste Disposal at Hanford*, WHC-SD-WM-EE-004, Rev. 1, Westinghouse Hanford Company, Richland, Washington.

Kincaid, C. T., M. P. Bergeron, C. R. Cole, M. D. Freshley, N. L. Hassig, V. G. Johnson, D. I. Kaplan, R. J. Serne, G. P. Streile, D. L. Strenge, P. D. Thorne, L. W. Vail, G. A. Whyatt, S. K. Wurstner, 1998, *Composite Analysis for Low-Level Waste Disposal in the 200 Area Plateau of the Hanford Site*, PNNL-11800, Pacific Northwest National Laboratory, Richland, Washington.

Law, A., S. Panday, C. Denslow, K. Fecht, and A. Knepp, 1996, *Hanford Sitewide Groundwater Flow and Transport Model Calibration Report*, BHI-00608, Rev. 1, Bechtel Hanford, Inc., Richland, Washington.

Lindsey, K. A., K. D. Reynolds, and S. E. Kos, 2001, *Vadose Zone Geology of Boreholes 299-E33-45 and 299-E33-46 B-BX-BY Waste Management Area, Hanford Site, South-Central Washington*, RPP-8681, Rev. 0, CH2M HILL Hanford Group, Inc., Richland, Washington.

Lu, A. H., 1996, *Contaminant Transport in the Unconfined Aquifer: Input to the Low Level Tank Waste Interim Performance Assessment*, WHC-SD-WM-RPT-241, Rev. 0, Westinghouse Hanford Company, Richland, Washington.

Mann, F. M., K. C. Burgard, W. R. Root, P. E. Lamont, R. J. Puigh, S. H. Finfrock, R. Khaleel, D. H. Bacon, E. J. Freeman, B. P. McGrail, and S. K. Wurstner, 2001, *Hanford Immobilized Low-Activity Waste Performance Assessment: 2001 Version*, DOE/ORP-2000-24, Rev. 0, Office of River Protection, Richland, Washington.

Millington, R. J., and J. P. Quirk, 1961, "Permeability of Porous Solids," Trans. Faraday Soc., 57:1200-1207.

Mualem, Y., 1976, "A New Model for Predicting the Hydraulic Conductivity of Unsaturated Porous Media, *Water Resources Research*, 12:513-522.

Polmann, D. J., 1990, *Application of Stochastic Methods to Transient Flow and Transport in Heterogeneous Unsaturated Soils*, Ph.D. Thesis, Massachusetts Institute of Technology, Cambridge, Massachusetts.

Resource Conservation and Recovery Act of 1976, 42 USC 6901, et seq.

Rittmann, P. D., 1999, *Exposure Scenarios and Unit Dose Factors for the Hanford Immobilized Low-Activity Tank Waste Performance Assessment*, HNF-SD-WM-TI-707, Rev. 1, (HNF-5636, Rev. 0), Fluor Federal Services, Richland, Washington.

Talbott, M. E., and L. W. Gelhar, 1994, *Performance Assessment of a Hypothetical Low-Level Waste Facility: Groundwater Flow and Transport Simulation*, NUREG/CR-6114, Vol. 3, U.S. Nuclear Regulatory Commission, Washington, D.C.

van der Kamp, G., L. D. Luba, J. A. Cherry, and H. Maathuis, 1994, "Field Study of a Long and Very Narrow Contaminant Plume," *Ground Water*, Vol. 32, No. 6, pp.1008-1016.

van Genuchten, M. Th., 1980, "A Closed-form Equation for Predicting the Hydraulic Conductivity of Unsaturated Soils," *Soil Sci. Soc. Am. J.*, 44:892-898.

van Genuchten, M. Th., F. J. Leij, and S. R. Yates, 1991, *The RETC Code for Quantifying the Hydraulic Functions of Unsaturated Soils*, EPA/600/2-91/065, U.S. Environmental Protection Agency, Washington, D.C.

WAC 173-340, "Model Toxics Control Act Cleanup Regulation," *Washington Administrative Code*, as amended.

White, M. D., and M. Oostrom, 2000a, *STOMP Subsurface Transport Over Multiple Phases, Version 2.0, Theory Guide*, PNNL-12030, UC-2010, Pacific Northwest National Laboratory, Richland, Washington.

White, M. D., and M. Oostrom, 2000b, *STOMP Subsurface Transport Over Multiple Phases, Version 2.0, User's Guide*, PNNL-12034, UC-2010, Pacific Northwest National Laboratory, Richland, Washington.

Yeh, T. -C. J., L. W. Gelhar, and A. L. Gutjahr, 1985, "Stochastic Analysis of Unsaturated Flow in Heterogeneous Soils, 2. Statistically Anisotropic Media with Variable α," *Water Resources Research*, Vol. 21, No. 4, pp 457-464.

This page intentionally left blank.

ATTACHMENT E1

BX TANK FARM SATURATION AND CONCENTRATION DISTRIBUTIONS

This page intentionally left blank.

CONTENTS

E1.1.0 CASE 1: BASE CASE, NO ACTION ALTERNATIVE E1-1

E1.2.0 CASE 2: BARRIER ALTERNATIVE AND NO WATER LINE LEAK E1-6

E1.3.0 CASE 3: NO INTERIM BARRIER AND WATER LINE LEAK OF 1 GPM FOR 20 YEARS E1-9

E1.4.0 CASE 4: NO INTERIM BARRIER AND WATER LINE LEAK OF 200,000 GALLONS OVER 5 DAYS E1-13

E1.5.0 CASE 5: ALTERNATE INVENTORY DISTRIBUTION AND NO INTERIM BARRIER E1-17

E1.6.0 CASE 6: ALTERNATE INVENTORY DISTRIBUTION WITH INTERIM BARRIER E1-21

E1.7.0 CASE 7: BASE CASE WITH 50 MM/YR METEORIC RECHARGE E1-24

E1.8.0 CASE 8: BASE CASE WITH 30 MM/YR METEORIC RECHARGE E1-28

E1.9.0 CASE 9: BASE CASE WITH 10 MM/YR METEORIC RECHARGE E1-32

E1.10.0 CASE 10: BASE CASE WITH KD = 0.1 ML/G FOR URANIUM-238 ..... E1-36

E1.11.0 CASE 11: BASE CASE WITH KD = 1 ML/G FOR URANIUM-238 ..... E1-38

FIGURES

E1.1. Case 1 (Base Case 100 mm/yr Recharge) Aqueous Phase Saturation Distributions at (a) Year 2000 and (b) Year 3000 ..... E1-2
E1.2. Case 1 (Base Case 100 mm/yr Recharge) Uranium-238 Aqueous Concentration Distribution at (a) Year 2000 and (b) Year 3000 ..... E1-3
E1.3. Case 1 (Base Case 100 mm/yr Recharge) Technetium-99 Aqueous Concentration Distribution at (a) Year 2000 and (b) Year 3000 ..... E1-4
E1.4. Case 1 (Base Case 100 mm/yr Recharge) Nitrate Aqueous Concentration Distribution at (a) Year 2000 and (b) Year 3000 ..... E1-5
E1.5. Case 2 (Interim Barrier) Aqueous Phase Saturation Distribution at Year 3000 ..... E1-7
E1.6. Case 2 (Interim Barrier) Uranium-238 Aqueous Concentration Distribution at Year 3000 ..... E1-7
E1.7. Case 2 (Interim Barrier) Aqueous (a) Technetium-99 and (b) Nitrate Concentration Distributions at Year 3000 ..... E1-8
E1.8. Case 3 (20-Year Water Line Leak at 1gpm) Aqueous Phase Saturation Distributions at (a) Year 2020 and (b) Year 3000 ..... E1-10
E1.9. Case 3 (20-Year Water Line Leak at 1gpm) Aqueous Uranium-238 Concentration Distributions at Year 3000 ..... E1-11
E1.10. Case 3 (20-Year Water Line Leak at 1gpm) Aqueous (a) Technetium-99 and (b) Nitrate Concentration Distributions at Year 3000 ..... E1-12
E1.11. Case 4 (200,000-Gallon Water Line Leak for 5 Days) Aqueous Saturation Distributions at (a) Year 2000 plus 5 days and (b) Year 3000 ..... E1-14
E1.12. Case 4 (200,000-Gallon Water Line Leak for 5 Days) Aqueous Uranium-238 Concentration Distribution at Year 3000 ..... E1-15
E1.13. Case 4 (200,000-Gallon Water Line Leak for 5 Days) Aqueous (a) Technetium-99 and (b) Nitrate Concentration Distributions at Year 3000 ..... E1-16
E1.14. Case 5 (Alternate Inventory) Aqueous Uranium-238 Concentration Distributions at (a) Year 2000 and (b) Year 3000 ..... E1-18
E1.15. Case 5 (Alternate Inventory) Aqueous Technetium-99 Concentration Distributions at (a) Year 2000 and (b) Year 3000 ..... E1-19
E1.16. Case 5 (Alternate Inventory) Aqueous Nitrate Concentration Distributions at (a) Year 2000 and (b) Year 3000 ..... E1-20
E1.17. Case 6 (Alternate Inventory with Interim Barrier) Uranium-238 Aqueous Concentration Distribution at Year 3000 ..... E1-22
E1.18. Case 6 (Alternate Inventory with Interim Barrier) Aqueous (a) Technetium-99 and (b) Nitrate Concentration Distributions at Year 3000 ..... E1-23
E1.19. Case 7 (50 mm/yr Recharge) Aqueous Phase Saturation Distributions at (a) Year 2000 and (b) Year 3000 ..... E1-25
E1.20. Case 7 (50 mm/yr Recharge) Uranium-238 Aqueous Concentration Distribution at Year 3000 ..... E1-26
E1.21. Case 7 (50 mm/yr Recharge) Aqueous (a) Technetium-99 and (b) Nitrate Concentration Distributions at Year 3000 ..... E1-27
E1.22. Case 8 (30 mm/yr Recharge) Aqueous Phase Saturation Distributions at (a) Year 2000 and (b) Year 3000 ..... E1-29

E1.23. Case 8 (30 mm/yr Recharge) Uranium-238 Aqueous Concentration Distribution at Year 3000 ..... E1-30
E1.24. Case 8 (30 mm/yr Recharge) Aqueous (a) Technetium-99 and (b) Nitrate Concentration Distributions at Year 3000 ..... E1-31
E1.25. Case 9 (10 mm/yr Recharge) Aqueous Phase Saturation Distributions at (a) Year 2000 and (b) Year 3000 ..... E1-33
E1.26. Case 9 (10 mm/yr Recharge) Uranium-238 Aqueous Concentration Distribution at Year 3000 ..... E1-34
E1.27. Case 9 (10 mm/yr Recharge) Aqueous (a) Technetium-99 and (b) Nitrate Concentration Distributions at Year 3000 ..... E1-35
E1.28. Case 10 (Uranium-238 K_d=0.1 mL/g) Aqueous Uranium-238 Concentration Distributions at (a) Year 2000 and (b) Year 3000 ..... E1-37
E1.29. Case 11 (Uranium-238 K_d=1 mL/g) Aqueous Uranium-238 Concentration Distributions at (a) Year 2000 and (b) Year 3000 ..... E1-39

This page intentionally left blank.

E1.1.0 CASE 1: BASE CASE, NO ACTION ALTERNATIVE

This scenario involves simulating flow and transport for the cross-section through tanks BX-108, BX-105, and BX-102, considering an initial recharge rate of 100 mm/yr, no water line leak, no interim barrier, a closure barrier at year 2040, a partitioning coefficient (Kd) of 0.6 mL/g for uranium-238, and an inventory distribution that extends east of tank BX-102 to the BX tank farm east fence line boundary.

Figure E1.1. Case 1 (Base Case 100 mm/yr Recharge) Aqueous Phase Saturation Distributions at (a) Year 2000 and (b) Year 3000

(a)

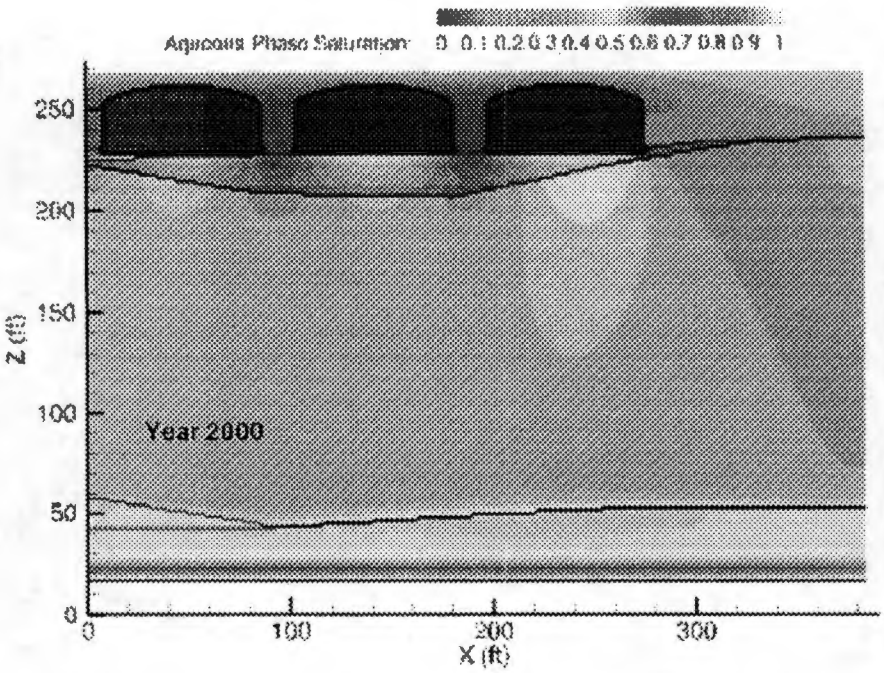

(b)

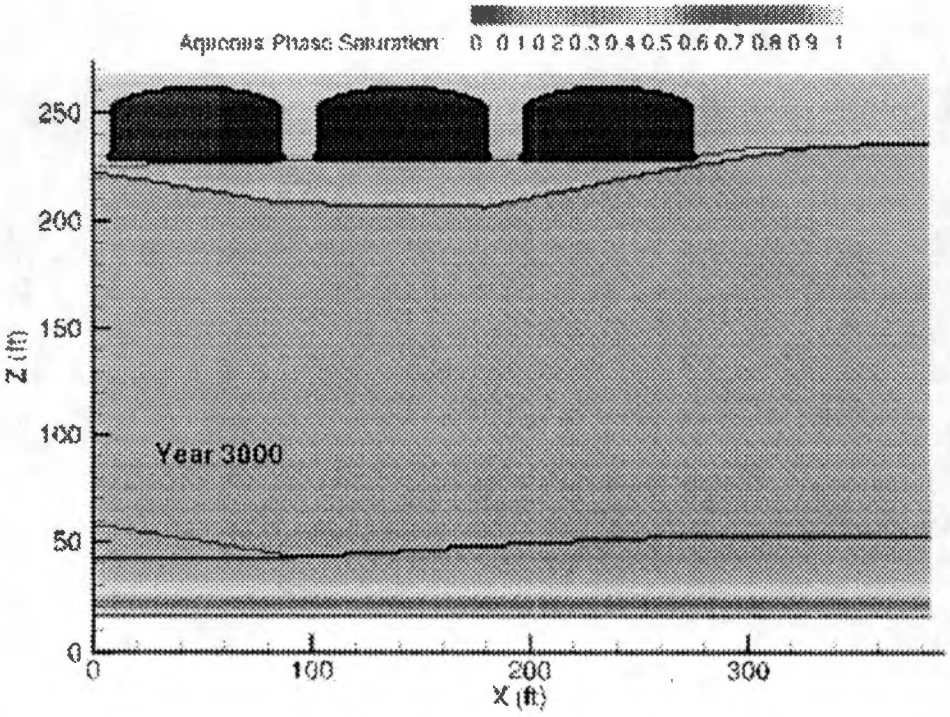

Figure E1.2. Case 1 (Base Case 100 mm/yr Recharge) Uranium-238 Aqueous Concentration Distribution at (a) Year 2000 and (b) Year 3000

(a)

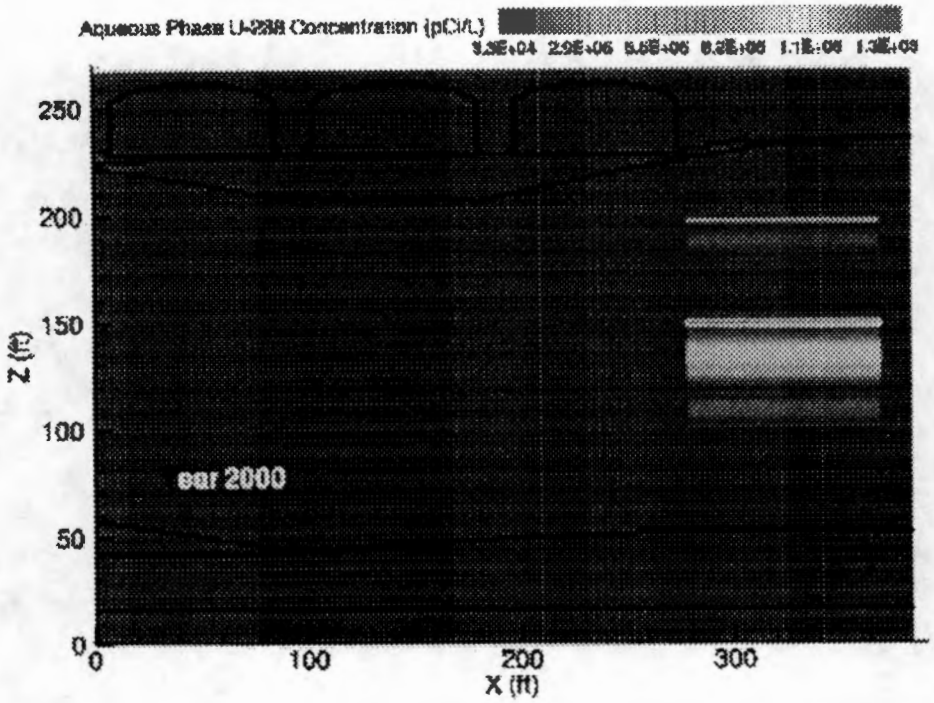

(b)

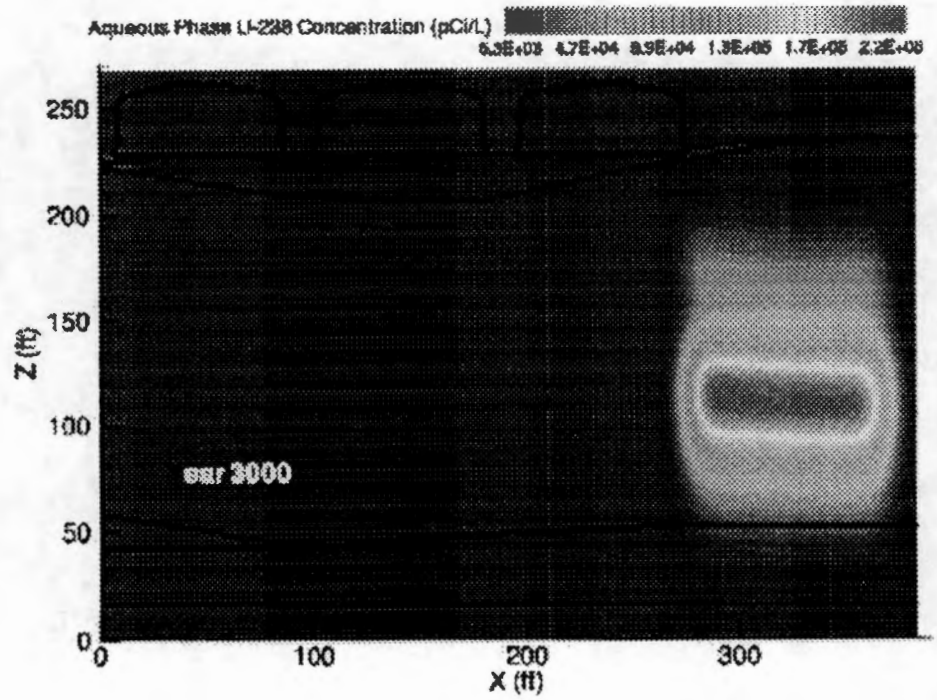

Figure E1.3. Case 1 (Base Case 100 mm/yr Recharge) Technetium-99 Aqueous Concentration Distribution at (a) Year 2000 and (b) Year 3000

(a)

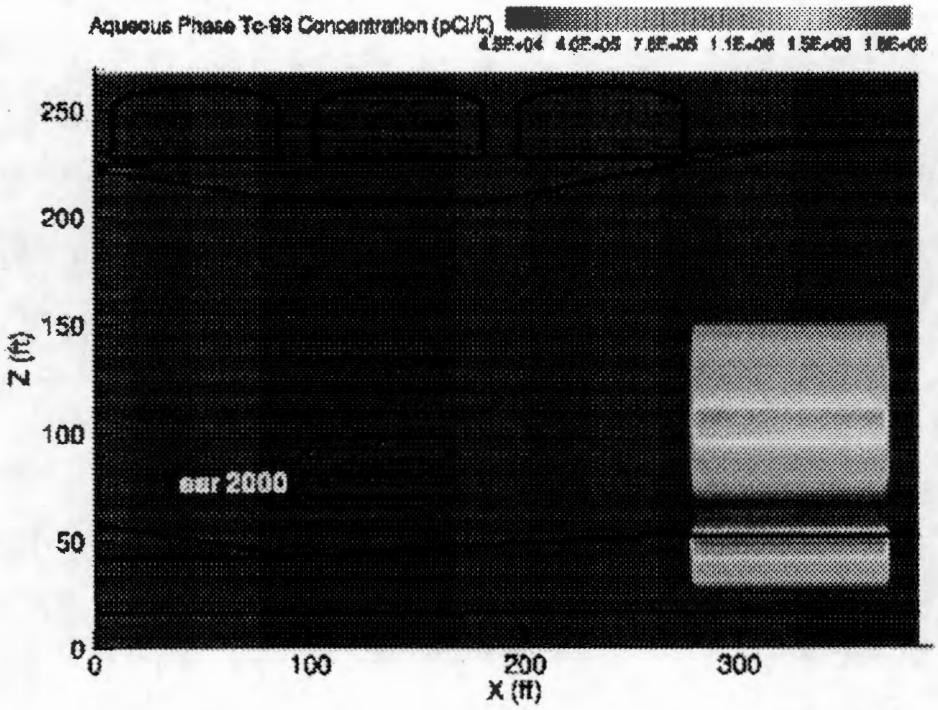

(b)

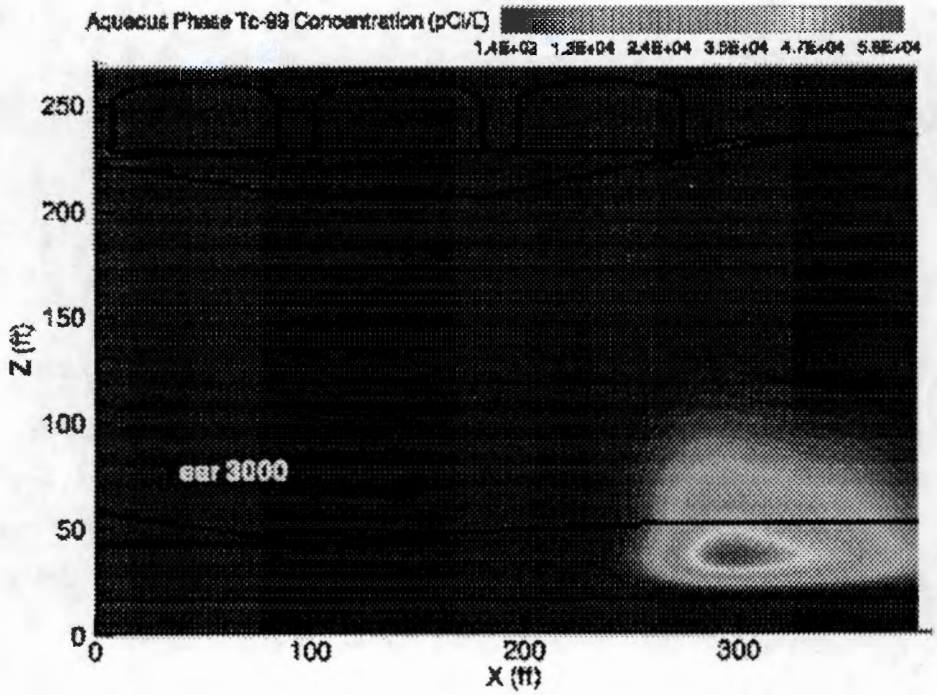

Figure E1.4. Case 1 (Base Case 100 mm/yr Recharge) Nitrate Aqueous Concentration Distribution at (a) Year 2000 and (b) Year 3000

(a)

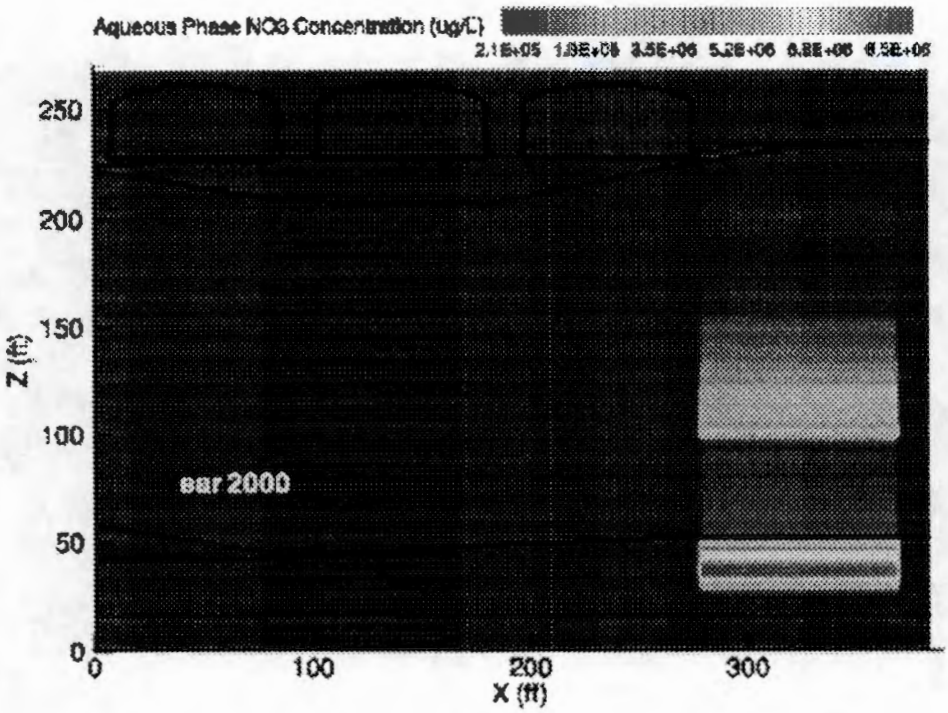

(b)

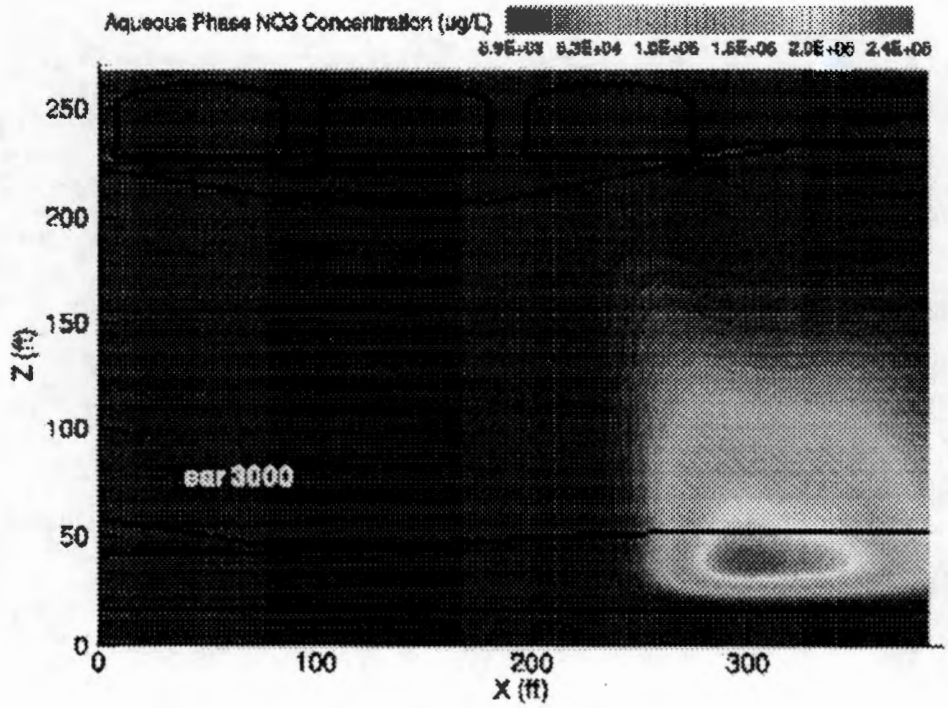

E1.2.0 CASE 2: BARRIER ALTERNATIVE AND NO WATER LINE LEAK

This scenario involves simulating flow and transport for the cross-section through tanks BX-108, BX-105, and BX-102, considering initial recharge rate of 100 mm/yr, placement of an interim barrier by 2010, a closure barrier at year 2040 (i.e., the interim barrier replaced by the closure barrier), no water line leak, a Kd of 0.6 mL/g for uranium-238, and an inventory distribution that extends east of tank BX-102 to the BX tank farm east fence line boundary.

Figure E1.5. Case 2 (Interim Barrier) Aqueous Phase Saturation Distribution at Year 3000

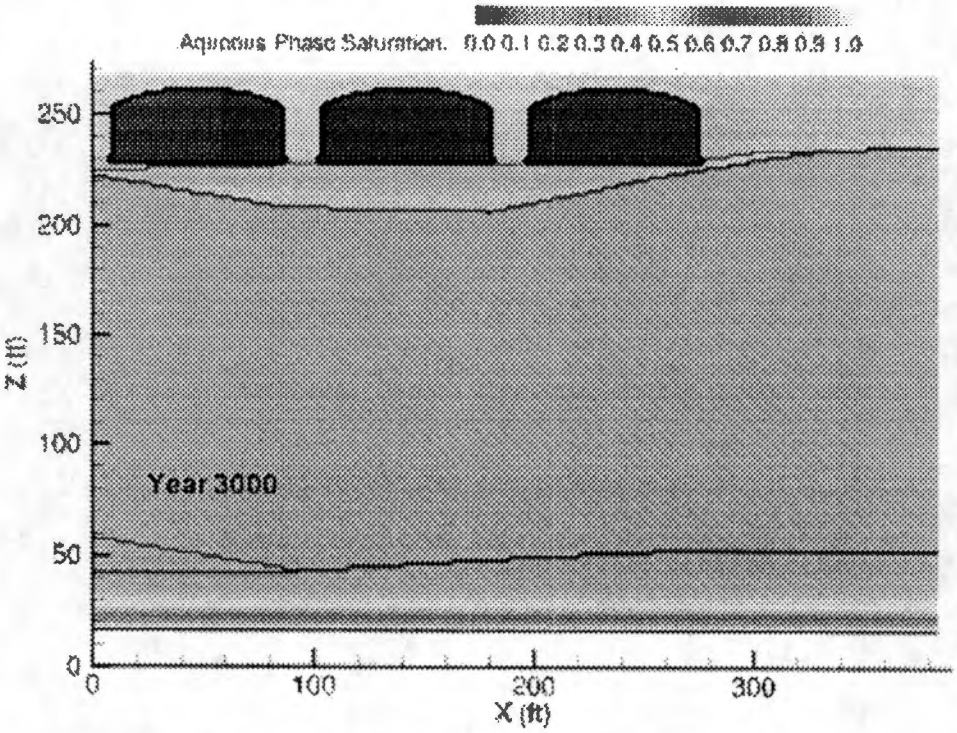

Figure E1.6. Case 2 (Interim Barrier) Uranium-238 Aqueous Concentration Distribution at Year 3000

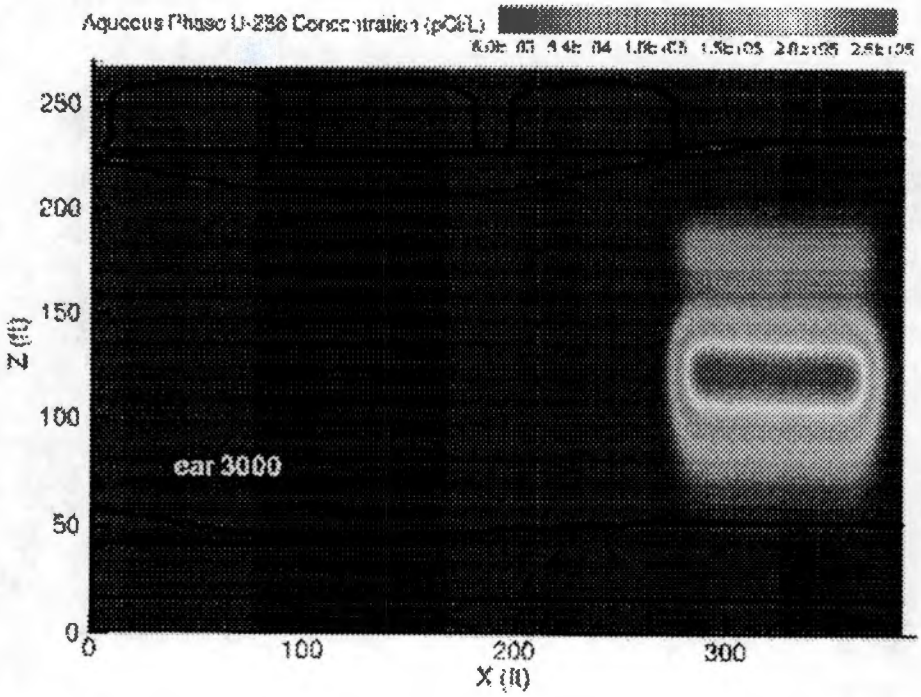

Figure E1.7. Case 2 (Interim Barrier) Aqueous (a) Technetium-99 and (b) Nitrate Concentration Distributions at Year 3000

(a)

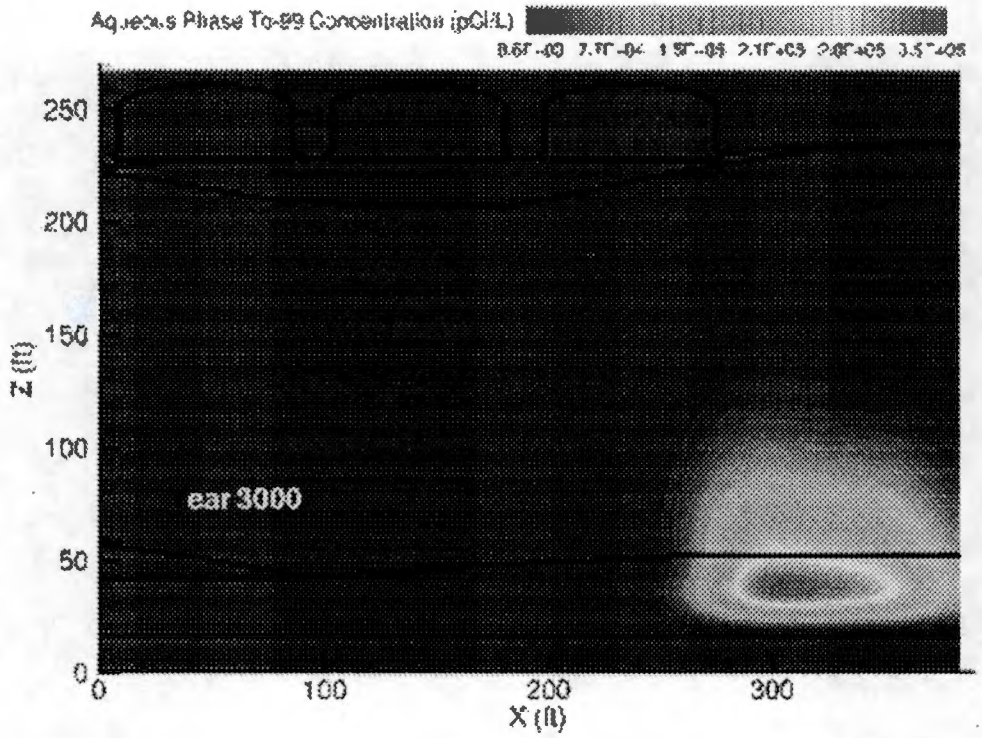

(b)

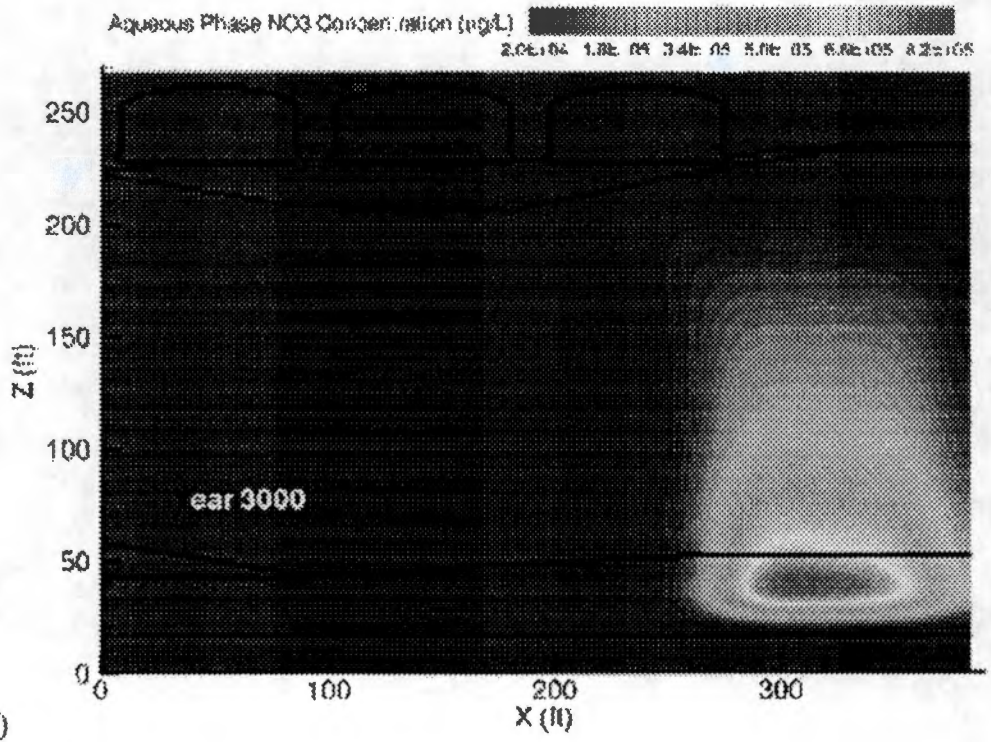

(b)

E1.3.0 CASE 3: NO INTERIM BARRIER AND WATER LINE LEAK OF 1 GPM FOR 20 YEARS

This scenario involves simulating flow and transport for the cross-section through tanks BX-108, BX-105, and BX-102, considering initial recharge rate of 100 mm/yr, water line leak (1 gpm for 20 years) for BX-102 only, no interim barrier until closure at year 2040, a Kd of 0.6 mL/g for uranium-238, and an inventory distribution that extends east of tank BX-102 to the BX fence line boundary. The water line leak occurs east of tank BX-102 over a 15-foot radius at the elevation of the top of the tank dome.

Figure E1.8. Case 3 (20-Year Water Line Leak at 1gpm) Aqueous Phase Saturation Distributions at (a) Year 2020 and (b) Year 3000

(a)

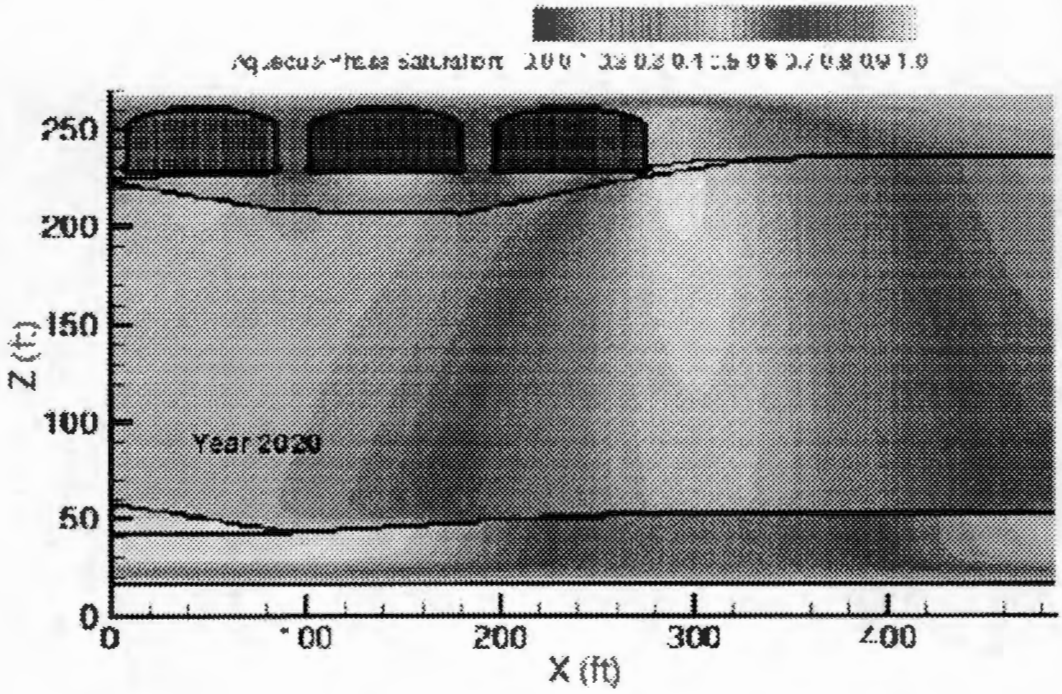

(b)

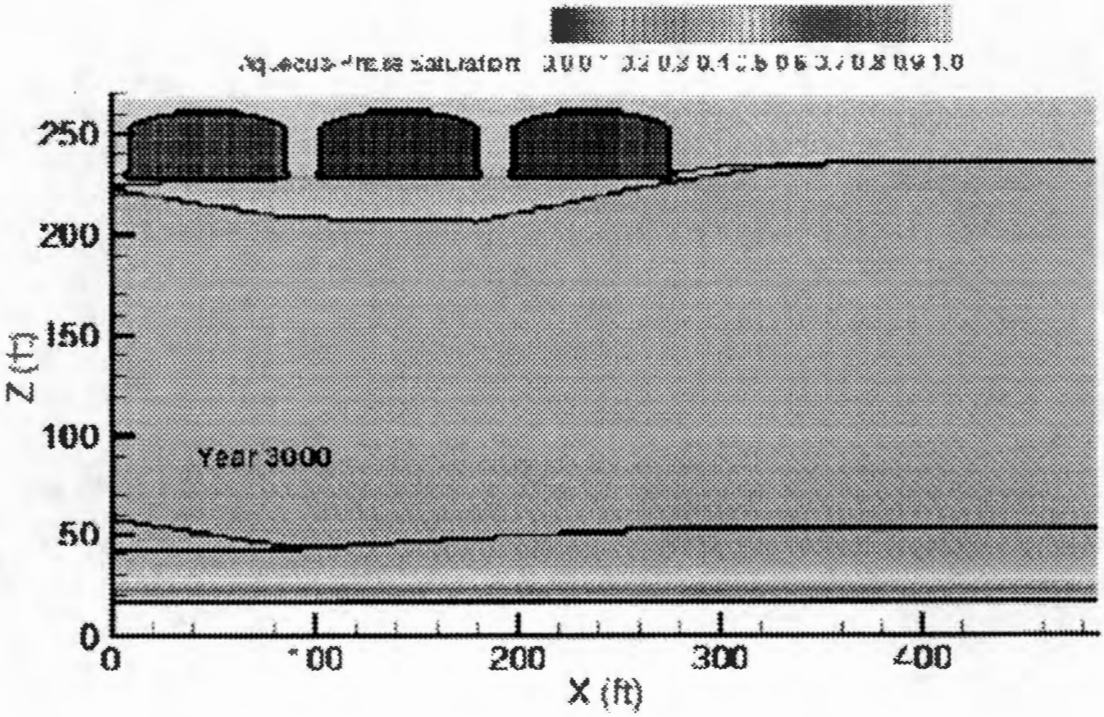

Figure E1.9. Case 3 (20-Year Water Line Leak at 1gpm) Aqueous Uranium-238 Concentration Distributions at Year 3000

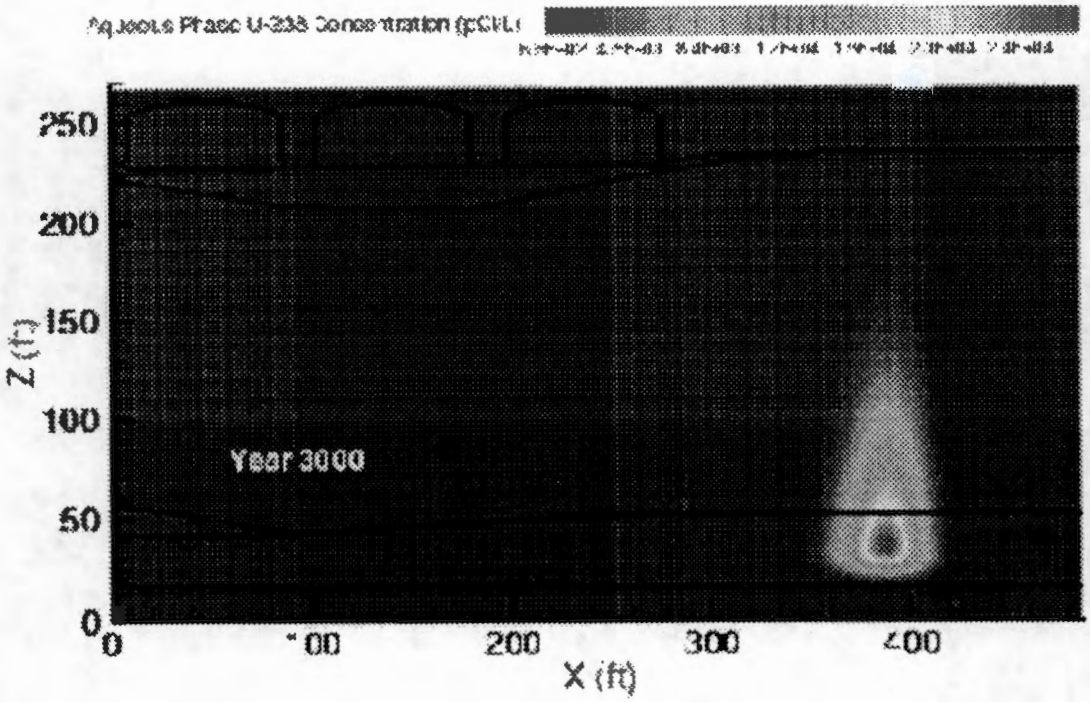

Figure E1.10. Case 3 (20-Year Water Line Leak at 1gpm) Aqueous (a) Technetium-99 and (b) Nitrate Concentration Distributions at Year 3000

(a)

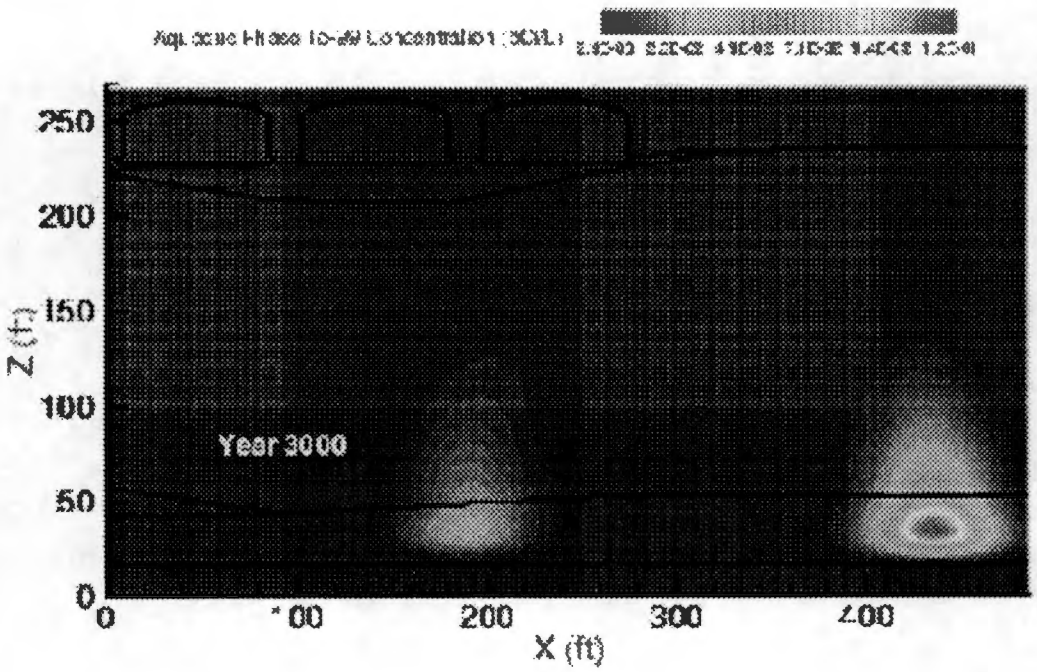

(b)

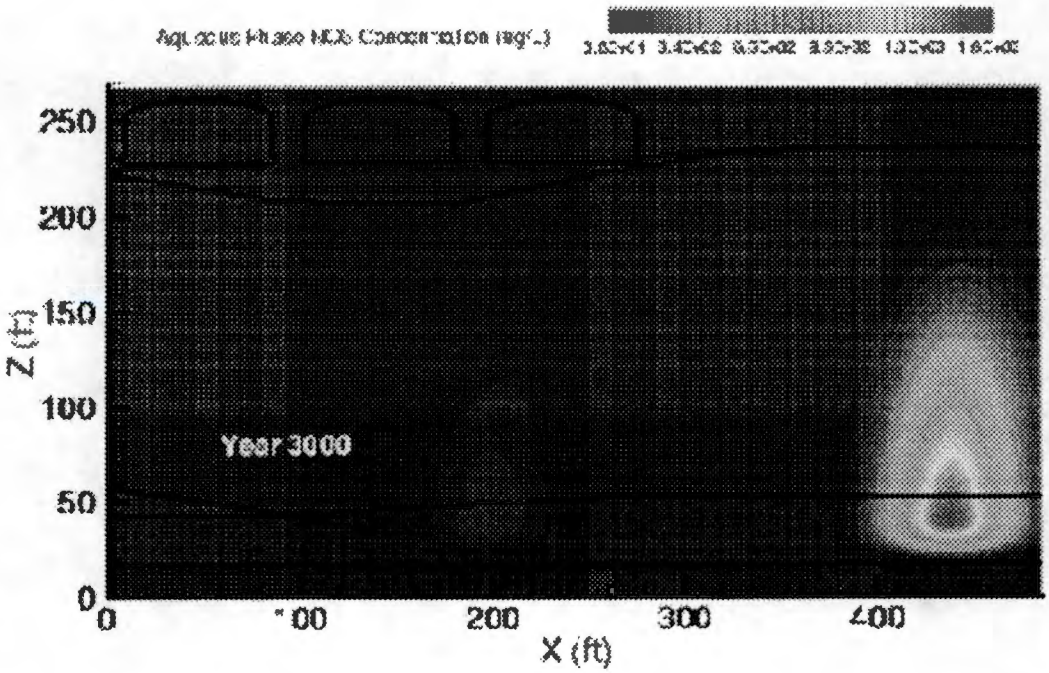

E1.4.0 CASE 4: NO INTERIM BARRIER AND WATER LINE LEAK OF 200,000 GALLONS OVER 5 DAYS

This scenario involves simulating flow and transport for the cross-section through tanks BX-108, BX-105, and BX-102, considering initial recharge rate of 100 mm/yr, water line leak (200,000 gallons in 5 days) for BX-102 only, no interim barrier until closure at year 2040, a Kd of 0.6 mL/g for uranium-238, and an inventory distribution that extends east of tank BX-102 to the BX tank farm fence line boundary. The water line leak occurs east of tank BX-102 over a 15-foot radius at the elevation of the top of the tank dome.

Figure E1.11. Case 4 (200,000-Gallon Water Line Leak for 5 Days) Aqueous Saturation Distributions at (a) Year 2000 plus 5 days and (b) Year 3000

(a)

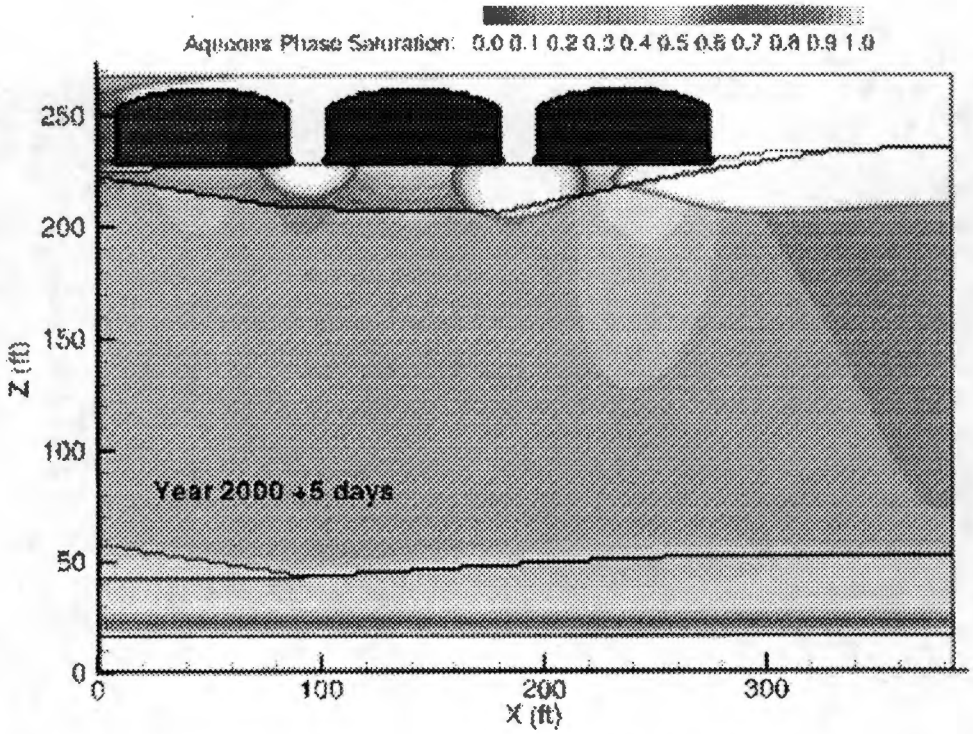

(b)

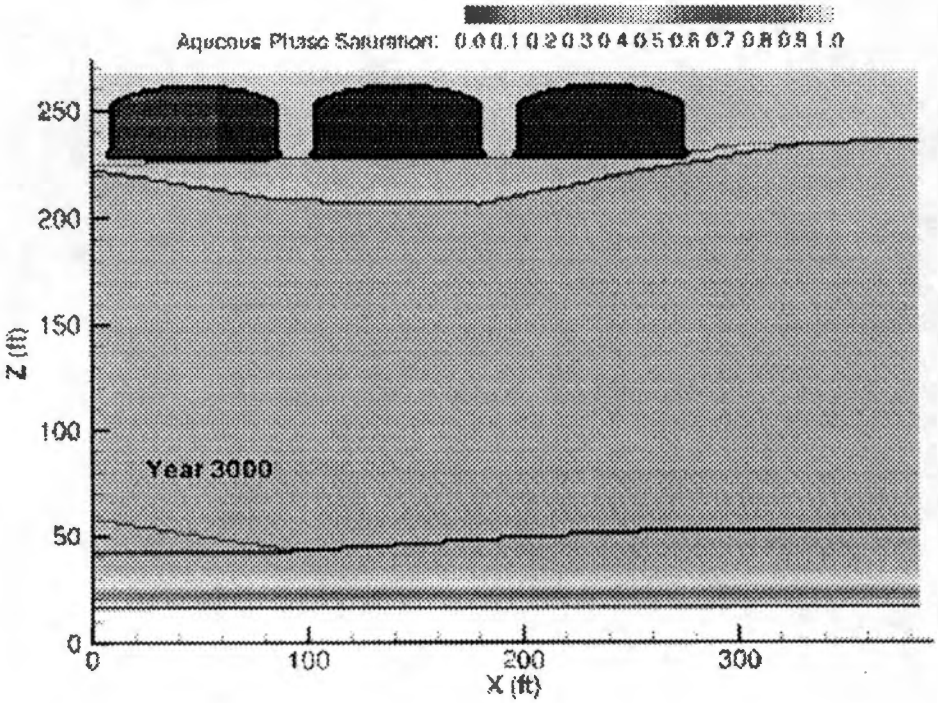

Figure E1.12. Case 4 (200,000-Gallon Water Line Leak for 5 Days) Aqueous Uranium-238 Concentration Distribution at Year 3000

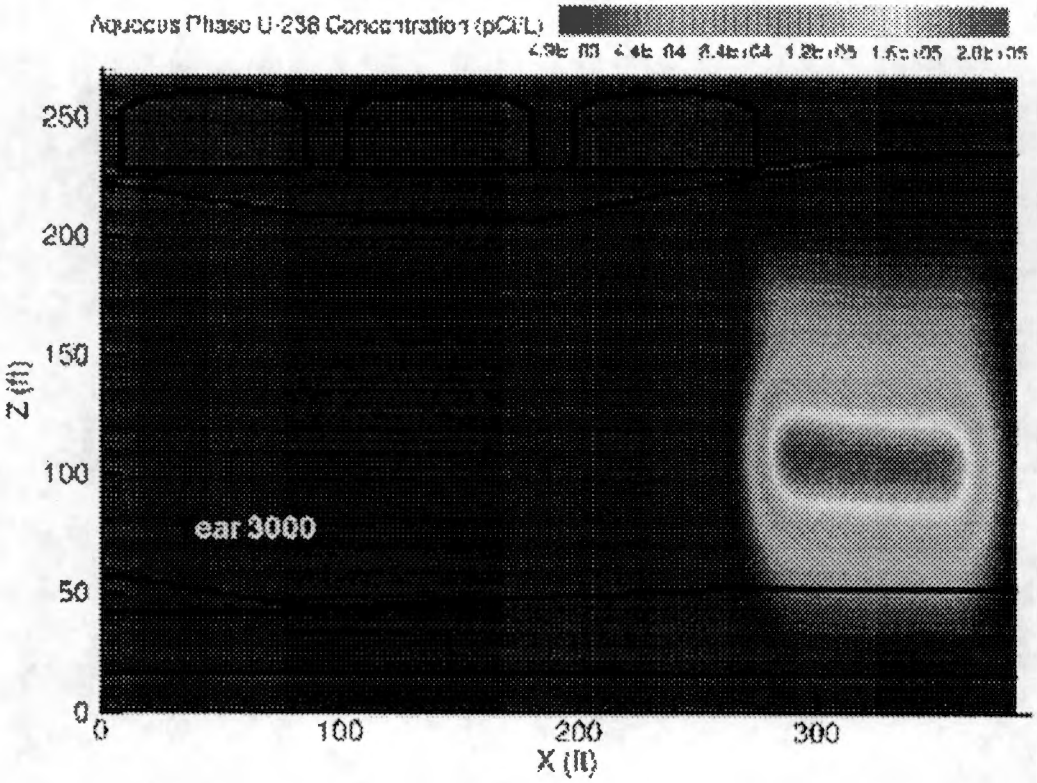

Figure E1.13. Case 4 (200,000-Gallon Water Line Leak for 5 Days) Aqueous (a) Technetium-99 and (b) Nitrate Concentration Distributions at Year 3000

(a)

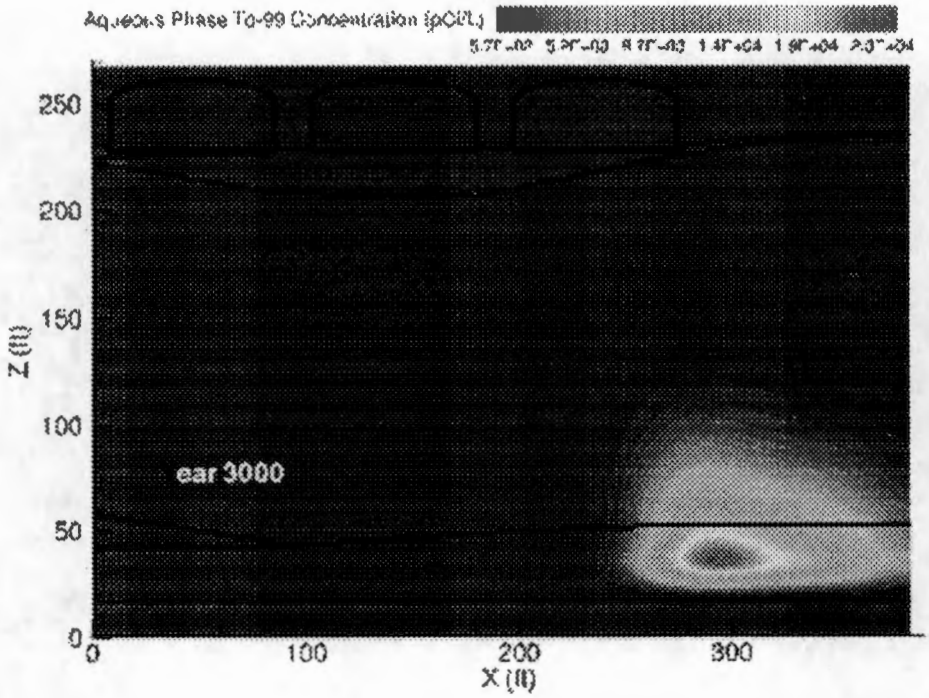

(b)

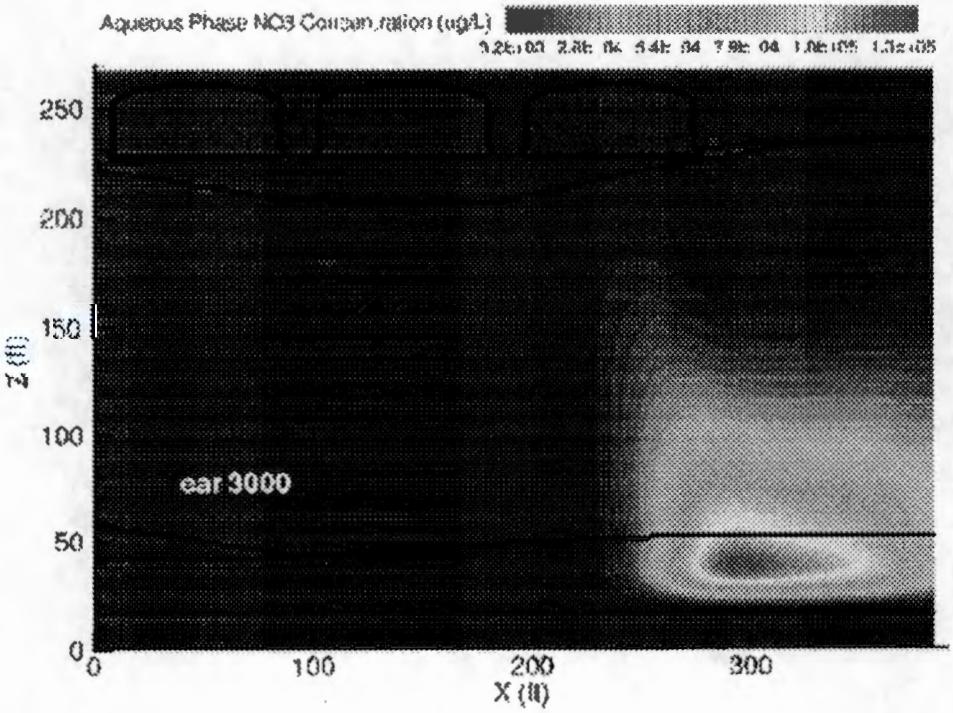

E1.5.0 CASE 5: ALTERNATE INVENTORY DISTRIBUTION AND NO INTERIM BARRIER

This scenario involves simulating flow and transport for the cross-section through tanks BX-108, BX-105, and BX-102, considering initial recharge rate of 100 mm/yr, no water line leak, no interim barrier until closure at year 2040, a Kd of 0.6 mL/g for uranium-238, and an inventory distribution that is centered between tanks BX-105 and BX-102.

Figure E1.14. Case 5 (Alternate Inventory) Aqueous Uranium-238 Concentration Distributions at (a) Year 2000 and (b) Year 3000

(a)

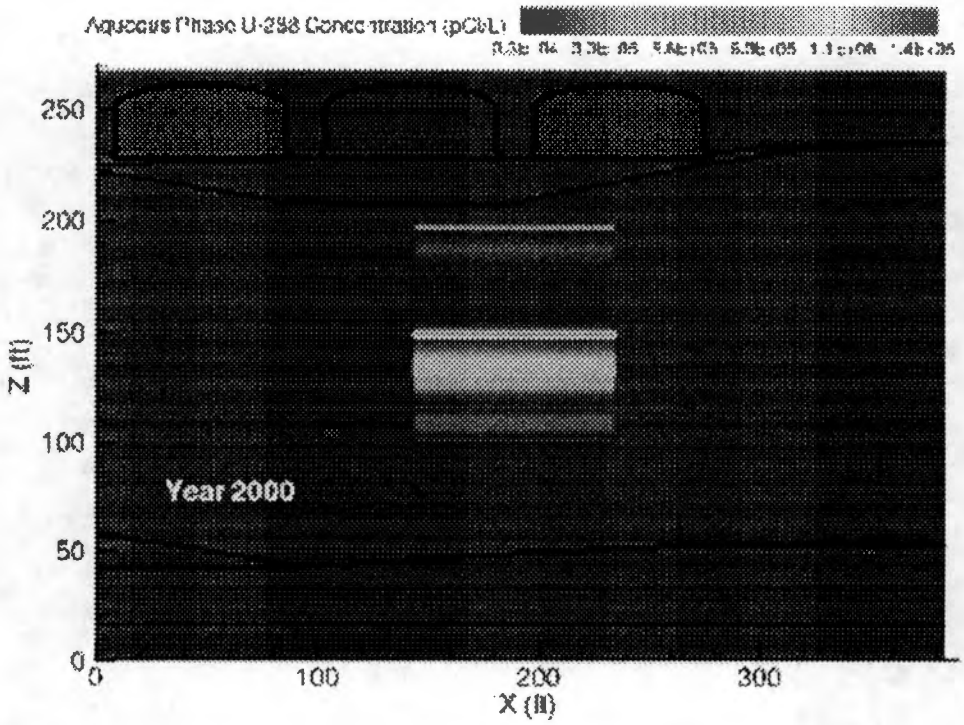

(b)

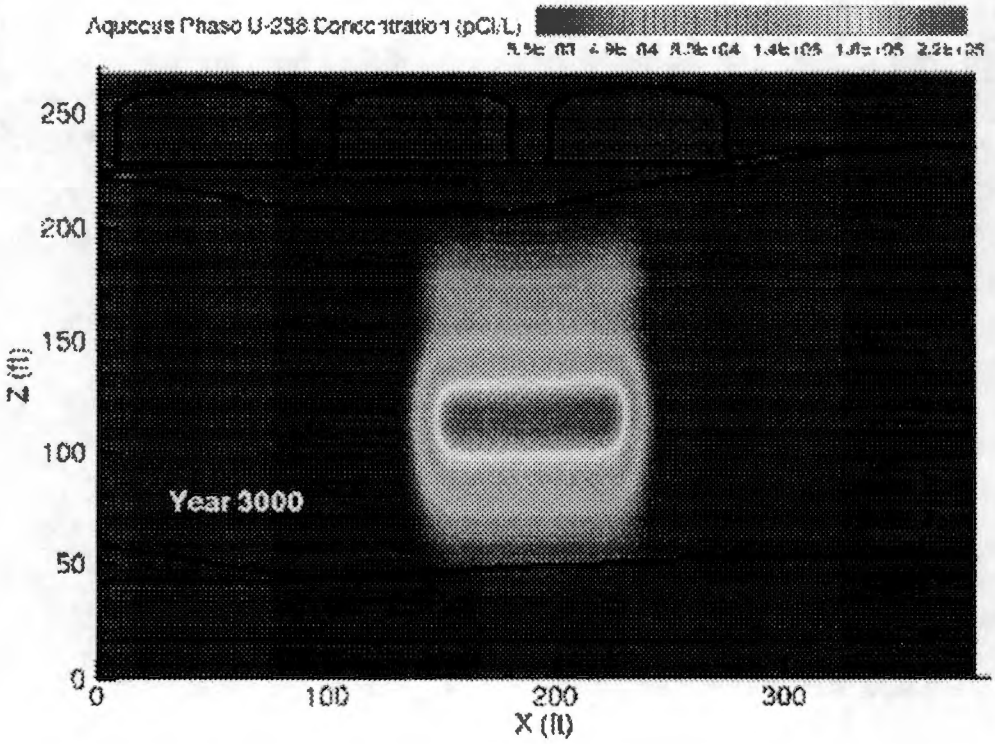

Figure E1.15. Case 5 (Alternate Inventory) Aqueous Technetium-99 Concentration Distributions at (a) Year 2000 and (b) Year 3000

(a)

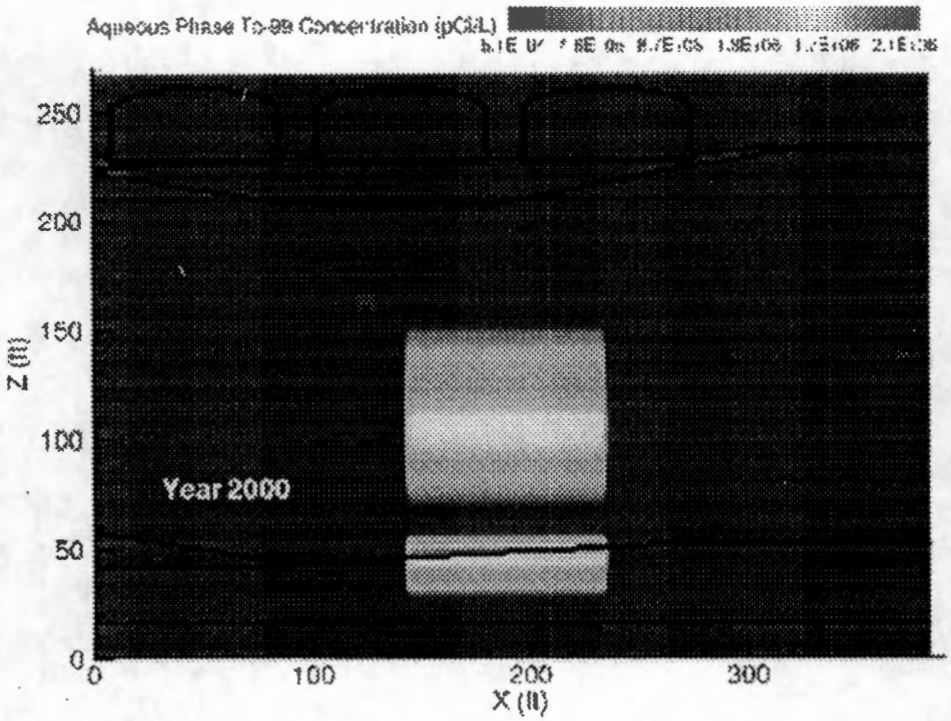

(b)

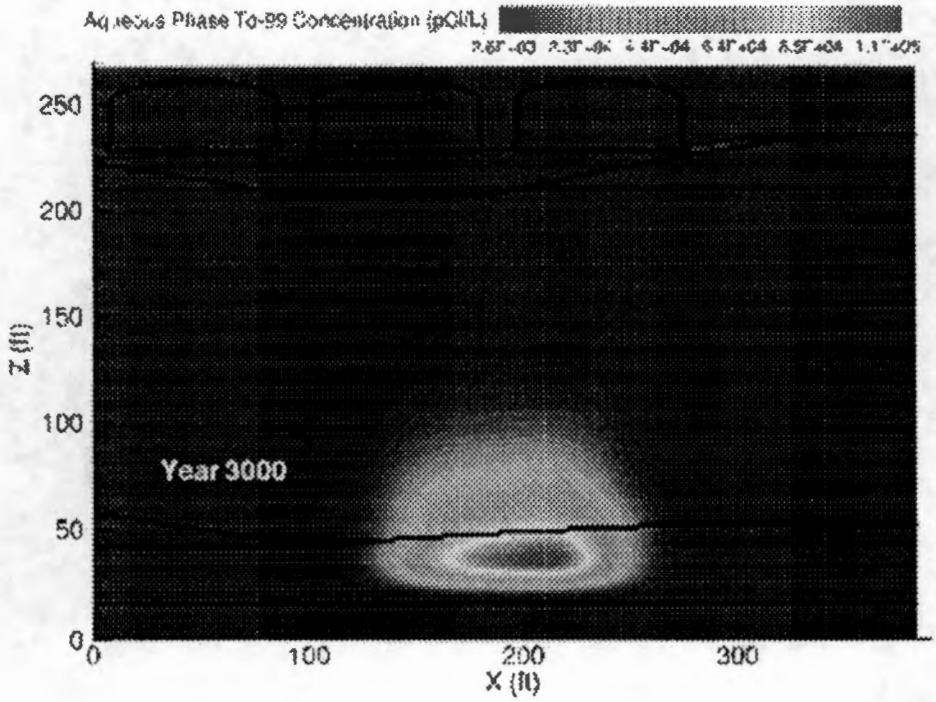

Figure E1.16. Case 5 (Alternate Inventory) Aqueous Nitrate Concentration Distributions at (a) Year 2000 and (b) Year 3000

(a)

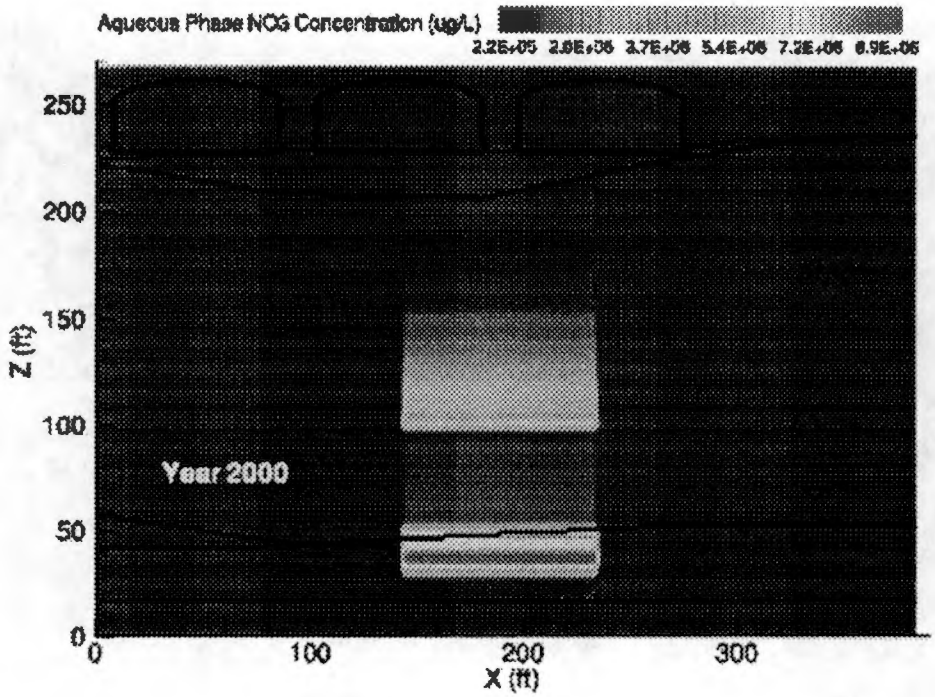

(b)

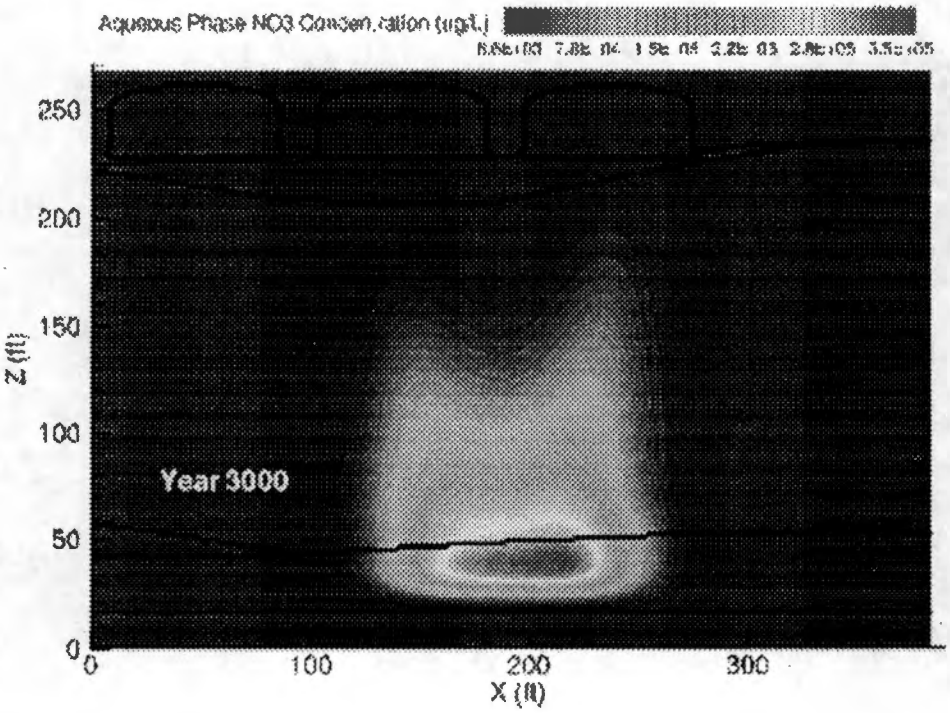

E1.6.0 CASE 6: ALTERNATE INVENTORY DISTRIBUTION WITH INTERIM BARRIER

This scenario involves simulating flow and transport for the cross-section through tanks BX-108, BX-105, and BX-102, considering initial recharge rate of 100 mm/yr, placement of an interim barrier at year 2010, a closure barrier at year 2040 (i.e., the interim barrier replaced by the closure barrier), no water line leak, a Kd of 0.6 mL/g for uranium-238, and an inventory distribution that is centered between tanks BX-105 and BX-102.

Figure E1.17. Case 6 (Alternate Inventory with Interim Barrier) Uranium-238 Aqueous Concentration Distribution at Year 3000

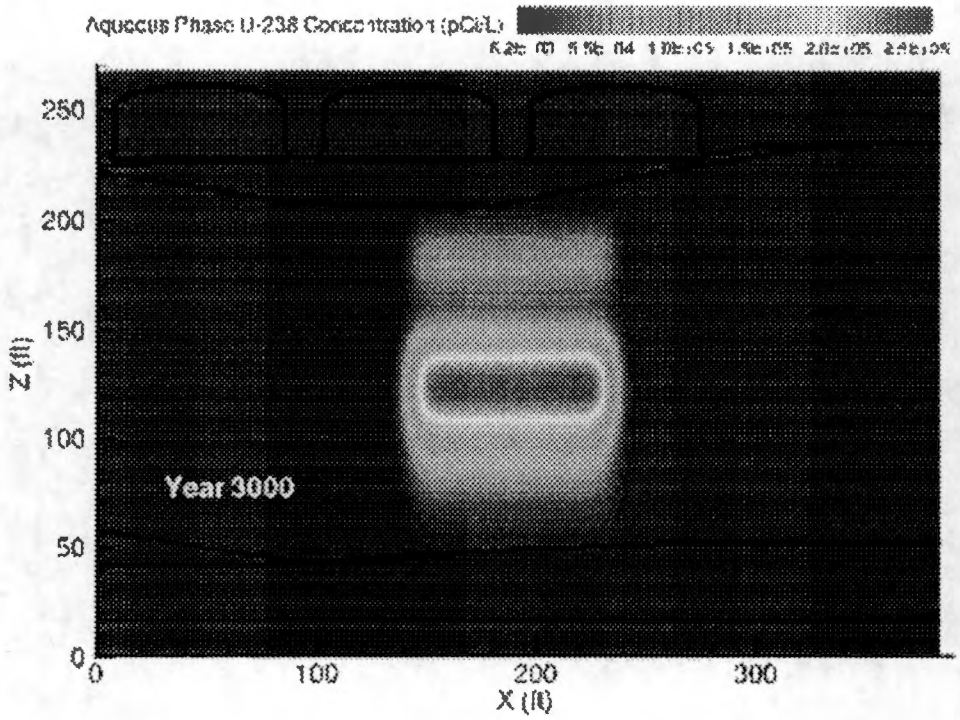

Figure E1.18. Case 6 (Alternate Inventory with Interim Barrier) Aqueous (a) Technetium-99 and (b) Nitrate Concentration Distributions at Year 3000

(a)

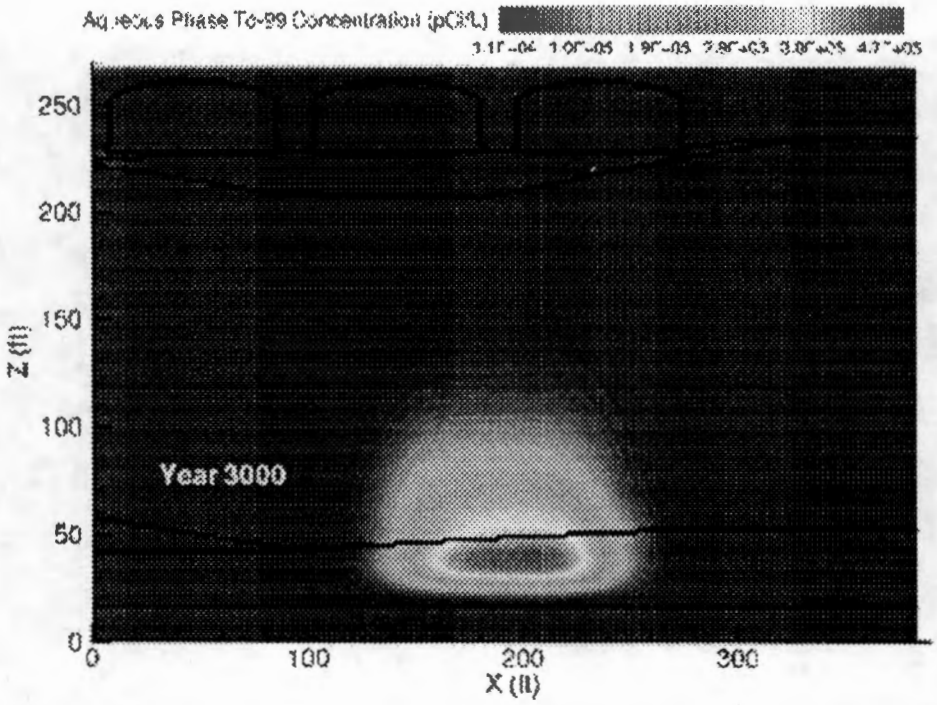

(b)

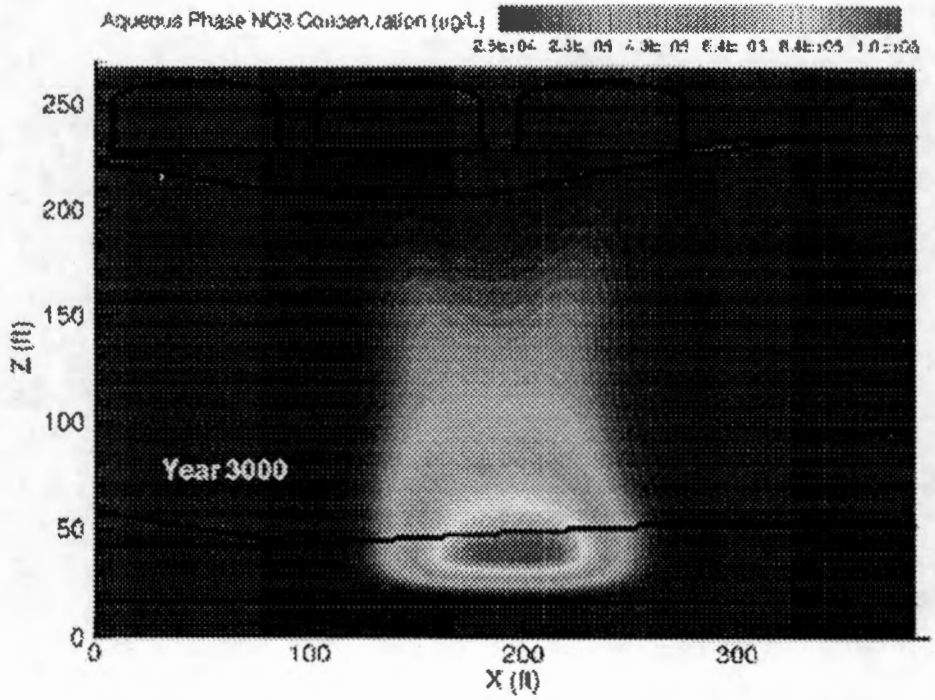

E1.7.0 CASE 7: BASE CASE WITH 50 MM/YR METEORIC RECHARGE

This scenario involves simulating flow and transport for the cross-section through tanks BX-108, BX-105, and BX-102, considering initial recharge rate of 50 mm/yr, no water line leak, no interim barrier until closure at year 2040, a Kd of 0.6 mL/g for uranium-238, and an inventory distribution that extends east of tank BX-102 to the BX tank farm fence line boundary.

Figure E1.19. Case 7 (50 mm/yr Recharge) Aqueous Phase Saturation Distributions at (a) Year 2000 and (b) Year 3000

(a)

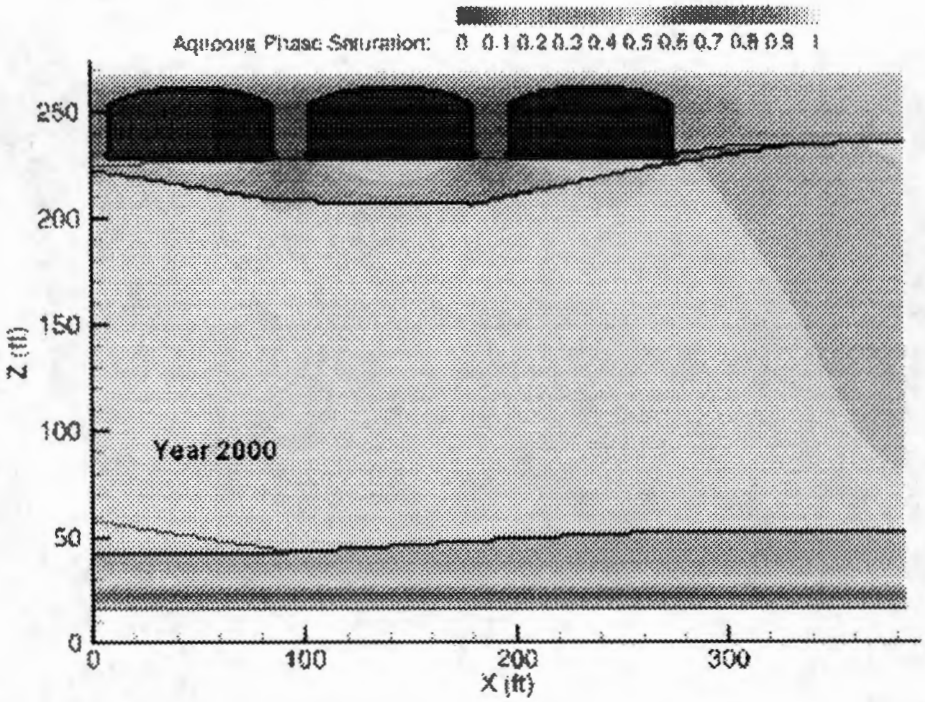

(b)

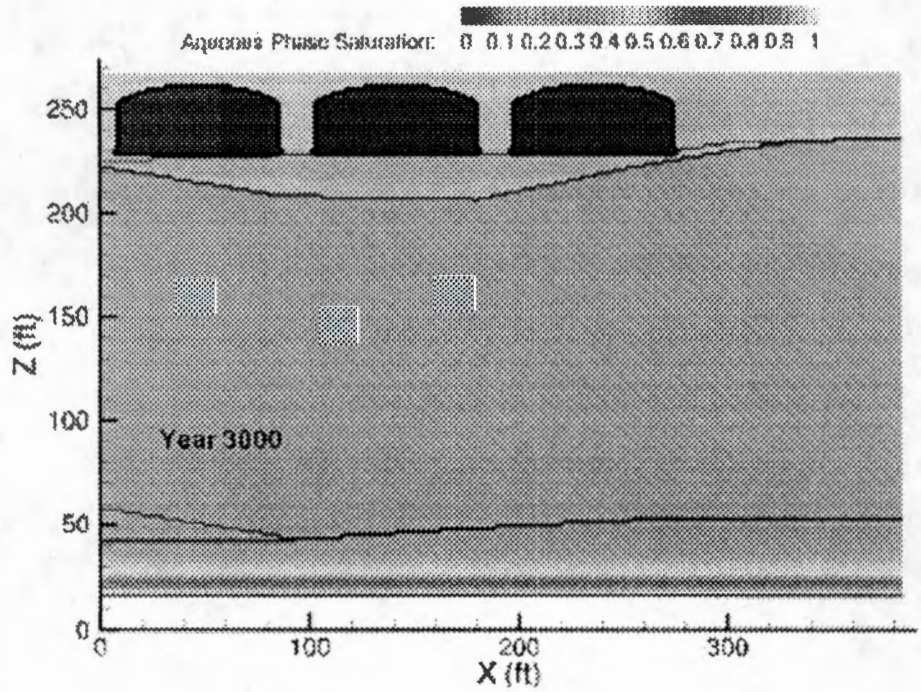

Figure E1.20. Case 7 (50 mm/yr Recharge) Uranium-238 Aqueous Concentration Distribution at Year 3000

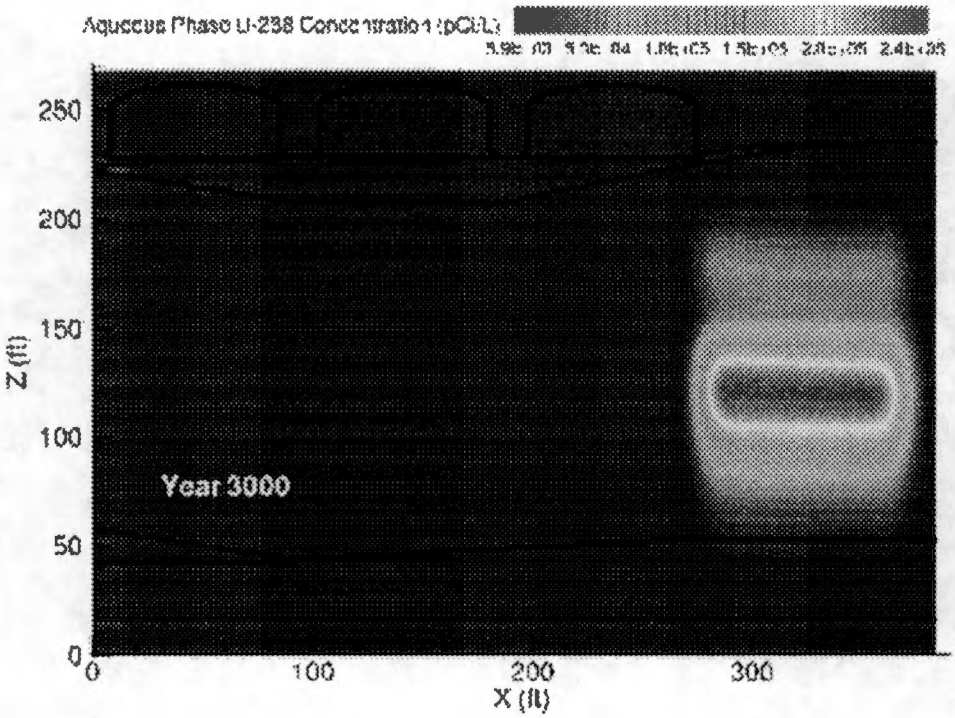

Figure E1.21. Case 7 (50 mm/yr Recharge) Aqueous (a) Technetium-99 and (b) Nitrate Concentration Distributions at Year 3000

(a)

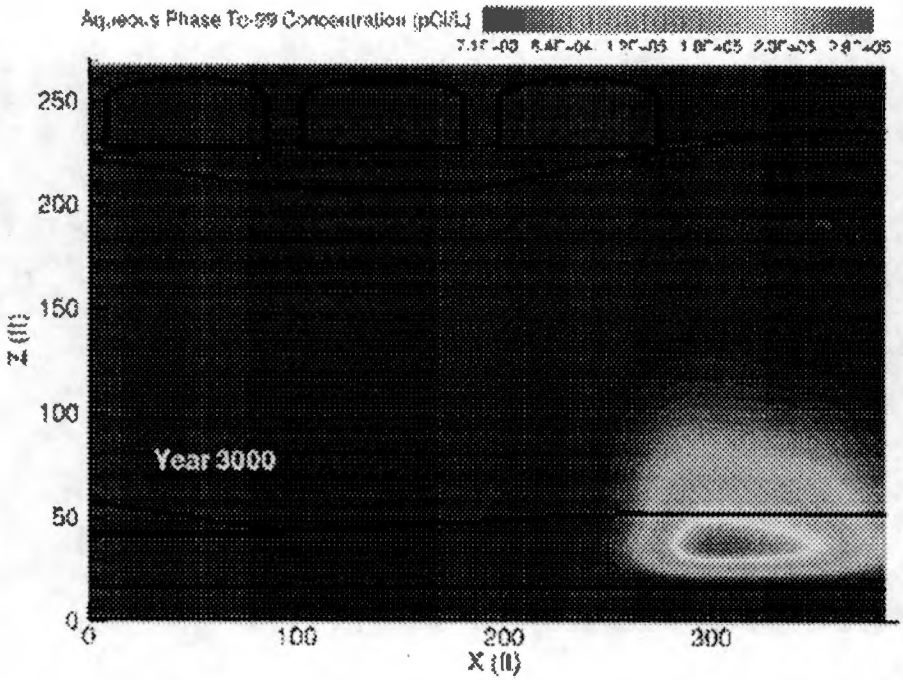

(b)

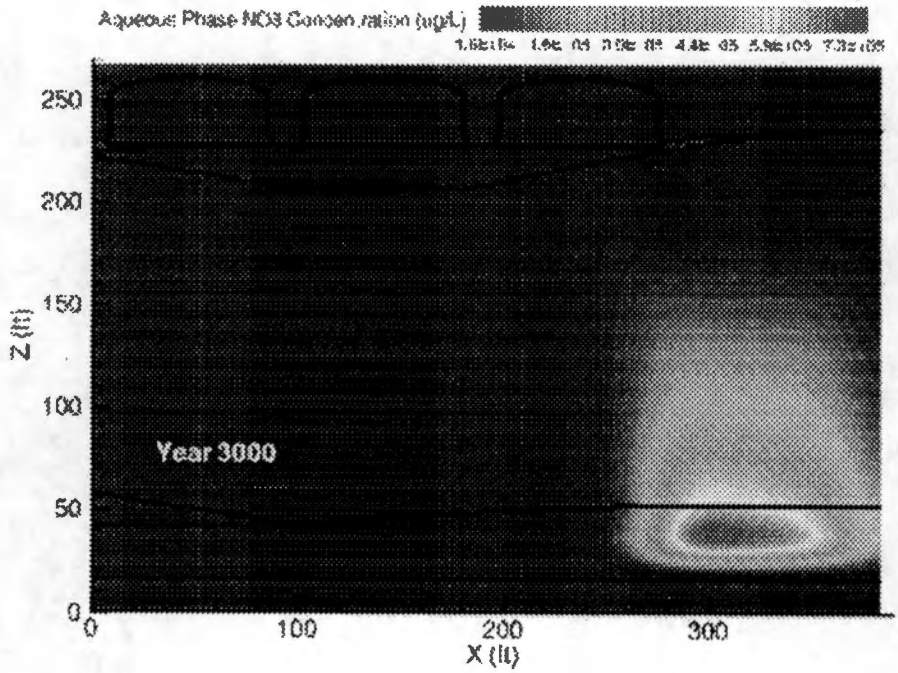

E1.8.0 CASE 8: BASE CASE WITH 30 MM/YR METEORIC RECHARGE

This scenario involves simulating flow and transport for the cross-section through tanks BX-108, BX-105, and BX-102, considering initial recharge rate of 30 mm/yr, no water line leak, no interim barrier until closure at year 2040, a Kd of 0.6 mL/g for uranium-238, and an inventory distribution that extends east of tank BX-102 to the BX tank farm fence line boundary.

Figure E1.22. Case 8 (30 mm/yr Recharge) Aqueous Phase Saturation Distributions at (a) Year 2000 and (b) Year 3000

(a)

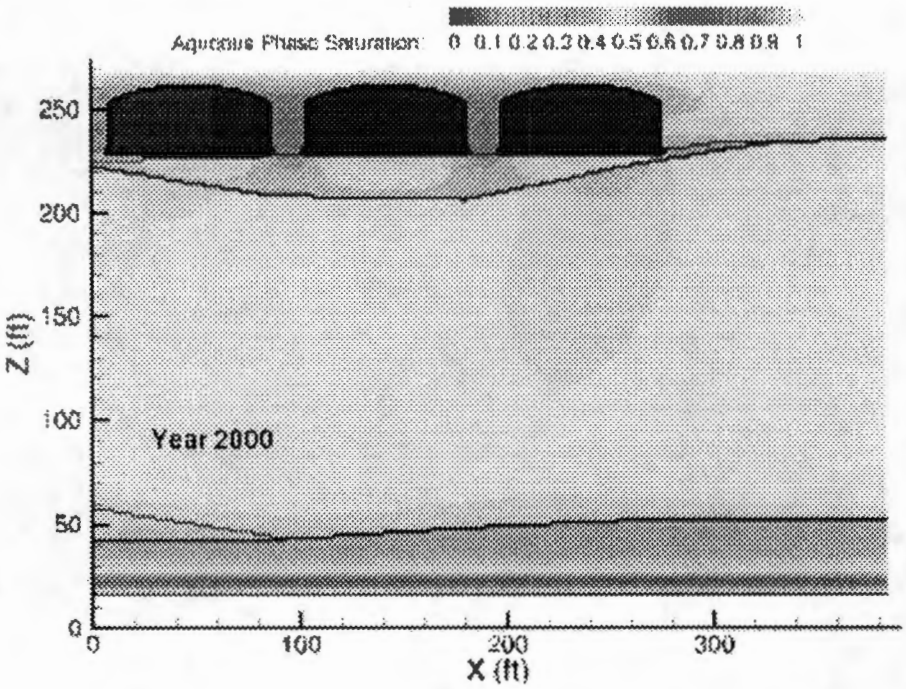

(b)

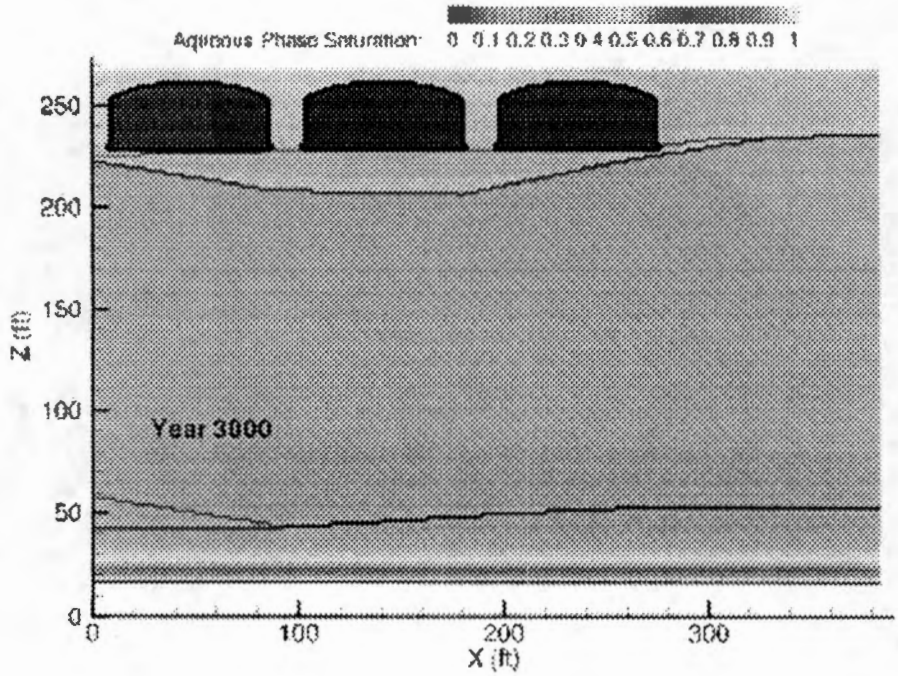

Figure E1.23. Case 8 (30 mm/yr Recharge) Uranium-238 Aqueous Concentration Distribution at Year 3000

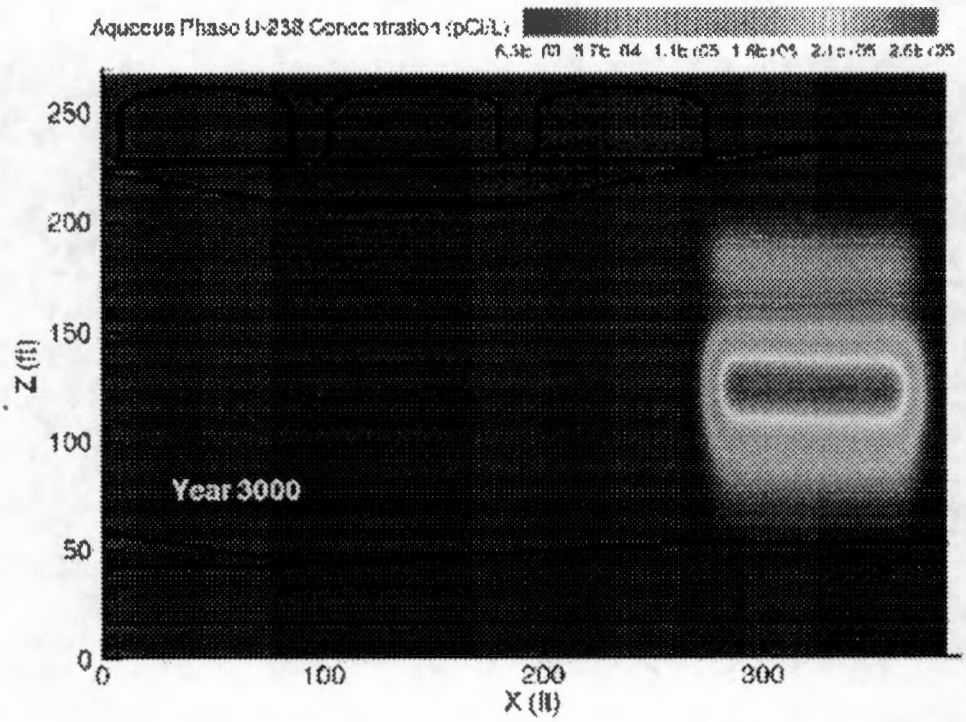

Figure E1.24. Case 8 (30 mm/yr Recharge) Aqueous (a) Technetium-99 and (b) Nitrate Concentration Distributions at Year 3000

(a)

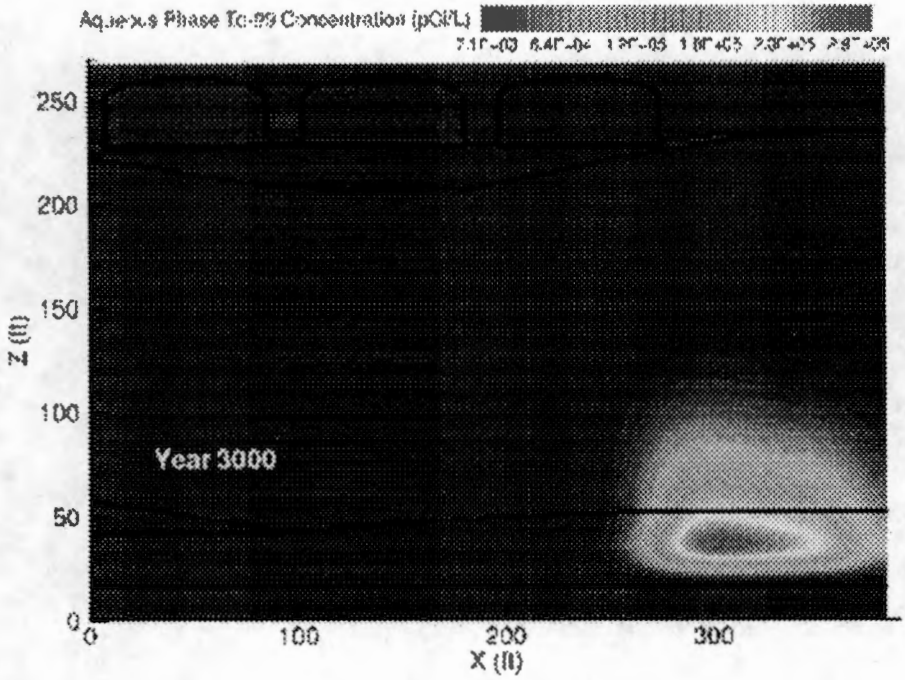

(b)

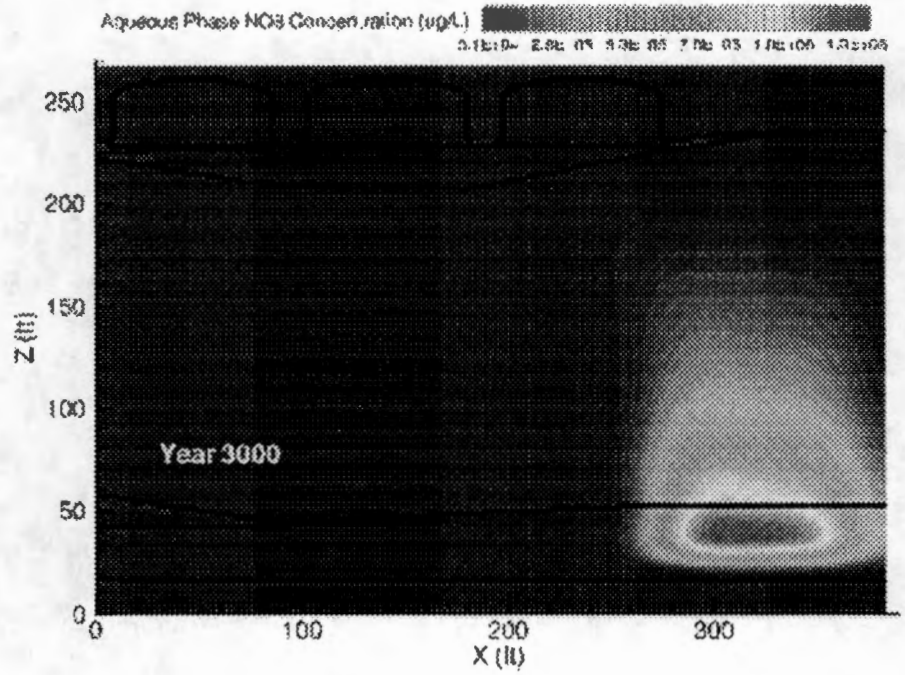

E1.9.0 CASE 9: BASE CASE WITH 10 MM/YR METEORIC RECHARGE

This scenario involves simulating flow and transport for the cross-section through tanks BX-108, BX-105, and BX-102, considering initial recharge rate of 10 mm/yr, no water line leak, no interim barrier until closure at year 2040, a Kd of 0.6 mL/g for uranium-238, and an inventory distribution that extends east of tank BX-102 to BX tank farm fence line boundary.

Figure E1.25. Case 9 (10 mm/yr Recharge) Aqueous Phase Saturation Distributions at (a) Year 2000 and (b) Year 3000

(a)

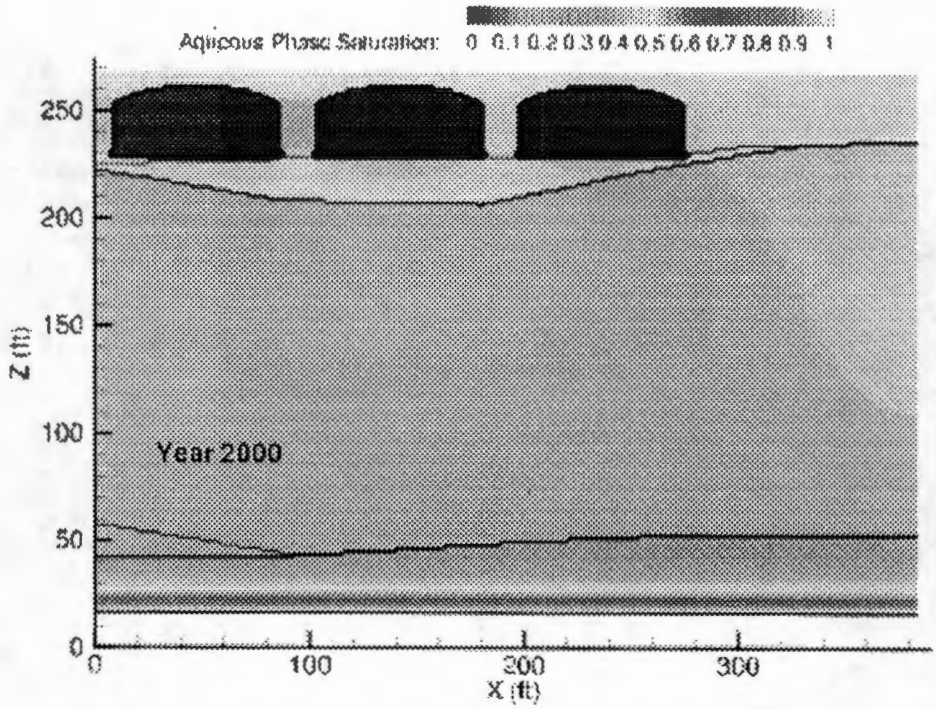

(b)

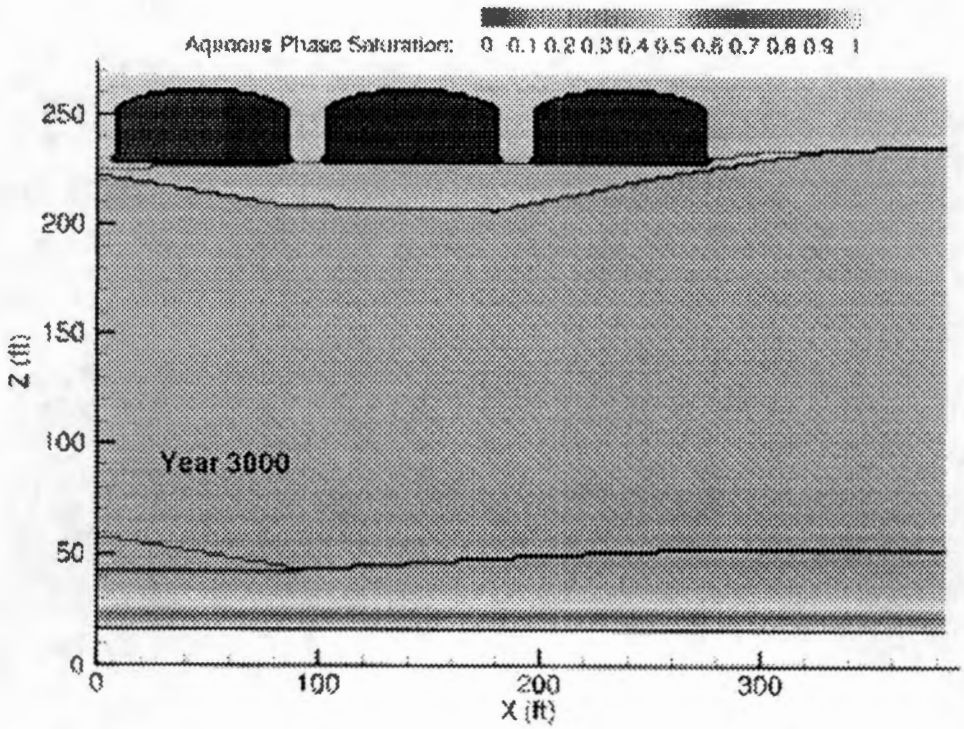

Figure E1.26. Case 9 (10 mm/yr Recharge) Uranium-238 Aqueous Concentration Distribution at Year 3000

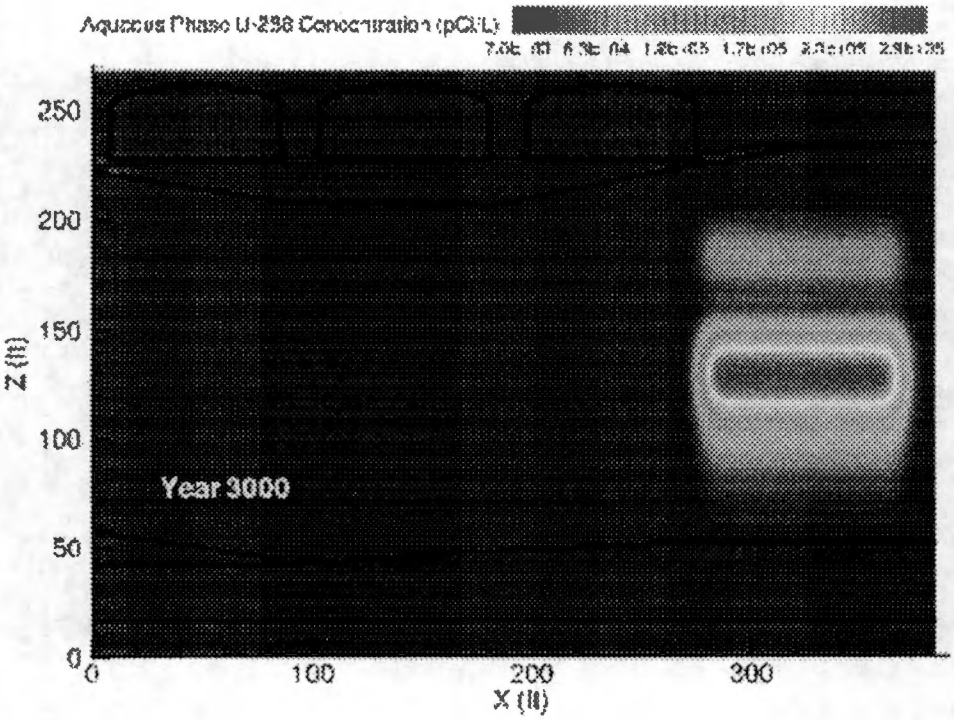

Figure E1.27. Case 9 (10 mm/yr Recharge) Aqueous (a) Technetium-99 and (b) Nitrate Concentration Distributions at Year 3000

(a)

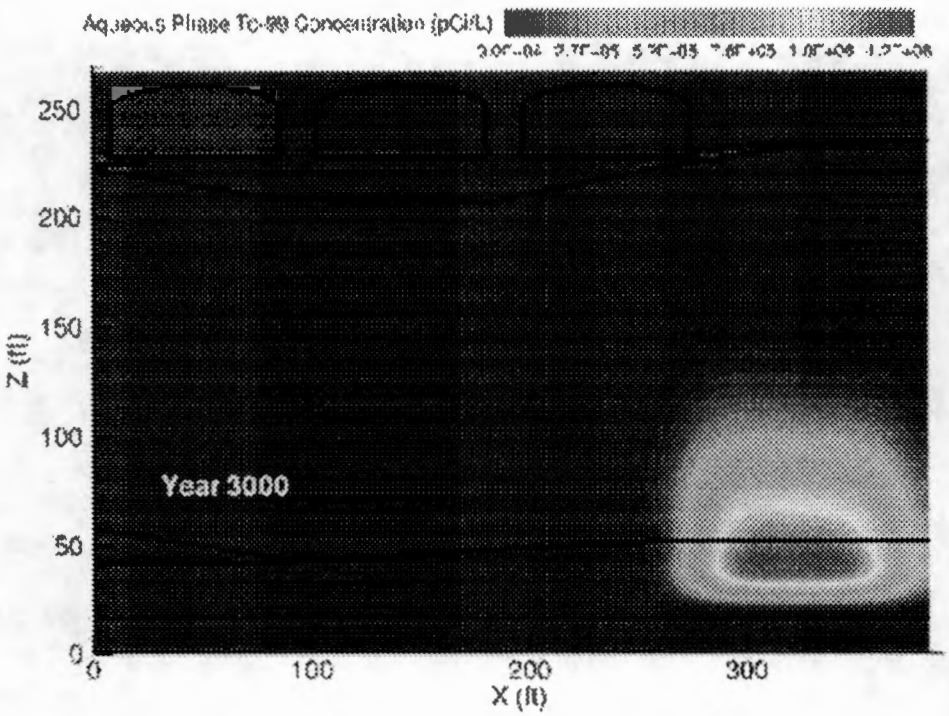

(b)

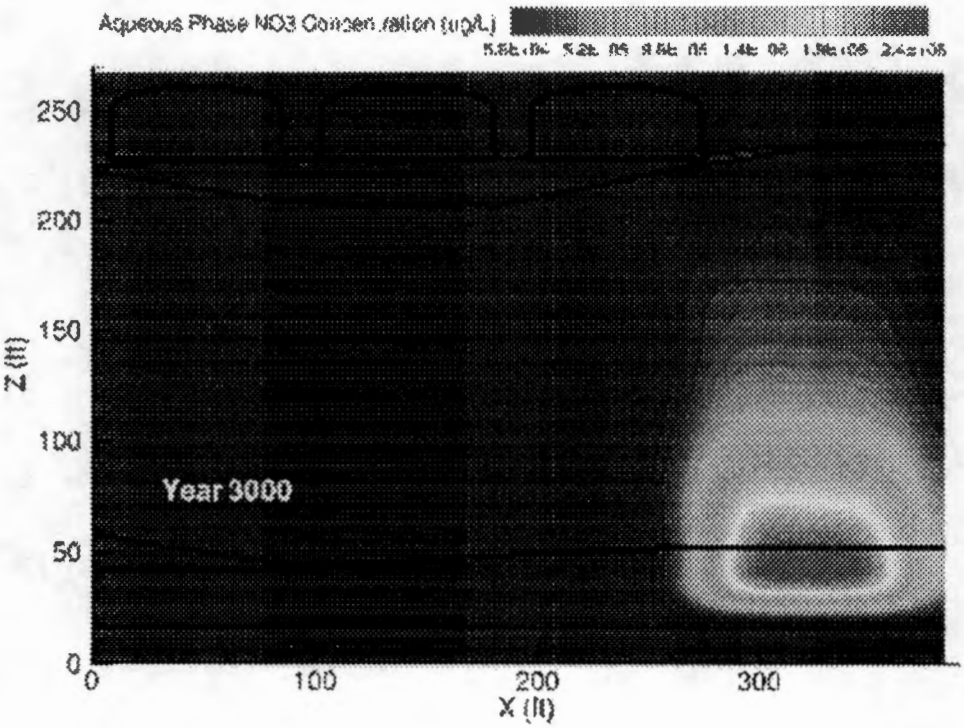

E1.10.0 CASE 10: BASE CASE WITH Kd = 0.1 ML/G FOR URANIUM-238

This scenario involves simulating flow and transport for the cross-section through tanks BX-108, BX-105, and BX-102, considering initial recharge rate of 100 mm/yr, no interim barrier until closure at year 2040, a partition coefficient (Kd) of 0.1 mL/g for uranium-238, and an inventory distribution that extends east of tank BX-102 to BX tank farm fence line boundary.

Figure E1.28. Case 10 (Uranium-238 K_d=0.1 mL/g) Aqueous Uranium-238 Concentration Distributions at (a) Year 2000 and (b) Year 3000

(a)

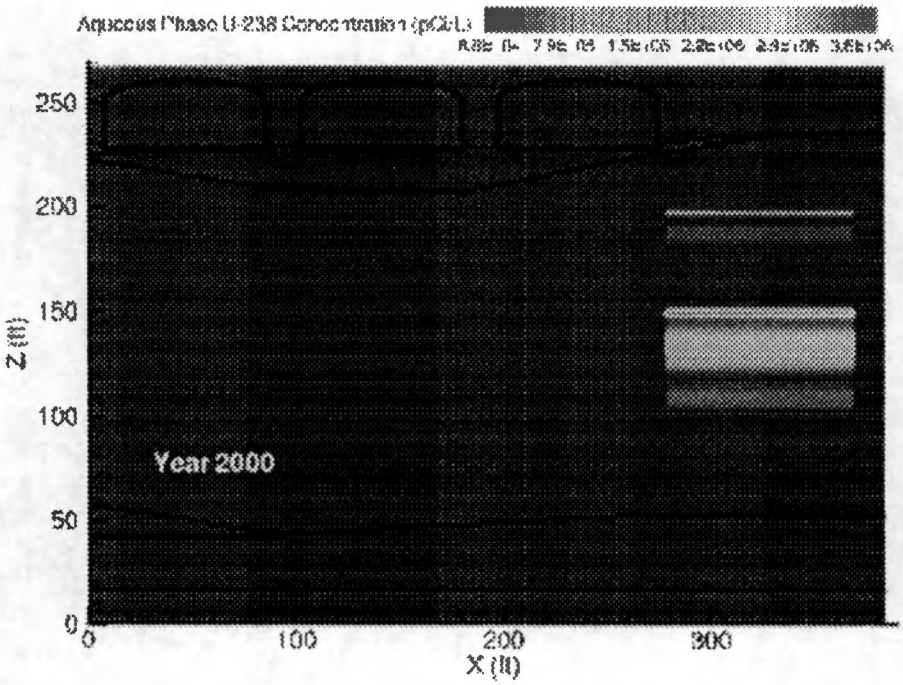

(b)

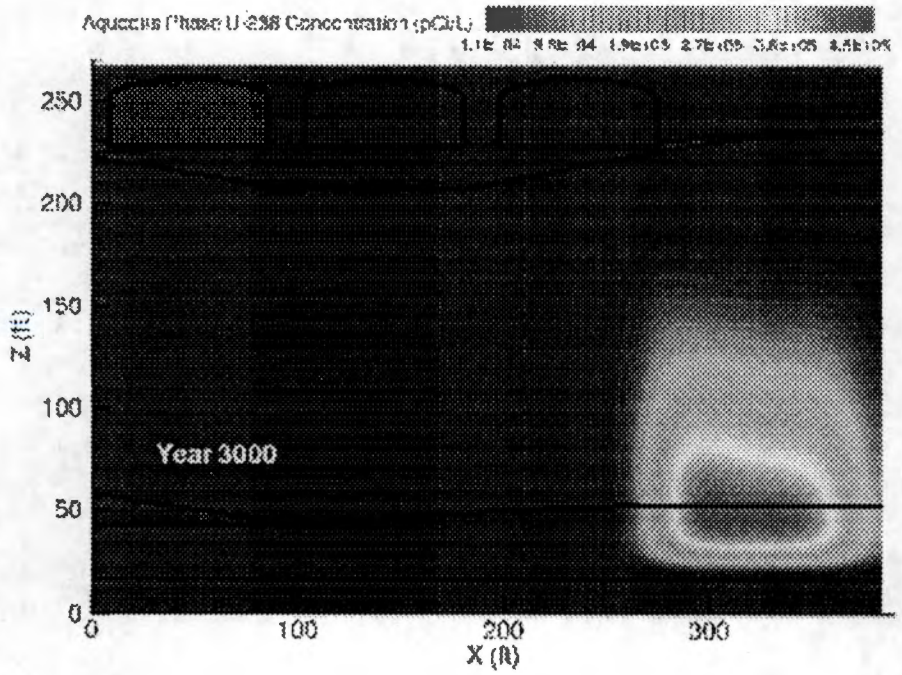

E1.11.0 CASE 11: BASE CASE WITH Kd = 1 ML/G FOR URANIUM-238

This scenario involves simulating flow and transport for the cross-section through tanks BX-108, BX-105, and BX-102, considering initial recharge rate of 100 mm/yr, no interim barrier until closure at year 2040, a partition coefficient (Kd) of 1.0 mL/g for uranium-238, and an inventory distribution that extends east of tank BX-102 to BX tank farm fence line boundary.

Figure E1.29. Case 11 (Uranium-238 K_d=1 mL/g) Aqueous Uranium-238 Concentration Distributions at (a) Year 2000 and (b) Year 3000

(a)

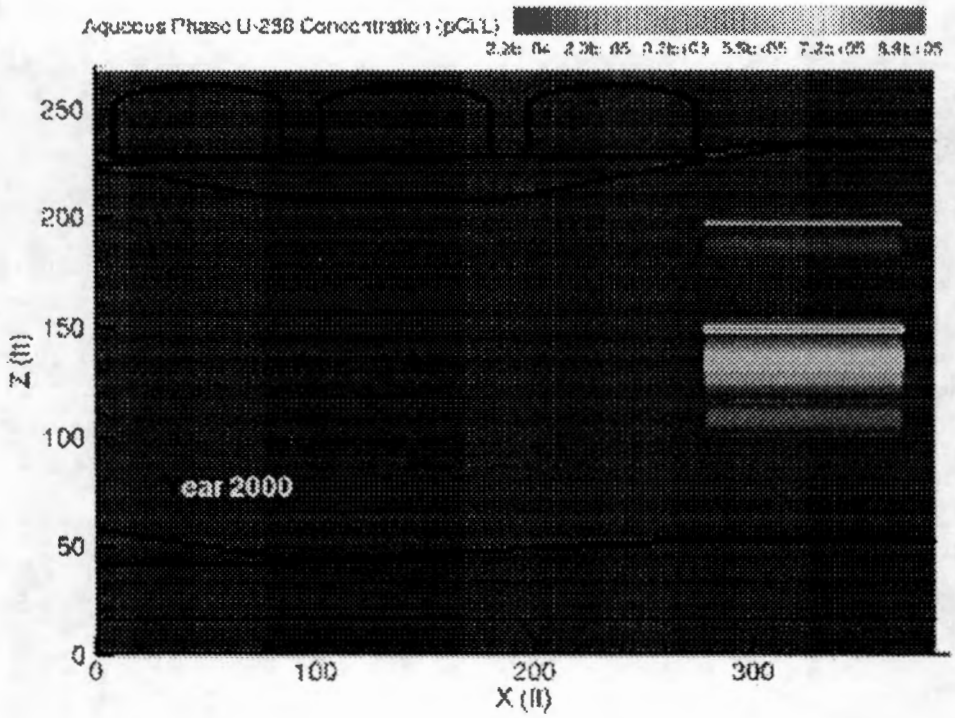

(b)

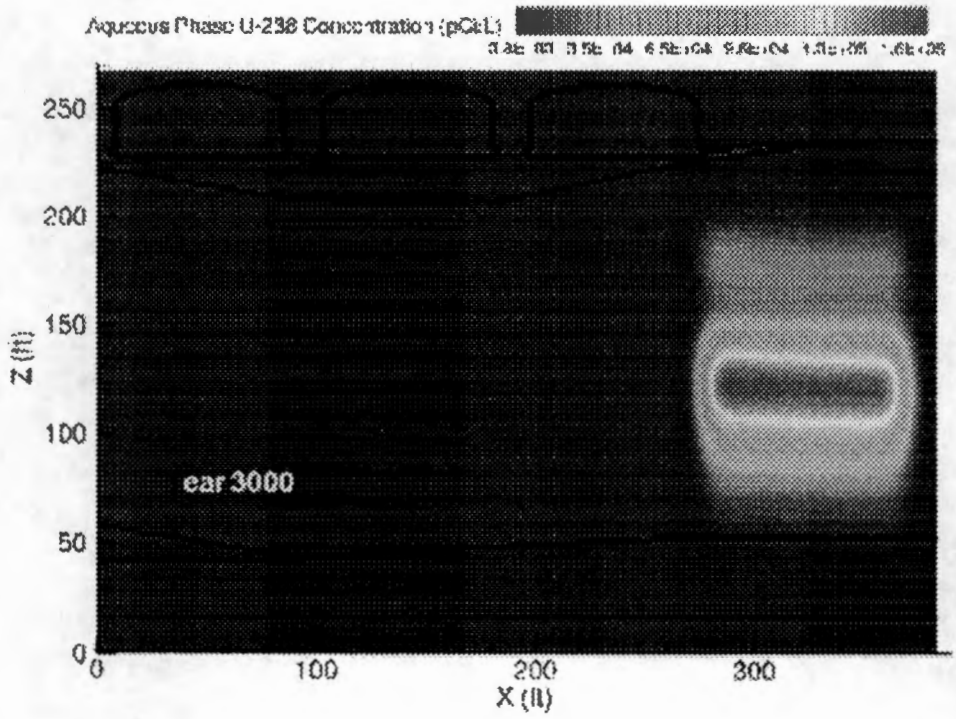

This page intentionally left blank.

ATTACHMENT E2

TRENCH 216-B-38 SATURATION AND CONCENTRATION DISTRIBUTIONS

This page intentionally left blank.

CONTENTS

E2.1.0 CASE 12: TRENCH B-38 WITH 55.4 MM/YR METEORIC RECHARGE E2-1

E2.2.0 CASE 13: TRENCH B-38 WITH 100 MM/YR METEORIC RECHARGE E2-8

E2.3.0 CASE 14: TRENCH B-38 WITH 100 MM/YR METEORIC RECHARGE AND DELAYED CLOSURE BARRIER E2-15

FIGURES

E2.1. Case 12 (55.4 mm/yr) Aqueous Phase Saturation Distribution at Year 1954 ..... E2-2
E2.2. Case 12 (55.4 mm/yr) Aqueous Phase Saturation Distributions at (a) Year 1955 and (b) Year 3000 ..... E2-3
E2.3. Case 12 (55.4 mm/yr) Aqueous Uranium-238 Concentration Distributions at (a) Year 1955 and (b) Year 3000 ..... E2-4
E2.4. Case 12 (55.4 mm/yr) Technetium-99 Concentration Distributions at (a) Year 1955 and (b) Year 2000 ..... E2-5
E2.5. Case 12 (55.4 mm/yr) Technetium-99 Concentration Distributions at (a) Year 2110 and (b) Year 2210 ..... E2-6
E2.6. Case 12 (55.4 mm/yr) Technetium-99 Concentration Distributions at (a) Year 2510 and (b) Year 3000 ..... E2-7
E2.7. Case 13 (100 mm/yr Recharge) Aqueous Phase Saturation Distribution at Year 1954 ..... E2-9
E2.8. Case 13 (100 mm/yr Recharge) Aqueous Phase Saturation Distributions at (a) Year 1955 and (b) Year 3000 ..... E2-10
E2.9. Case 13 (100 mm/yr Recharge) Aqueous Uranium-238 Concentration Distributions at (a) Year 1955 and (b) Year 3000 ..... E2-11
E2.10. Case 13 (100 mm/yr Recharge) Technetium-99 Concentration Distributions at (a) Year 1955 and (b) Year 2000 ..... E2-12
E2.11. Case 13 (100 mm/yr Recharge) Technetium-99 Concentration Distributions at (a) Year 2110 and (b) Year 2210 ..... E2-13
E2.12. Case 13 (100 mm/yr Recharge) Technetium-99 Concentration Distributions at (a) Year 2510 and (b) Year 3000 ..... E2-14
E2.13. Case 14 (100 mm/yr Recharge) with Delayed Closure Barrier Aqueous Phase Saturation Distribution at Year 3000 ..... E2-16
E2.14. Case 14 (100 mm/yr Recharge) with Delayed Closure Barrier Uranium-238 Aqueous Concentration Distribution at Year 3000 ..... E2-16
E2.15. Case 14 (100 mm/yr Recharge) with Delayed Closure Barrier Technetium-99 Concentration Distributions at (a) Year 2110 and (b) Year 2210 ..... E2-17
E2.16. Case 14 (100 mm/yr Recharge) with Delayed Closure Barrier Technetium-99 Concentration Distributions at (a) Year 2510 and (b) Year 3000 ..... E2-18

This page intentionally left blank.

E2.1.0 CASE 12: TRENCH B-38 WITH 55.4 MM/YR METEORIC RECHARGE

This scenario involves simulating flow and transport for a cross-section west of tank BX-11I, considering initial recharge rate of 55.4 mm/yr, a 378,000-gallon leak in 1954, no water line leak, no interim barrier until closure at year 2010, and a unit inventory distribution for a sorbed species (i.e., uranium-238, Kd = 0.6 mL/g) and a non-sorbing species (i.e., technetium-99 and nitrate). The unit inventory results are also scaled to the uranium-238, technetium-99, and nitrate inventory estimates for trench B-38 and all of the B trenches.

Figure E2.1. Case 12 (55.4 mm/yr) Aqueous Phase Saturation Distribution at Year 1954

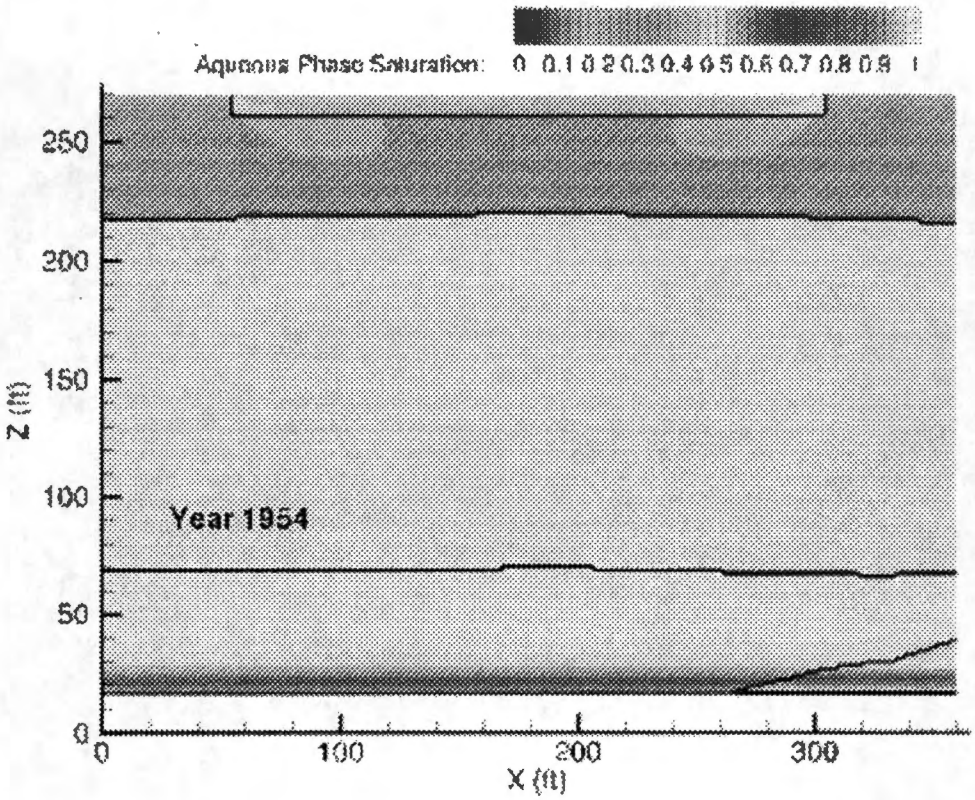

Figure E2.2. Case 12 (55.4 mm/yr) Aqueous Phase Saturation Distributions at (a) Year 1955 and (b) Year 3000

(a)

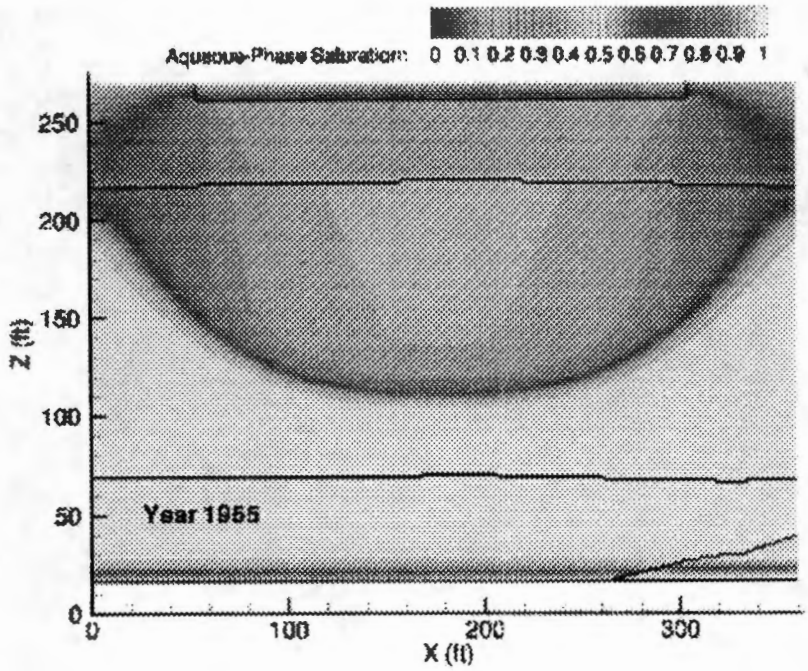

(b)

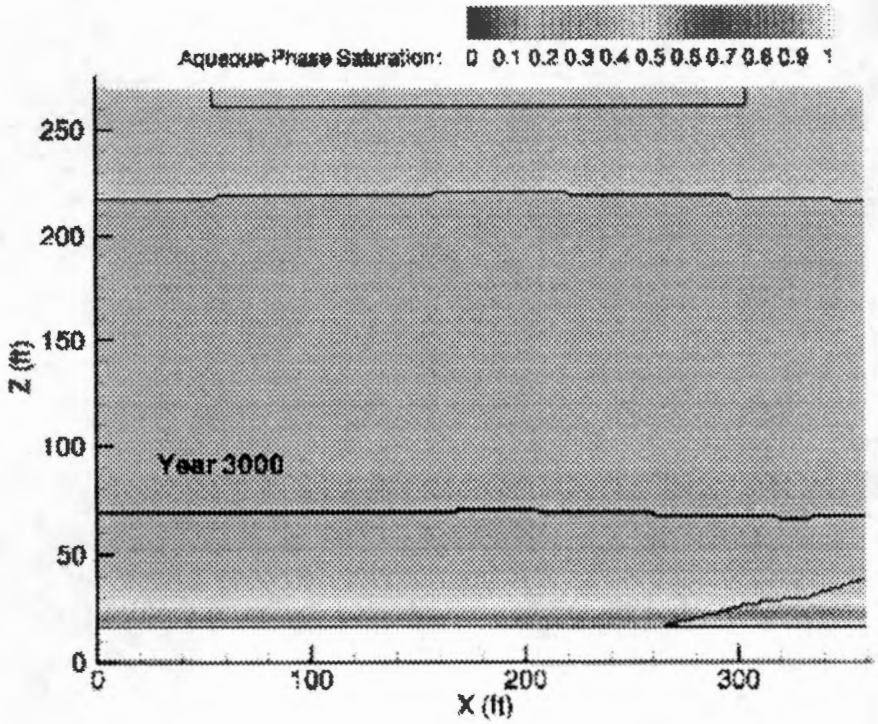

Figure E2.3. Case 12 (55.4 mm/yr) Aqueous Uranium-238 Concentration Distributions at (a) Year 1955 and (b) Year 3000

(a)

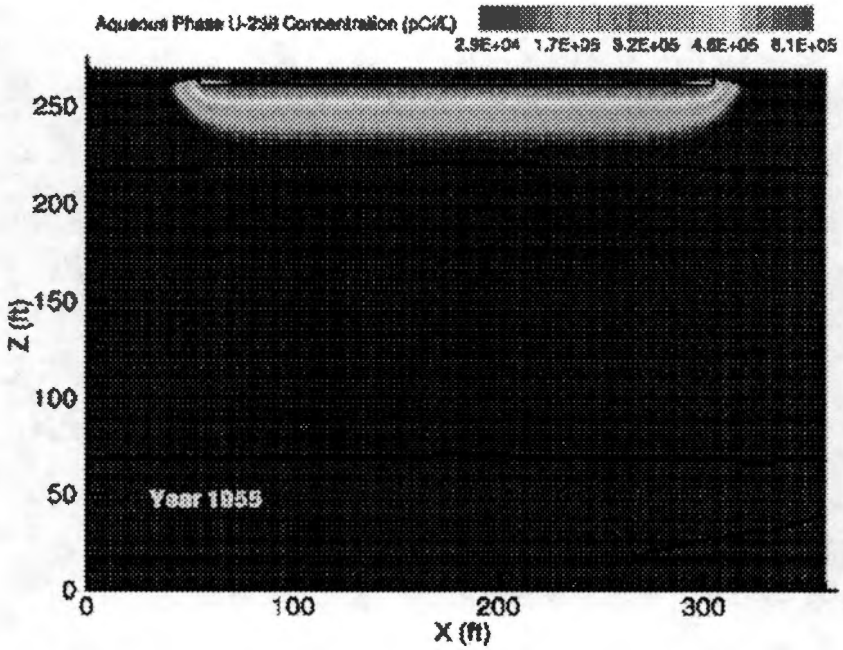

(b)

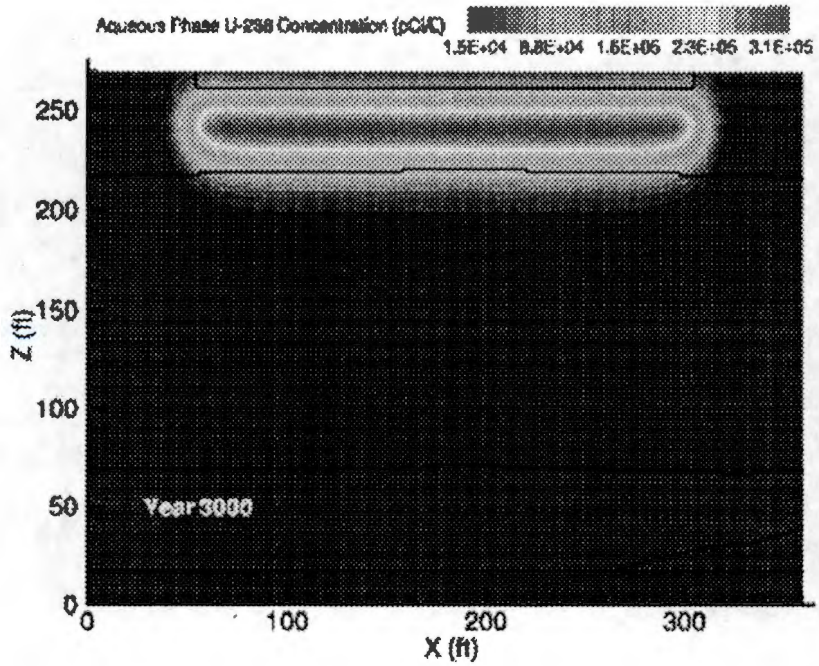

Figure E2.4. Case 12 (55.4 mm/yr) Technetium-99 Concentration Distributions at (a) Year 1955 and (b) Year 2000

(a)

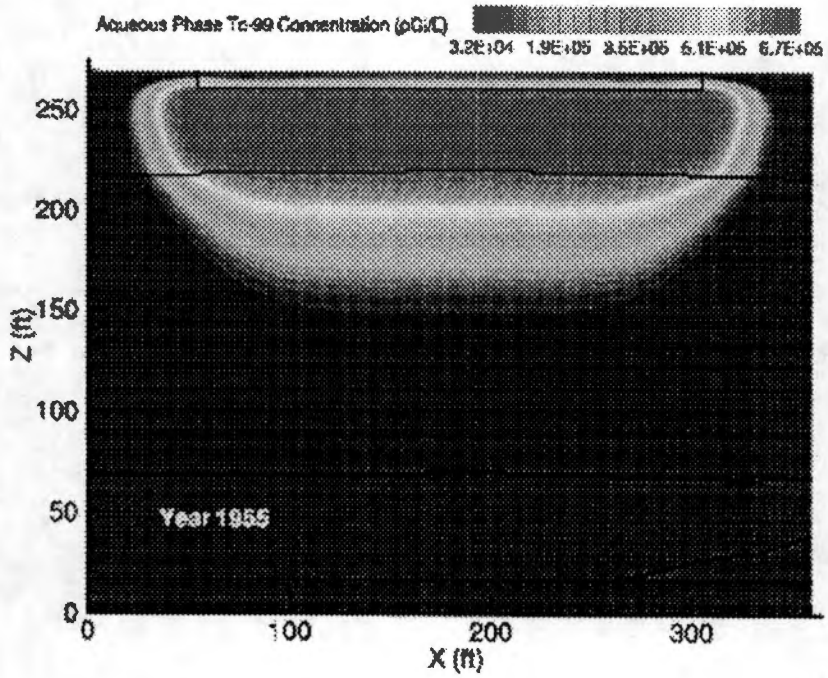

(b)

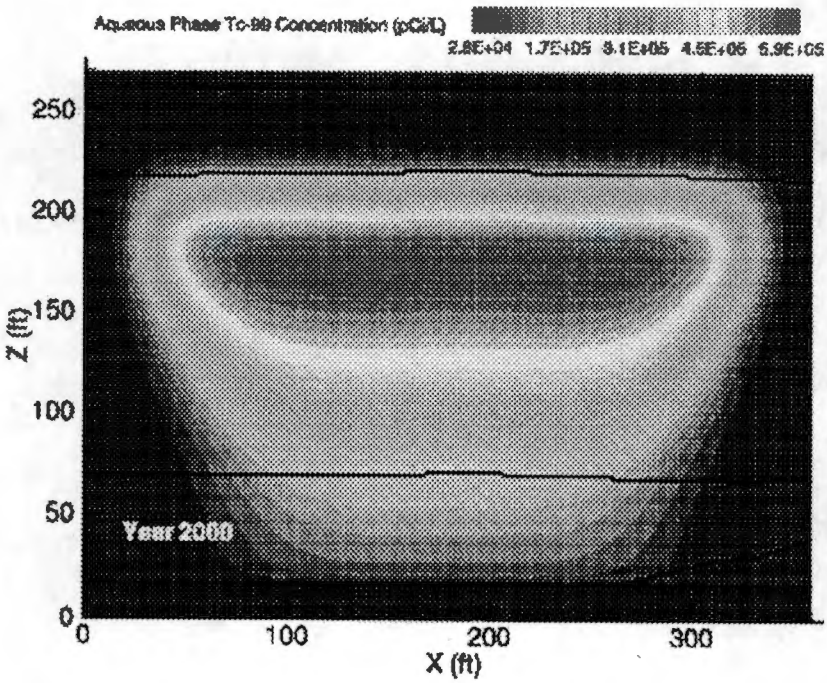

Figure E2.5. Case 12 (55.4 mm/yr) Technetium-99 Concentration Distributions at (a) Year 2110 and (b) Year 2210

(a)

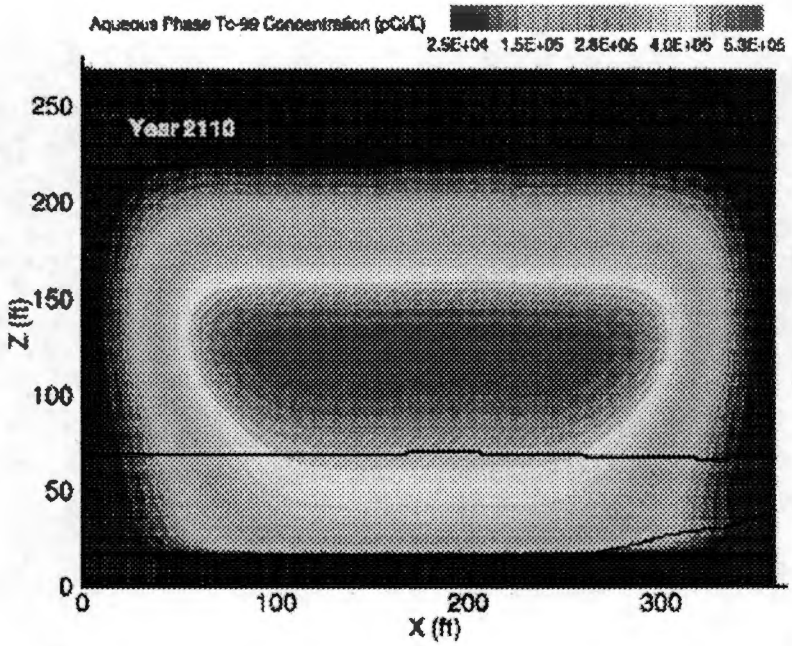

(b)

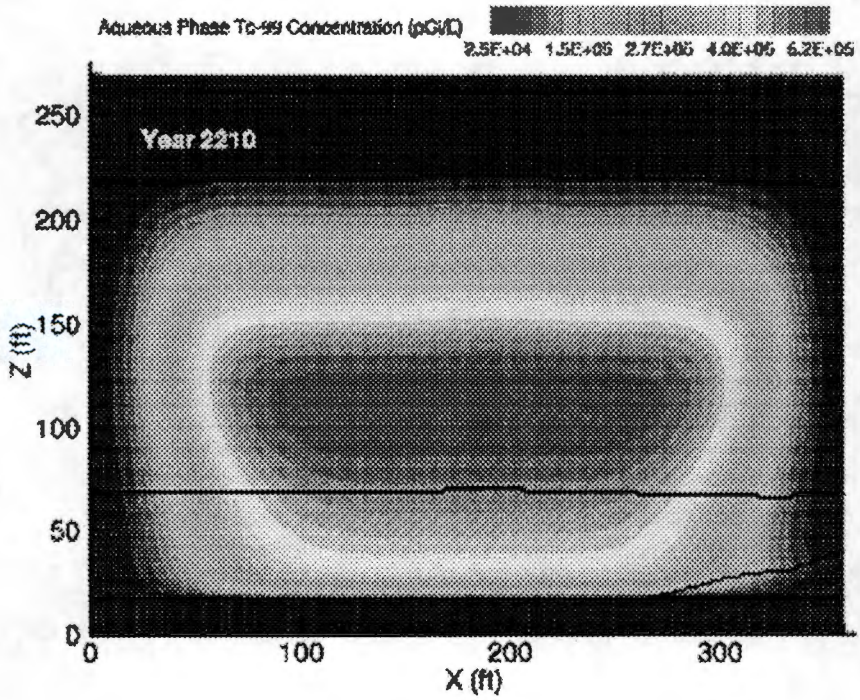

Figure E2.6. Case 12 (55.4 mm/yr) Technetium-99 Concentration Distributions at (a) Year 2510 and (b) Year 3000

(a)

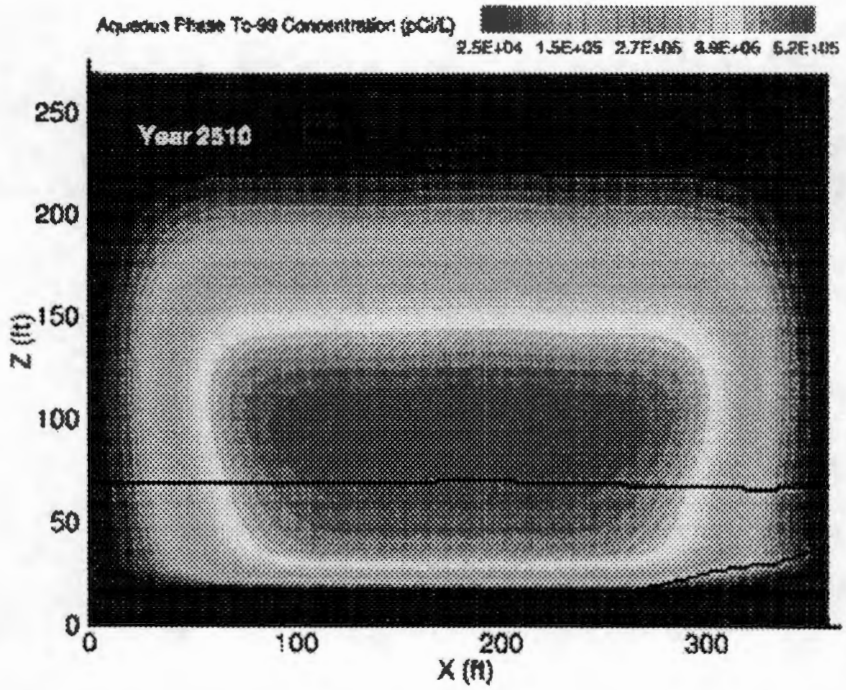

(b)

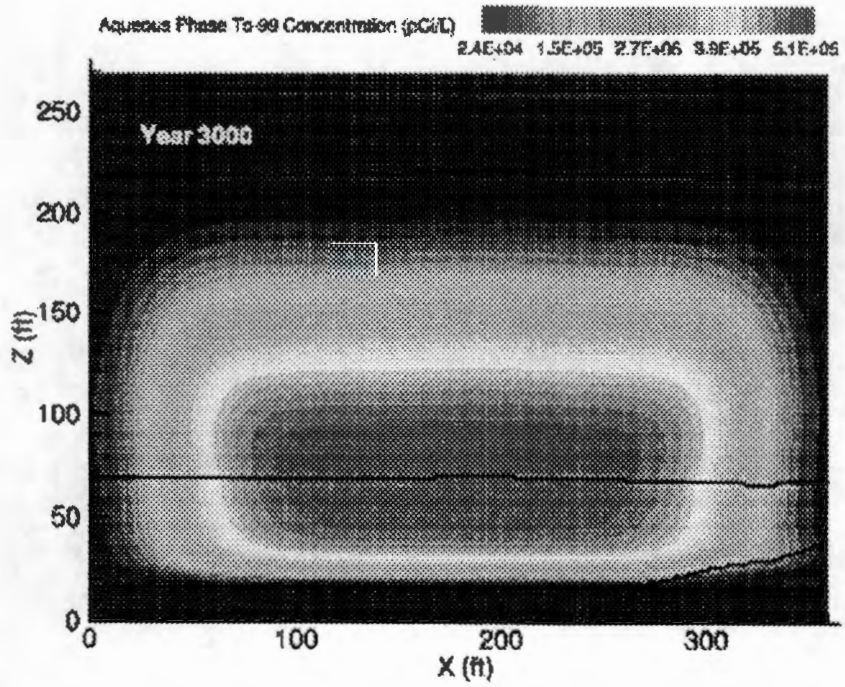

E2.2.0 CASE 13: TRENCH B-38 WITH 100 MM/YR METEORIC RECHARGE

This scenario involves simulating flow and transport for a cross-section west of tank BX-111, considering initial recharge rate of 100 mm/yr, a 378,000-gallon leak in 1954, no interim barrier until closure at year 2010, and a unit inventory distribution for a sorbed species (i.e., uranium-238, Kd = 0.6 mL/g) and a non-sorbing species (i.e., technetium-99 and nitrate). The unit inventory results are also scaled to the uranium-238, technetium-99, and nitrate inventory estimates for trench B-38 and all of the B trenches.

Figure E2.7. Case 13 (100 mm/yr Recharge) Aqueous Phase Saturation Distribution at Year 1954

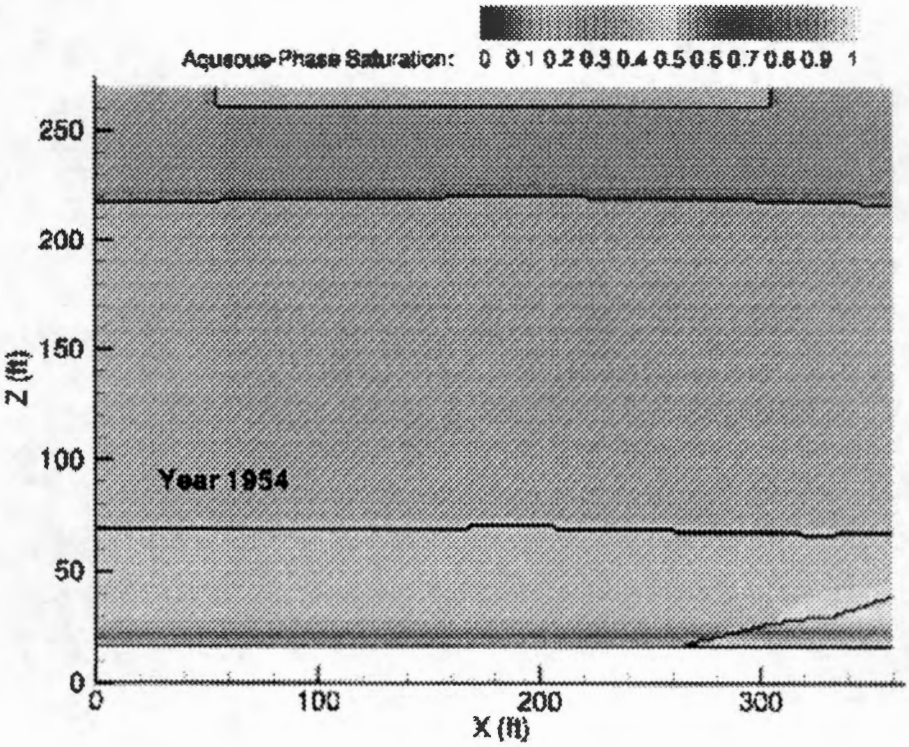

Figure E2.8. Case 13 (100 mm/yr Recharge) Aqueous Phase Saturation Distributions at (a) Year 1955 and (b) Year 3000

(a)

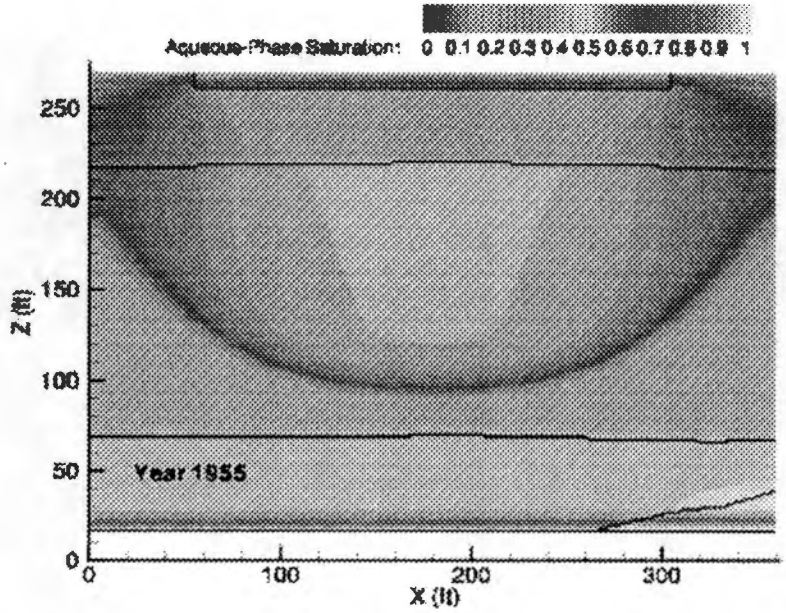

(b)

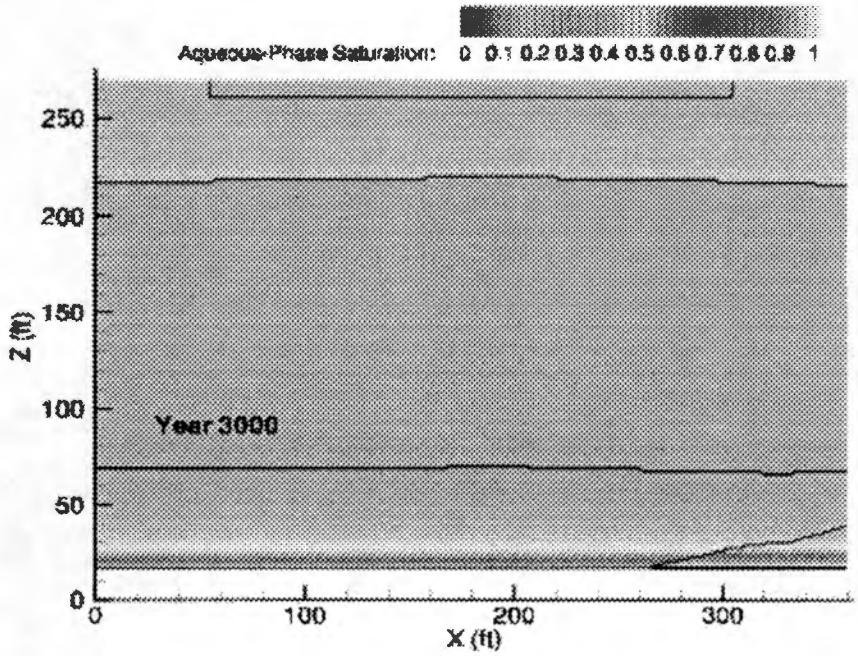

Figure E2.9. Case 13 (100 mm/yr Recharge) Aqueous Uranium-238 Concentration Distributions at (a) Year 1955 and (b) Year 3000

(a)

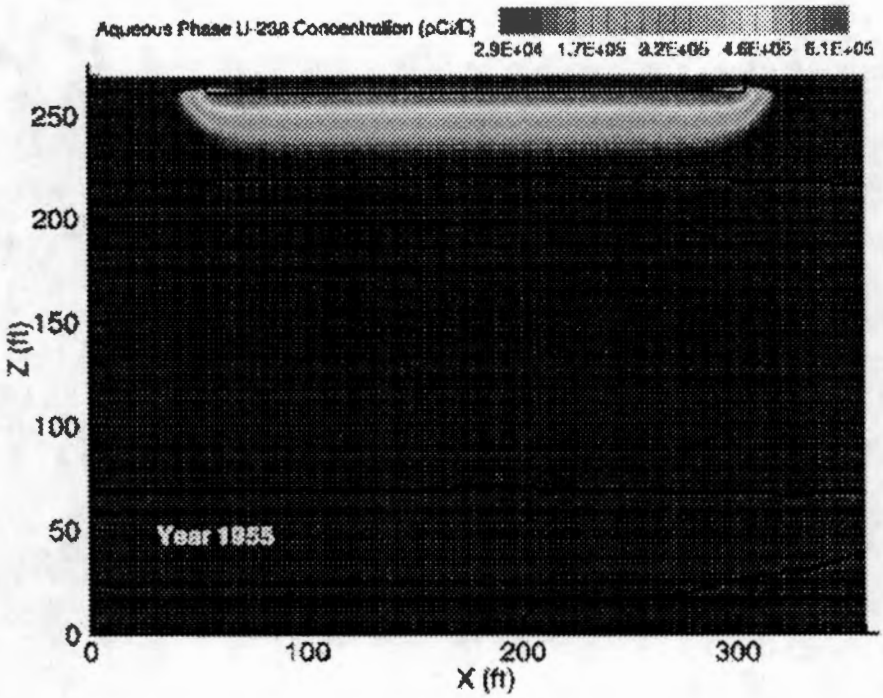

(b)

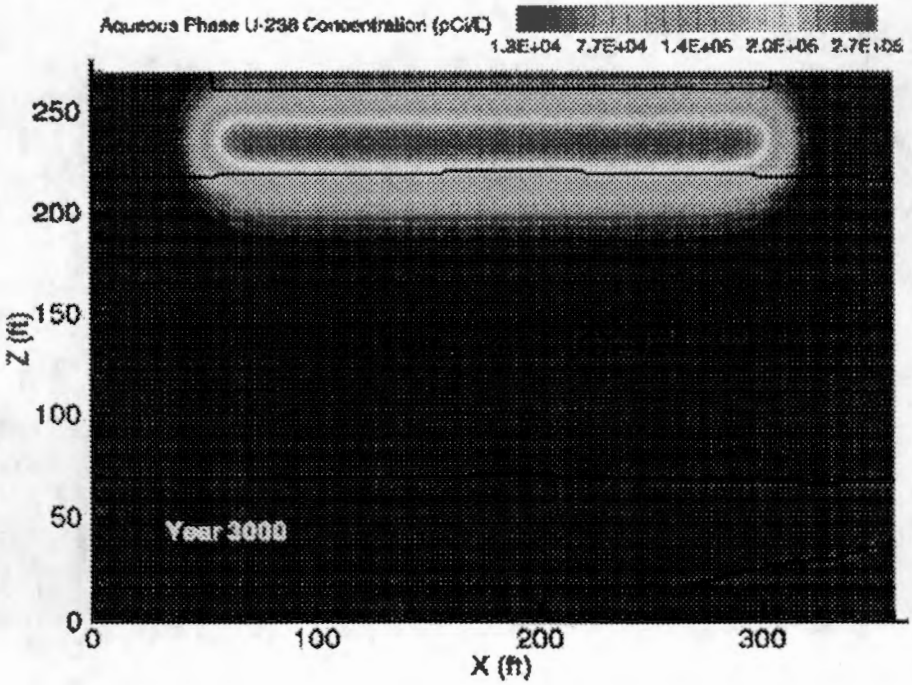

Figure E2.10. Case 13 (100 mm/yr Recharge) Technetium-99 Concentration Distributions at (a) Year 1955 and (b) Year 2000

(a)

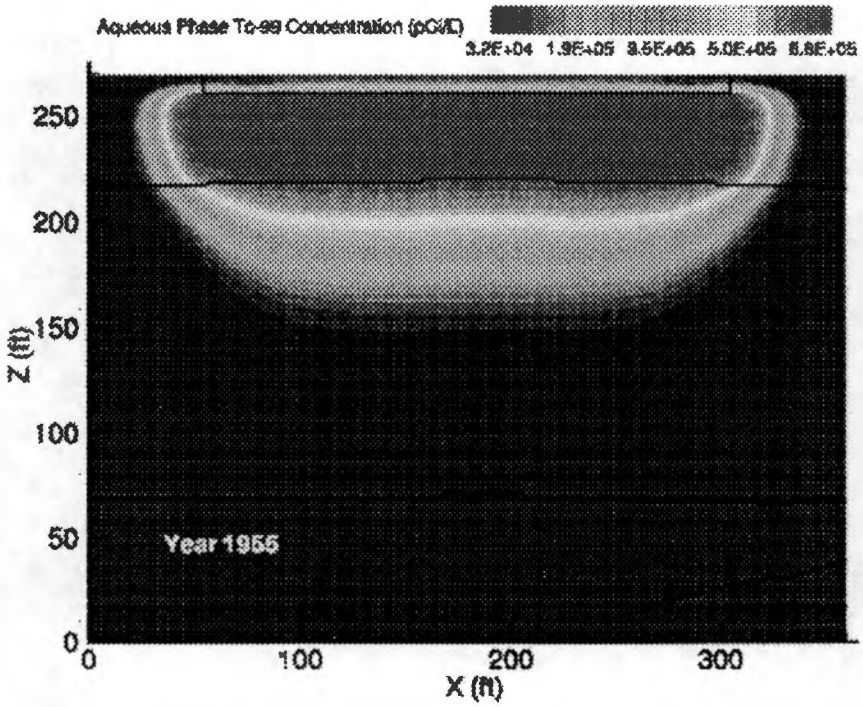

(b)

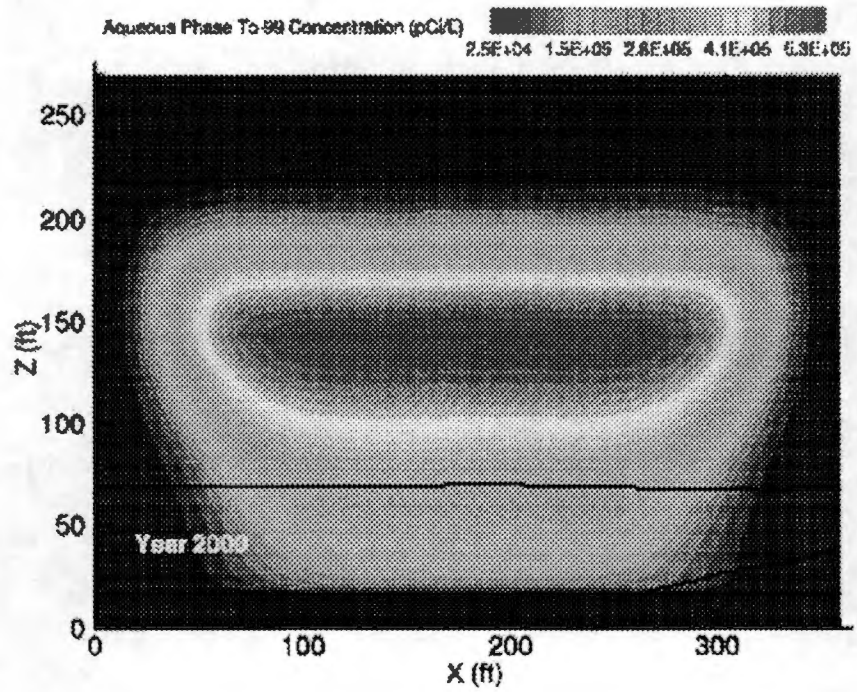

Figure E2.11. Case 13 (100 mm/yr Recharge) Technetium-99 Concentration Distributions at (a) Year 2110 and (b) Year 2210

(a)

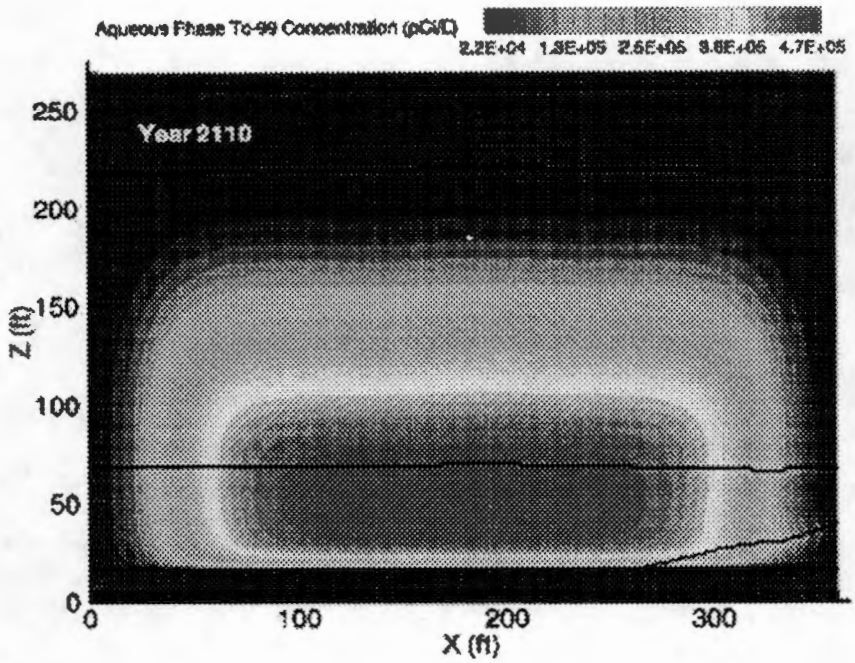

(b)

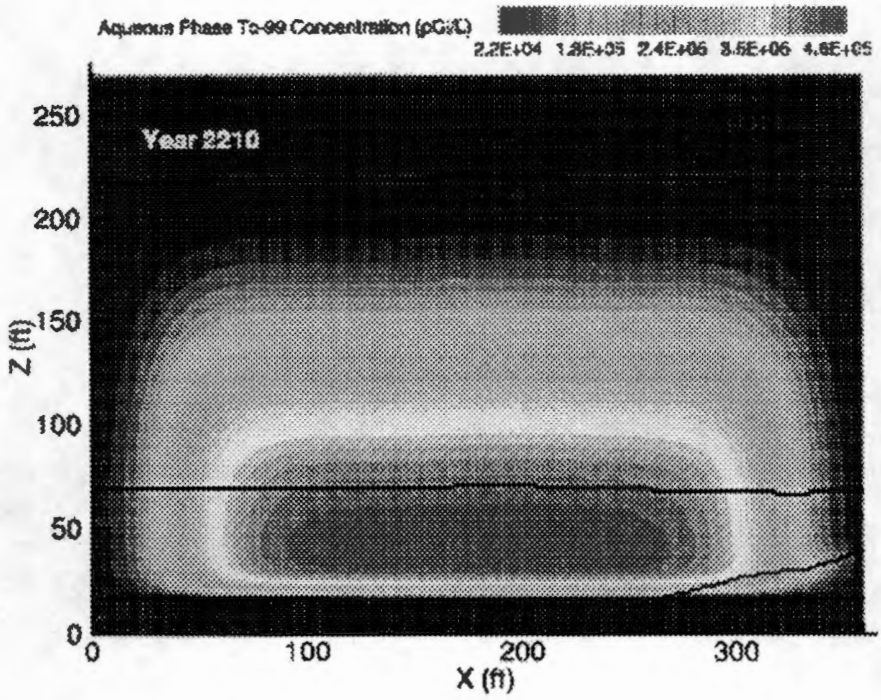

Figure E2.12. Case 13 (100 mm/yr Recharge) Technetium-99 Concentration Distributions at (a) Year 2510 and (b) Year 3000

(a)

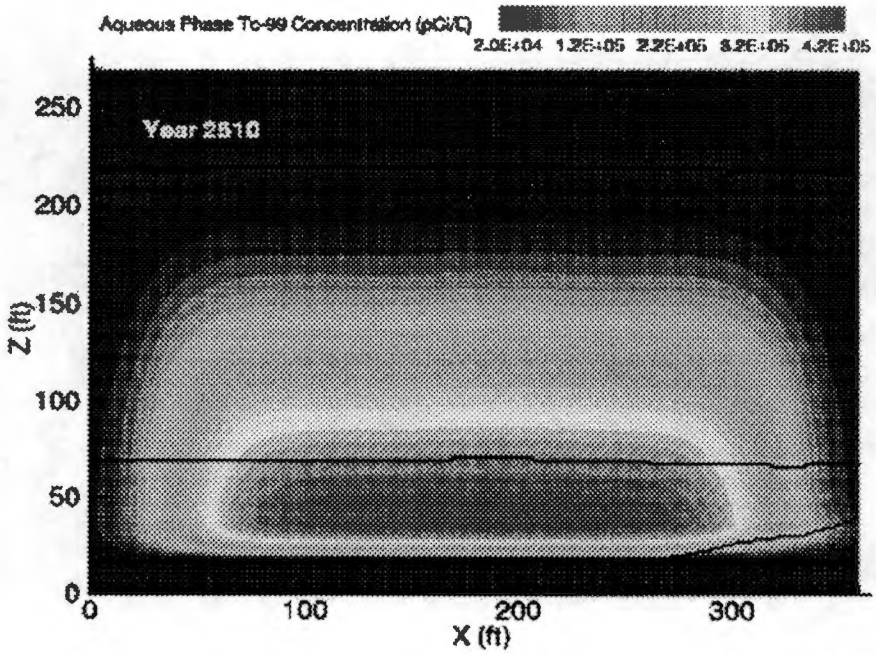

(b)

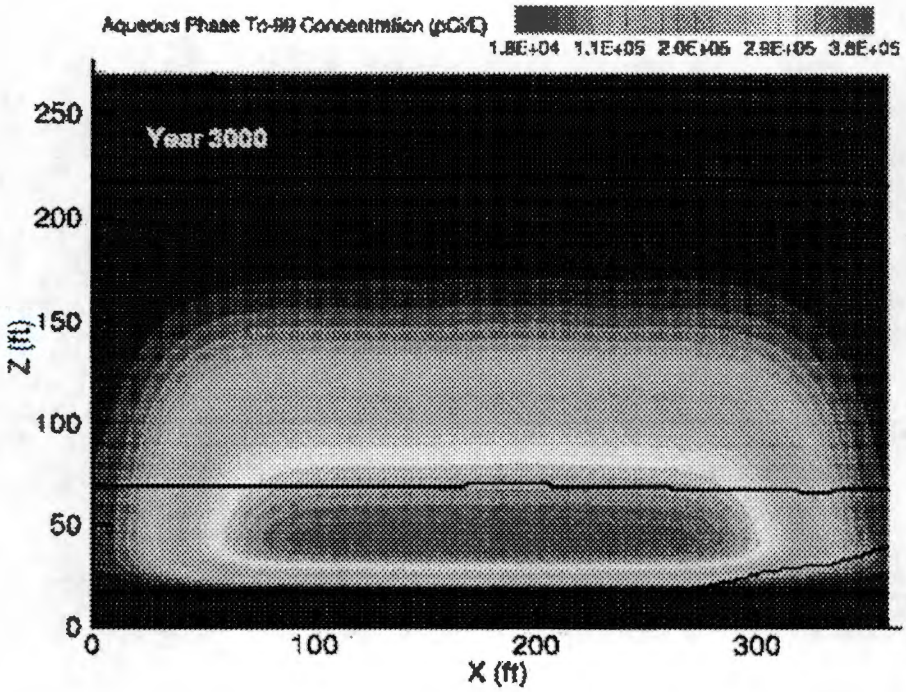

E2.3.0 CASE 14: TRENCH B-38 WITH 100 MM/YR METEORIC RECHARGE AND DELAYED CLOSURE BARRIER

This scenario involves simulating flow and transport for a cross-section west of tank BX-111, considering initial recharge rate of 100 mm/yr, a 378,000-gallon leak in 1954, no interim barrier until closure at year 2040, and a unit inventory distribution for a sorbed species (i.e., uranium-238, Kd = 0.6 mL/g) and a non-sorbing species (i.e., technetium-99 and nitrate). The unit inventory results are also scaled to the uranium-238, technetium-99, and nitrate inventory estimates for trench B-38 and all of the B trenches.

Figure E2.13. Case 14 (100 mm/yr Recharge) with Delayed Closure Barrier Aqueous Phase Saturation Distribution at Year 3000

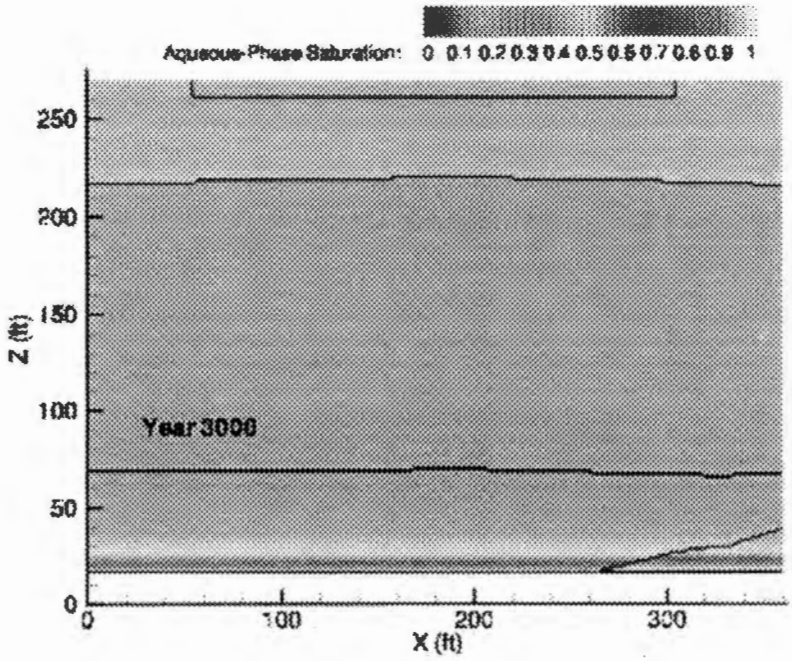

Figure E2.14. Case 14 (100 mm/yr Recharge) with Delayed Closure Barrier Uranium-238 Aqueous Concentration Distribution at Year 3000

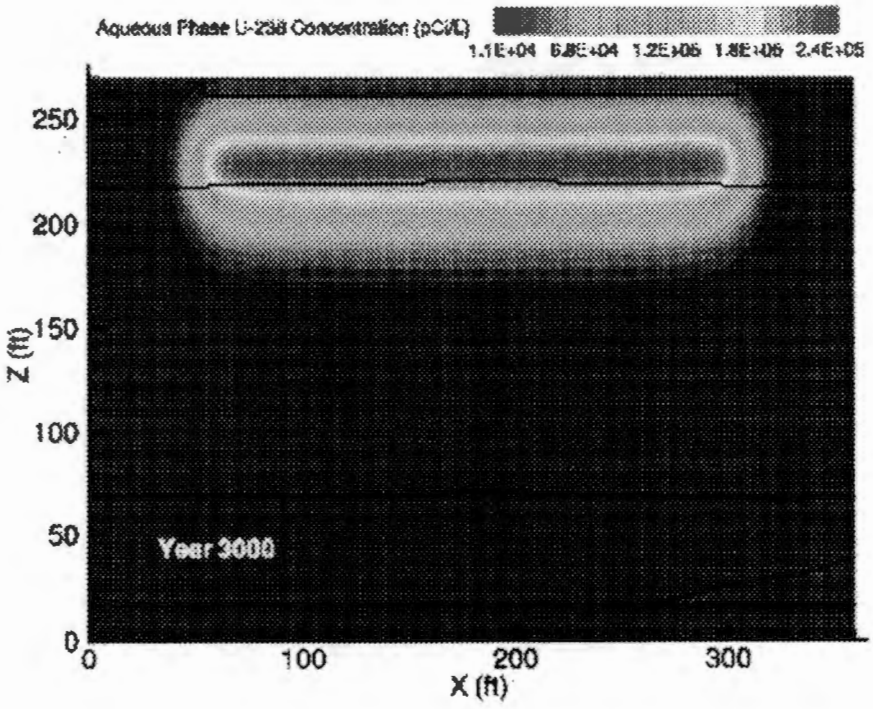

Figure E2.15. Case 14 (100 mm/yr Recharge) with Delayed Closure Barrier Technetium-99 Concentration Distributions at (a) Year 2110 and (b) Year 2210

(a)

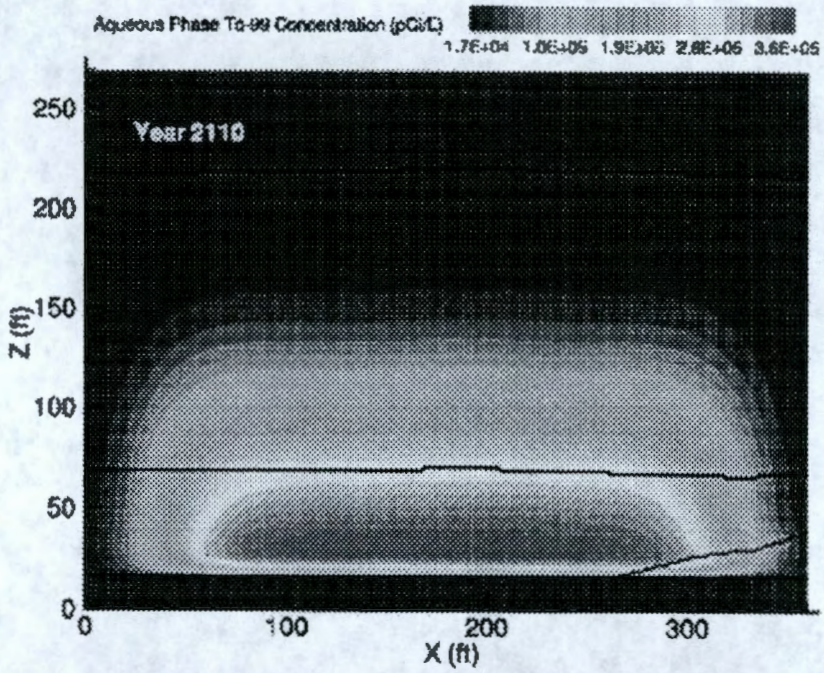

(b)

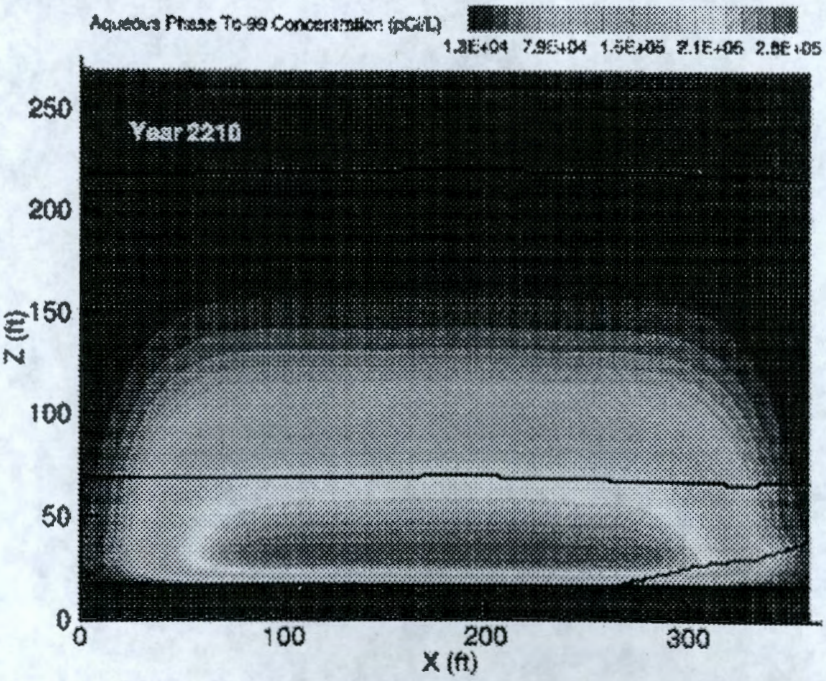

Figure E2.16. Case 14 (100 mm/yr Recharge) with Delayed Closure Barrier Technetium-99 Concentration Distributions at (a) Year 2510 and (b) Year 3000

(a)

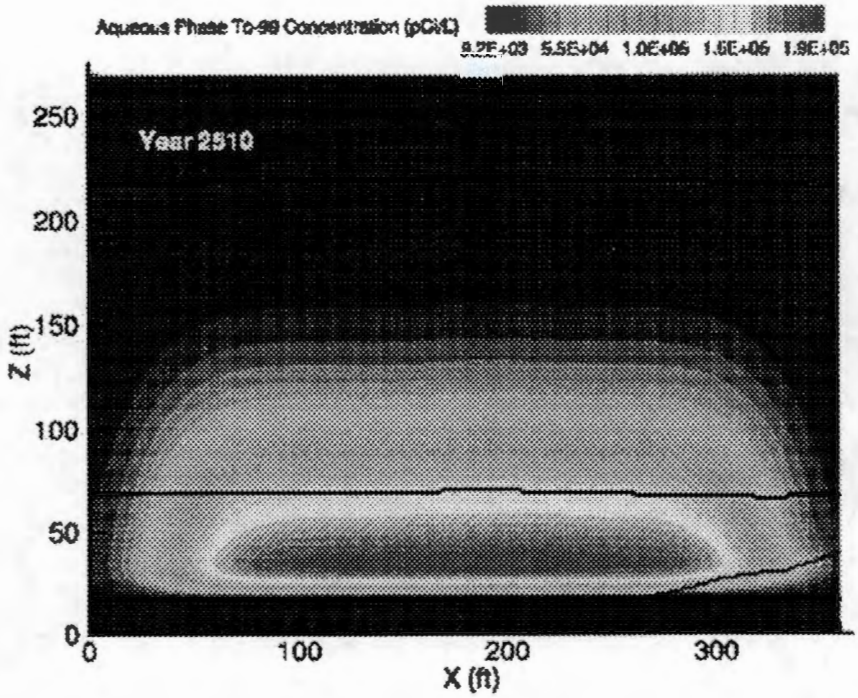

(b)

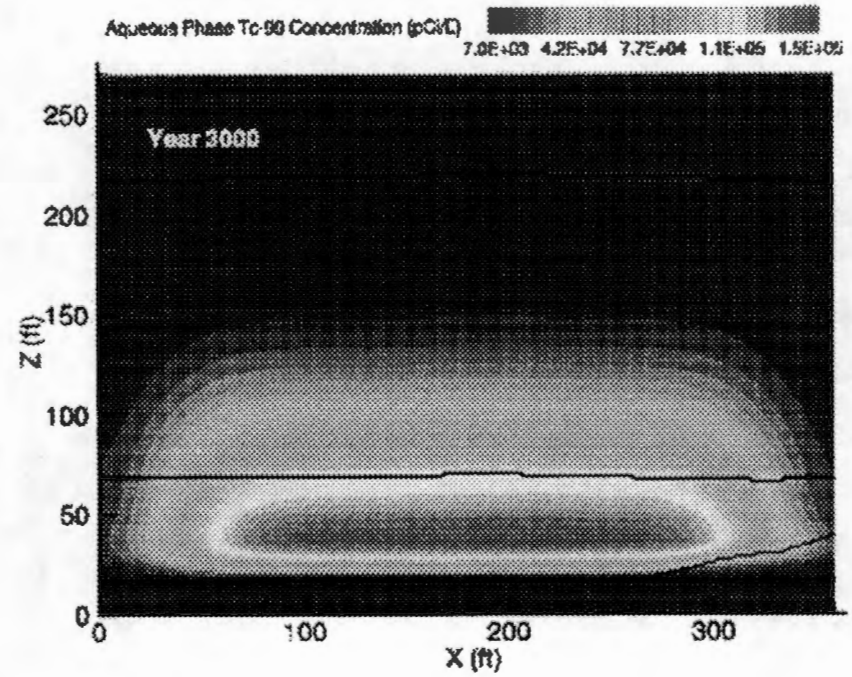

ATTACHMENT E3

BX TANK FARM MASS FLUX AND BREAKTHROUGH CURVES

This page intentionally left blank.

CONTENTS

E3.1.0 CASE 1: BASE CASE, NO ACTION ALTERNATIVE E3-1

E3.2.0 CASE 2: BARRIER ALTERNATIVE AND NO WATER LINE LEAK E3-5

E3.3.0 CASE 3: NO INTERIM BARRIER AND WATER LINE LEAK OF 1 GPM FOR 20 YEARS E3-9

E3.4.0 CASE 4: NO INTERIM BARRIER AND WATER LINE LEAK OF 200,000 GALLONS OVER 5 DAYS E3-13

E3.5.0 CASE 5: ALTERNATE INVENTORY DISTRIBUTION AND NO INTERIM BARRIER E3-17

E3.6.0 CASE 6: ALTERNATE INVENTORY DISTRIBUTION WITH INTERIM BARRIER E3-21

E3.7.0 CASE 7: BASE CASE WITH 50 MM/YR METEORIC RECHARGE E3-25

E3.8.0 CASE 8: BASE CASE WITH 30 MM/YR METEORIC RECHARGE E3-29

E3.9.0 CASE 9: BASE CASE WITH 10 MM/YR METEORIC RECHARGE E3-33

E3.10.0 CASE 10: BASE CASE WITH KD = 0.1 ML/G FOR URANIUM-238 ..... E3-37

E3.11.0 CASE 11: BASE CASE WITH KD = 1 ML/G FOR URANIUM-238 ..... E3-39

FIGURES

E3.1. Uranium-238 (a) Mass Flux and (b) Breakthrough Curves for Case 1 (Base Case 100 mm/yr Recharge) E3-2
E3.2. Technetium-99 (a) Mass Flux and (b) Breakthrough Curves for Case 1 (Base Case 100 mm/yr Recharge) E3-3
E3.3. Nitrate (a) Mass Flux and (b) Breakthrough Curves for Case 1 (Base Case 100 mm/yr Recharge) E3-4
E3.4. Uranium-238 (a) Mass Flux and (b) Breakthrough Curves for Case 2 (Interim Barrier) E3-6
E3.5. Technetium-99 (a) Mass Flux and (b) Breakthrough Curves for Case 2 (Interim Barrier) E3-7
E3.6. Nitrate (a) Mass Flux and (b) Breakthrough Curves for Case 2 (Interim Barrier) E3-8
E3.7. Uranium-238 (a) Mass Flux and (b) Breakthrough Curves for Case 3 (20-Year Water Line Leak at 1 gpm) E3-10
E3.8. Technetium-99 (a) Mass Flux and (b) Breakthrough Curves for Case 3 (20-Year Water Line Leak at 1 gpm) E3-11
E3.9. Nitrate (a) Mass Flux and (b) Breakthrough Curves for Case 3 (20-Year Water Line Leak at 1 gpm) E3-12
E3.10. Uranium-238 (a) Mass Flux and (b) Breakthrough Curves for Case 4 (200,000-Gallon Water Line Leak for 5 Days) E3-14
E3.11. Technetium-99 (a) Mass Flux and (b) Breakthrough Curves for Case 4 (200,000-Gallon Water Line Leak for 5 Days) E3-15
E3.12. Nitrate (a) Mass Flux and (b) Breakthrough Curves for Case 4 (200,000-Gallon Water Line Leak for 5 Days) E3-16
E3.13. Uranium-238 (a) Mass Flux and (b) Breakthrough Curves for Case 5 (Alternate Inventory) E3-18
E3.14. Technetium-99 (a) Mass Flux and (b) Breakthrough Curves for Case 5 (Alternate Inventory) E3-19
E3.15. Nitrate (a) Mass Flux and (b) Breakthrough Curves for Case 5 (Alternate Inventory) E3-20
E3.16. Uranium-238 (a) Mass Flux and (b) Breakthrough Curves for Case 6 (Alternate Inventory with Interim Barrier) E3-22
E3.17. Technetium-99 (a) Mass Flux and (b) Breakthrough Curves for Case 6 (Alternate Inventory with Interim Barrier) E3-23
E3.18. Nitrate (a) Mass Flux and (b) Breakthrough Curves for Case 6 (Alternate Inventory with Interim Barrier) E3-24
E3.19. Uranium-238 (a) Mass Flux and (b) Breakthrough Curves for Case 7 (50 mm/yr Recharge) E3-26
E3.20. Tecnetium-99 (a) Mass Flux and (b) Breakthrough Curves for Case 7 (50 mm/yr Recharge) E3-27
E3.21. Nitrate (a) Mass Flux and (b) Breakthrough Curves for Case 7 (50 mm/yr Recharge) E3-28
E3.22. Uranium-238 (a) Mass Flux and (b) Breakthrough Curves for Case 8 (30 mm/yr Recharge) E3-30

E3.23. Technetium-99 (a) Mass Flux and (b) Breakthrough Curves for Case 8 (30 mm/yr Recharge) E3-31
E3.24. Nitrate (a) Mass Flux and (b) Breakthrough Curves for Case 8 (30 mm/yr Recharge) E3-32
E3.25. Uranium-238 Mass Flux for Case 9 (10 mm/yr Recharge) E3-34
E3.26. Technetium-99 (a) Mass Flux and (b) Breakthrough Curves for Case 9 (10 mm/yr Recharge) E3-35
E3.27. Nitrate (a) Mass Flux and (b) Breakthrough Curves for Case 9 (10 mm/yr Recharge) E3-36
E3.28. Uranium-238 (a) Mass Flux and (b) Breakthrough Curves for Case 10 (Uranium-238 Kd=0.1 mL/g) E3-38
E3.29. Uranium-238 (a) Mass Flux and (b) Breakthrough Curves for Case 11 (Uranium-238 Kd=1 mL/g) E3-40

This page intentionally left blank.

E3.1.0 CASE 1: BASE CASE, NO ACTION ALTERNATIVE

This scenario involves simulating flow and transport for the cross-section through tanks BX-108, BX-105, and BX-102, considering an initial recharge rate of 100 mm/yr, no water line leak, no interim barrier, a closure barrier at year 2040, a partitioning coefficient (Kd) of 0.6 mL/g for uranium-238, and an inventory distribution that extends east of tank BX-102 to the BX tank farm fence line boundary.

Figure E3.1. Uranium-238 (a) Mass Flux and (b) Breakthrough Curves for Case 1 (Base Case 100 mm/yr Recharge)

(a)

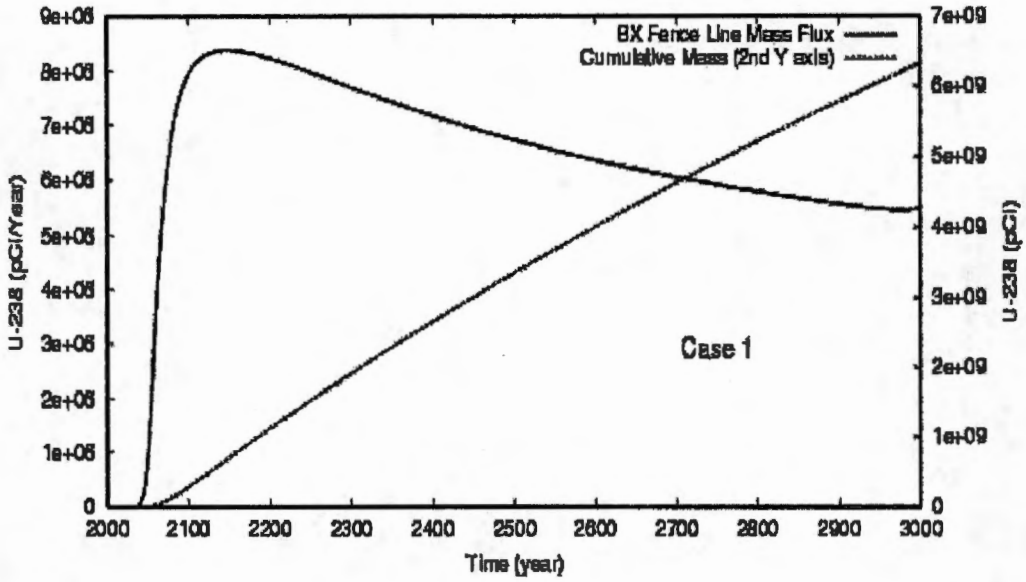

(b)

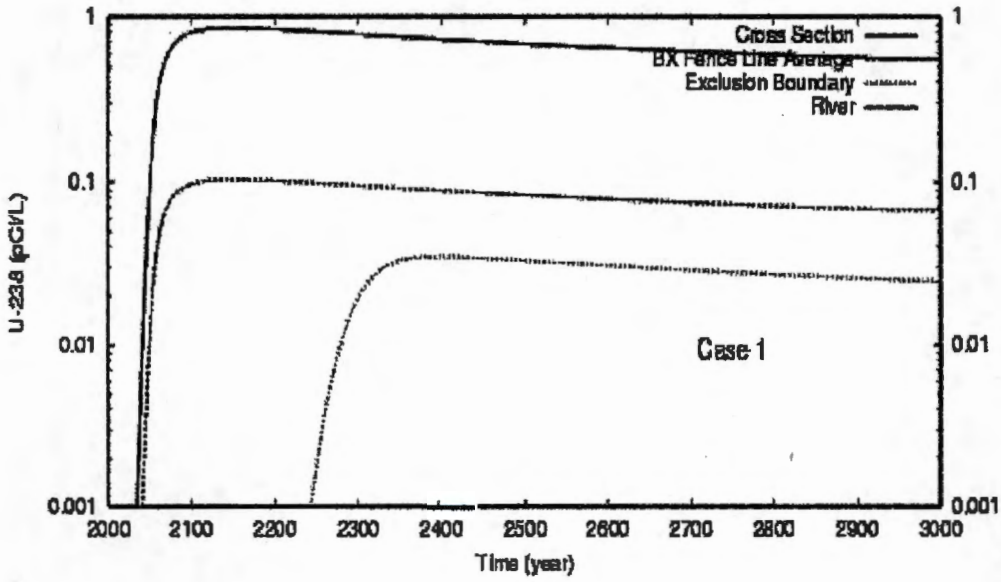

Figure E3.2. Technetium-99 (a) Mass Flux and (b) Breakthrough Curves for Case 1 (Base Case 100 mm/yr Recharge)

(a)

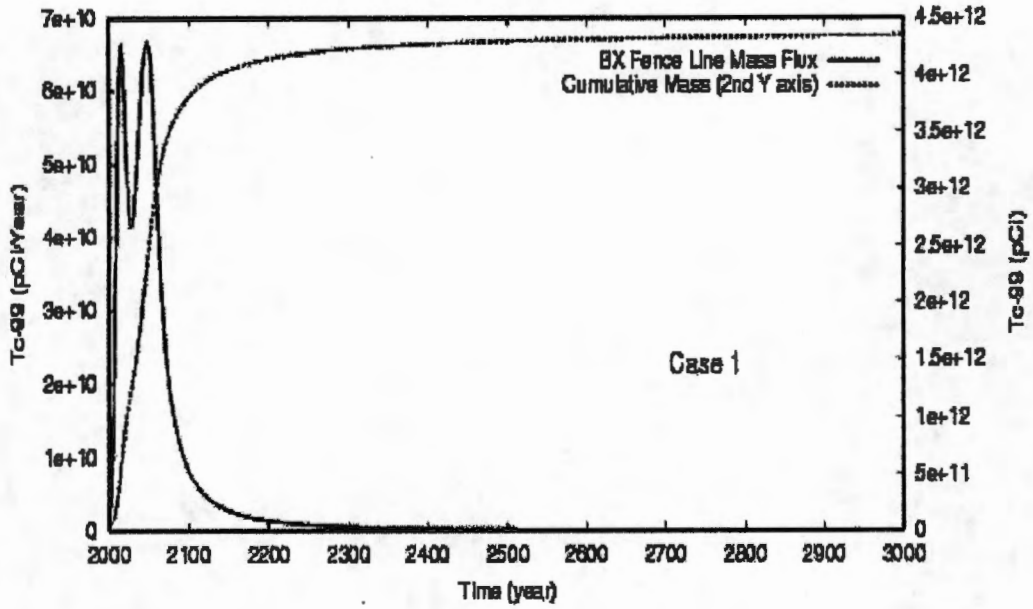

(b)

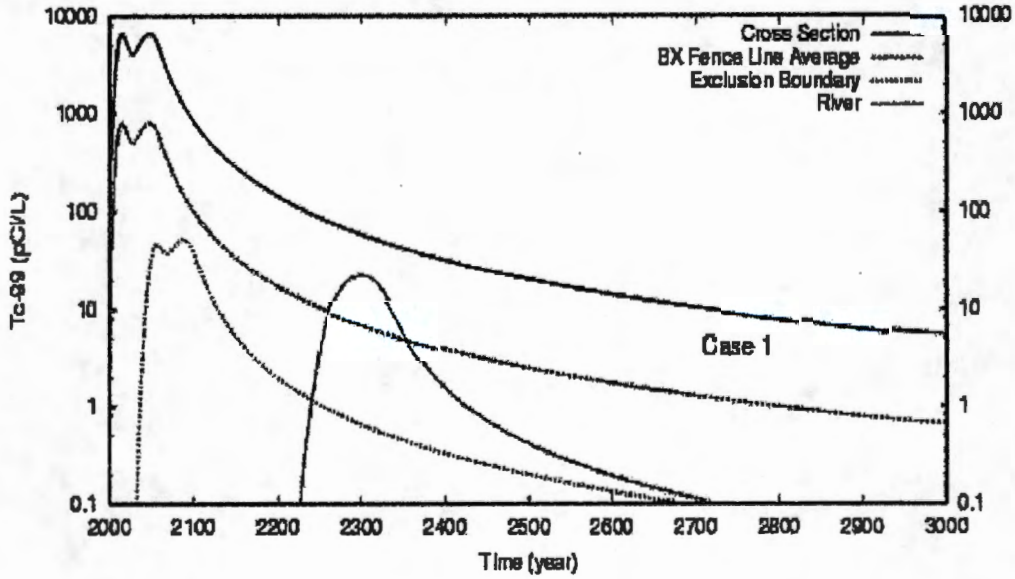

Figure E3.3. Nitrate (a) Mass Flux and (b) Breakthrough Curves for Case 1 (Base Case 100 mm/yr Recharge)

(a)

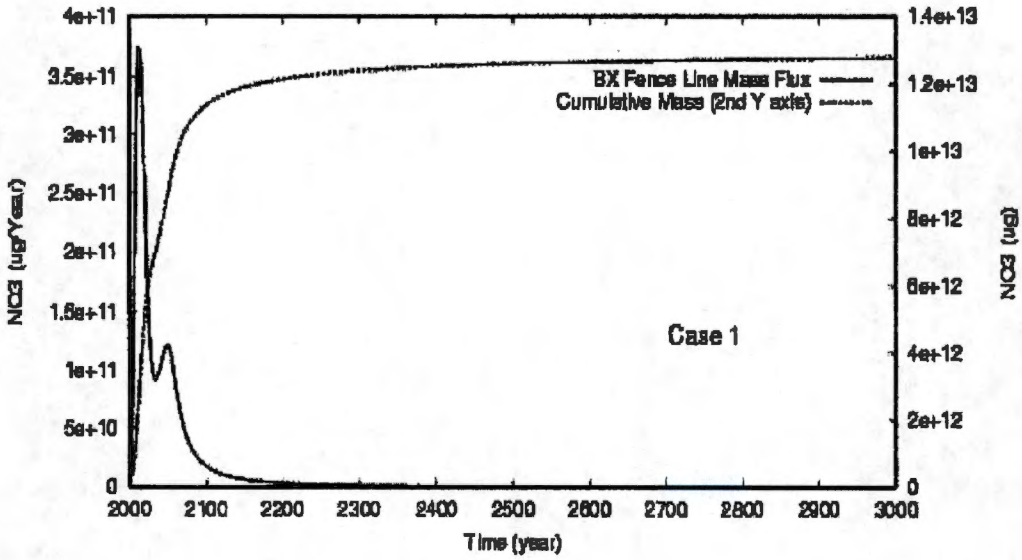

(b)

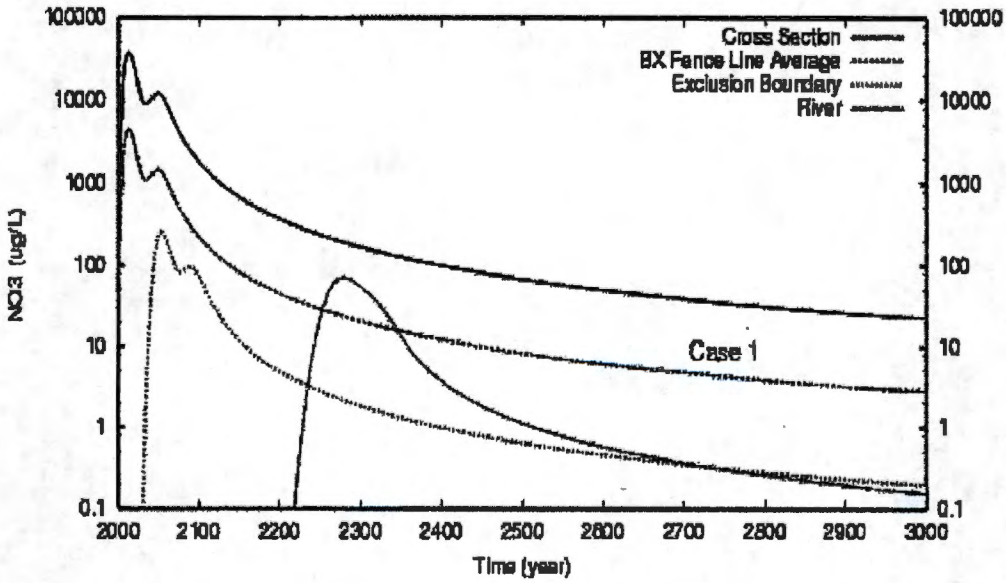

E3.2.0 CASE 2: BARRIER ALTERNATIVE AND NO WATER LINE LEAK

This scenario involves simulating flow and transport for the cross-section through tanks BX-108, BX-105, and BX-102, considering initial recharge rate of 100 mm/yr, placement of an interim barrier by 2010, a closure barrier at year 2040 (i.e., the interim barrier replaced by the closure barrier), no water line leak, a Kd of 0.6 mL/g for uranium-238, and an inventory distribution that extends east of tank BX-102 to the BX fence line boundary.

Figure E3.4. Uranium-238 (a) Mass Flux and (b) Breakthrough Curves for Case 2 (Interim Barrier)

(a)

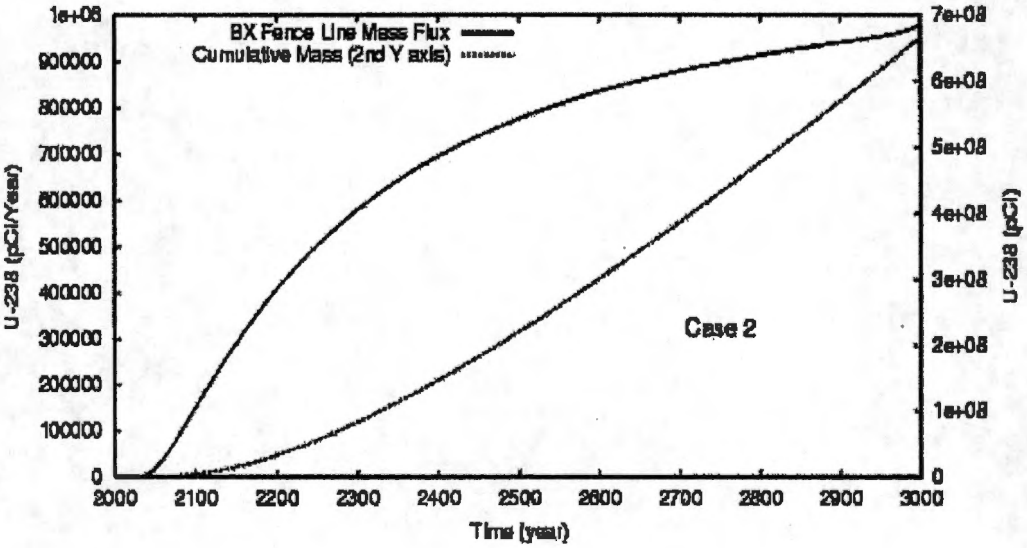

(b)

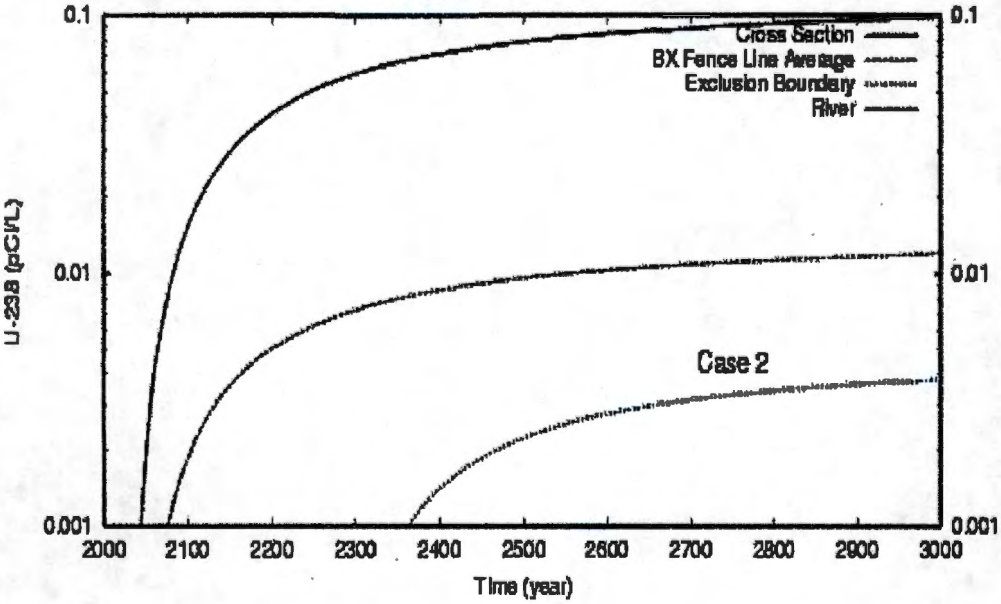

Figure E3.5. Technetium-99 (a) Mass Flux and (b) Breakthrough Curves for Case 2 (Interim Barrier)

(a)

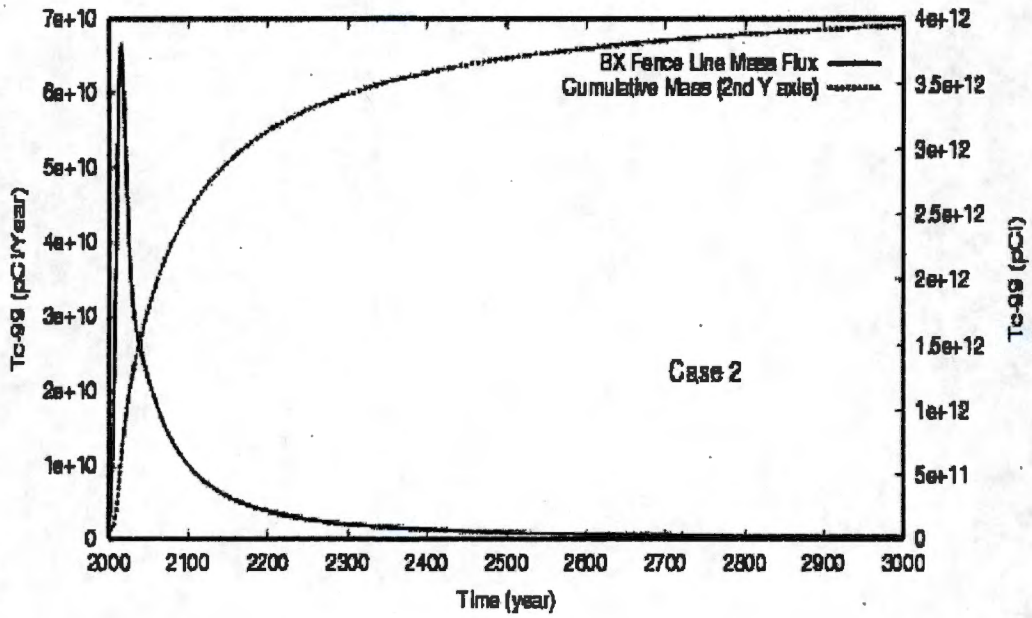

(b)

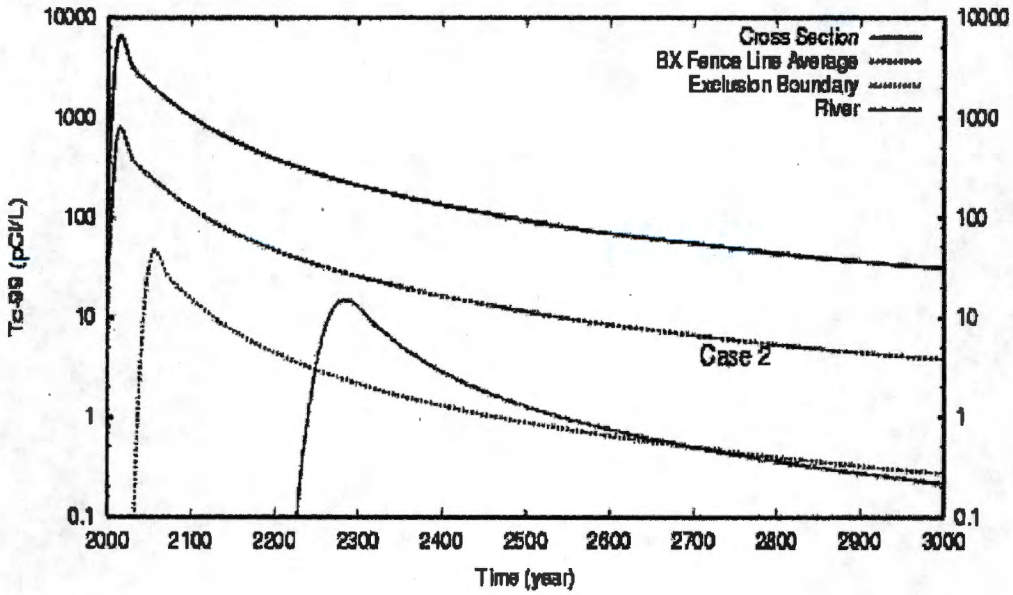

Figure E3.6. Nitrate (a) Mass Flux and (b) Breakthrough Curves for Case 2 (Interim Barrier)

(a)

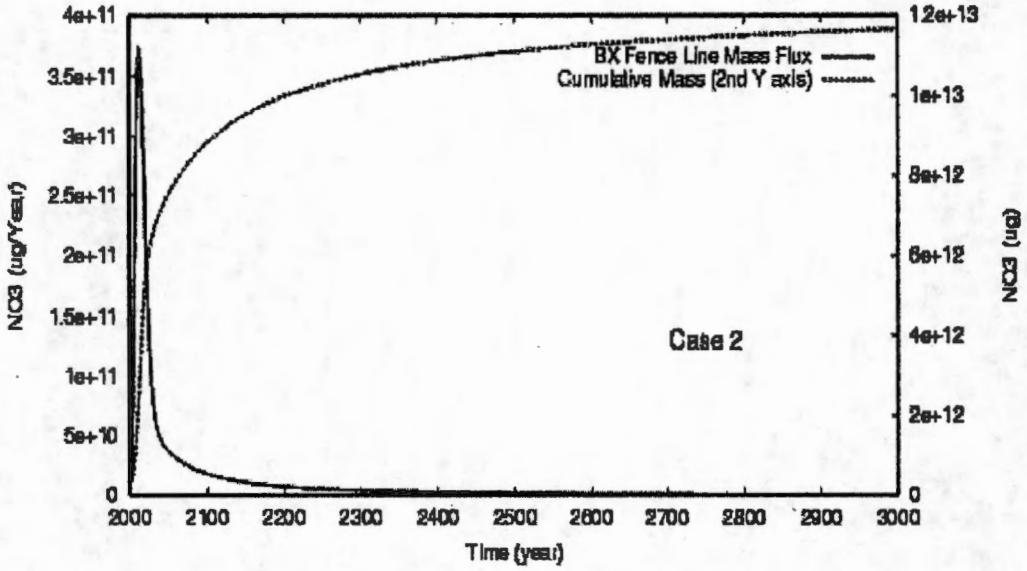

(b)

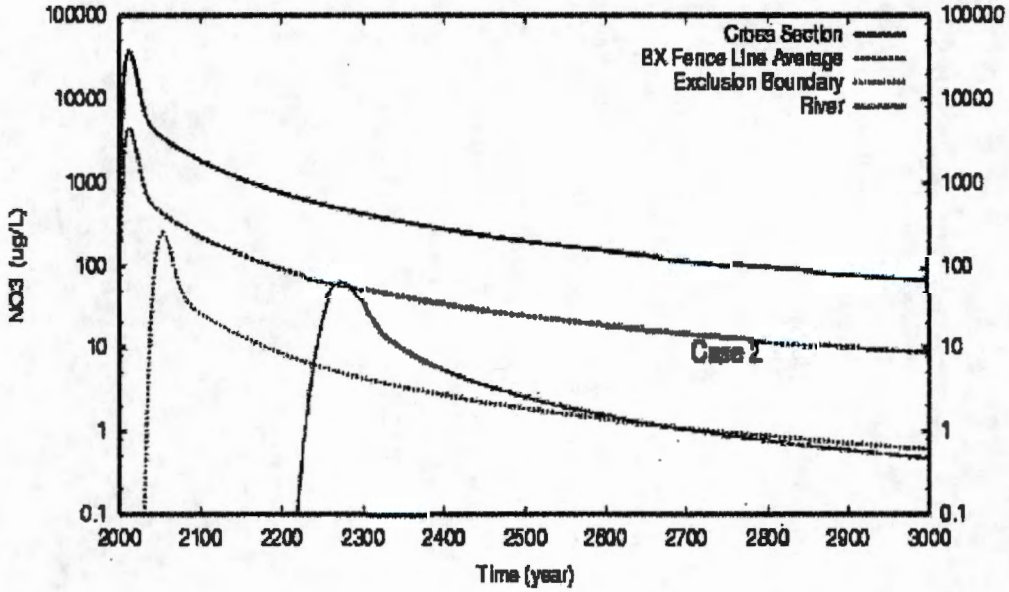

E3.3.0 CASE 3: NO INTERIM BARRIER AND WATER LINE LEAK OF 1 GPM FOR 20 YEARS

This scenario involves simulating flow and transport for the cross-section through tanks BX-108, BX-105, and BX-102, considering initial recharge rate of 100 mm/yr, water line leak (1 gpm for 20 years) for BX-102 only, no interim barrier until closure at year 2040, a Kd of 0.6 mL/g for uranium-238, and an inventory distribution that extends east of tank BX-102 to the BX tank farm fence line boundary. The water line leak occurs east of tank BX-102 over a 15-foot radius at the elevation of the top of the tank dome.

Figure E3.7. Uranium-238 (a) Mass Flux and (b) Breakthrough Curves for Case 3 (20-Year Water Line Leak at 1 gpm)

(a)

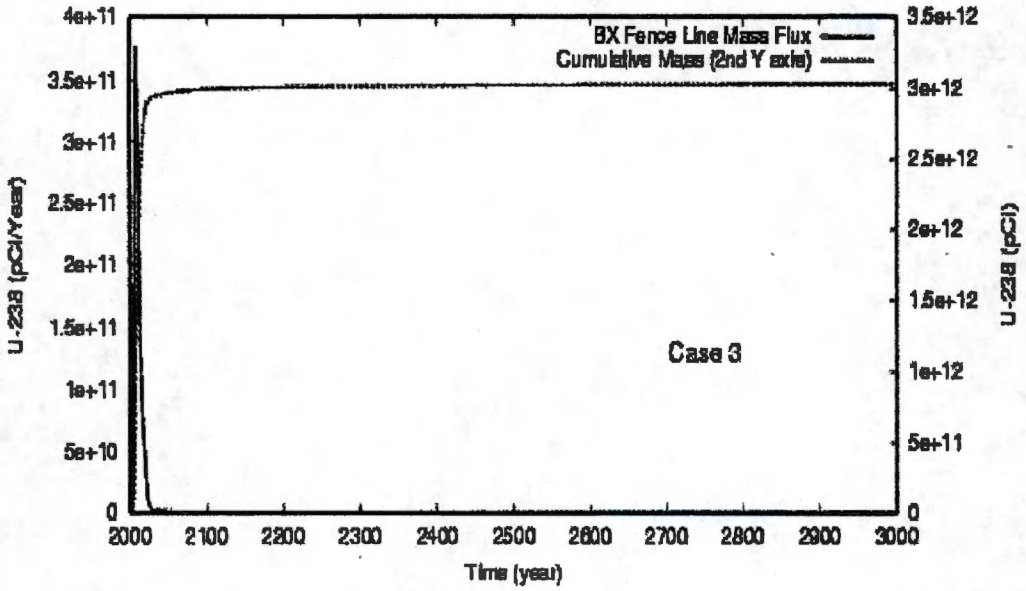

(b)

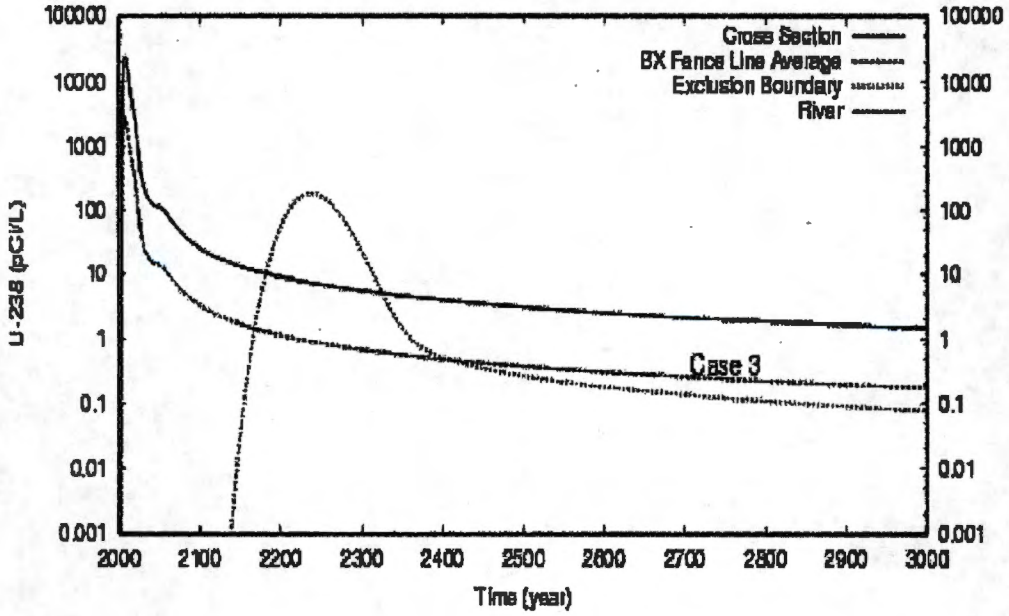

Figure E3.8. Technetium-99 (a) Mass Flux and (b) Breakthrough Curves for Case 3 (20-Year Water Line Leak at 1 gpm)

(a)

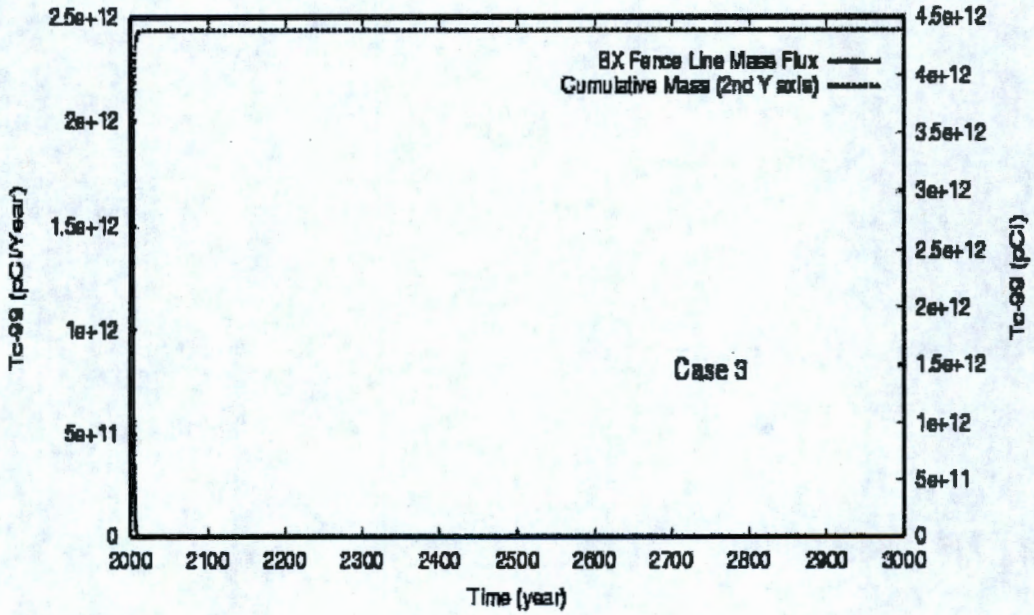

(b)

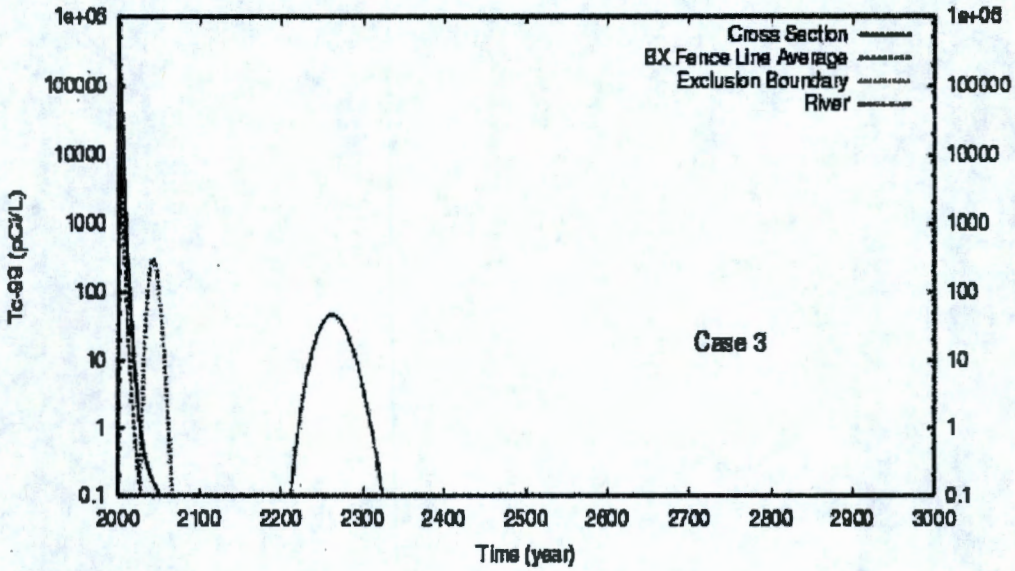

Figure E3.9. Nitrate (a) Mass Flux and (b) Breakthrough Curves for Case 3 (20-Year Water Line Leak at 1 gpm)

(a)

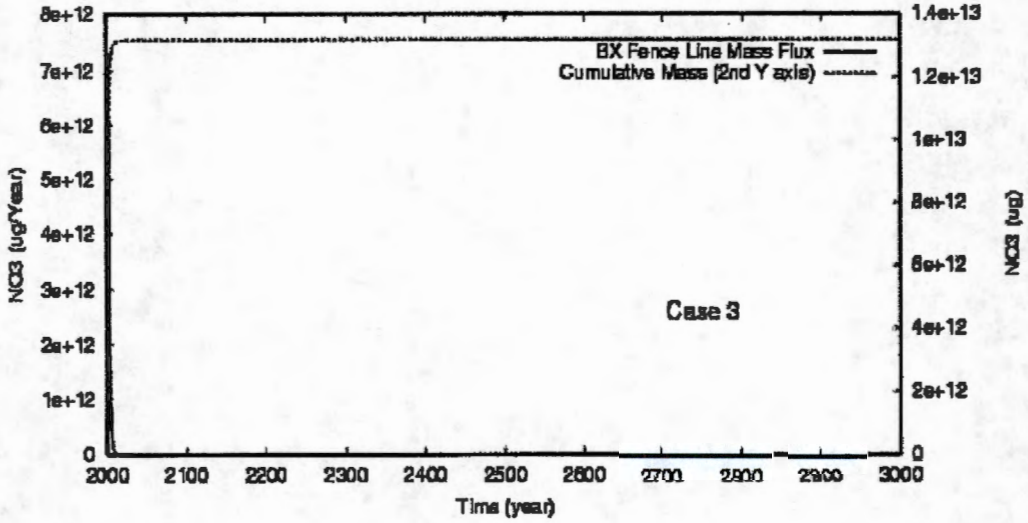

(b)

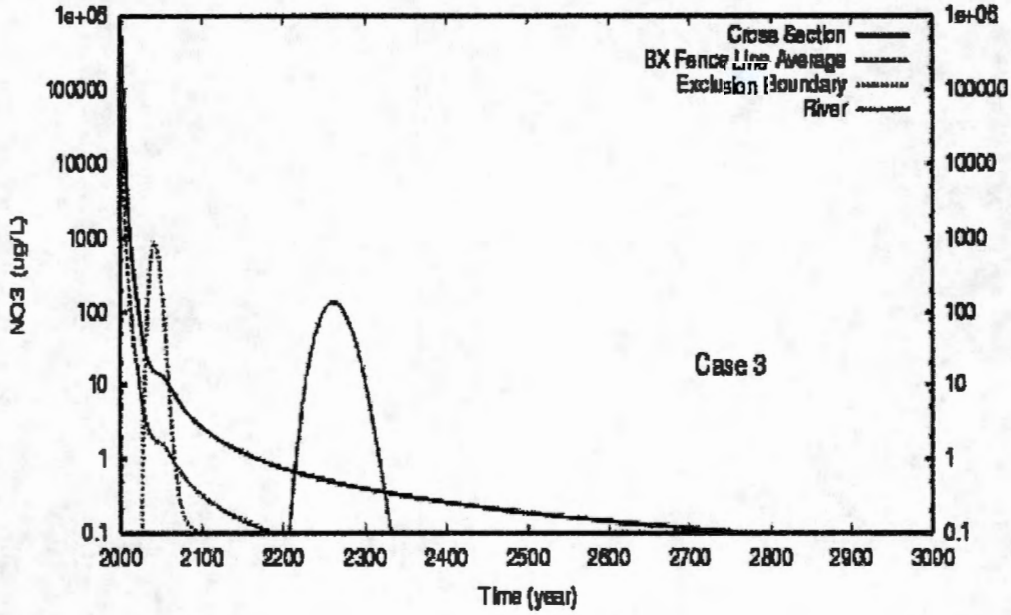

E3.4.0 CASE 4: NO INTERIM BARRIER AND WATER LINE LEAK OF 200,000 GALLONS OVER 5 DAYS

This scenario involves simulating flow and transport for the cross-section through tanks BX-108, BX-105, and BX-102, considering initial recharge rate of 100 mm/yr, water line leak (200,000 gallons in 5 days) for BX-102 only, no interim barrier until closure at year 2040, a Kd of 0.6 mL/g for uranium-238, and an inventory distribution that extends east of tank BX-102 to the BX tank farm fence line boundary. The water line leak occurs east of tank BX-102 over a 15-foot radius at the elevation of the top of the tank dome.

Figure E3.10. Uranium-238 (a) Mass Flux and (b) Breakthrough Curves for Case 4 (200,000-Gallon Water Line Leak for 5 Days)

(a)

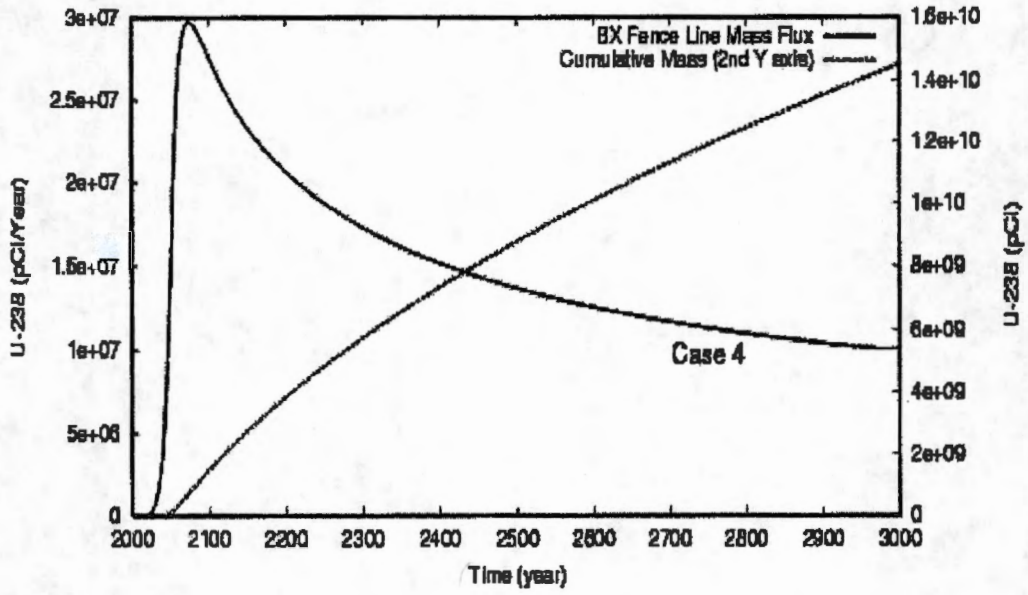

(b)

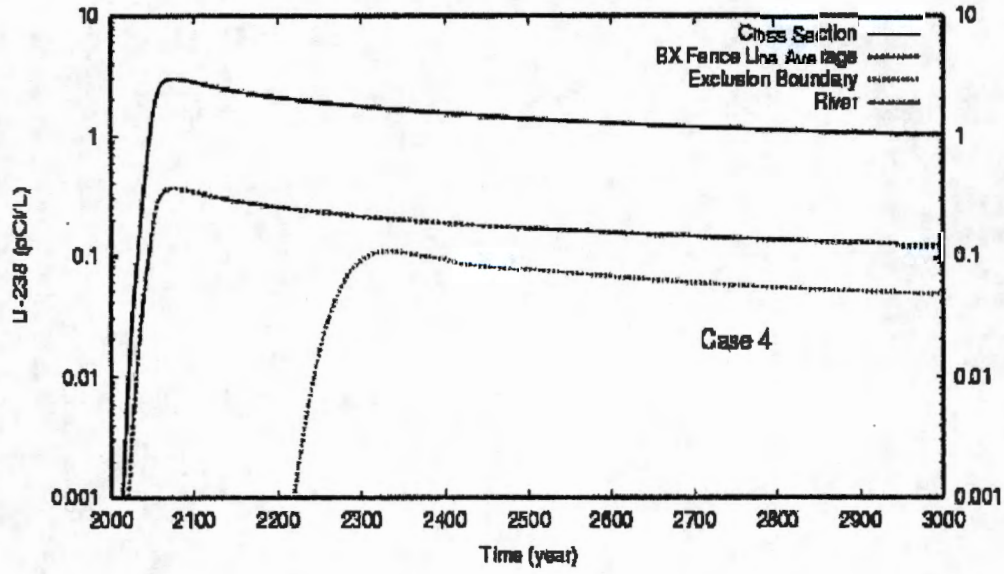

Figure E3.11. Technetium-99 (a) Mass Flux and (b) Breakthrough Curves for Case 4 (200,000-Gallon Water Line Leak for 5 Days)

(a)

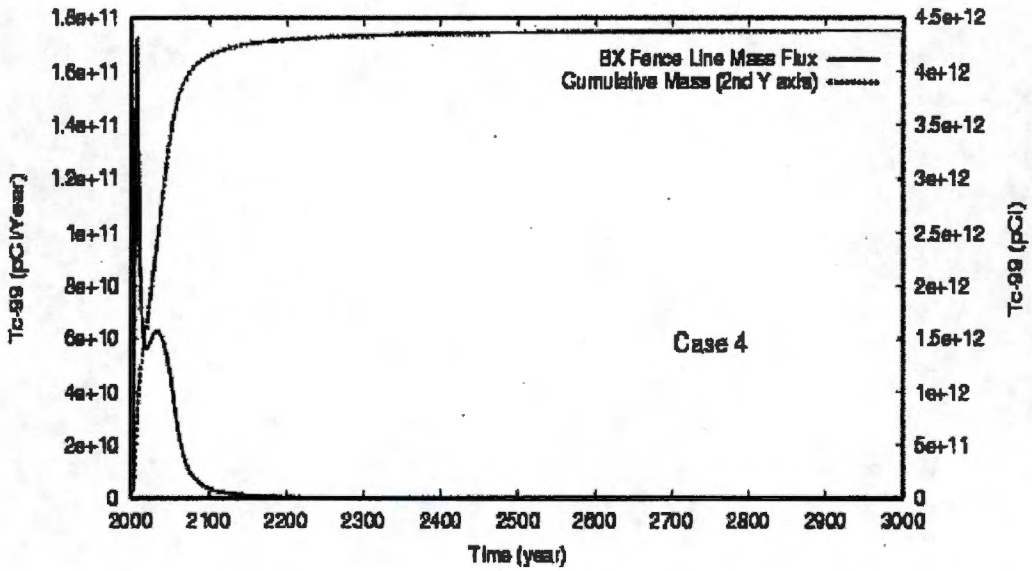

(b)

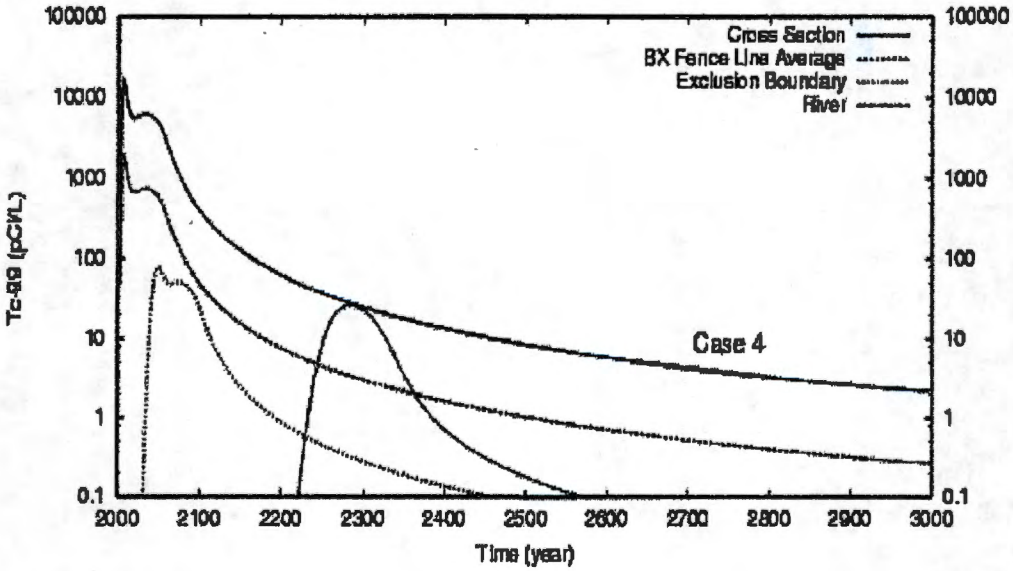

Figure E3.12. Nitrate (a) Mass Flux and (b) Breakthrough Curves for Case 4 (200,000-Gallon Water Line Leak for 5 Days)

(a)

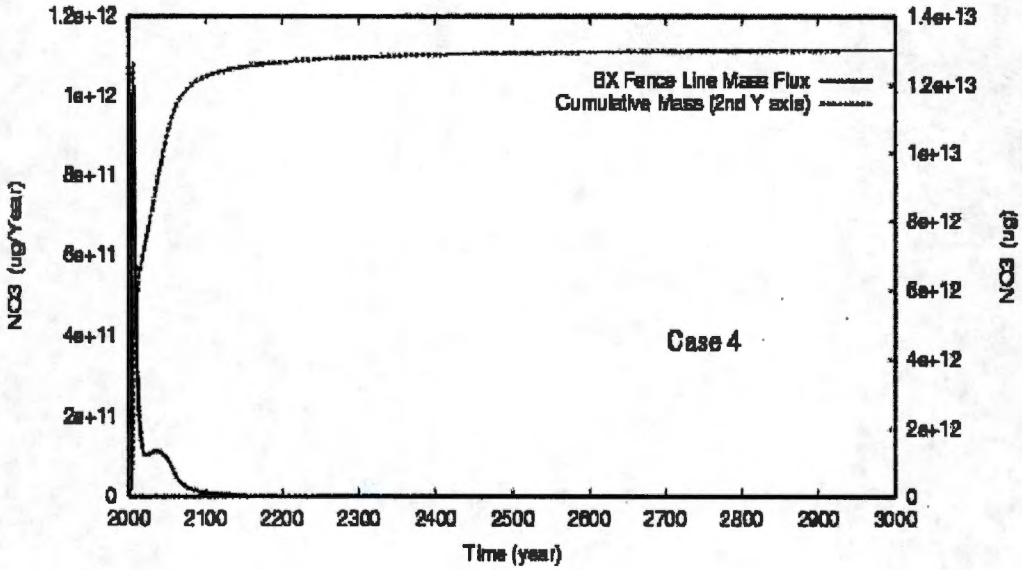

(b)

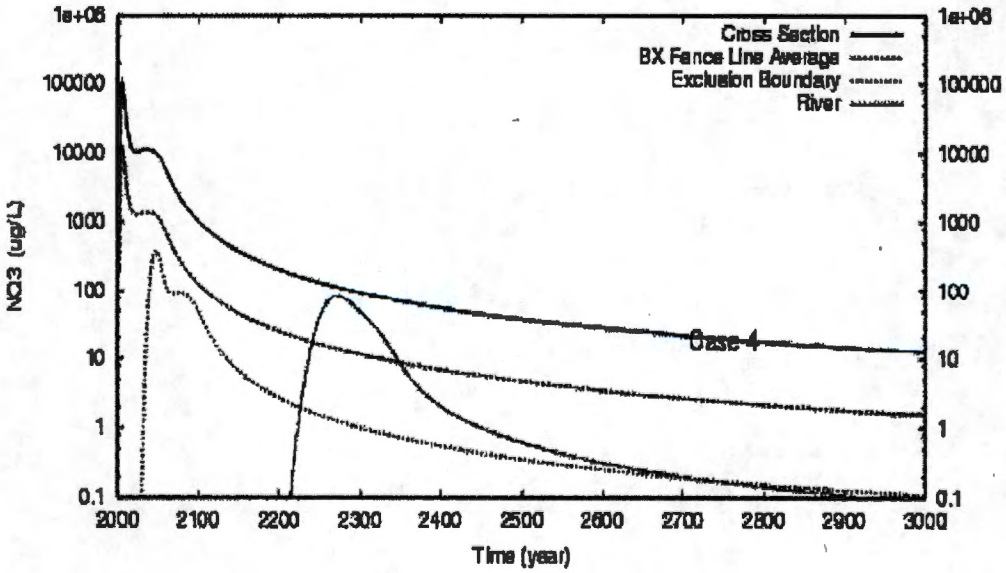

E3.5.0 CASE 5: ALTERNATE INVENTORY DISTRIBUTION AND NO INTERIM BARRIER

This scenario involves simulating flow and transport for the cross-section through tanks BX-108, BX-105, and BX-102, considering initial recharge rate of 100 mm/yr, no water line leak, no interim barrier until closure at year 2040, a Kd of 0.6 mL/g for uranium-238, and an inventory distribution that is centered between tanks BX-105 and BX-102.

Figure E3.13. Uranium-238 (a) Mass Flux and (b) Breakthrough Curves for Case 5 (Alternate Inventory)

(a)

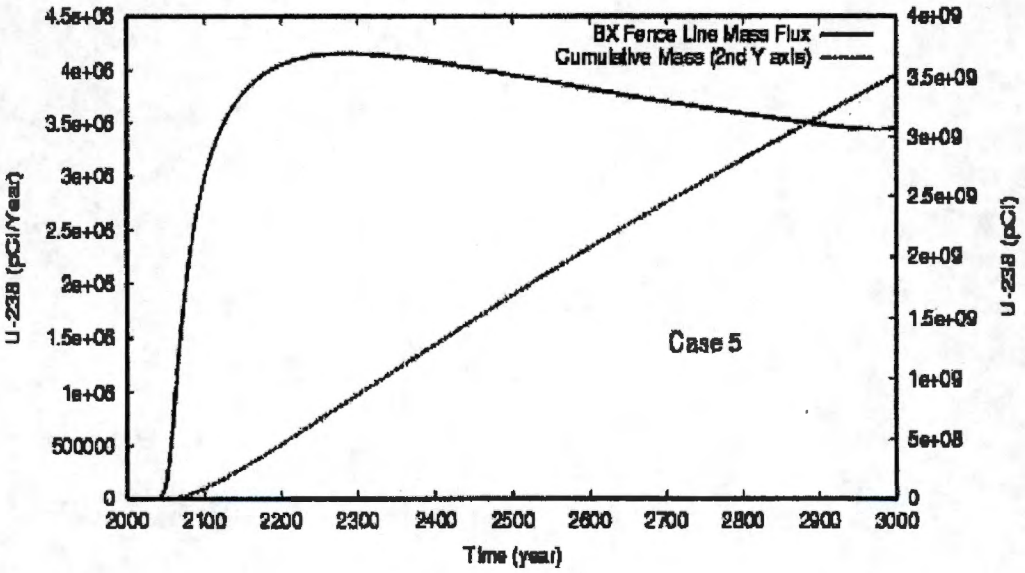

(b)

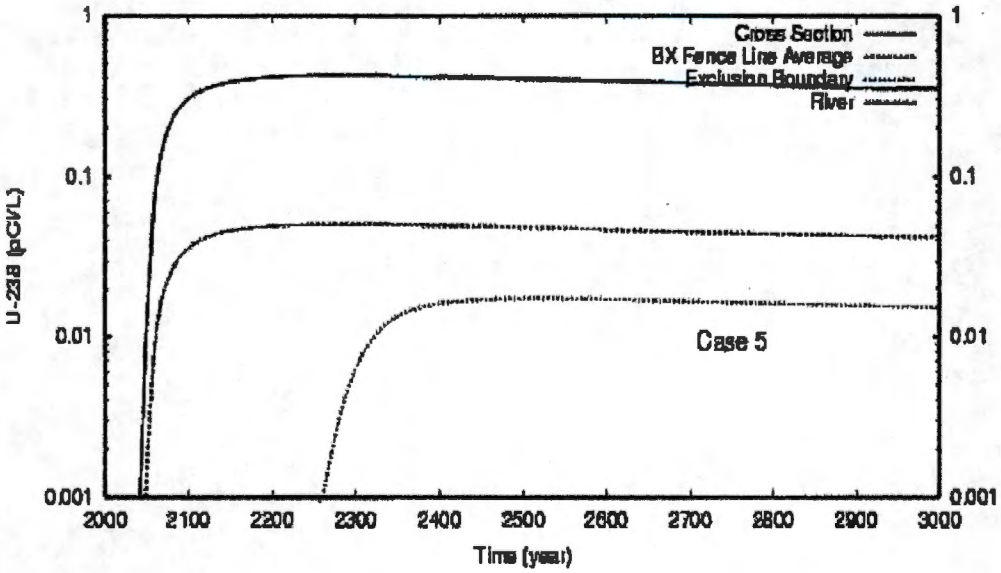

Figure E3.14. Technetium-99 (a) Mass Flux and (b) Breakthrough Curves for Case 5 (Alternate Inventory)

(a)

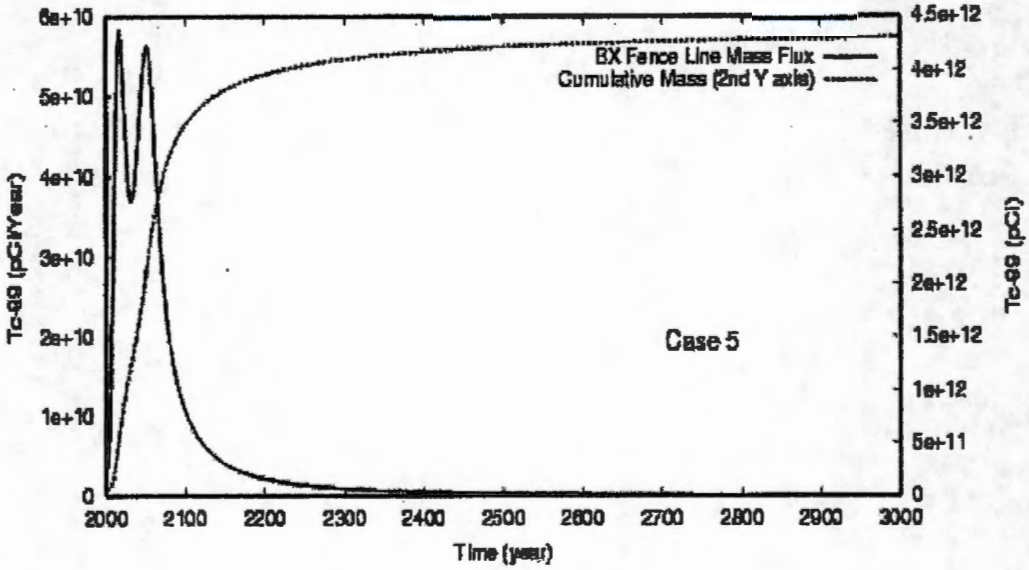

(b)

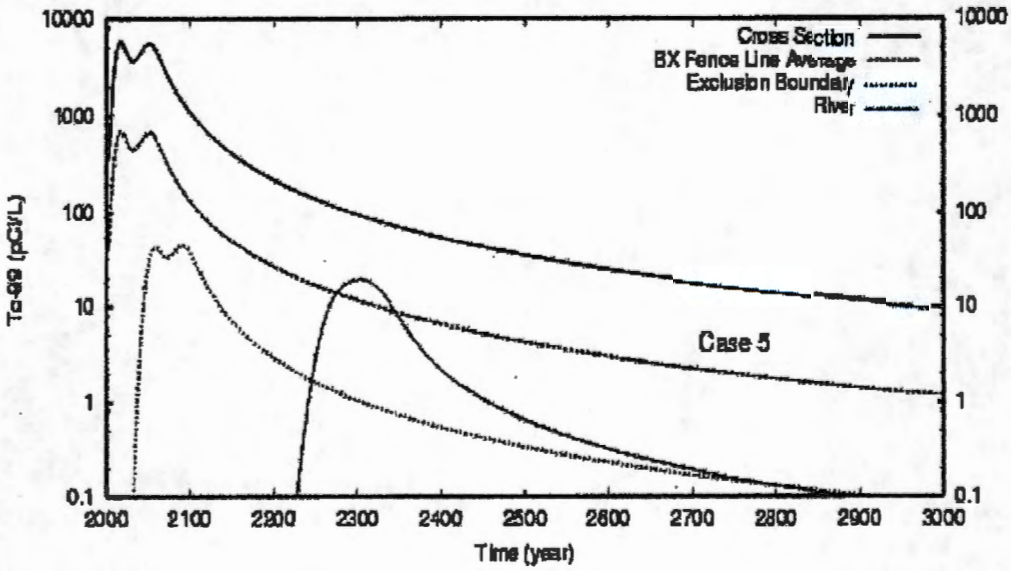

Figure E3.15. Nitrate (a) Mass Flux and (b) Breakthrough Curves for Case 5 (Alternate Inventory)

(a)

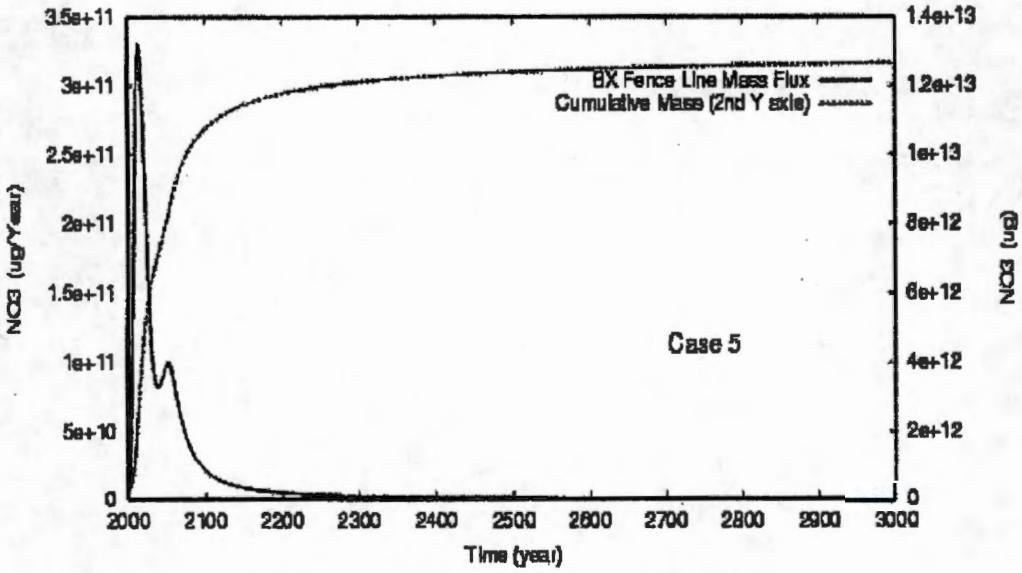

(b)

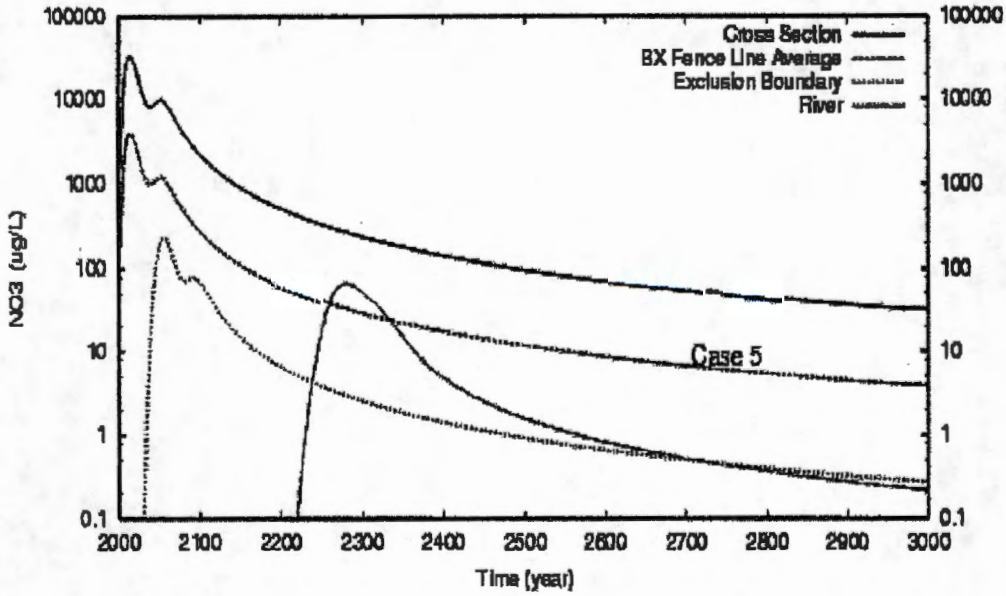

E3.6.0 CASE 6: ALTERNATE INVENTORY DISTRIBUTION WITH INTERIM BARRIER

This scenario involves simulating flow and transport for the cross-section through tanks BX-108, BX-105, and BX-102, considering initial recharge rate of 100 mm/yr, placement of an interim barrier at year 2010, a closure barrier at year 2040 (i.e., the interim barrier replaced by the closure barrier), no water line leak, a Kd of 0.6 mL/g for uranium-238, and an inventory distribution that is centered between tanks BX-105 and BX-102.

Figure E3.16. Uranium-238 (a) Mass Flux and (b) Breakthrough Curves for Case 6 (Alternate Inventory with Interim Barrier)

(a)

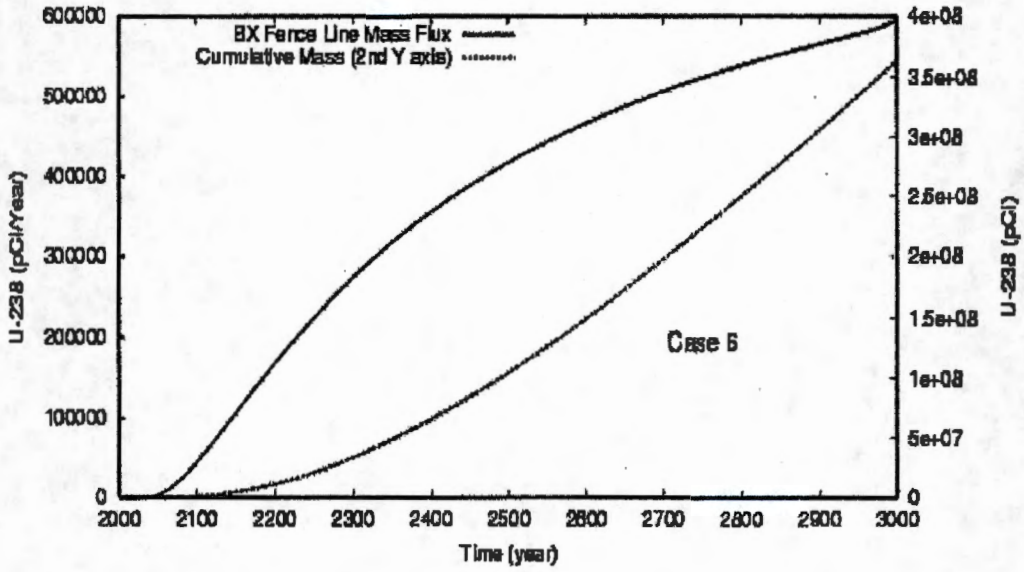

(b)

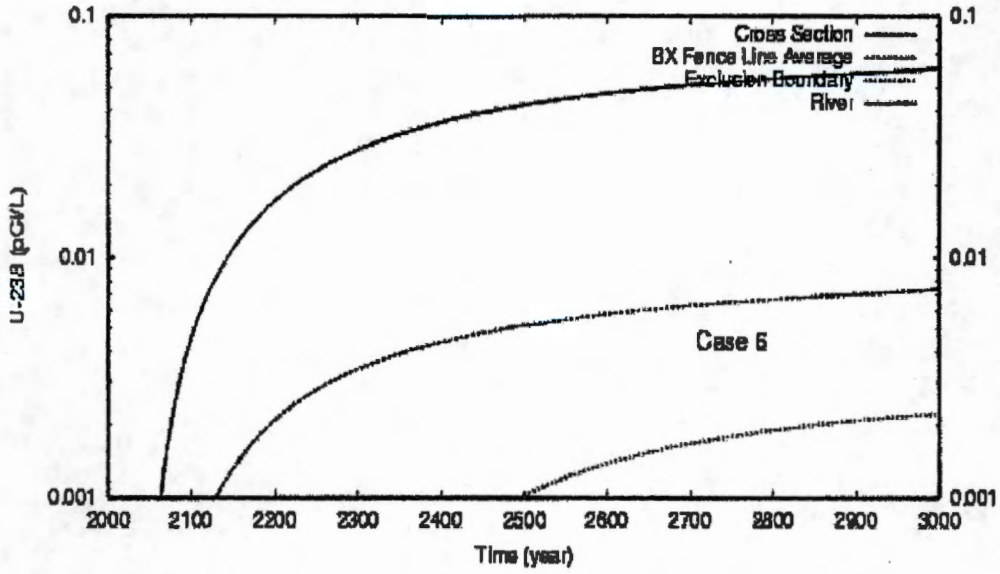

Figure E3.17. Technetium-99 (a) Mass Flux and (b) Breakthrough Curves for Case 6 (Alternate Inventory with Interim Barrier)

(a)

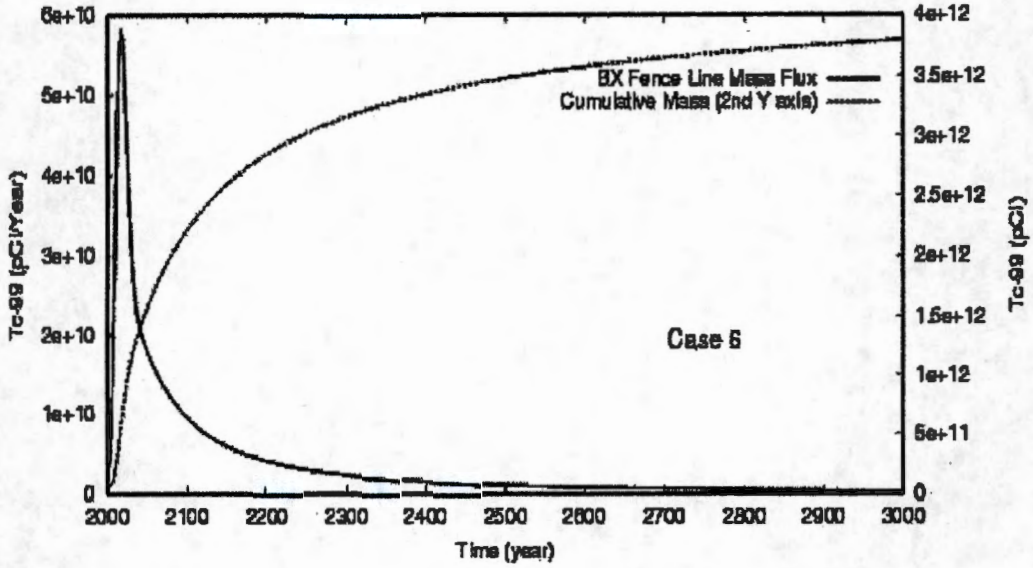

(b)

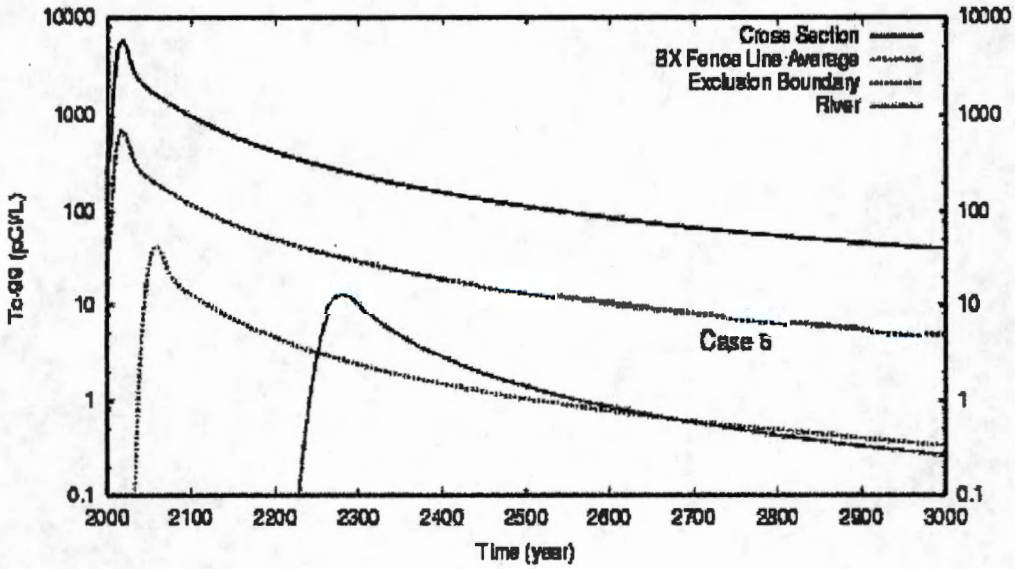

Figure E3.18. Nitrate (a) Mass Flux and (b) Breakthrough Curves for Case 6 (Alternate Inventory with Interim Barrier)

(a)

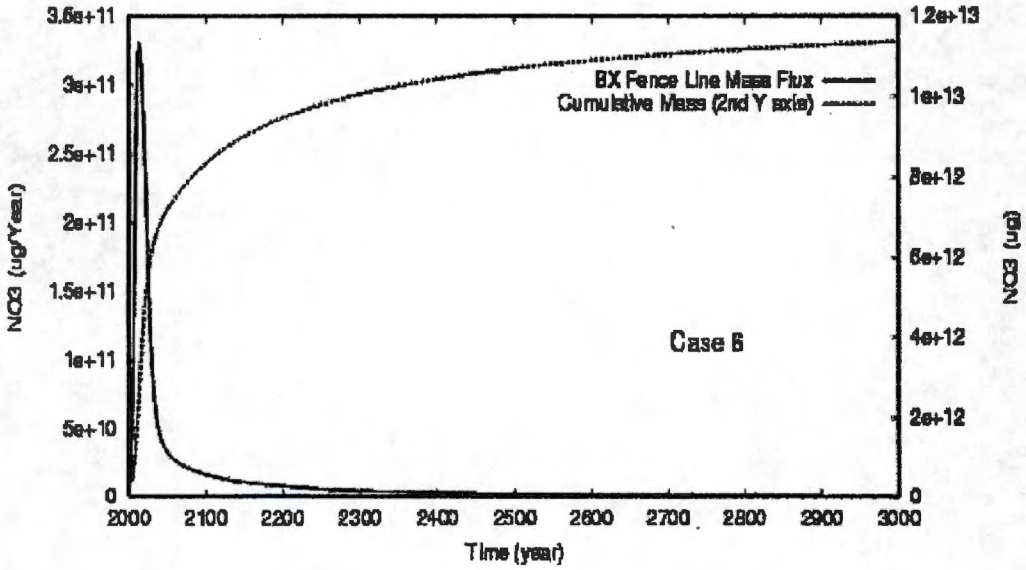

(b)

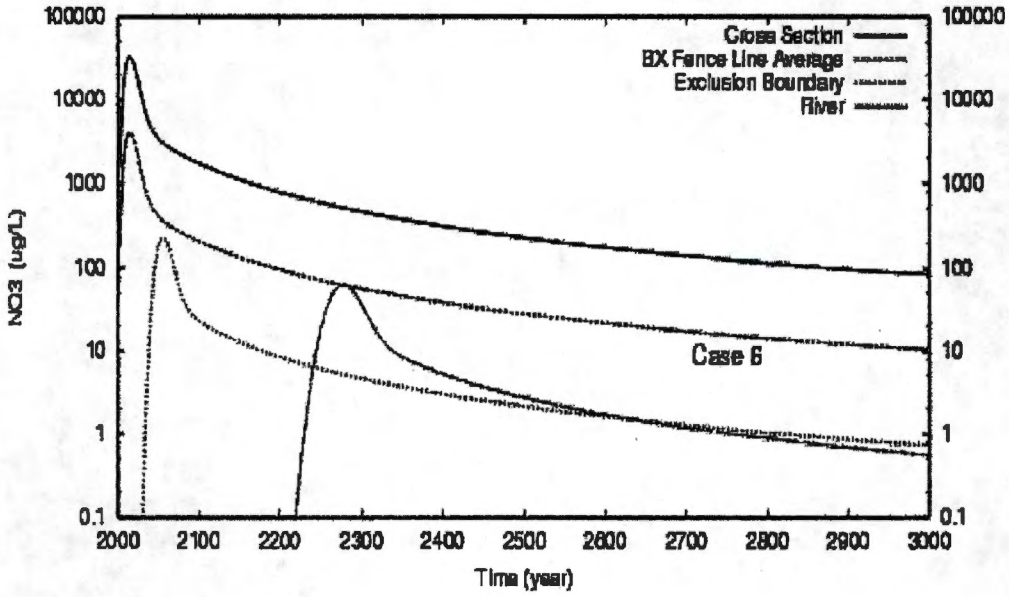

E3.7.0 CASE 7: BASE CASE WITH 50 MM/YR METEORIC RECHARGE

This scenario involves simulating flow and transport for the cross-section through tanks BX-108, BX-105, and BX-102, considering initial recharge rate of 50 mm/yr, no water line leak, no interim barrier until closure at year 2040, a Kd of 0.6 mL/g for uranium-238, and an inventory distribution that extends east of tank BX-102 to the BX tank farm fence line boundary.

Figure E3.19. Uranium-238 (a) Mass Flux and (b) Breakthrough Curves for Case 7 (50 mm/yr Recharge)

(a)

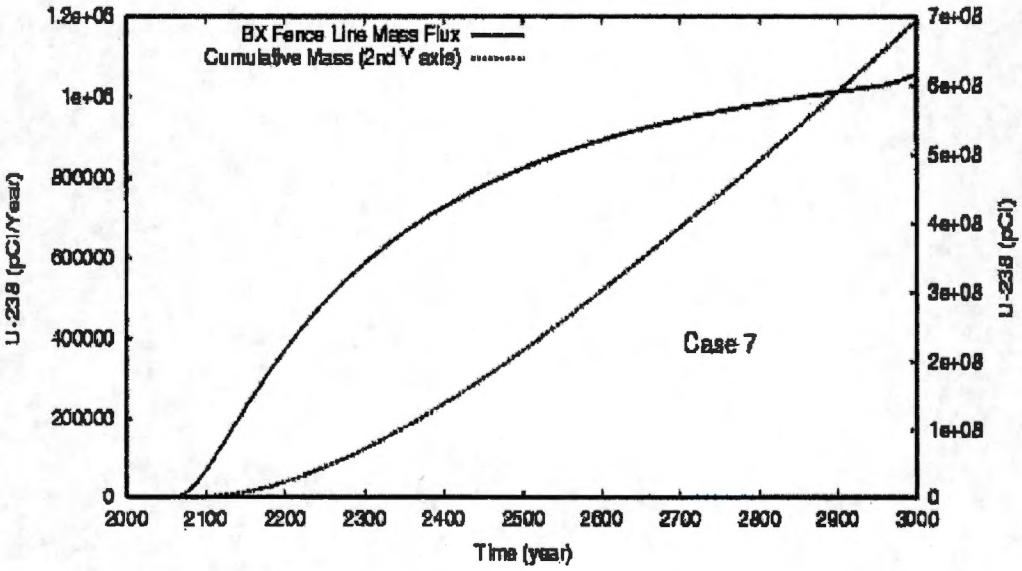

(b)

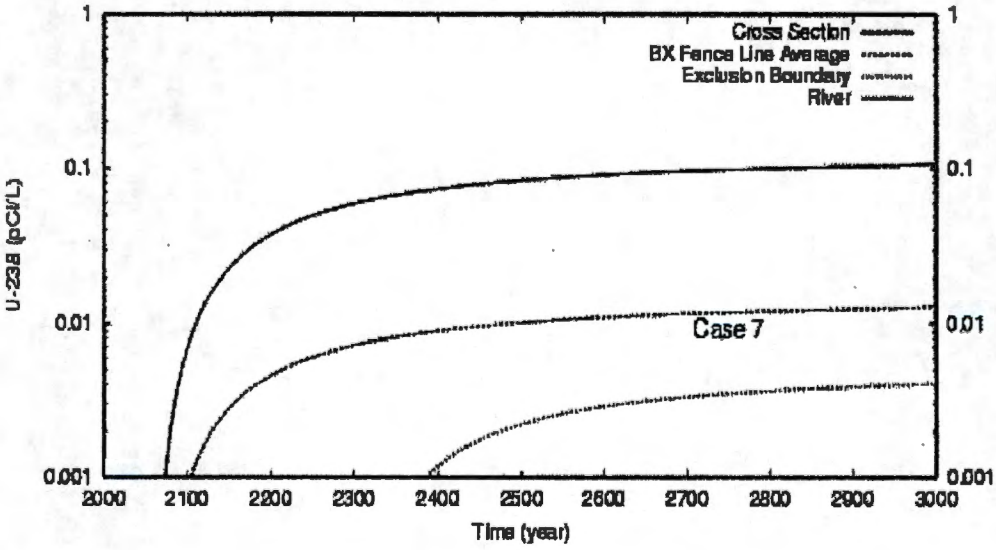

Figure E3.20. Tecnetium-99 (a) Mass Flux and (b) Breakthrough Curves for Case 7 (50 mm/yr Recharge)

(a)

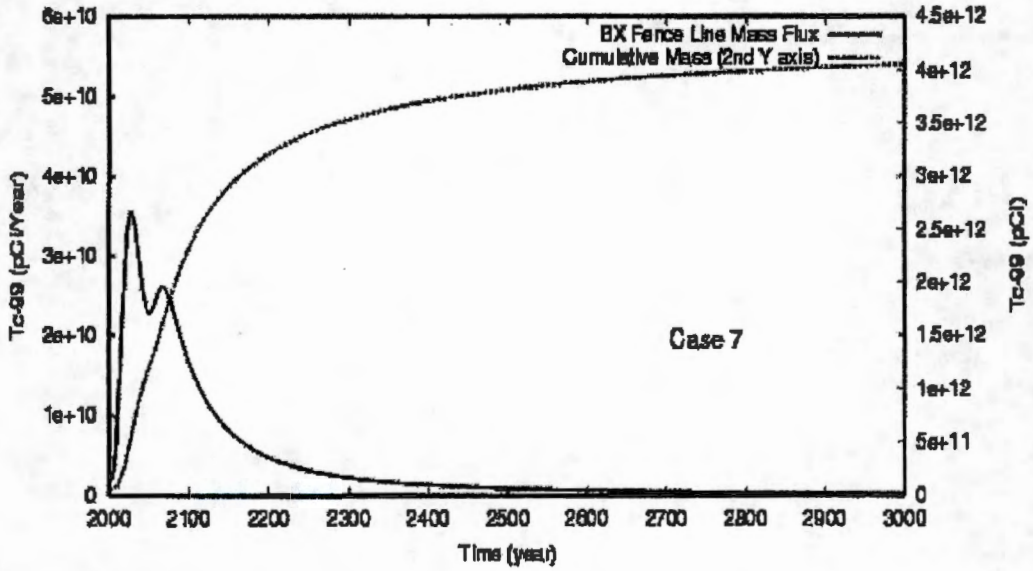

(b)

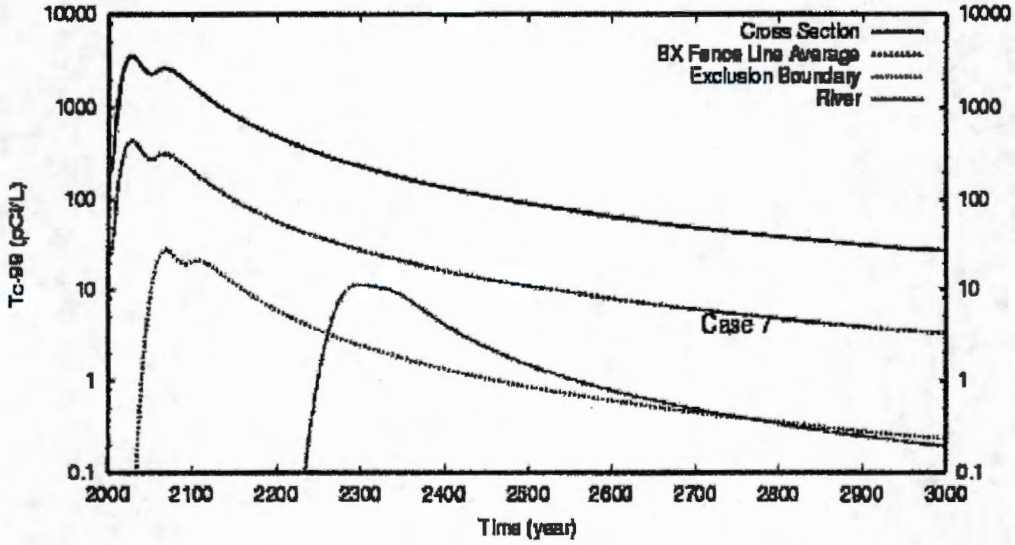

Figure E3.21. Nitrate (a) Mass Flux and (b) Breakthrough Curves for Case 7 (50 mm/yr Recharge)

(a)

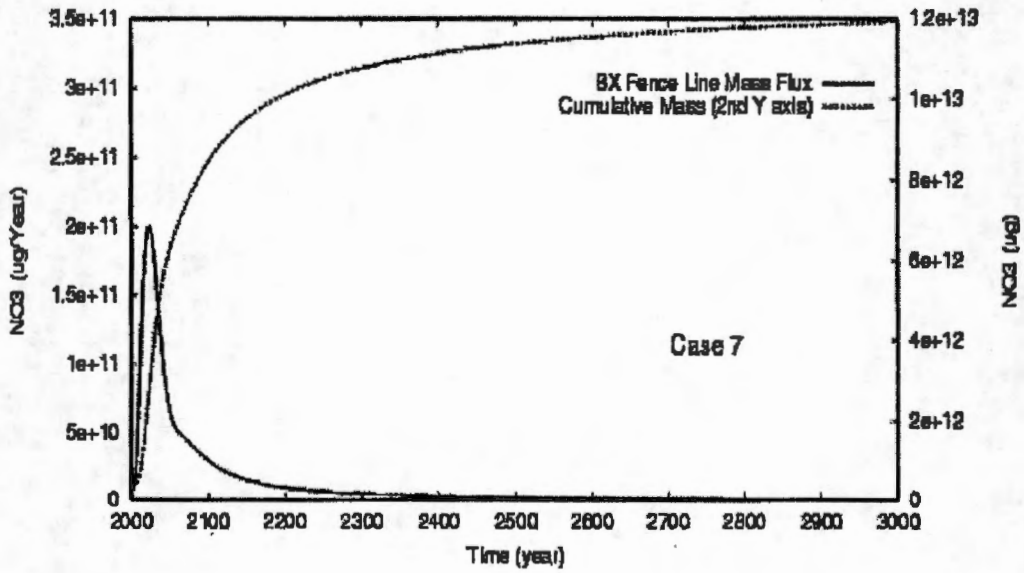

(b)

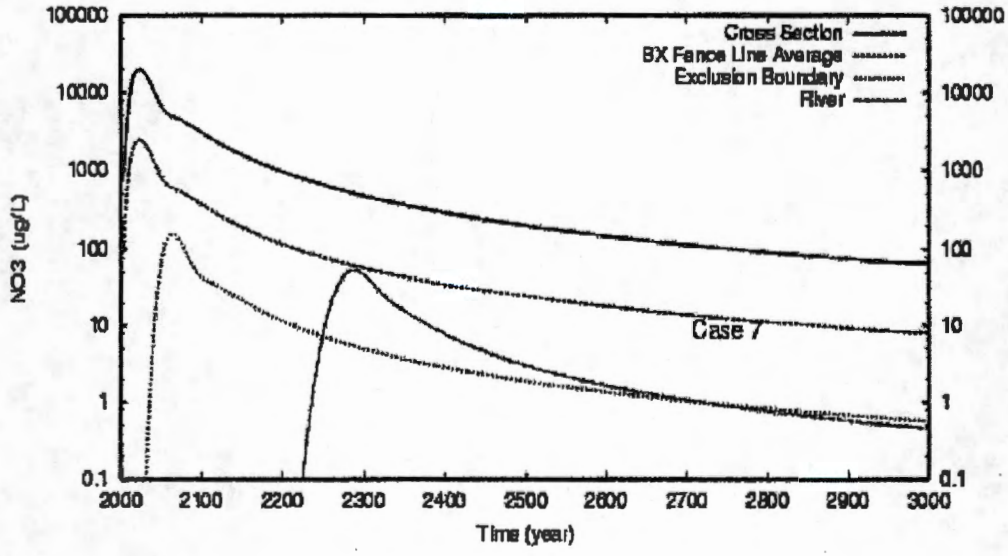

E3.8.0 CASE 8: BASE CASE WITH 30 MM/YR METEORIC RECHARGE

This scenario involves simulating flow and transport for the cross-section through tanks BX-108, BX-105, and BX-102, considering initial recharge rate of 30 mm/yr, no water line leak, no interim barrier until closure at year 2040, a Kd of 0.6 mL/g for uranium-238, and an inventory distribution that extends east of tank BX-102 to the BX tank farm fence line boundary.

Figure E3.22. Uranium-238 (a) Mass Flux and (b) Breakthrough Curves for Case 8 (30 mm/yr Recharge)

(a)

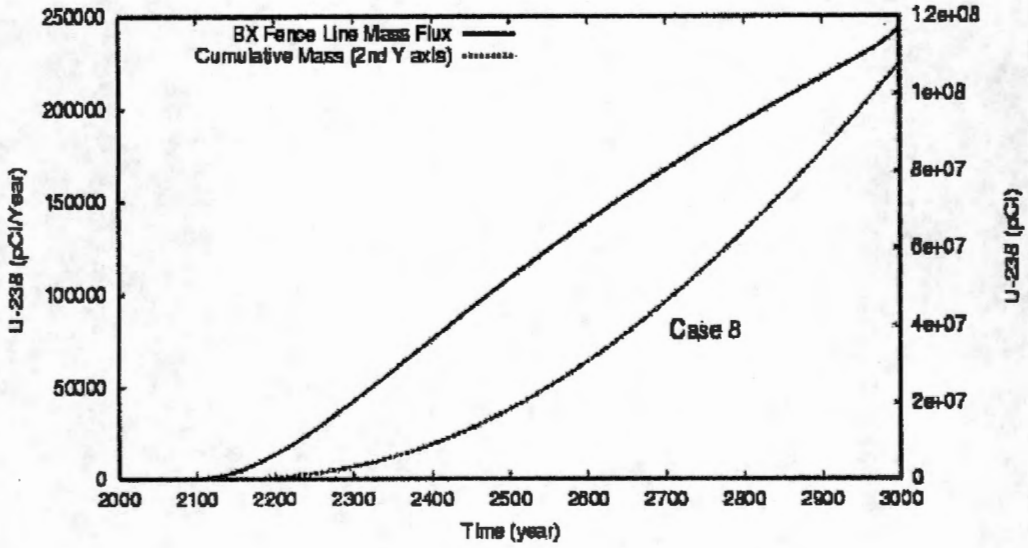

(b)

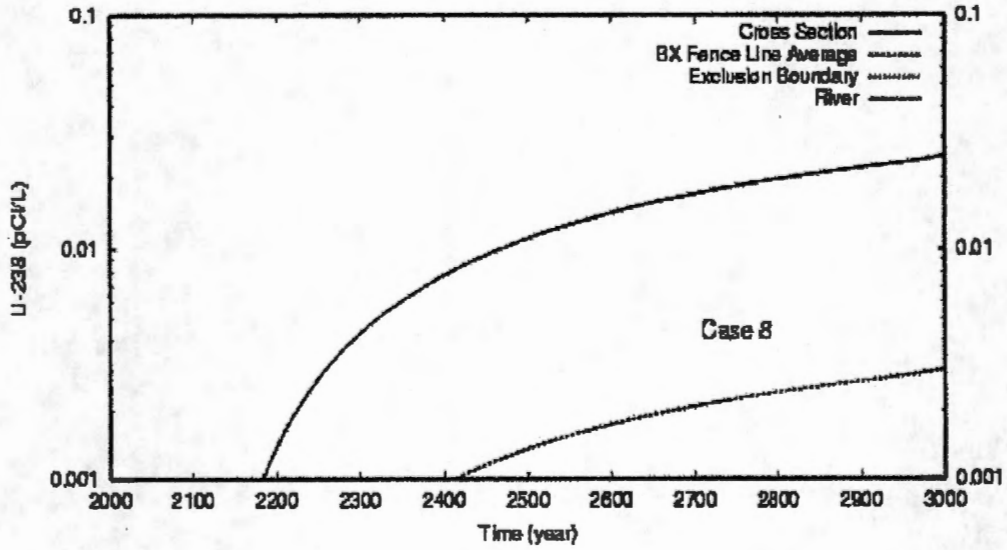

Figure E3.23. Technetium-99 (a) Mass Flux and (b) Breakthrough Curves for Case 8 (30 mm/yr Recharge)

(a)

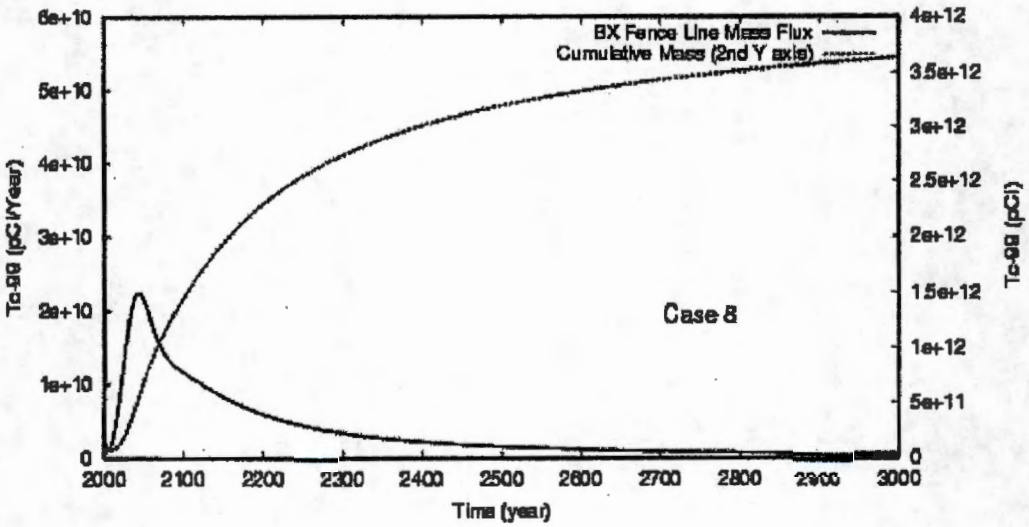

(b)

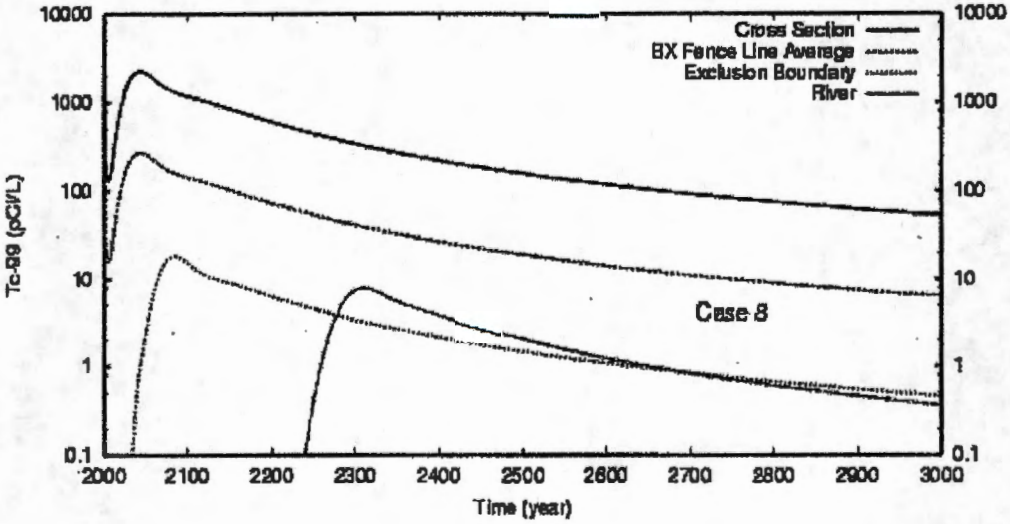

Figure E3.24. Nitrate (a) Mass Flux and (b) Breakthrough Curves for Case 8 (30 mm/yr Recharge)

(a)

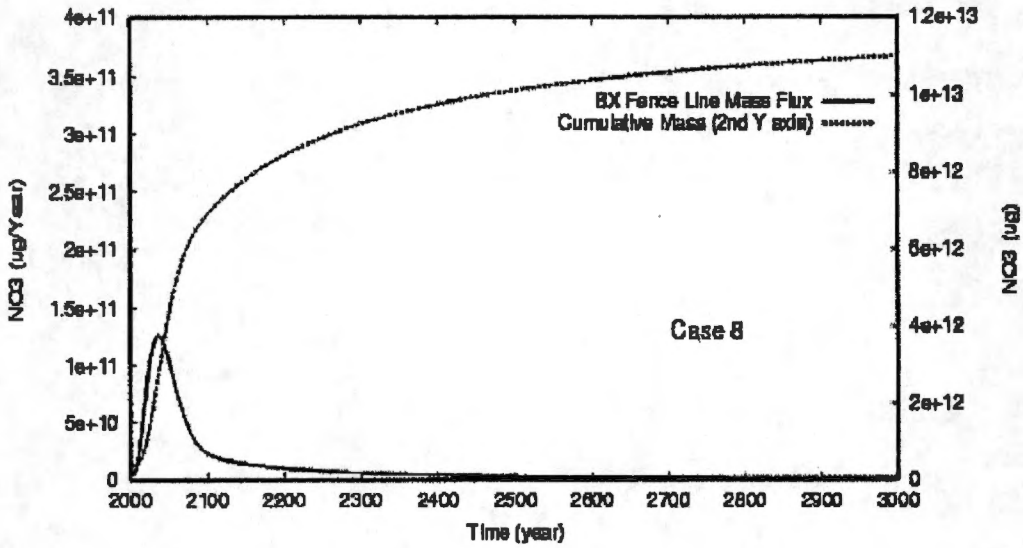

(b)

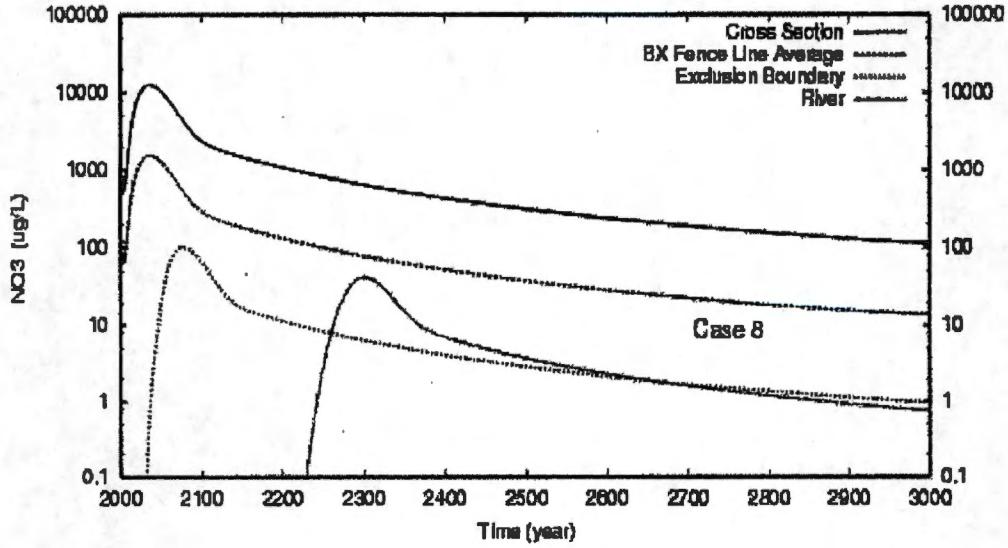

E3.9.0 CASE 9: BASE CASE WITH 10 MM/YR METEORIC RECHARGE

This scenario involves simulating flow and transport for the cross-section through tanks BX-108, BX-105, and BX-102, considering initial recharge rate of 10 mm/yr, no water line leak, no interim barrier until closure at year 2040, a Kd of 0.6 mL/g for uranium-238, and an inventory distribution that extends east of tank BX-102 to the BX tank farm fence line boundary.

Figure E3.25. Uranium-238 Mass Flux for Case 9 (10 mm/yr Recharge)

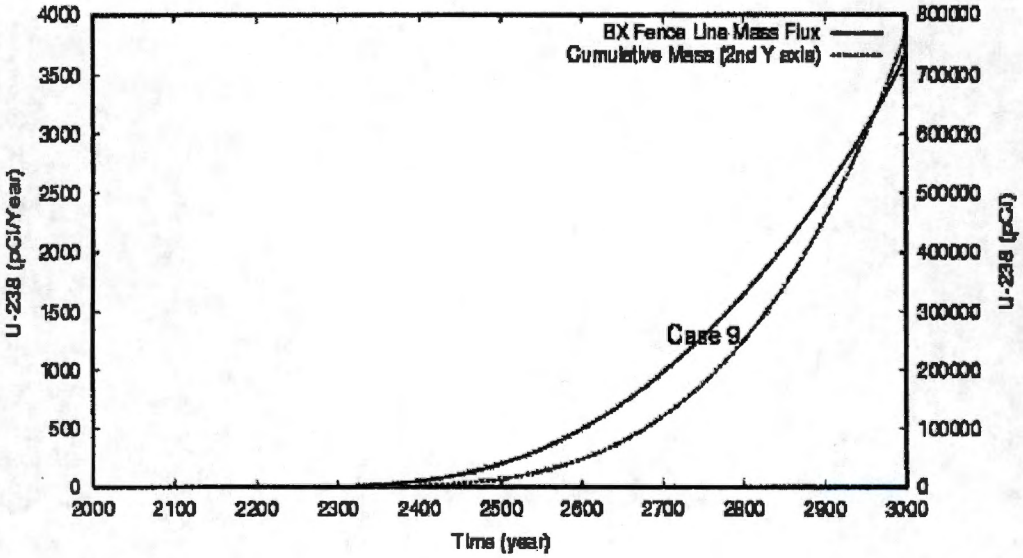

Figure E3.26. Technetium-99 (a) Mass Flux and (b) Breakthrough Curves for Case 9 (10 mm/yr Recharge)

(a)

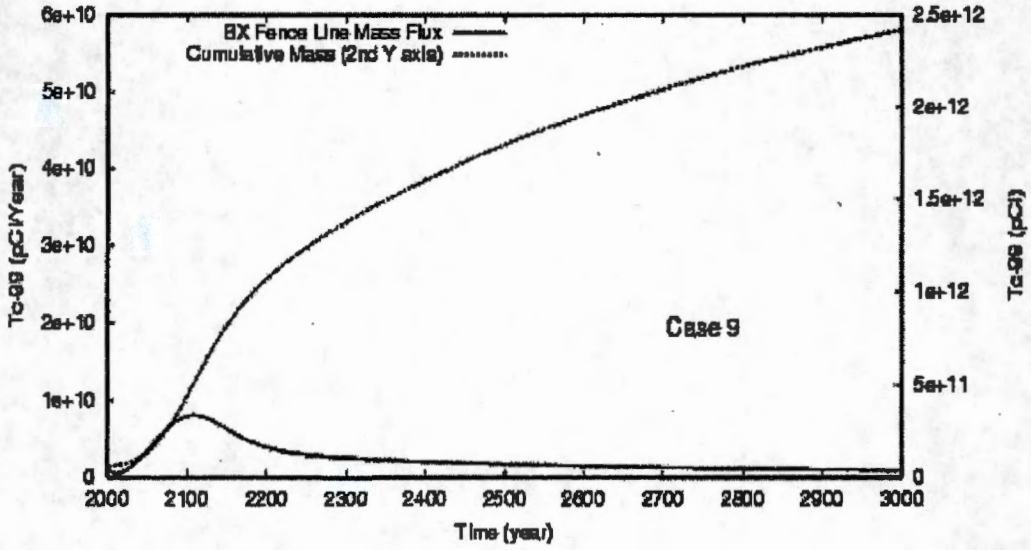

(b)

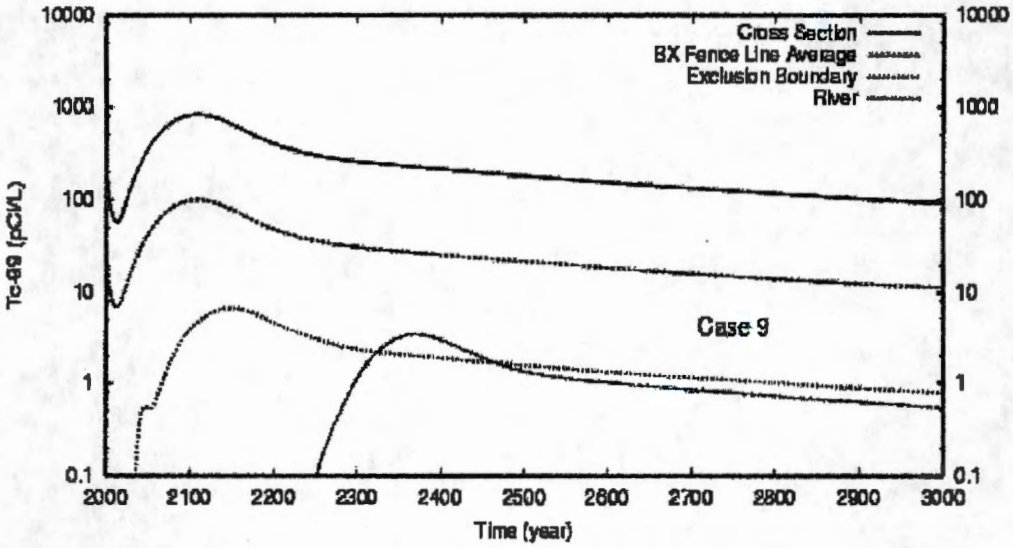

Figure E3.27. Nitrate (a) Mass Flux and (b) Breakthrough Curves for Case 9 (10 mm/yr Recharge)

(a)

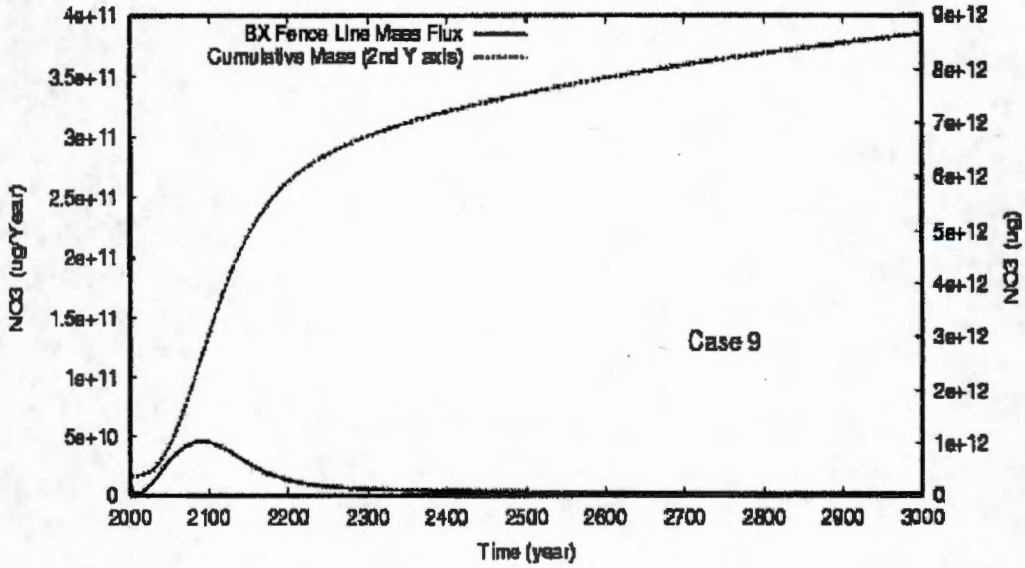

(b)

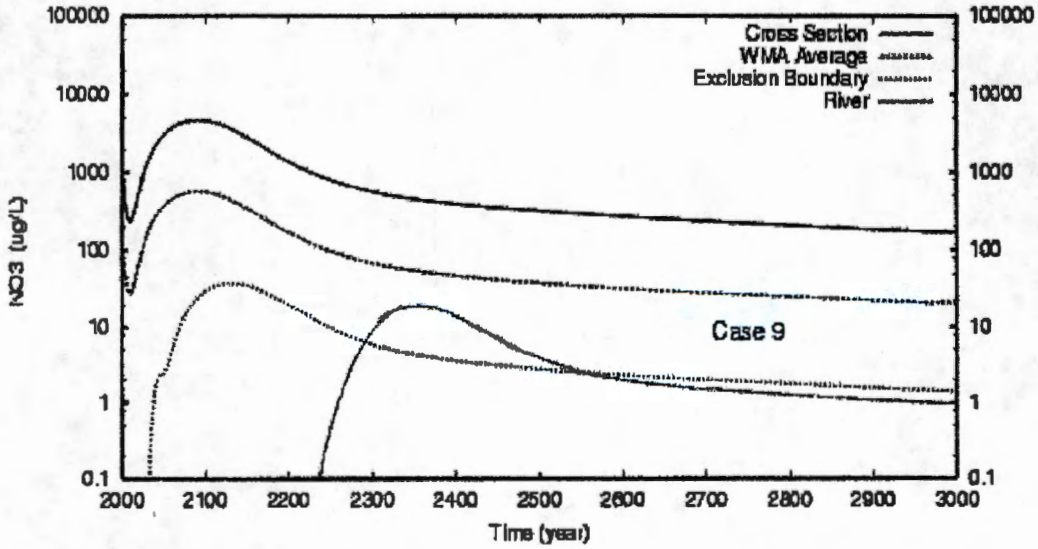

Figure E3.26. Technetium-99 (a) Mass Flux and (b) Breakthrough Curves for Case 9 (10 mm/yr Recharge)

(a)

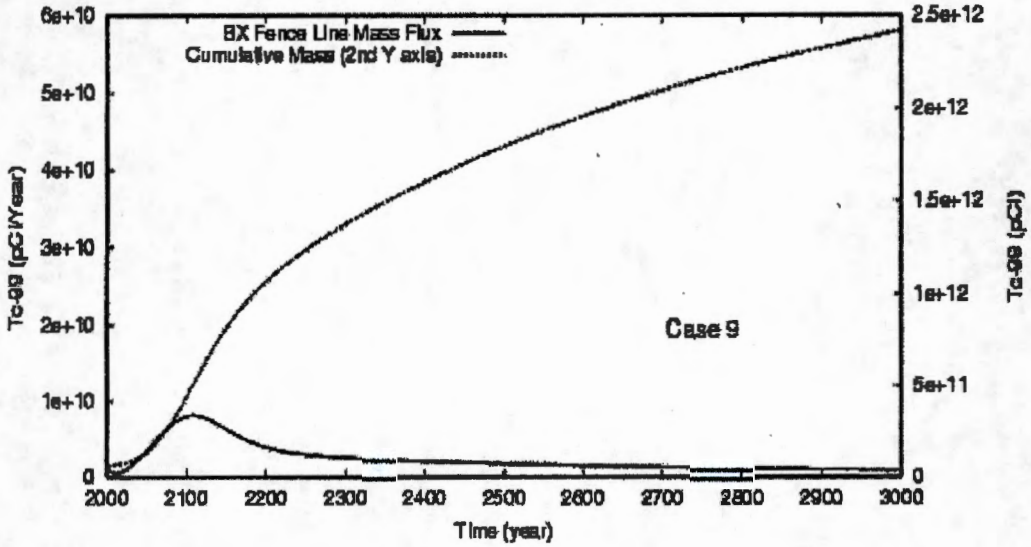

(b)

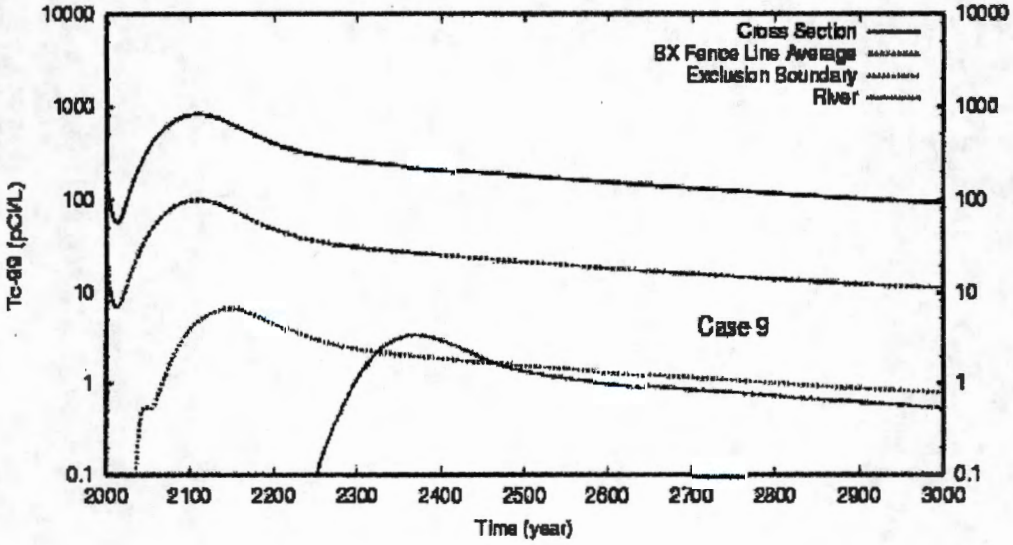

Figure E3.27. Nitrate (a) Mass Flux and (b) Breakthrough Curves for Case 9 (10 mm/yr Recharge)

(a)

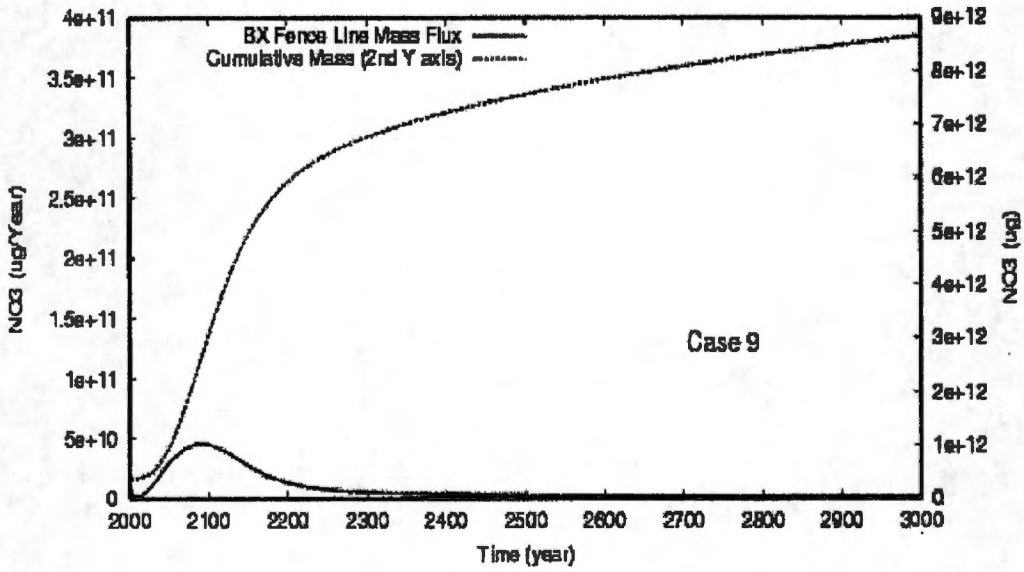

(b)

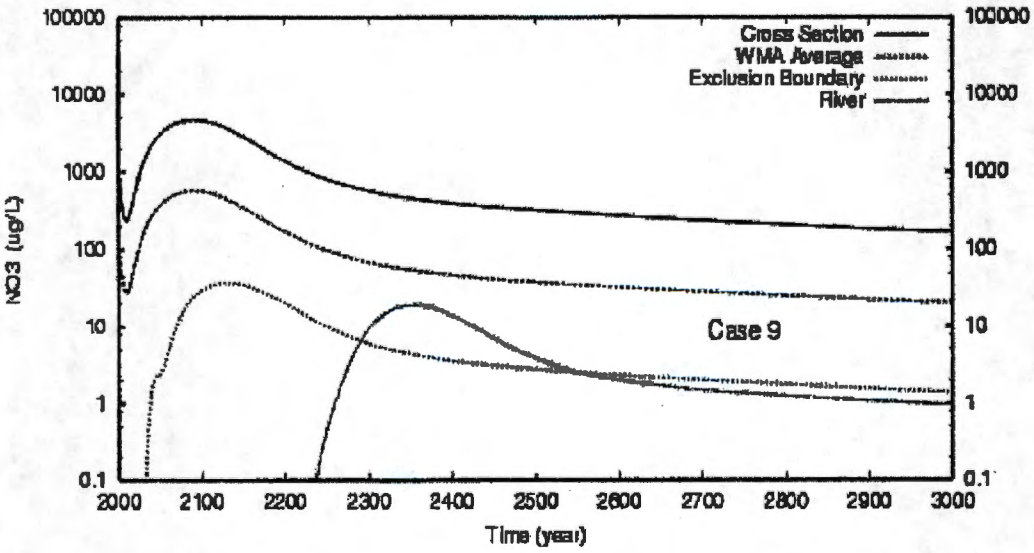

E3.10.0 CASE 10: BASE CASE WITH Kd = 0.1 ML/G FOR URANIUM-238

This scenario involves simulating flow and transport for the cross-section through tanks BX-108, BX-105, and BX-102, considering initial recharge rate of 100 mm/yr, no interim barrier until closure at year 2040, a partition coefficient (Kd) of 0.1 mL/g for uranium-238, and an inventory distribution that extends east of tank BX-102 to the BX tank farm fence line boundary.

Figure E3.28. Uranium-238 (a) Mass Flux and (b) Breakthrough Curves for Case 10 (Uranium-238 Kd=0.1 mL/g)

(a)

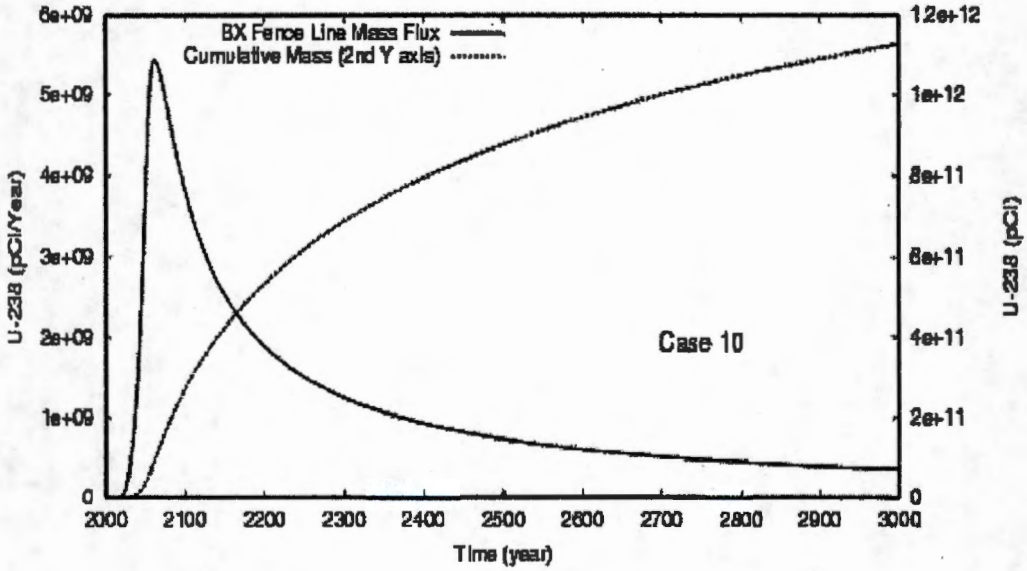

(b)

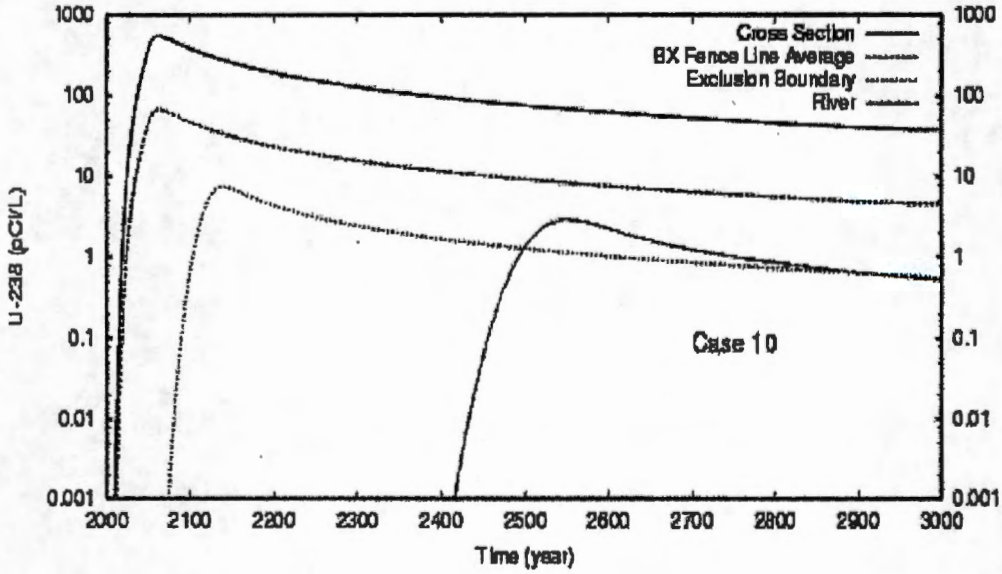

E3.11.0 CASE 11: BASE CASE WITH Kd = 1 ML/G FOR URANIUM-238

This scenario involves simulating flow and transport for the cross-section through tanks BX-108, BX-105, and BX-102, considering initial recharge rate of 100 mm/yr, no interim barrier until closure at year 2040, a partition coefficient (Kd) of 1.0 mL/g for uranium-238, and an inventory distribution that extends east of tank BX-102 to the BX tank farm fence line boundary.

Figure E3.29. Uranium-238 (a) Mass Flux and (b) Breakthrough Curves for Case 11 (Uranium-238 Kd=1 mL/g)

(a)

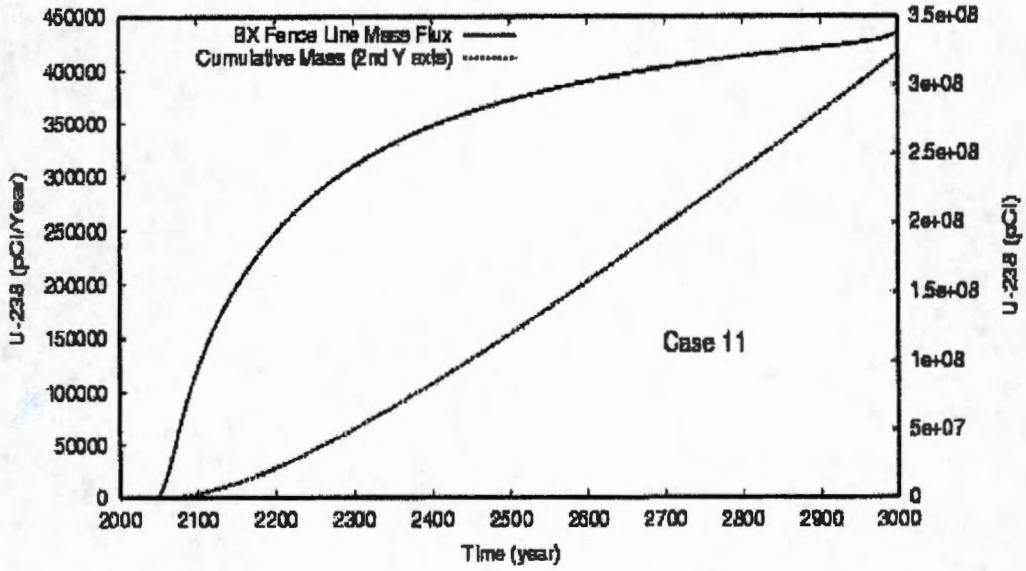

(b)

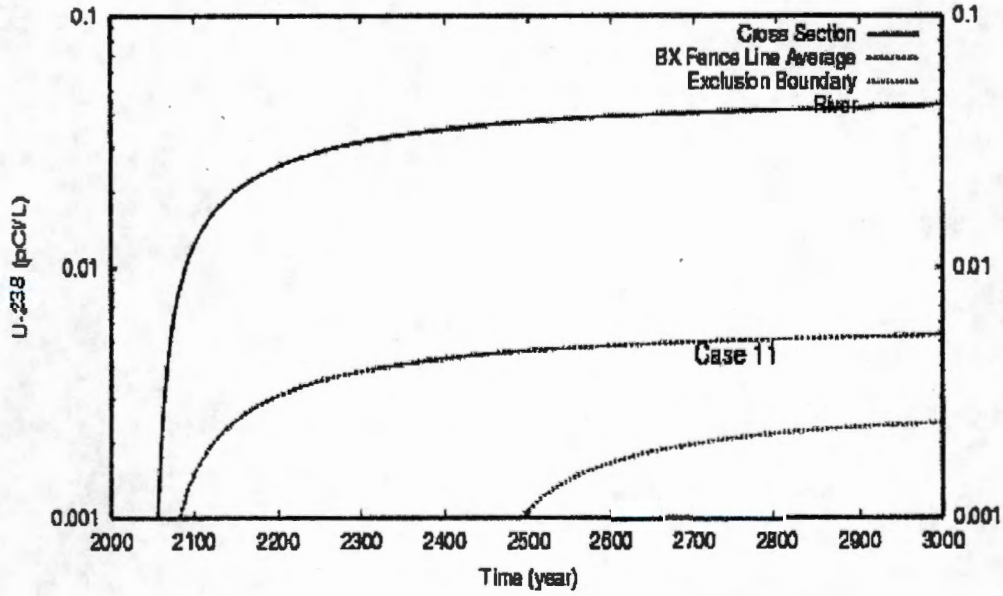

ATTACHMENT E4

TRENCH 216-B-38 MASS FLUX AND BREAKTHROUGH CURVES

This page intentionally left blank.

CONTENTS

E4.1.0 CASE 12: TRENCH B-38 WITH 55.4 MM/YR METEORIC RECHARGE E4-1

E4.2.0 CASE 13: TRENCH B-38 WITH 100 MM/YR METEORIC RECHARGE E4-8

E4.3.0 CASE 14: TRENCH B-38 WITH 100 MM/YR METEORIC RECHARGE AND DELAYED CLOSURE BARRIER E4-15

FIGURES

E4.1. Case 12 Technetium-99 (a) Mass Flux and (b) Breakthrough Curves for Trench B-38 with Unit Inventory E4-2
E4.2. Case 12 Nitrate (a) Mass Flux and (b) Breakthrough Curves for Trench B-38 with Unit Inventory E4-3
E4.3. Case 12 Technetium-99 (a) Mass Flux and (b) Breakthrough Curves for Trench B-38 ..... E4-4
E4.4. Case 12 Nitrate (a) Mass Flux and (b) Breakthrough Curves for Trench B-38 ..... E4-5
E4.5. Case 12 Technetium-99 (a) Mass Flux and (b) Breakthrough Curves for all Eight Trenches E4-6
E4.6. Case 12 Nitrate (a) Mass Flux and (b) Breakthrough Curves for all Eight Trenches E4-7
E4.7. Case 13 Technetium-99 (a) Mass Flux and (b) Breakthrough Curves for Trench B-38 with Unit Inventory E4-9
E4.8. Case 13 Nitrate (a) Mass Flux and (b) Breakthrough Curves for Trench B-38 with Unit Inventory E4-10
E4.9. Case 13 Technetium-99 (a) Mass Flux and (b) Breakthrough Curves for Trench B-38 ..... E4-11
E4.10. Case 13 Nitrate (a) Mass Flux and (b) Breakthrough Curves for Trench B-38 ..... E4-12
E4.11. Case 13 Technetium-99 (a) Mass Flux and (b) Breakthrough Curves for all Eight Trenches E4-13
E4.12. Case 13 Nitrate (a) Mass Flux and (b) Breakthrough Curves for all Eight Trenches E4-14
E4.13. Case 14 Technetium-99 (a) Mass Flux and (b) Breakthrough Curves for Trench B-38 with Unit Inventory E4-16
E4.14. Case 14 Nitrate (a) Mass Flux and (b) Breakthrough Curves for Trench B-38 with Unit Inventory E4-17
E4.15. Case 14 Technetium-99 (a) Mass Flux and (b) Breakthrough Curves for Trench B-38 ..... E4-18
E4.16. Case 14 Nitrate (a) Mass Flux and (b) Breakthrough Curves for Trench B-38 ..... E4-19
E4.17. Case 14 Technetium-99 (a) Mass Flux and (b) Breakthrough Curves for all Eight Trenches E4-20
E4.18. Case 14 Nitrate (a) Mass Flux and (b) Breakthrough Curves for all Eight Trenches E4-21

This page intentionally left blank.

E4.1.0 CASE 12: TRENCH B-38 WITH 55.4 MM/YR METEORIC RECHARGE

This scenario involves simulating flow and transport for a cross-section west of tank BX-111, considering initial recharge rate of 55.4 mm/yr, a 378,000-gallon leak in 1954, no water line leak, no interim barrier until closure at year 2010, and a unit inventory distribution for a sorbed species (i.e., uranium-238, Kd = 0.6 mL/g) and a non-sorbing species (i.e., technetium-99 and nitrate). The unit inventory results are also scaled to the U-238, technetium-99, and nitrate inventory estimates for trench B-38 and all of the B trenches.

Figure E4.1. Case 12 Technetium-99 (a) Mass Flux and (b) Breakthrough Curves for Trench B-38 with Unit Inventory

(a)

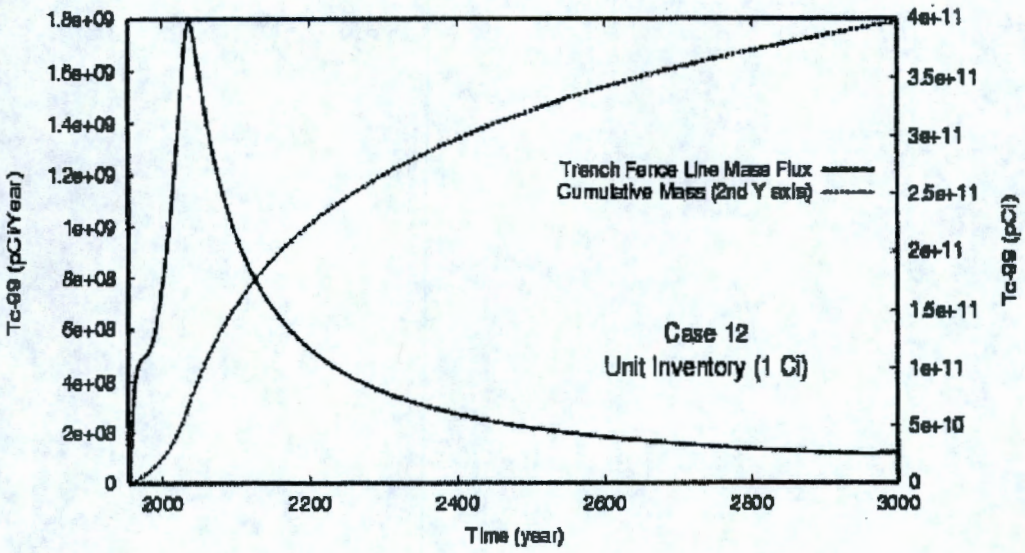

(b)

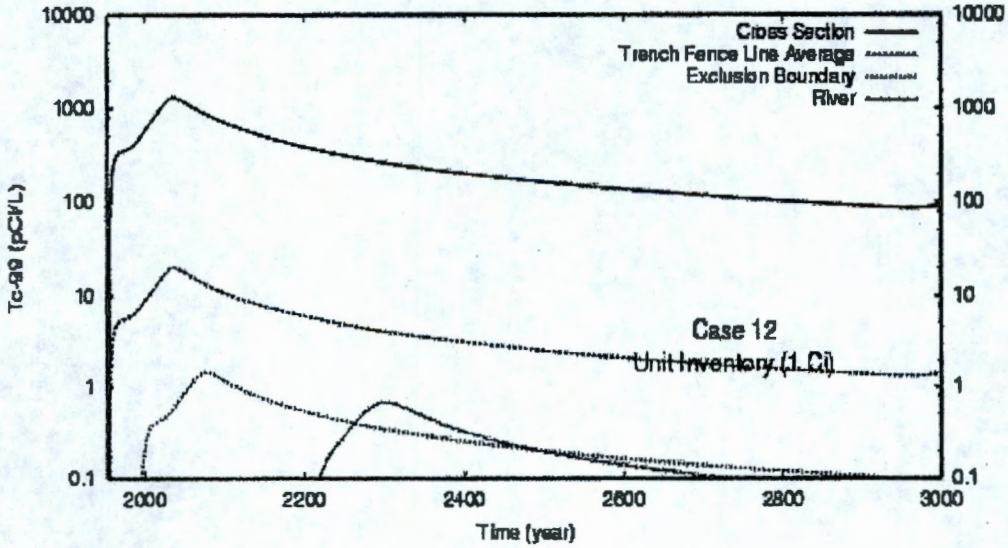

Figure E4.2. Case 12 Nitrate (a) Mass Flux and (b) Breakthrough Curves for Trench B-38 with Unit Inventory

(a)

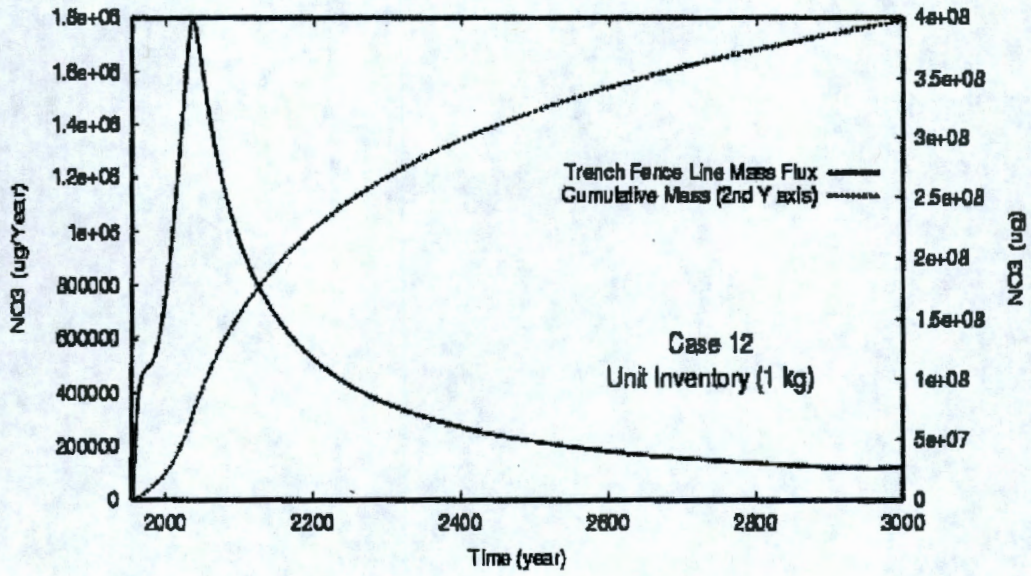

(b)

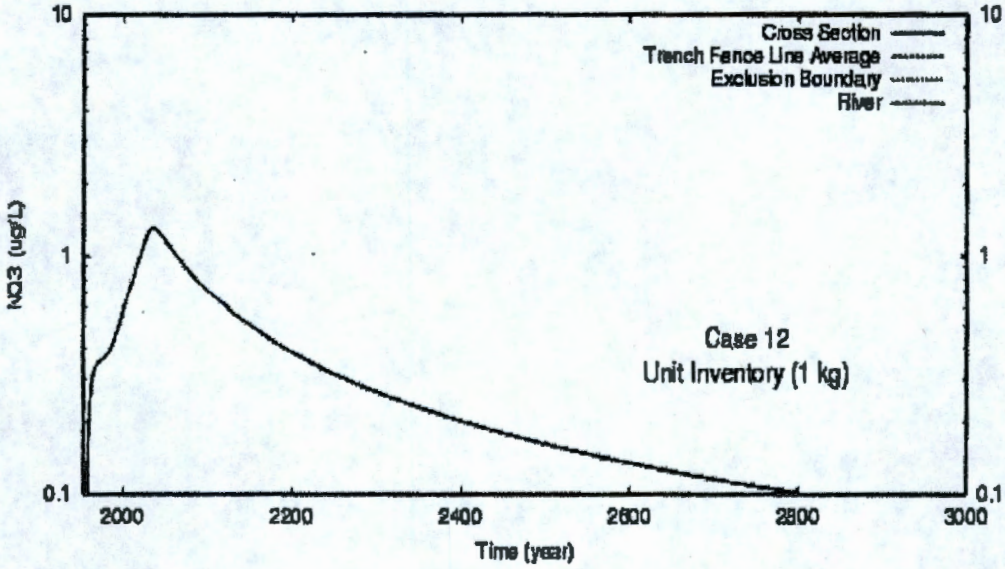

Figure E4.3. Case 12 Technetium-99 (a) Mass Flux and (b) Breakthrough Curves for Trench B-38

(a)

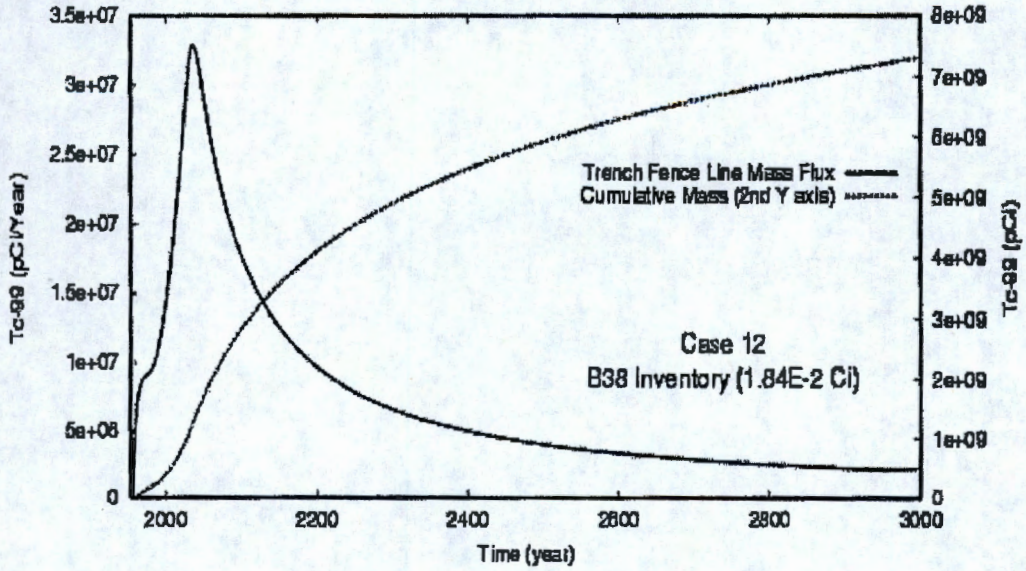

(b)

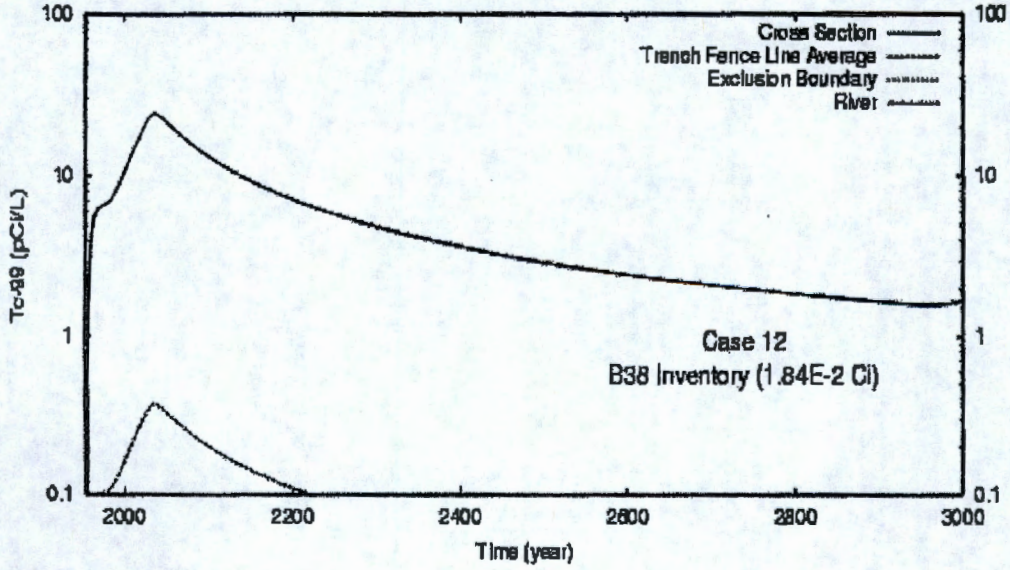

Figure E4.4. Case 12 Nitrate (a) Mass Flux and (b) Breakthrough Curves for Trench B-38

(a)

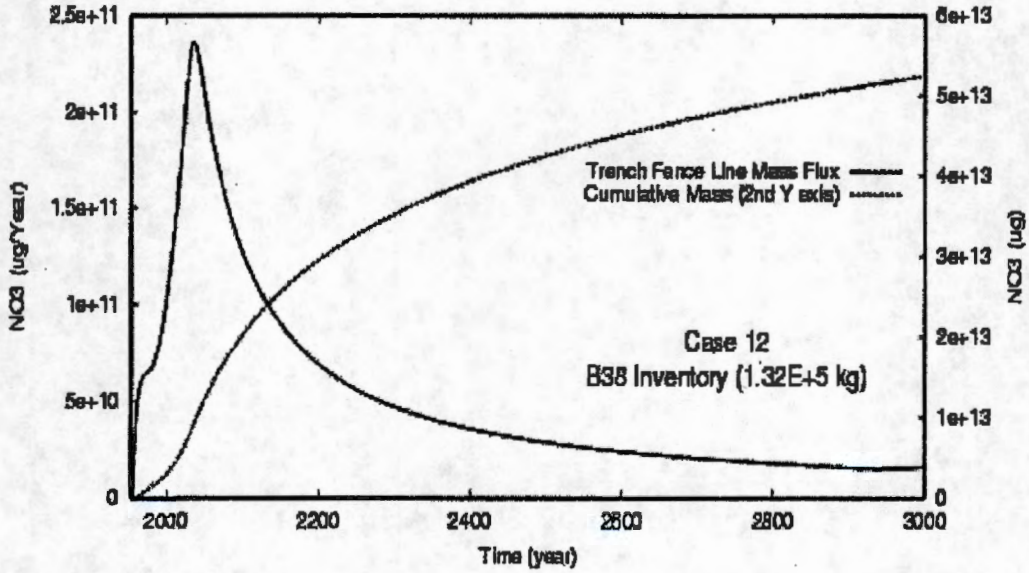

(b)

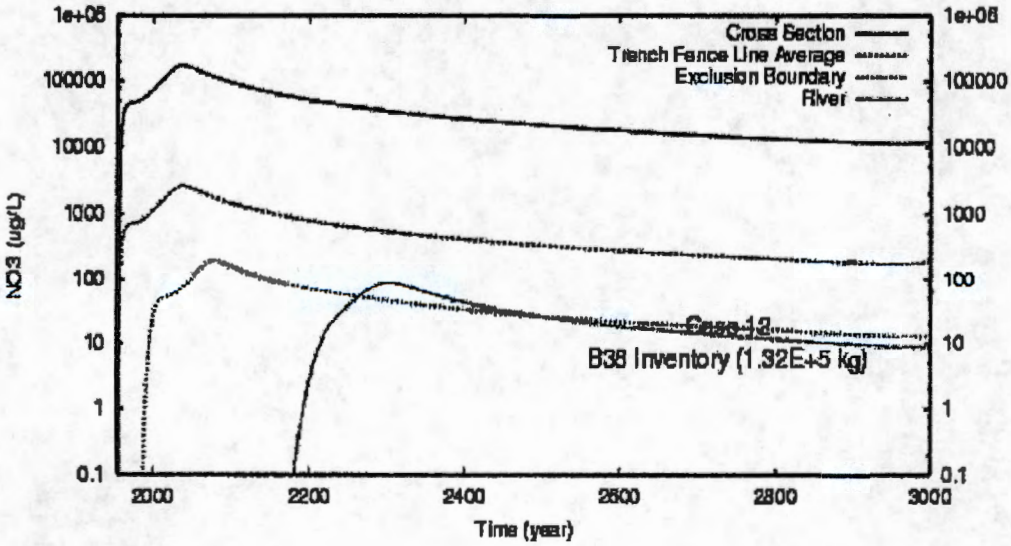

Figure E4.5. Case 12 Technetium-99 (a) Mass Flux and (b) Breakthrough Curves for all Eight Trenches

(a)

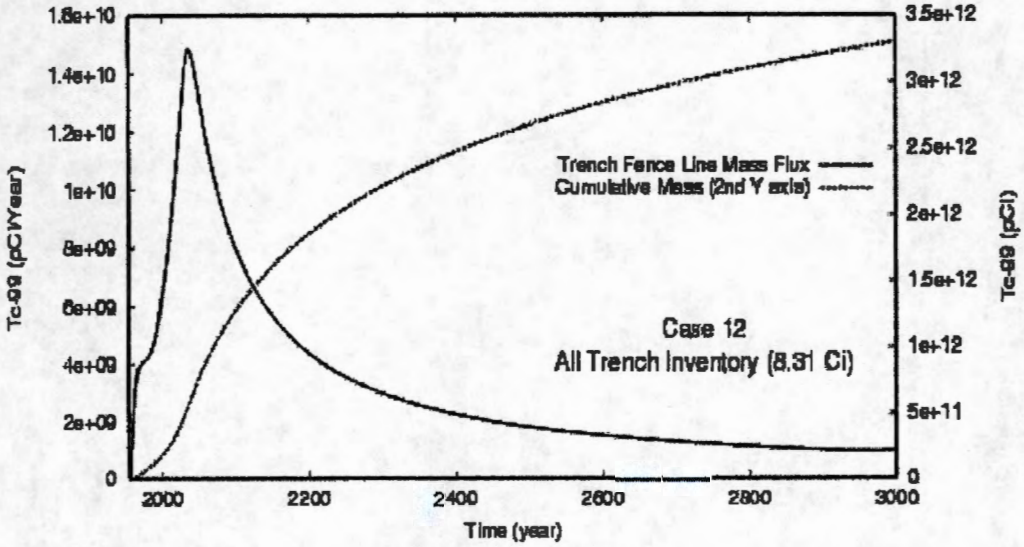

(b)

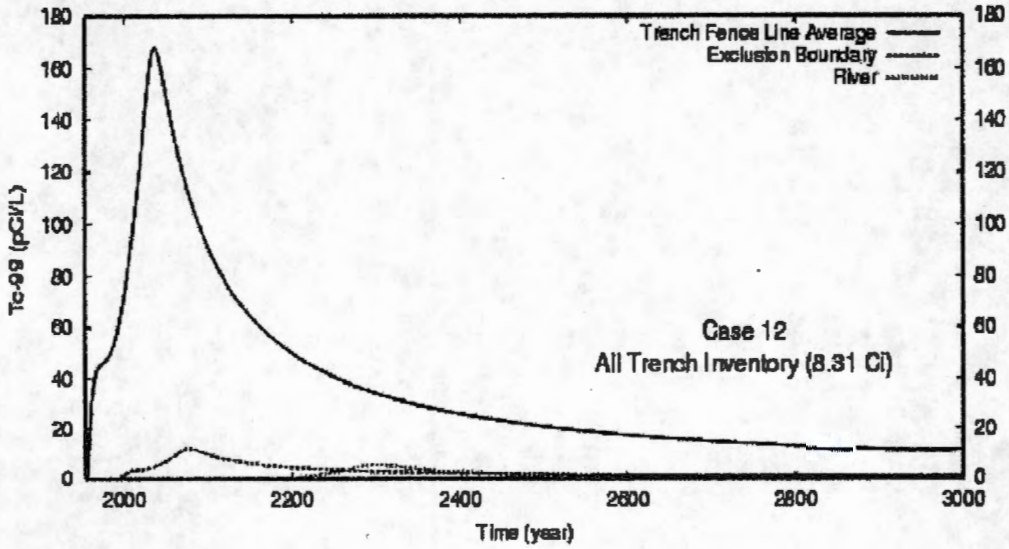

Figure E4.6. Case 12 Nitrate (a) Mass Flux and (b) Breakthrough Curves for all Eight Trenches

(a)

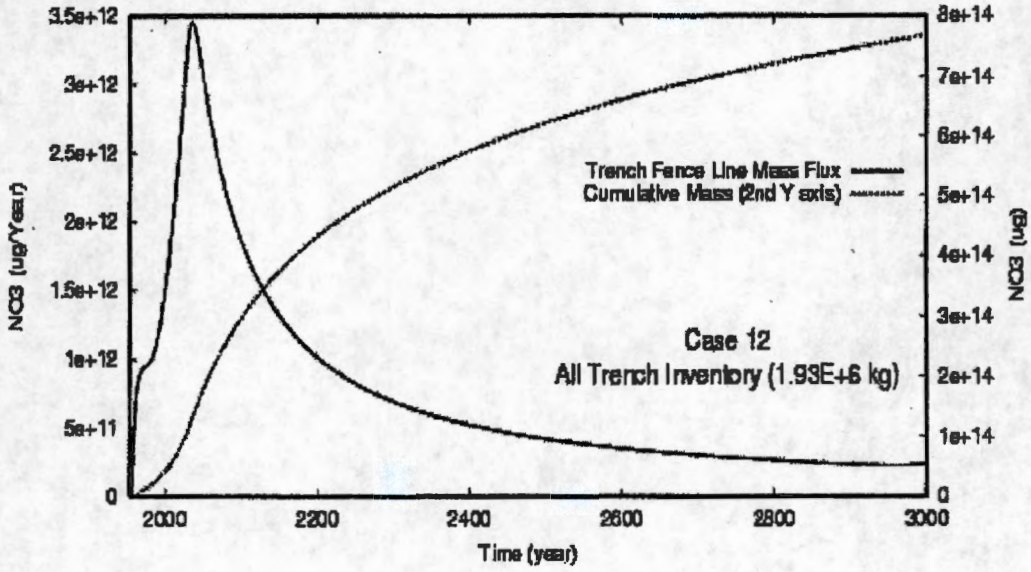

(b)

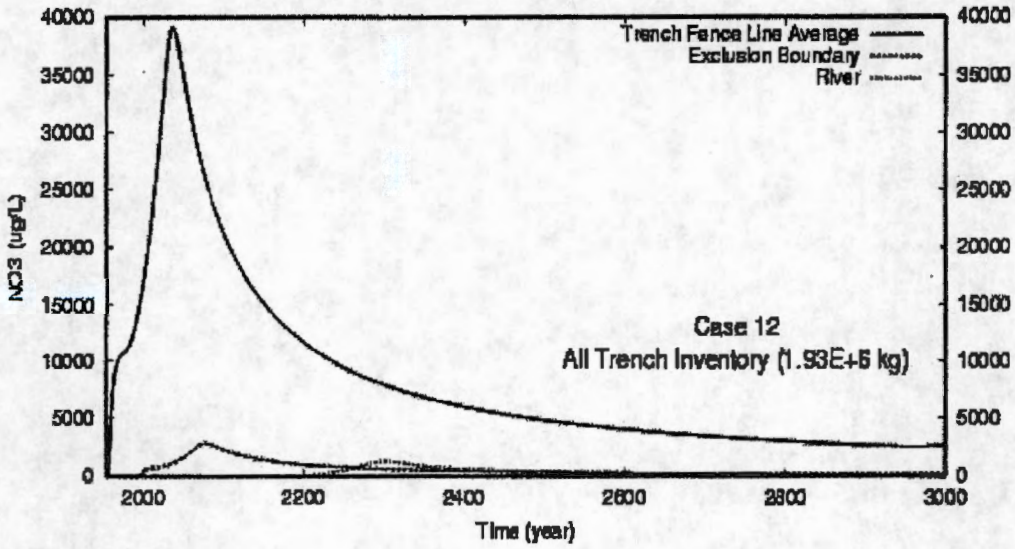

E4.2.0 CASE 13: TRENCH B-38 WITH 100 MM/YR METEORIC RECHARGE

This scenario involves simulating flow and transport for a cross-section west of tank BX-111, considering initial recharge rate of 100 mm/yr, a 378,000-gallon leak in 1954, no interim barrier until closure at year 2010, and a unit inventory distribution for a sorbed species (i.e., uranium-238, Kd = 0.6 mL/g) and a non-sorbing species (i.e., technetium-99 and nitrate). The unit inventory results are also scaled to the uranium-238, technetium-99, and nitrate inventory estimates for trench B-38 and all of the B trenches..

Figure E4.7. Case 13 Technetium-99 (a) Mass Flux and (b) Breakthrough Curves for Trench B-38 with Unit Inventory

(a)

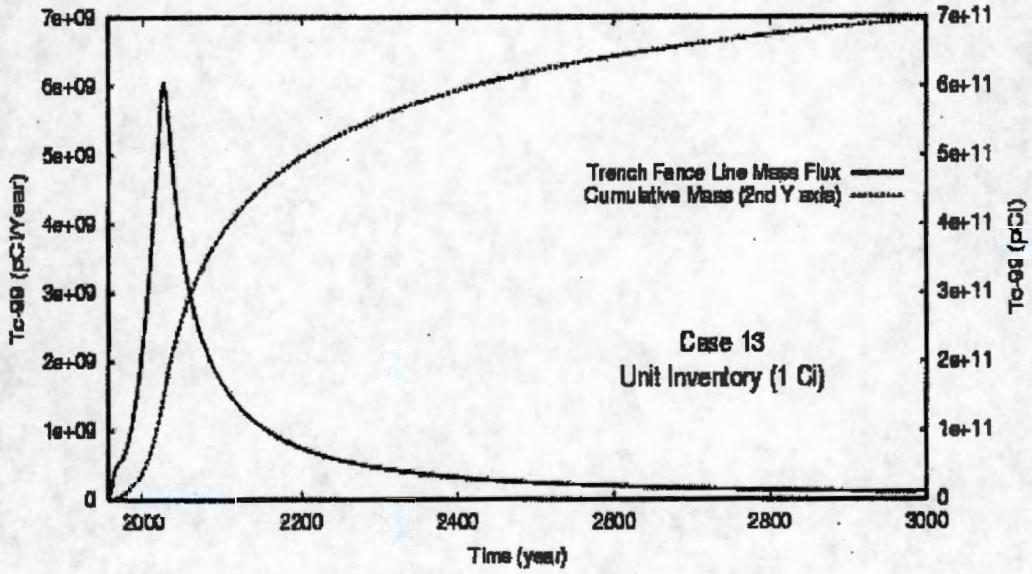

(b)

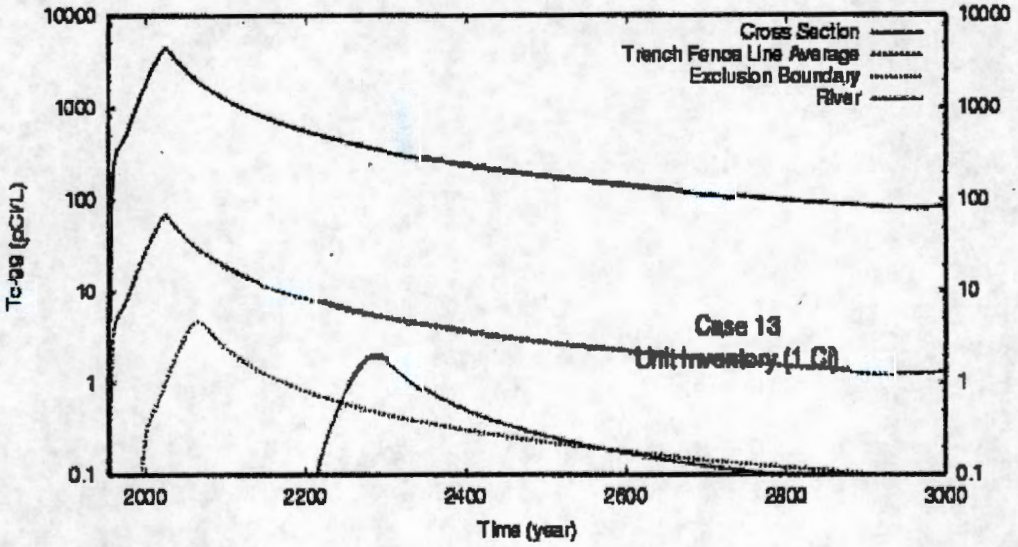

Figure E4.8. Case 13 Nitrate (a) Mass Flux and (b) Breakthrough Curves for Trench B-38 with Unit Inventory

(a)

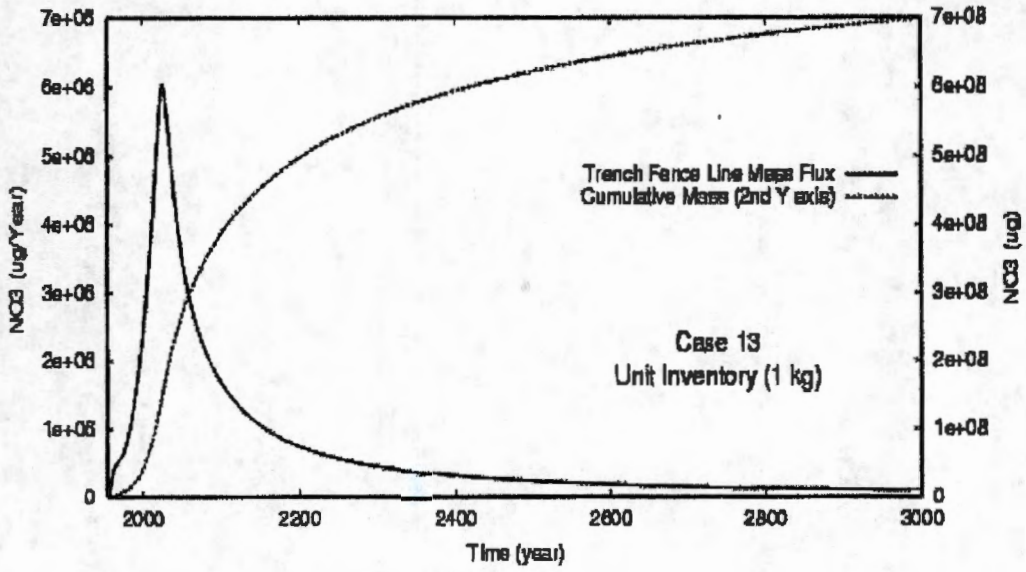

(b)

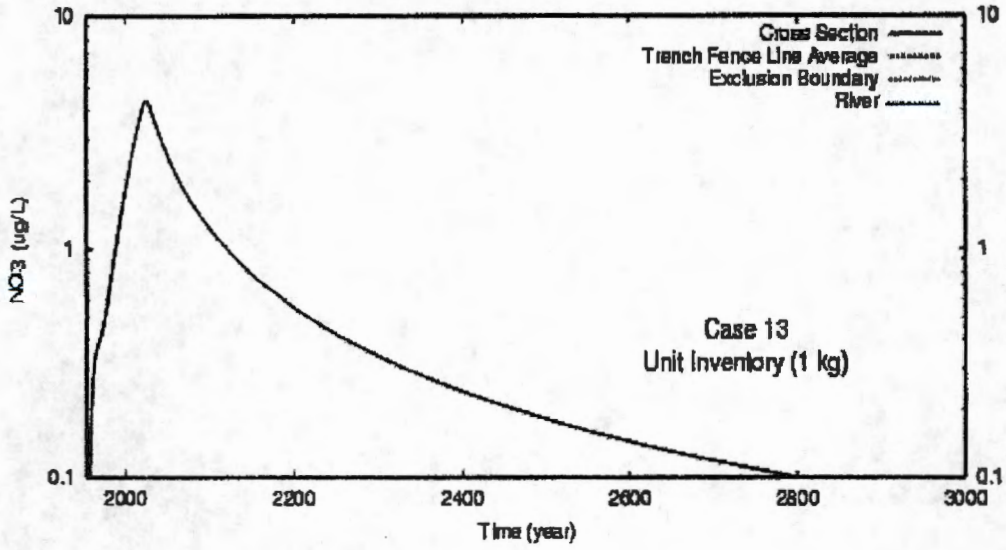

Figure E4.9. Case 13 Technetium-99 (a) Mass Flux and (b) Breakthrough Curves for Trench B-38

(a)

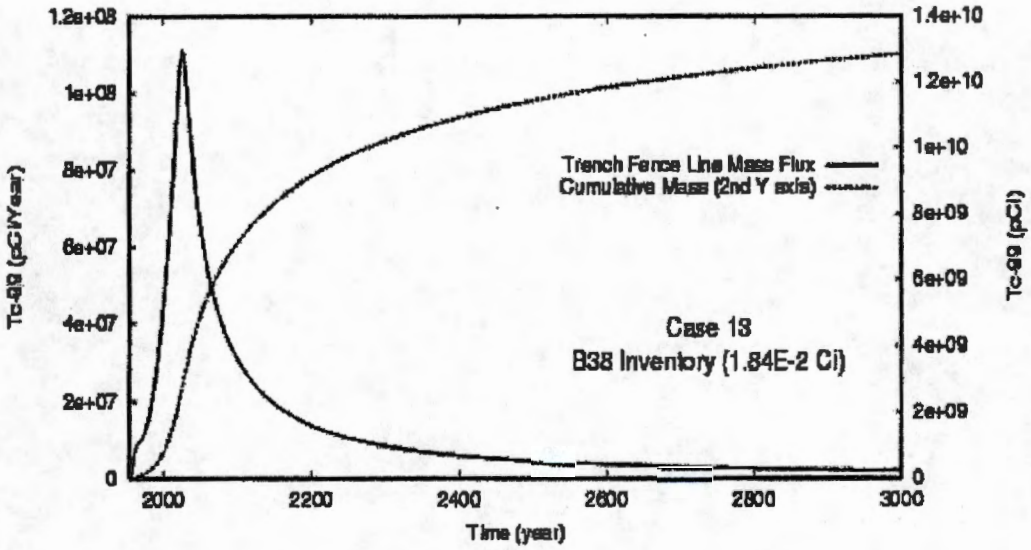

(b)

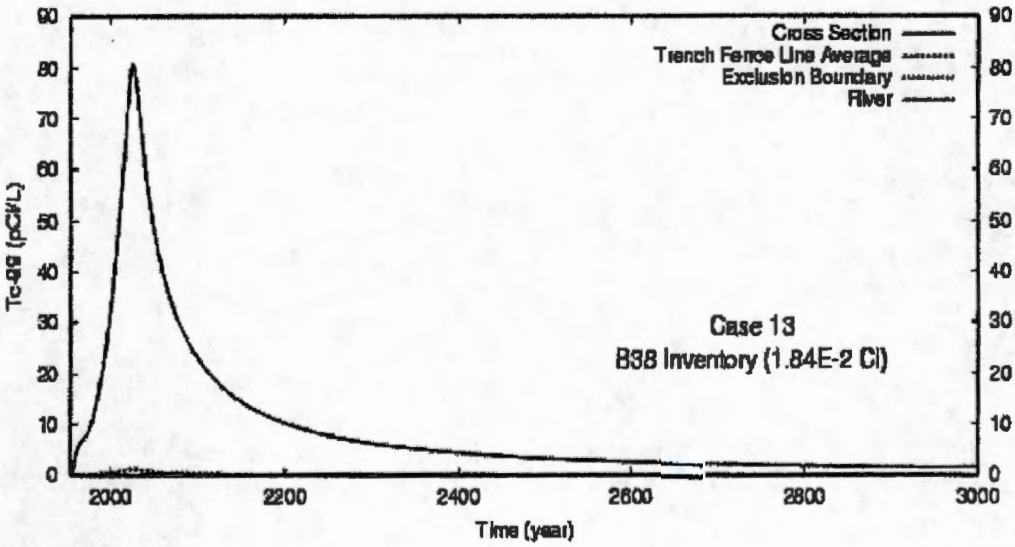

Figure E4.10. Case 13 Nitrate (a) Mass Flux and (b) Breakthrough Curves for Trench B-38

(a)

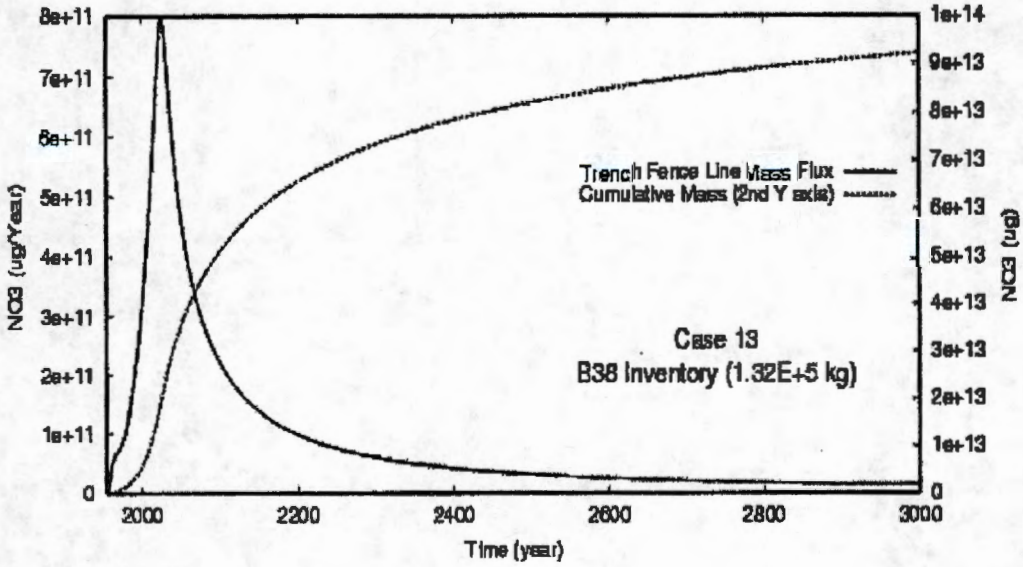

(b)

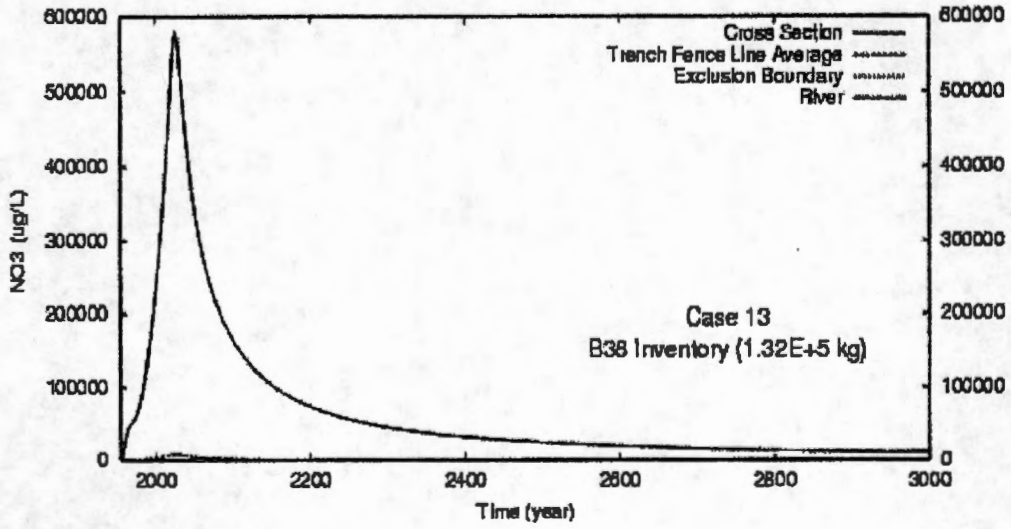

Figure E4.11. Case 13 Technetium-99 (a) Mass Flux and (b) Breakthrough Curves for all Eight Trenches

(a)

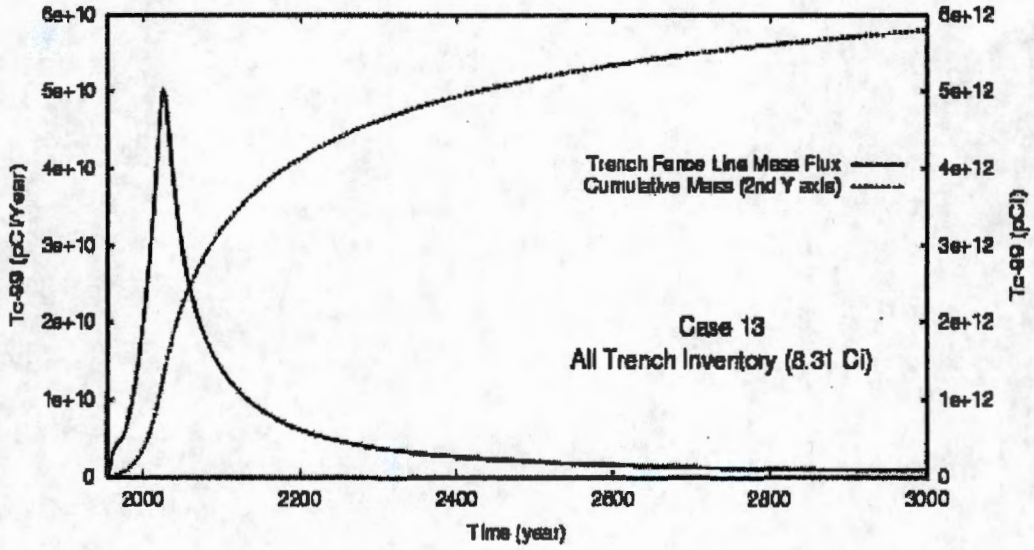

(b)

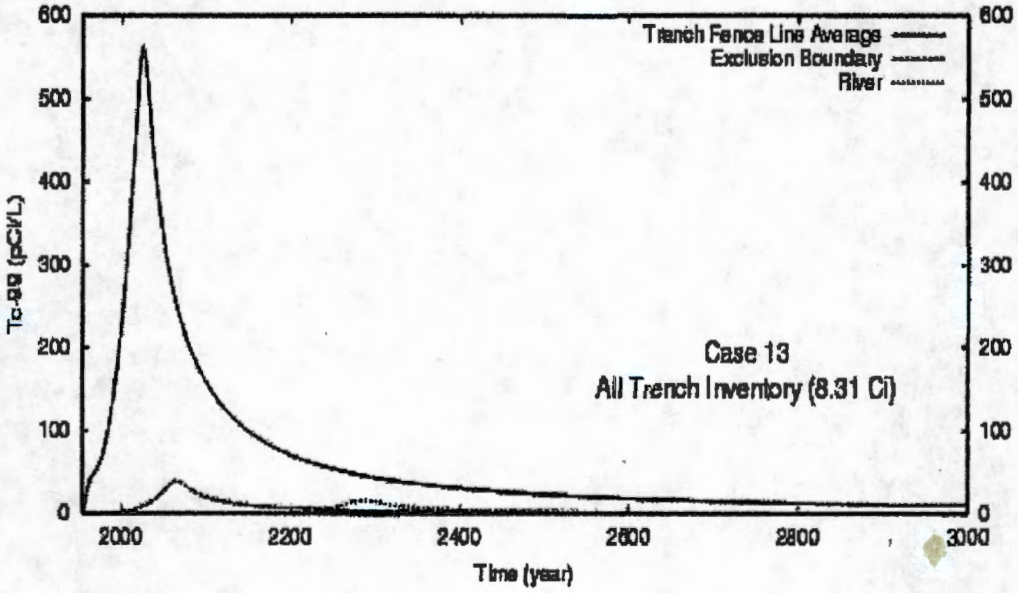

Figure E4.12. Case 13 Nitrate (a) Mass Flux and (b) Breakthrough Curves for all Eight Trenches

(a)

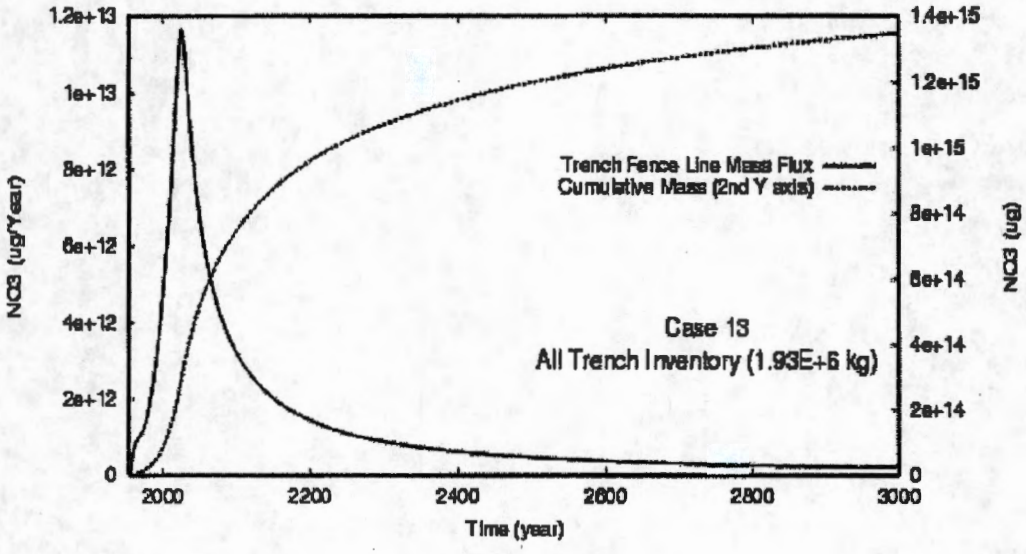

(b)

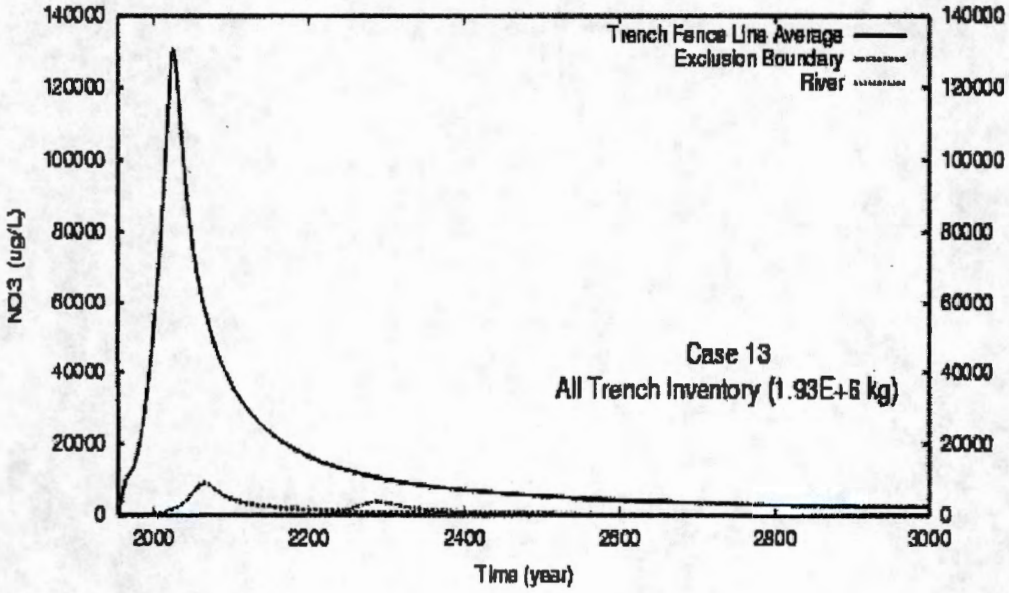

E4.3.0 CASE 14: TRENCH B-38 WITH 100 MM/YR METEORIC RECHARGE AND DELAYED CLOSURE BARRIER

This scenario involves simulating flow and transport for a cross-section west of tank BX-111, considering initial recharge rate of 100 mm/yr, a 378,000-gallon leak in 1954, no interim barrier until closure at year 2040, and a unit inventory distribution for a sorbed species (i.e., uranium-238, Kd = 0.6 mL/g) and a non-sorbing species (i.e., technetium-99 and nitrate). The unit inventory results are also scaled to the uranium-238, technetium-99, and nitrate inventory estimates for trench B-38 and all of the B trenches.

Figure E4.13. Case 14 Technetium-99 (a) Mass Flux and (b) Breakthrough Curves for Trench B-38 with Unit Inventory

(a)

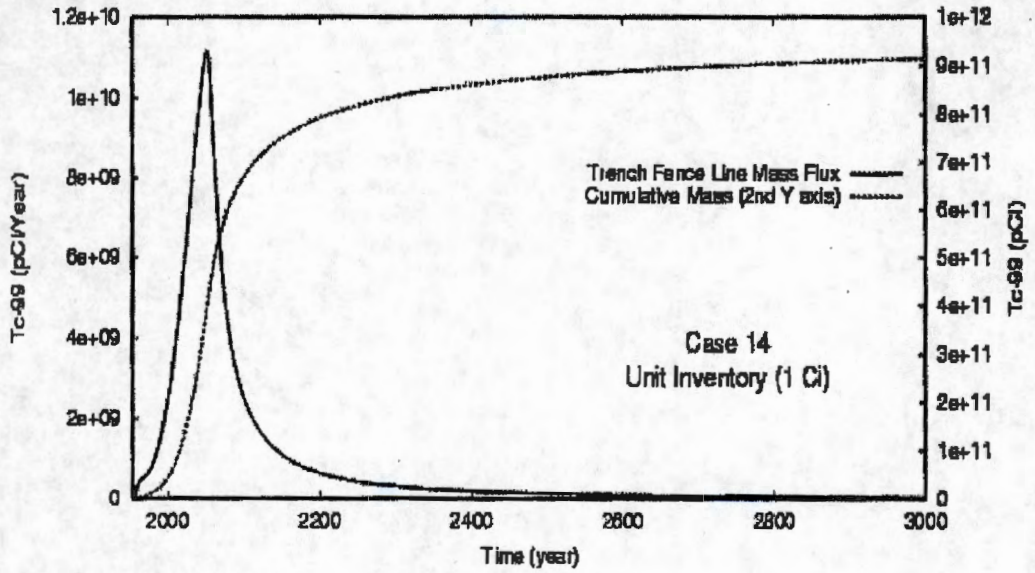

(b)

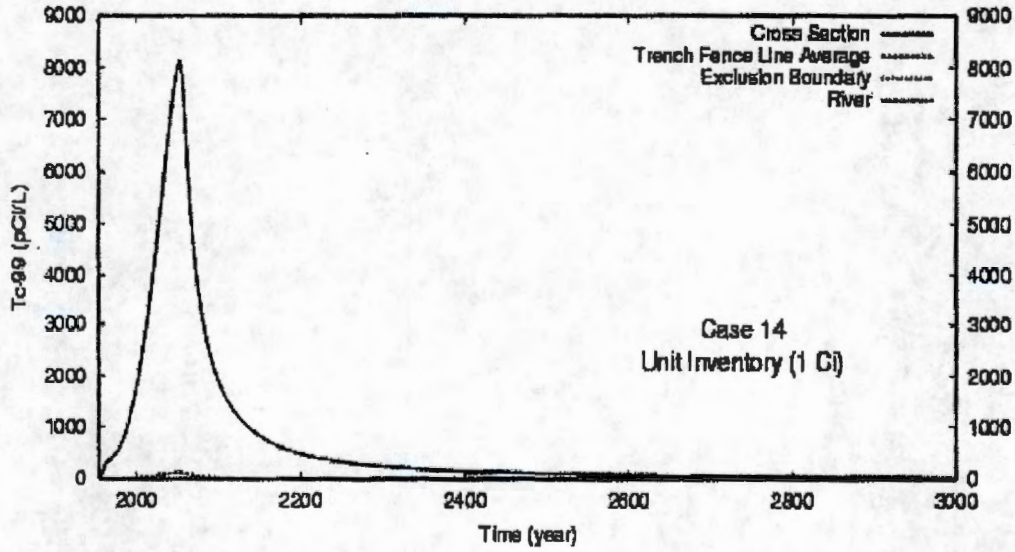

Figure E4.14. Case 14 Nitrate (a) Mass Flux and (b) Breakthrough Curves for Trench B-38 with Unit Inventory

(a)

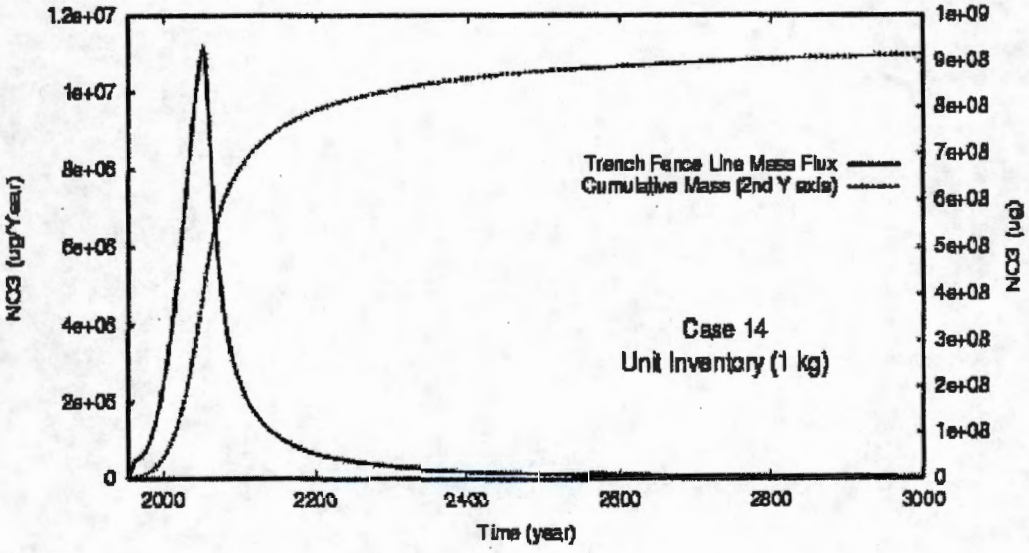

(b)

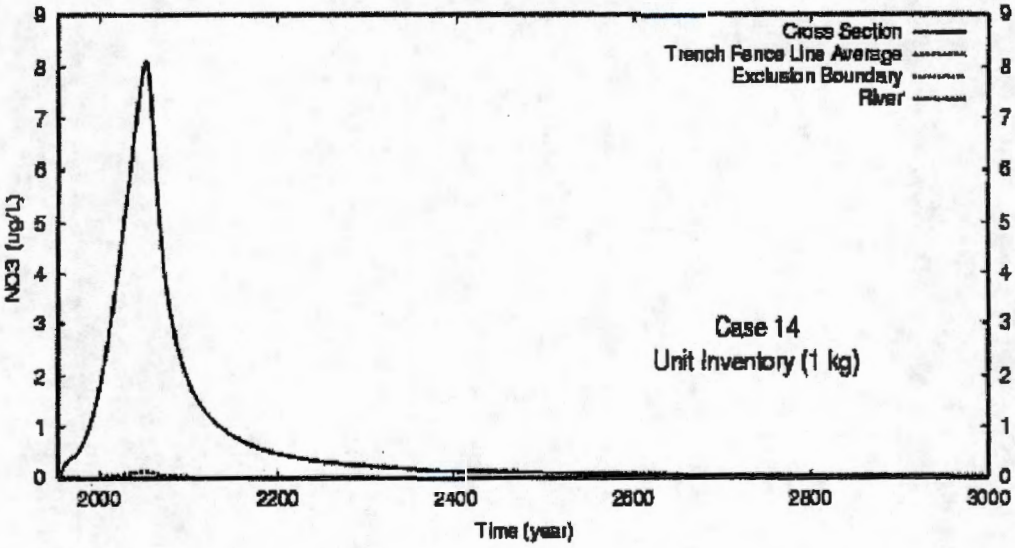

Figure E4.15. Case 14 Technetium-99 (a) Mass Flux and (b) Breakthrough Curves for Trench B-38

(a)

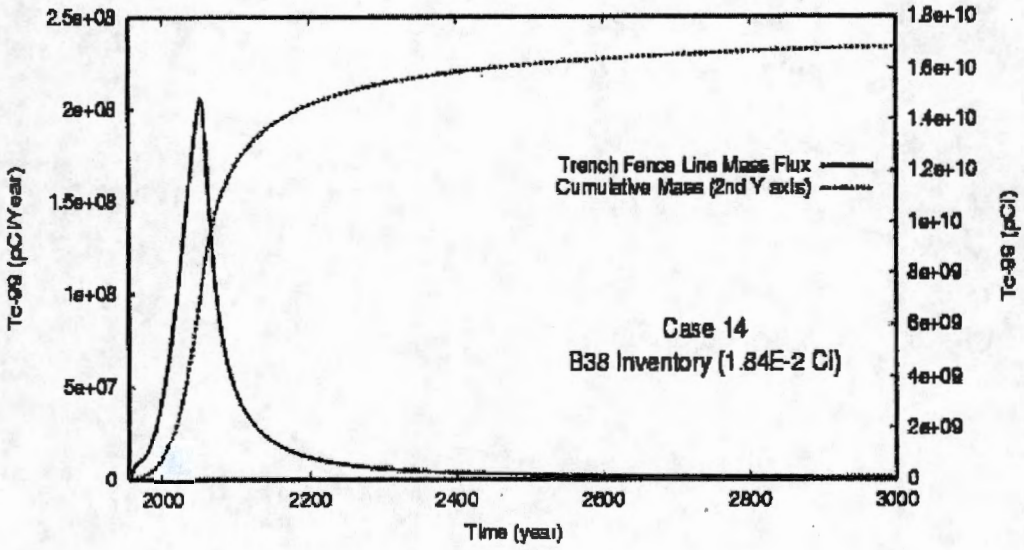

(b)

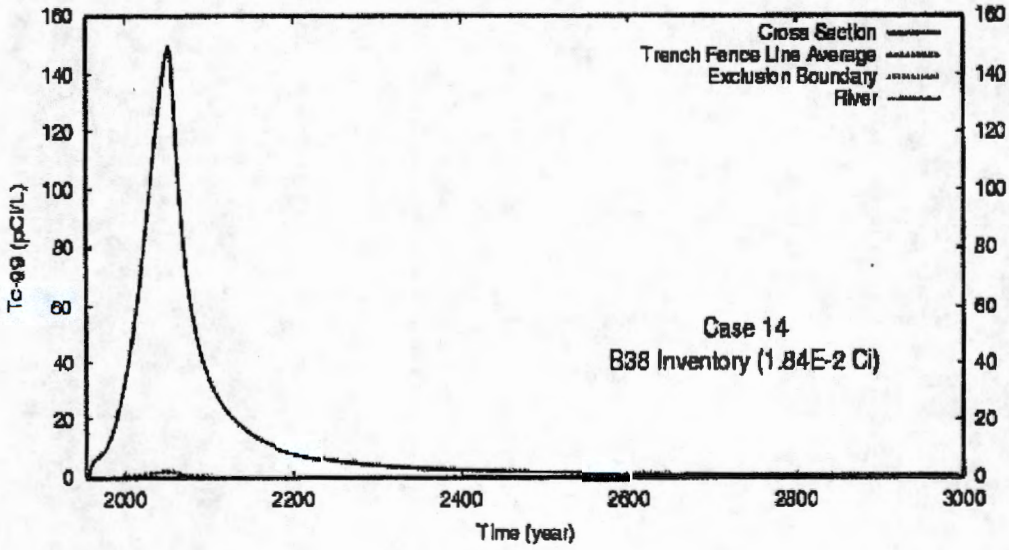

Figure E4.16. Case 14 Nitrate (a) Mass Flux and (b) Breakthrough Curves for Trench B-38

(a)

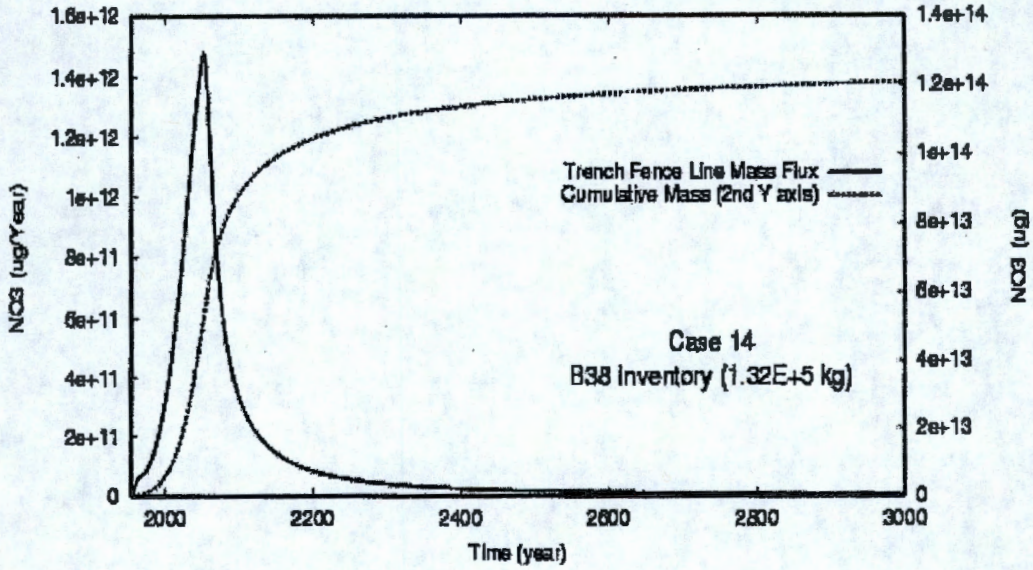

(b)

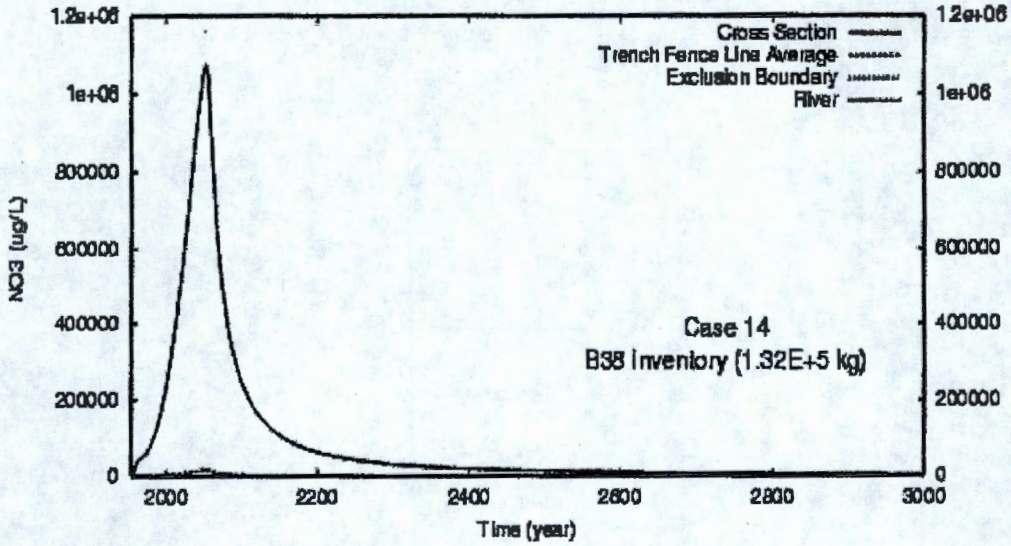

Figure E4.17. Case 14 Technetium-99 (a) Mass Flux and (b) Breakthrough Curves for all Eight Trenches

(a)

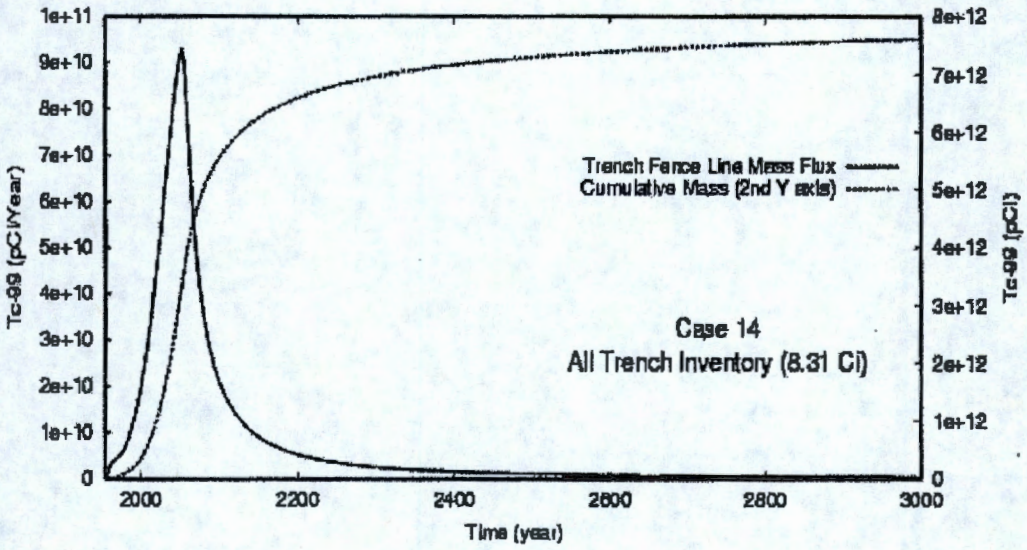

(b)

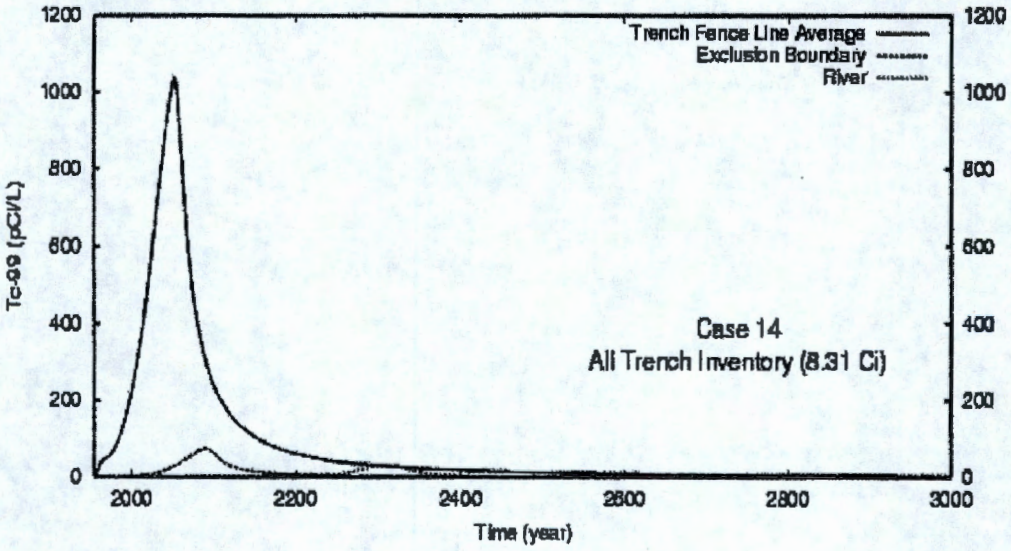

Figure E4.18. Case 14 Nitrate (a) Mass Flux and (b) Breakthrough Curves for all Eight Trenches

(a)

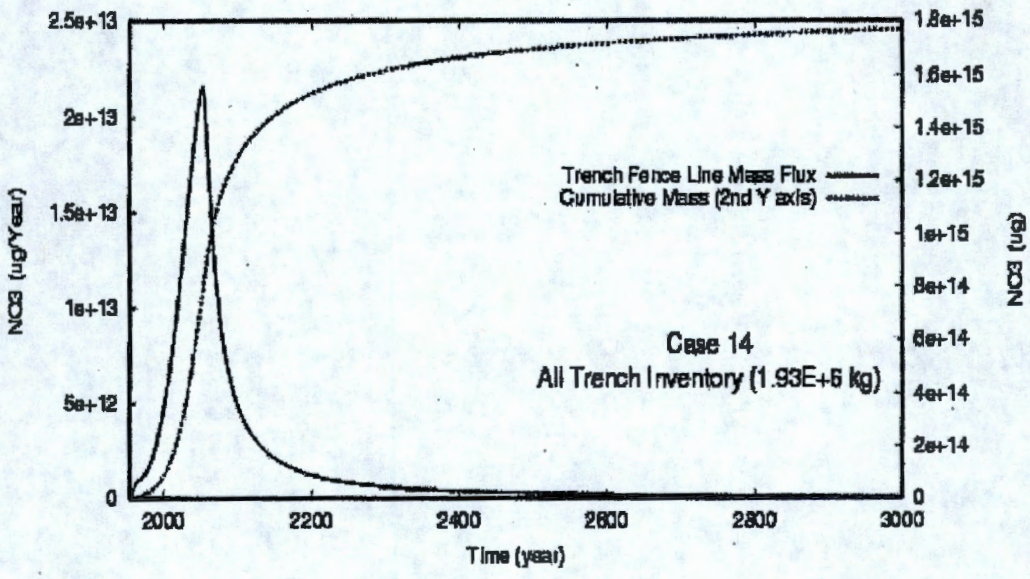

(b)

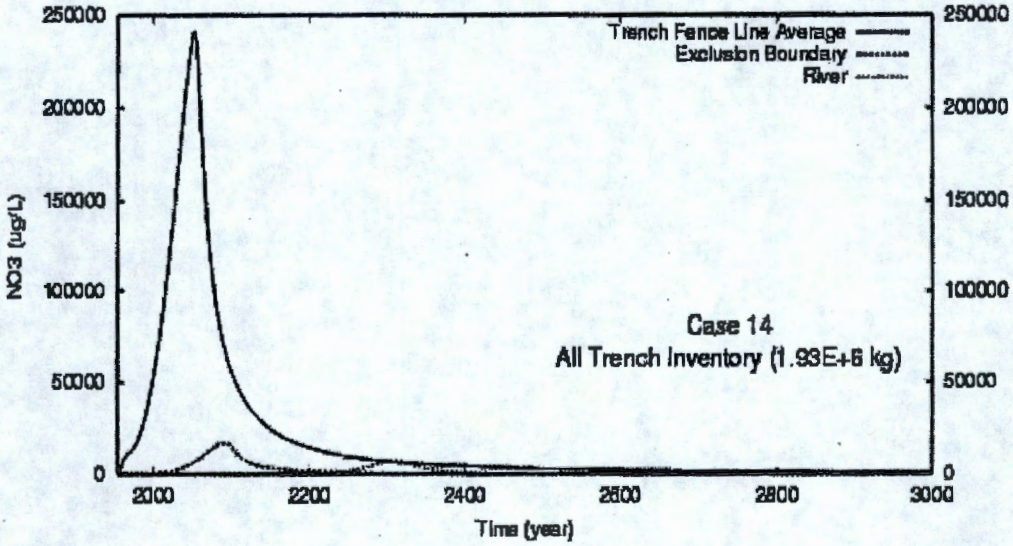

This page intentionally left blank.

ATTACHMENT E5

PEAK CONCENTRATIONS AND ARRIVAL TIMES

This page intentionally left blank.

CONTENTS

E5.1.0 PEAK CONCENTRATIONS AND ARRIVAL TIMES E5-1

TABLES

E5.1. Predicted Peak Uranium-238 Aqueous Concentrations and Arrival Times (DWS 21 pCi/L) E5-1
E5.2. Predicted Peak Technetium-99 Aqueous Concentrations and Arrival Times (DWS 900 pCi/L) E5-2
E5.3. Predicted Peak Nitrate Aqueous Concentrations and Arrival Times (DWS 45,000 μg/L) E5-3

This page intentionally left blank.

E5.1.0 PEAK CONCENTRATIONS AND ARRIVAL TIMES

Table E5.1. Predicted Peak Uranium-238 Aqueous Concentrations[a] and Arrival Times (DWS [b] 21 pCi/L)

U-238 Concentration	Cross-Section		BX Fence Line Boundary		Exclusion Boundary		Columbia River	
(pCi/L)	Time	Concentration	Time	Concentration	Time	Concentration	Time	Concentration
Case 1	2149	8.50E-01	2147	1.04E-01	2395	3.49E-02	—	—
Case 2	2999	9.96E-02	2999	1.21E-02	2999	3.80E-03	—	—
Case 3	2007	2.31E+04	2007	2.82E+03	2237	1.87E+02	—	—
Case 4	2075	2.99E+00	2075	3.65E-01	2333	1.10E-01	—	—
Case 5	2284	4.22E-01	2283	5.14E-02	2521	1.74E-02	—	—
Case 6	2999	6.06E-02	2999	7.39E-03	2999	2.23E-03	—	—
Case 7	2999	1.08E-01	2999	1.32E-02	2999	4.09E-03	—	—
Case 8	2999	2.48E-02	2999	3.02E-03	2999	7.80E-04	—	—
Case 9	2999	3.72E-04	2999	4.53E-05	2999	5.98E-06	—	—
Case 10	2063	5.44E+02	2063	6.63E+01	2139	7.43E+00	2552	2.91E+00
Case 11	2999	4.43E-02	2999	5.39E-03	2999	2.40E-03	—	—

Table entries marked with a dash (—) indicate that peak concentrations were insignificant.

[a] Simulated uranium-238 peak concentrations for the trench cases (i.e., cases 12, 13, and 14) were insignificant.

[b] Drinking water standard (DWS) based on a limit of 30 μg/L and a conversion factor of 6.93×10^{-7} Ci/g.

Table E5.2. Predicted Peak Technetium-99 Aqueous Concentrations and Arrival Times (DWS 900 pCi/L)

Tc-99 Concentration	Cross-Section		BX Fence Line Boundary		Exclusion Boundary		Columbia River	
(pCi /L)	Time	Concentration	Time	Concentration	Time	Concentration	Time	Concentration
Case 1	2048	6.65E+03	2048	8.05E+02	2087	5.31E+01	2300	2.27E+01
Case 2	2015	6.58E+03	2015	7.97E+02	2056	4.67E+01	2283	1.49E+01
Case 3	2002	1.40E+05	2002	1.69E+04	2042	3.02E+02	2262	4.68E+01
Case 4	2007	1.67E+04	2007	2.02E+03	2049	7.84E+01	2283	2.62E+01
Case 5	2017	5.79E+03	2017	7.02E+02	2091	4.46E+01	2303	1.95E+01
Case 6	2017	5.78E+03	2017	7.00E+02	2058	4.21E+01	2283	1.34E+01
Case 7	2028	3.59E+03[a]	2028	4.35E+02[a]	2069	2.80E+01	2300	1.15E+01
Case 8	2043	2.27E+03[a]	2043	2.75E+02[a]	2084	1.82E+01	2310	8.01E+00
Case 9	2109	8.33E+02[a]	2109	1.01E+02[a]	2149	6.78E+00	2370	3.39E+00
Case 10	2048	6.65E+03	2048	8.05E+02	2087	5.31E+01	2300	2.27E+01
Case 11	2048	6.65E+03	2048	8.05E+02	2087	5.31E+01	2300	2.27E+01
Unit Inventory								
Case 12	2036	1.31E+03	2036	2.02E+01	2077	1.46E+00	2301	6.74E-01
Case 13	2025	4.39E+03	2025	6.75E+01	2065	4.75E+00	2288	1.98E+00
Case 14	2052	8.11E+03	2052	1.25E+02	2090	8.90E+00	2307	3.76E+00
B-38 Trench								
Case 12	2036	2.41E+01	2036	3.71E-01	2077	2.69E-02	2301	1.24E-02
Case 13	2025	8.08E+01	2025	1.24E+00	2065	8.74E-02	2288	3.64E-02
Case 14	2052	1.49E+02	2052	2.30E+00	2090	1.64E-01	2307	6.92E-02
All Trenches								
Case 12	NA	NA	2036	1.69E+02	2077	1.21E+01	2301	5.60E+00
Case 13	NA	NA	2025	5.61E+02	2065	3.95E+01	2288	1.65E+01
Case 14	NA	NA	2052	1.04E+03	2090	7.40E+01	2307	3.12E+01

[a]Actual cross-section peak is ~600 pCi/L and actual average WMA fence peak is ~ 20 Ci/L. Both peaks occur in the year 2000 due to initial conditions near the water table. Values in table represent changes in peak concentrations due to variations in meteoric recharge.

DWS = drinking water standard
NA = not applicable

Table E5.3. Predicted Peak Nitrate Aqueous Concentrations and Arrival Times (DWS 45,000 μg/L)

NO_3 Concentration	Cross-Section		BX Fence Line Boundary		Exclusion Boundary		Columbia River	
(μg/L)	Time	Concentration	Time	Concentration	Time	Concentration	Time	Concentration
Case 1	2012	3.69E+04	2012	4.51E+03	2053	2.54E+02	2279	7.14E+01
Case 2	2012	3.69E+04	2012	4.50E+03	2053	2.53E+02	2276	6.63E+01
Case 3	2002	5.06E+05	2002	6.17E+04	2042	8.92E+02	2262	1.39E+02
Case 4	2006	1.05E+05	2006	1.28E+04	2047	3.88E+02	2272	8.42E+01
Case 5	2000	3.46E+04	2000	4.22E+03	2055	2.32E+02	2280	6.76E+01
Case 6	2000	2.46E+04	2000	4.22E+03	2055	2.31E+02	2277	6.32E+01
Case 7	2023	2.01E+04[a]	2023	2.45E+03[a]	2064	1.56E+02	2288	5.44E+01
Case 8	2036	1.26E+04[a]	2036	1.54E+03[a]	2077	1.01E+02	2301	4.23E+01
Case 9	2091	4.65E+03[a]	2091	5.68E+02[a]	2131	3.81E+01	2353	1.91E+01
Case 10	2012	3.69E+04	2012	4.51E+03	2053	2.54E+02	2279	7.14E+01
Case 11	2012	3.69E+04	2012	4.51E+03	2053	2.54E+02	2279	7.14E+01
Unit Inventory								
Case 12	2036	1.31E+00	2036	2.02E-02	2077	1.46E-03	2301	6.74E-04
Case 13	2025	4.39E+00	2025	6.76E-02	2065	4.75E-03	2288	1.98E-03
Case 14	2052	8.11E+00	2052	1.25E-01	2090	8.90E-03	2307	3.76E-03
B-38 Trench								
Case 12	2036	1.73E+05	2036	2.67E+03	2077	1.93E+02	2301	8.90E+01
Case 13	2025	5.79E+05	2025	8.93E+03	2065	6.27E+02	2288	2.61E+02
Case 14	2052	1.07E+06	2052	1.65E+04	2090	1.17E+03	2307	4.96E+02
All Trenches								
Case 12	NA	NA	2036	3.90E+04	2077	2.82E+03	2301	1.30E+03
Case 13	NA	NA	2025	1.30E+05	2065	9.17E+03	2288	3.82E+03
Case 14	NA	NA	2052	2.41E+05	2090	1.72E+04	2307	7.26E+03

[a]Actual cross-section peak is 3.5×10^4 μg/L and actual average WMA fence peak is $\sim 4 \times 10^3$ μg/L. Both peaks occur in the year 2000 due to initial conditions near the water table. Values in table represent changes in peak concentrations due to variations in meteoric recharge.

DWS = drinking water standard
NA = not applicable

This page intentionally left blank.

APPENDIX F

COST AND IMPLEMENTABILITY OF INTERIM CORRECTIVE MEASURES

This page intentionally left blank.

CONTENTS

F.1.0 INTRODUCTION F-1

F.2.0 INTERIM CORRECTIVE MEASURES F-2
F.2.1 IDENTIFICATION OF POTENTIAL NEAR-TERM INTERIM CORRECTIVE MEASURES F-2
F.2.2 NEAR-SURFACE BARRIER F-3
F.2.2.1 Description F-3
F.2.2.2 Implementation at Waste Management Area B-BX-BY F-3
F.2.2.3 Cost F-4
F.2.2.4 Evaluation Criteria F-4
F.2.3 INTERIM SURFACE BARRIER F-6
F.2.3.1 Description F-6
F.2.3.2 Implementation at Waste Management Area B-BX-BY F-6
F.2.3.3 Cost F-6
F.2.3.4 Evaluation Criteria F-6
F.2.4 OVERHEAD STRUCTURE F-8
F.2.4.1 Description F-8
F.2.4.2 Implementation at Waste Management Area B-BX-BY F-8
F.2.4.3 Cost F-9
F.2.4.4 Evaluation Criteria F-9
F.2.5 NEAR-TERM INTERIM CORRECTIVE MEASURES SUMMARY F-11
F.2.6 ADDITIONAL POTENTIAL INTERIM CORRECTIVE MEASURES F-12
F.2.6.1 Interim Corrective Measure Technologies for Soil Contamination F-12
F.2.6.2 Interim Corrective Measure Technologies for Groundwater Contamination F-16

F.3.0 REFERENCES F-21

TABLES

F.1. B Tank Farm Near-Surface Barrier Evaluation F-4
F.2. BX Tank Farm Near-Surface Barrier Evaluation F-5
F.3. BY Tank Farm Near-Surface Barrier Evaluation F-5
F.4. B Tank Farm Interim Surface Barrier Evaluation F-7
F.5. BX Tank Farm Interim Surface Barrier Evaluation F-7
F.6. BY Tank Farm Interim Surface Barrier Evaluation F-8
F.7. B Tank Farm Overhead Structure Evaluation F-9
F.8. BX Tank Farm Overhead Structure Evaluation F-10
F.9. BY Tank Farm Overhead Structure Evaluation F-10
F.10. Interim Corrective Measures Cost Summary F-11
F.11. Interim Corrective Measures Evaluation Summary F-11

LIST OF TERMS

CMS	corrective measures study
ICM	interim corrective measure
WMA	waste management area

F.1.0 INTRODUCTION

This appendix describes the interim corrective measures (ICMs) that have been evaluated as they relate to waste management area (WMA) B-BX-BY. ICMs are response actions having the objective of reducing contaminant migration to groundwater to acceptable regulatory levels and which require a balancing of risks, benefits, and costs.

In general, ICMs involve a substantial commitment of resources, require a more thorough evaluation, and are intended to provide a more permanent solution to the long-term threats posed by a release. For those measures where engineering studies have been performed, results from those studies will be summarized. For other potential ICMs, it is premature to provide a detailed discussion of the associated cost and implementability issues. Detailed evaluation of the ICMs will be undertaken in a corrective measures study (CMS) or an accelerated corrective measures study pending results of this field investigation report.

F.2.0 INTERIM CORRECTIVE MEASURES

ICMs have the same overall purpose as interim measures. Because of their size, complexity, or impact to operations, a more careful study must be performed before ICMs are implemented. Many potential ICMs have been identified; however, it is recognized that some of these potential ICMs are likely to be implemented sooner than others. Thus, this section describes the two sets of ICMs separately.

F.2.1 IDENTIFICATION OF POTENTIAL NEAR-TERM INTERIM CORRECTIVE MEASURES

The activities that have been undertaken to identify potential ICMs for the WMAs are described below.

- In 1992, an engineering study that evaluated four approaches for reducing surface infiltration at the WMAs, *Single-Shell Tank Interim Cover Engineering Study* (Schroeder and Carvo 1992), was completed. The approaches evaluated were: 1) polymer-modified asphalt, 2) fine-soil cover, 3) buildings (structures), and 4) flexible membrane liners. Cost and other factors were the reasons that none of the approaches were implemented.

- On May 4 through 6, 1999, an innovative treatment remediation demonstration forum was held in Richland, Washington to discuss techniques for reducing and monitoring infiltration at the single-shell tank farms. The U.S. Department of Energy, Hanford Site contractors, and various vendors from throughout the United States and Canada attended. Pacific Northwest National Laboratory summarized this conference in a two-volume report, "Reducing Water Infiltration Around Hanford Tanks" (Molton 1999). Four technical sessions were conducted to discuss: 1) moisture monitoring and characterization, 2) structures or buildings to cover the WMAs, 3) surface modifications or covers, and 4) near-surface modifications (i.e., barriers and permeability reduction techniques). The forum concluded that existing commercial capabilities could be employed to reduce and monitor infiltration in the WMAs, but that no one technology was appropriate for all seven WMAs. Another conclusion of the forum was that the costs shown in Schroeder and Carvo (1992) were 50% to 80% higher than those reflected by the vendors attending the forum. During the course of the forum, a number of U.S. Department of Energy officials and Hanford Site subcontractors addressed site-specific constraints that the vendors may not have taken into account before they submitted their estimated or typical unit costs.

- In June 2000, the U.S. Department of Energy revised *Phase 1 RCRA Facility Investigation/Corrective Measures Study Work Plan for Single-Shell Tank Waste Management Areas* (DOE-RL 2000). Section 4.2 of DOE-RL (2000) identifies a number of general response actions, and technology and process options associated with each general response action. Each option was screened based on effectiveness, ability to implement, worker safety, and cost. While the majority of the processes discussed fell into the ICM category, surface caps, overhead structures, and run-on and run-off controls, that are considered interim measures, were identified.

- In April 2001, an engineering report (Anderson 2001) was completed. In addition to evaluating water lines and wells within the WMAs, the report also evaluated surface water both from natural causes and catastrophic events. Alternatives considered in that report include: 1) no action, 2) site grading, 3) geo-fabric liners, 4) asphalt concrete paving, 5) building enclosure with asphalt apron, and 6) run-on control. The report recommends that a combination of a building enclosure with asphalt apron and run-on control be implemented. While the building enclosure was not the preferred option (because of the cost), the report concluded that it provided the best operational and technical alternative.

- In March 2002, Tank Farm Corrective Action Projects issued *White Paper on Interim Surface Barriers* (Anderson 2002). Interim surface barriers dovetail with other completed or planned interim measures at single-shelled tanks to eliminate or significantly reduce liquids added to the soil column that may carry or drive contamination located outside of the tanks downward toward the groundwater. A polyurea or polyurethane coating sprayed on an underlying fiber mat could be installed over the contamination surrounding tanks within the farms for the purposes of stabilizing that material. A demonstration of this technique is proposed for fiscal year 2003.

The three potentially viable ICMs selected from among those identified were: 1) near-surface barriers, 2) surface barriers, and 3) overhead structures. The following sections describe how each of those three near-term ICMs would apply to WMA B-BX-BY.

F.2.2 NEAR-SURFACE BARRIER

This section describes and evaluates the near-surface barrier option as a near-term ICM, its implementation at WMA B-BX-BY, and rough order of magnitude costs.

F.2.2.1 Description

The near-surface barrier would consist of an impervious, geo-fabric (geomembrane liner or geosynthetic clay) system over the entire WMA B-BX-BY to direct surface water to the outer boundaries of the tank farm. A run-off collection system consisting of ditches and pipes would be required to route collected surface water to existing drainage routes.

F.2.2.2 Implementation at Waste Management Area B-BX-BY

Implementation of a near-surface barrier would be disruptive to other tank farm activities. The entire B farm complex totals 53,500 m^2 (576,000 ft^2), with B farm consisting of 17,500 m^2 (188,000 ft^2), BX farm consisting of 18,000 m^2 (194,000 ft^2), and BY farm consisting of 18,000 m^2 (194,000 ft^2). This area would require hand excavation to remove 30 cm (12 in.) of existing soil and subsequent replacement of this soil as a cover over the liner to allow for traffic. The soil would have to be hand excavated because of tank dome-loading restrictions and the many utilities within the tank farm. Some of these utilities may require support during construction or relocation to a depth below the liner. Installation of the near-surface barrier would require additional time from a typical installation because of the many obstructions protruding above the surface. Vibratory compaction of the soil could adversely affect tank

stability. During the period that the near-surface barrier is required to control surface water, repairs would be required if any tank farm activities required work below the liner.

F.2.2.3 Cost

The estimated rough order of magnitude costs cited in the engineering report (Anderson 2001) for implementation of a subsurface barrier are $24.4 million for the B farm complex including $6.8, $7.1, and $10.5 million for B, BX, and BY tank farms, respectively.

F.2.2.4 Evaluation Criteria

Tables F.1, F.2, and F.3 show decision criteria, weight factors, and score for the near-surface barrier option for the B, BX, and BY tank farms. For this evaluation, the weight factor was multiplied by one through five to determine the weighted score. A score of one represents little or no impact of the activity to the decision criterion, and a score of five represents a greatly increased impact of the activity. Note that the weighted factor and decision criteria are the same for all three viable ICMs.

Table F.1. B Tank Farm Near-Surface Barrier Evaluation

Decision Criteria	Weight Factor	Score	Weighted Score	Highest Possible
Safety	5	4	20	25
Regulatory compliance	3	1	3	15
Life cycle cost analysis	2	2	4	10
Tank integrity	5	3	15	25
Future retrieval and processing	4	2	8	20
Schedule	3	2	6	15
Proven technology	3	1	3	15
Maintainability	3	2	6	15
Operability	2	2	4	10
Constructability	3	3	9	15
Decontamination, decommissioning, and disposal	4	3	12	20
Total Weighted Score			**90**	**185**

Source: Anderson 2001

Table F.2. BX Tank Farm Near-Surface Barrier Evaluation

Decision Criteria	Weight Factor	Score	Weighted Score	Highest Possible
Safety	5	4	20	25
Regulatory compliance	3	1	3	15
Life cycle cost analysis	2	3	6	10
Tank integrity	5	3	15	25
Future retrieval and processing	4	2	8	20
Schedule	3	1	3	15
Proven technology	3	2	6	15
Maintainability	3	3	9	15
Operability	2	2	4	10
Constructability	3	4	12	15
Decontamination, decommissioning, and disposal	4	3	12	20
Total Weighted Score			**99**	**185**

Source: Anderson 2001

Table F.3. BY Tank Farm Near-Surface Barrier Evaluation

Decision Criteria	Weight Factor	Score	Weighted Score	Highest Possible
Safety	5	4	20	25
Regulatory compliance	3	1	3	15
Life cycle cost analysis	2	2	4	10
Tank integrity	5	3	15	25
Future retrieval and processing	4	2	8	20
Schedule	3	3	9	15
Proven technology	3	1	3	15
Maintainability	3	2	6	15
Operability	2	2	4	10
Constructability	3	3	9	15
Decontamination, decommissioning, and disposal	4	3	12	20
Total Weighted Score			**93**	**185**

Source: Anderson 2001

F.2.3 INTERIM SURFACE BARRIER

This section describes and evaluates the interim surface barrier option as a near-term ICM, its implementation at WMA B-BX-BY, and cost.

F.2.3.1 Description

The only surface barrier evaluated is a 6 cm (2.5 in.) layer of asphalt cement pavement. Surface barriers that were not evaluated, but have been used successfully on other projects, include various liquid and solid reagents that are applied and allowed to penetrate the surface materials or are mixed with the surface materials to form a crust. A run-off collection system consisting of ditches and pipes would be required to route collected surface water to existing drainage routes.

F.2.3.2 Implementation at Waste Management Area B-BX-BY

Implementation of a surface barrier would be disruptive to other tank farm activities. The entire B farm complex totals 53,500 m^2 (576,000 ft^2), with B farm consisting of 17,500 m^2 (188,000 ft^2), BX farm consisting of 18,000 m^2 (194,000 ft^2), and BX farm consisting of 18,000 m^2 (194,000 ft^2). This area would require hand excavation to remove 10 cm (4 in.) of existing gravel cover, which would be taken from the site for disposal if contaminated or used in the production of the asphalt if not contaminated. The material would have to be hand excavated because of tank dome loading restrictions and the many utilities within the tank farm. Some of these utilities may require relocation if they are near the surface following removal of the 10 cm (4 in.) of existing materials. Installation of the surface barrier would also take additional time from typical installations to seal the numerous obstructions protruding above the surface.

Vibratory compaction of 10 cm (4 in.) of asphalt could adversely affect tank stability. Adequate compaction of both the subgrade and the asphalt would not be obtained because of the obstructions within the tank farm and tank dome loading restrictions. During the period that the surface barrier is required to control surface water, traffic loading could do substantial damage to the surface barrier. The cost to repair the asphalt barrier using the special fine mix could be excessive.

F.2.3.3 Cost

The estimated rough order of magnitude costs cited in the engineering report (Anderson 2001) for implementation of a surface barrier for the B farm complex are $11.3 million including $3.3, $3.4, and $4.6 million for B, BX, and BY tank farms, respectively.

F.2.3.4 Evaluation Criteria

Tables F.4, F.5, and F.6 show decision criteria, weight factors, and score for the interim surface barrier option for the B, BX, and BY tank farms. For this evaluation, the weight factor was multiplied by one through five to determine the weighted score. A score of one represents little or no impact of the activity to the decision criterion, while a score of five represents a greatly increased impact of the activity. Note that the weighted factor and decision criteria are the same for all three viable ICMs.

Table F.4. B Tank Farm Interim Surface Barrier Evaluation

Decision Criteria	Weight Factor	Score	Weighted Score	Highest Possible
Safety	5	3	15	25
Regulatory compliance	3	1	3	15
Life cycle cost analysis	2	3	6	10
Tank integrity	5	3	15	25
Future retrieval and processing	4	3	12	20
Schedule	3	3	9	15
Proven technology	3	2	6	15
Maintainability	3	3	9	15
Operability	2	2	4	10
Constructability	3	3	9	15
Decontamination, decommissioning, and disposal	4	4	16	20
Total Weighted Score			**104**	**185**

Source: Anderson 2001

Table F.5. BX Tank Farm Interim Surface Barrier Evaluation

Decision Criteria	Weight Factor	Score	Weighted Score	Highest Possible
Safety	5	3	15	25
Regulatory compliance	3	1	3	15
Life cycle cost analysis	2	3	6	10
Tank integrity	5	3	15	25
Future retrieval and processing	4	3	12	20
Schedule	3	3	9	15
Proven technology	3	2	6	15
Maintainability	3	4	12	15
Operability	2	2	4	10
Constructability	3	4	12	15
Decontamination, decommissioning, and disposal	4	4	16	20
Total Weighted Score			**110**	**185**

Source: Anderson 2001

Table F.6. BY Tank Farm Interim Surface Barrier Evaluation

Decision Criteria	Weight Factor	Score	Weighted Score	Highest Possible
Safety	5	3	15	25
Regulatory compliance	3	1	3	15
Life cycle cost analysis	2	3	6	10
Tank integrity	5	3	15	25
Future retrieval and processing	4	3	12	20
Schedule	3	3	9	15
Proven technology	3	2	6	15
Maintainability	3	2	6	15
Operability	2	2	4	10
Constructability	3	3	9	15
Decontamination, decommissioning, and disposal	4	4	16	20
Total Weighted Score			**101**	**185**

Source: Anderson 2001

F.2.4 OVERHEAD STRUCTURE

This section describes and evaluates the overhead structure option as a near-term ICM, its implementation at WMA B-BX-BY, and cost.

F.2.4.1 Description

The overhead structure would consist of an enclosed shelter covering the majority of the surface water control area of the WMA. An asphalt apron would be constructed around the perimeter of the structure to capture surface water and route that water to a run-off collection system.

F.2.4.2 Implementation at Waste Management Area B-BX-BY

Erection of the overhead structure would be more complicated than typical erections because of tank dome loading limitations. This option may require larger than normal cranes for erection of the structure and coverings. To span the entire width of the B, BX, BY tank farms would limit the weight of equipment that could be attached to the structure (e.g., monorails; lighting; heating, ventilation, and air conditioning). Engineers would have to determine if foundations could be constructed between the tanks at the B, BX, and BY farms to decrease the free span distance and to allow greater auxiliary loading of the structural supports.

The evaluation of which overhead structure to construct must take into account the free span distances. To provide a structure with this free span, a rigid-framed structure may be required. An evaluation should be made of intermediate supports to be located between the tanks. This would allow the structure to be equipped with accessories that may increase productivity of

future tank farm operations (e.g., monorail; lighting; and heating, ventilation, and air conditioning). The use of intermediate supports would also allow the use of enclosure systems other than a rigid frame structure.

The evaluation of overhead structures should also include recently emerging or advanced technologies, (e.g., a domed structure). This technology is purported to provide greater strengths at less cost than conventional structures.

F.2.4.3 Cost

The estimated costs presented in the engineering report (Anderson 2001) for implementation of a building enclosure with an asphalt apron at the B farm complex are $55.6 million including $19.0, $18.2, and $18.4 million for B, BX, and BY tank farms, respectively. Depending on the closure technology used at WMA B-BX-BY, a confinement facility would be required (DOE-RL 2000). If a confinement facility is not required, production would be increased 30% by working within an enclosure (Anderson 2001). Credit was not given to these items in determination of the costs.

F.2.4.4 Evaluation Criteria

Tables F.7, F.8, and F.9 show decision criteria, weight factors, and score for the overhead structure option at the B, BX, and BY tank farms. For this evaluation, the weight factor was multiplied by one through five to determine the weighted score. A score of one represents little or no impact of the activity to the decision criterion, while a score of five represents a greatly increased impact of the activity. Note that the weighted factor and decision criteria are the same for all three viable ICMs.

Table F.7. B Tank Farm Overhead Structure Evaluation

Decision Criteria	Weight Factor	Score	Weighted Score	Highest Possible
Safety	5	2	10	25
Regulatory compliance	3	1	3	15
Life cycle cost analysis	2	5	10	10
Tank integrity	5	2	10	25
Future retrieval and processing	4	1	4	20
Schedule	3	2	6	15
Proven technology	3	1	3	15
Maintainability	3	2	6	15
Operability	2	1	2	10
Constructability	3	2	6	15
Decontamination, decommissioning, and disposal	4		12	20
Total Weighted Score			**72**	**185**

Source: Anderson 2001

Table F.8. BX Tank Farm Overhead Structure Evaluation

Decision Criteria	Weight Factor	Score	Weighted Score	Highest Possible
Safety	5	2	10	25
Regulatory compliance	3	1	3	15
Life cycle cost analysis	2	5	10	10
Tank integrity	5	2	10	25
Future retrieval and processing	4	1	4	20
Schedule	3	2	6	15
Proven technology	3	1	3	15
Maintainability	3	2	6	15
Operability	2	1	2	10
Constructability	3	2	6	15
Decontamination, decommissioning, and disposal	4	4	16	20
Total Weighted Score			**76**	**185**

No credit was given for an estimated 30% productivity improvement for tank farm activities following structure construction or that closure activities may require an enclosure.

Source: Anderson 2001

Table F.9. BY Tank Farm Overhead Structure Evaluation

Decision Criteria	Weight Factor	Score	Weighted Score	Highest Possible
Safety	5	2	10	25
Regulatory compliance	3	1	3	15
Life cycle cost analysis	2	5	10	10
Tank integrity	5	2	10	25
Future retrieval and processing	4	1	4	20
Schedule	3	2	6	15
Proven technology	3	1	3	15
Maintainability	3	2	6	15
Operability	2	1	2	10
Constructability	3	2	6	15
Decontamination, decommissioning, and disposal	4	4	16	20
Total Weighted Score			**76**	**185**

No credit was given for an estimated 30% productivity improvement for tank farm activities following structure construction or that closure activities may require an enclosure.

Source: Anderson 2001

F.2.5 NEAR-TERM INTERIM CORRECTIVE MEASURES SUMMARY

This section summarizes the evaluation of the three potential near-term ICMs (i.e., near-surface barriers, surface barriers, overhead structures) and provides a comparison of the evaluation criteria and conclusions based on the evaluation. The near-surface barrier, surface barrier, and overhead structures options evaluated presented problems for implementation. Implementation of the near-surface and surface barriers would require extensive hand labor because of tank dome loading restrictions and numerous obstructions protruding to the surface. Implementation of the overhead structures would require free span distances that may stretch the limits of current technologies involved in construction or would require foundations to be constructed in the area between tanks. Table F.10 summarizes the estimated costs for each option by tank farm.

Table F.10. Interim Corrective Measures Cost Summary

Option	B Tank Farm Estimated Costs	BX Tank Farm Estimated Costs	BY Tank Farm Estimated Costs
Near-surface barriers	$6,844,000	$7,121,000	$10,476,000
Surface barriers	$3,261,000	$3,415,000	$4,589,000
Overhead structures	$19,027,000	$18,245,000	$18,385,000

Table F.11 summarizes the evaluation criteria and weighted scores for the options evaluated for minimizing infiltration at the B, BX, and BY tank farms.

Table F.11. Interim Corrective Measures Evaluation Summary

Decision Criteria	Weighted Score B Tank Farm			Weighted Score BX Tank Farm			Weighted Score BY Tank Farm		
	Subsurface Barrier	Surface Barrier	Overhead Structure	Subsurface Barrier	Surface Barrier	Overhead Structure	Subsurface Barrier	Surface Barrier	Overhead Structure
Safety	20	15	10	20	15	10	20	15	10
Regulatory compliance	3	3	3	3	3	3	3	3	3
Life cycle cost analysis	4	6	10	6	6	10	4	6	10
Tank integrity	15	15	10	15	15	10	15	15	10
Future retrieval and processing	8	12	4	8	12	4	8	12	4
Schedule	6	9	6	3	9	6	9	9	6
Proven technology	3	6	3	6	6	3	3	6	3
Maintainability	6	9	6	9	12	6	6	6	6
Operability	4	4	2	4	4	2	4	4	2
Constructability	9	9	6	12	12	6	9	9	6
Decontamination, decommissioning, and disposal	12	16	12	12	16	12	12	16	16
Total Weighted Score	**90**	**104**	**72**	**99+**	**110**	**76**	**93**	**101**	**76**

Source: Anderson 2001

Any of the three potential near-term ICMs could be implemented to reduce infiltration at WMA B-BX-BY. The cost versus benefits (i.e., reduction in contaminant concentrations in the groundwater) of implementing any of the interim measures should be considered because sufficient time may have elapsed between when the leaks occurred and the present to effectively reduce the contaminant concentrations in the groundwater. Additionally, implementing ICMs may divert funding from other tank waste remediation activities such as waste retrieval.

The evaluation of options in Anderson (2001) resulted in a recommendation to implement the overhead structure. This recommendation is based on the summary of the evaluation criteria that ranked the overhead structure lowest for B, BX, and BY tank farms. The weighted scores presented are subjective and represent a best estimate effort to account for the relative importance of the different evaluation criteria presented. The estimated cost for the overhead structure is considerably higher than the other options evaluated and this variation is not well captured in the weighted ranking. Anderson (2001) did not provide credit for an estimated 30% productivity gain for tank farm operations within the enclosure or that an enclosure would be required for certain tank farm closure alternatives.

F.2.6 ADDITIONAL POTENTIAL INTERIM CORRECTIVE MEASURES

This section identifies additional potential ICMs for consideration at WMA B-BX-BY. These ICMs generally involve a greater commitment of resources than those interim measures discussed above and require a more thorough site-specific evaluation before selecting an ICM for implementation at WMA B-BX-BY. Any evaluation of ICMs needs to include consideration of continued storage of waste in the tanks and future plans to retrieve waste from the tanks as well as cost versus benefits of the technologies in terms of reducing groundwater impacts. If warranted, detailed evaluation of ICMs for WMA B-BX-BY would be conducted in a corrective measures study.

F.2.6.1 Interim Corrective Measure Technologies for Soil Contamination

This section describes the ICM technologies for soil contamination that are described in the *Phase 1 RCRA Facility Investigation/Corrective Measures Study Work Plan for Single-Shell Tank Waste Management Areas* (DOE-RL 2000) and in *Feasibility Study of Tank Leakage Mitigation Using Subsurface Barriers* (Treat et al. 1995).

F.2.6.1.1. Containment Technologies. Containment technologies use physical measures to isolate and reduce the horizontal and vertical movement of contaminants.

Grout Walls. Grout walls are formed by either injecting grout under pressure directly into the soil matrix (permeation grouting) or in conjunction with drilling (jet grouting) at regularly spaced intervals to form a continuous low-permeability barrier. Grout walls could be installed either vertically or directionally in an effort to create a barrier underneath the contaminant plume in the soil (DOE-RL 2000). A large number of boreholes would be required to construct a barrier. A grout containment barrier was previously evaluated for the AX tank farm as a means to contain potential retrieval leakage (Norman 1999). In the AX tank farm study, grout injection borings would be directionally drilled beneath the tanks on approximately 1.5 m (5 ft) centers. Installation of a horizontal grout blanket beneath the four tanks in the AX tank farm was

estimated to cost approximately $200 million. One of the issues identified with this technology was the difficulty in verifying the integrity of the grout barrier. Grout walls are potentially applicable at WMA B-BX-BY; however, the contamination has reached the groundwater and that contamination remaining in the vadose has limited mobility. The usefulness of implementing this technology and determining its effectiveness are of concern and would require further evaluation.

Cryogenic Barrier. Cryogenic (or freeze-wall) barriers are formed by recirculating chilled brine or other refrigerants through an array of closely spaced wells or freeze pipes. As the soil surrounding and between these wells or freeze pipes cools and freezes, the water in the voids freezes and expands. The freezing and expanding water effectively creates an impermeable barrier. Cryogenic barriers may be applicable at WMA B-BX-BY although it is unclear if the technology would perform as planned if it were necessary to inject supplemental water into the highly transmissive soils of the Hanford Site. In addition, maintenance of a cryogenic barrier requires a long-term commitment of resources. As noted above, contamination has reached the groundwater and that contamination remaining in the vadose zone has limited mobility.

Dynamic Compaction. Dynamic compaction is used to densify the soil, compact buried solid waste, and reduce the void spaces in the soil, which can reduce the saturated hydraulic conductivity of the soil and the mobility of contaminants, and under unsaturated conditions, this technology may be counter productive. This process is accomplished by dropping a heavy weight onto the ground surface. This technology is commonly used in coordination with caps and it would have limited application in the tank farm area because of the graveled surface and the potential tank dome loading during the compaction process.

Circulating Air Barriers. The circulating air barrier technology would create a dry zone under the area of confinement through which no liquids could penetrate until a critical liquid saturation was exceeded. For most sediments at the Hanford Site, critical saturation is on the order of 5% to 25%. The water beneath the tanks is essentially immobile when kept at or below the critical saturation value. Circulating air barrier technology injects dry air from an array of either vertical or horizontal wells. The air is drawn through porous soils to extraction wells, vaporizing water in the process. Some difficulty could be experienced as progressively more saturated air is moved through the vadose zone, as zones of greater than critical liquid saturation could be created. Circulating air barrier technology is applicable at WMA B-BX-BY although no large-scale field tests have been performed.

Radio Frequency Desiccating Subsurface Barriers. A radio frequency heating process can be used for the formation of an active desiccating barrier beneath underground storage tanks. Electrodes are installed in the soil between the source of the contamination and groundwater using horizontal drilling techniques. The radio frequency energy applied to the electrodes heats a 2 to 3 m (6 to 10 ft) thick layer of soil to temperatures above 100 °C (212 °F) to evaporate the moisture. Electrode arrays are part of a perforated pipe system that is maintained under vacuum to remove the steam and volatile organics for aboveground treatment and disposal. Radio frequency desiccating subsurface barriers may be applicable at WMA B-BX-BY although the concept has not been tested at the Hanford Site.

Close-Coupled Injected Chemical Barriers. Unlike the concept of subsurface barriers installed at some depth below the tanks or below a containment plume as discussed previously for grout walls and cryogenic barriers, close-coupled injected chemical barriers are formed against the sides and bottom of an individual underground storage tank. It is unlikely that the close-coupled chemical barrier concept would be applicable at WMA B-BX-BY because of the problems of induced stresses on the tanks and the inability of installing a conical jet grout shell given the confining limitations among the Hanford Site underground storage tanks. In addition, the concept has not been tested outside of the laboratory.

Induced Liquefaction Barriers. Induced liquefaction is a close-coupled subsurface barrier option that combines the concepts of sheet metal piling to create a vertical barrier with caisson-drilled horizontal jet grouting. Although this technology may be applicable at WMA B-BX-BY, no full-scale application of this technology for waste management or environmental restoration purposes is known. The tank farm infrastructure would further limit the applicability of this alternative.

F.2.6.1.2. Removal Technologies. Removal technologies include the excavation of contaminated soils or buried solid waste. After removal, the soil and debris may require ex situ treatment to meet disposal requirements or to reduce waste volume. Removal technologies could be considered for localized areas in the tank farms where leaks occurred from piping or diversion boxes at near-surface to mid-depth. Removal would not likely be effective for capturing the mobile contaminants because of the known depth of occurrence.

F.2.6.1.3. In Situ Treatment Technologies. In situ treatment technologies are oriented at treating the contamination in place to either extract the contaminants of concern or to stabilize and isolate contaminated soil to prevent migration to the groundwater.

Electrokinetic Separation. Electrokinetic separation can be used for organic, inorganic, and radioactive contaminants. This technology involves applying an electrical potential across the contaminated zone by using electrodes placed in the ground. Remediation by electrokinetics is based on the migration of water and ions in an electrical field. The application of electrokinetic separation at the tank farms may be limited because water is required to move ions between electrodes. Application in unsaturated soils may require water addition that could cause unwanted migration of contaminants.

In Situ Biodegradation. In situ biodegradation relies on microbial transformation of organic contaminants. Biodegradation is effective on organic contaminants but is not effective on radionuclides or inorganics; therefore, this technology would have limited application in the tank farm area.

Solidification. Solidification can be used for organic, inorganic, and radiological contaminants. This process involves drilling holes to the desired depth then injecting the solidification and stabilization agents into the soil with high pressure pumps. Variations of solidification include jet injection and shallow soil mixing. Jet injection involves drilling a small diameter hole using a downward jet of air or water then pumping the solidification agent out laterally through jets located near the bottom of the drill pipe. Shallow soil mixing is performed using a crane mounted auger head to mix the soil and solidification agent. Solidification methods are

potentially applicable at WMA B-BX-BY. Access to contaminants beneath the tanks would be difficult and would require directional drilling or angle drilling. Solidification requires an understanding of the location and distribution of contaminants. Stabilization of large plumes extending from the base of the tank to the groundwater would require a substantial commitment of time and resources. Solidification technologies could serve to delay the migration of contaminants to the groundwater.

Grout Injection. Grout is injected into the soil matrix, encapsulating the contaminants. The injection process produces a monolithic block that can be left in place or excavated for disposal elsewhere. Although grout injection is applicable at WMA B-BX-BY, future use of the site may be limited if the encapsulated contaminants are left in place. Grouting contaminated soils deep in the vadose zone beneath the tanks would be an issue.

Deep Soil Mixing. Deep soil mixing is performed using large augers and injector head systems to inject and mix solidifying agents into contaminated soil. Although deep soil mixing is applicable at WMA B-BX-BY, future use of the site may be limited if the encapsulated contaminants are left in place. Using this technology to mix contaminated soil deep in the vadose zone directly beneath or adjacent to the tanks would be problematic.

Vitrification. Vitrification can be used for organics, heavy metals, and radionuclides. In situ vitrification involves the application of an electrical current to the soil to bring it to a temperature of 1400 to 2000 °C (2552 to 3632 °F) that is sufficient to melt the soil. The process forms a stable, vitrified mass when cooled, chemically incorporates most inorganics including heavy metals and radionuclides, and destroys or removes organic contaminants. In situ vitrification is probably not applicable at WMA B-BX-BY because process depths are limited and the technology has very limited potential for use in tank farms or near tanks that are storing waste.

Soil Flushing. Soil flushing can be used for organics, inorganics, and radioactive contaminants. In situ soil flushing involves the extraction of contaminants from the soil by injecting an extractant or elutant (e.g., water or other suitable solvent) through the contaminated soils. The extraction fluids solubilize or elute the contaminant from the soil. The resultant solution must be recovered through extraction wells and treated at the surface by a treatment system (e.g., ion-exchange system). Soil flushing is potentially applicable at WMA B-BX-BY.

Soil Vapor Extraction. The soil vapor extraction process induces airflow through the soil matrix with an applied vacuum that facilitates the mass transfer of adsorbed, dissolved, or free phases of the contaminant to the vapor phase. Because soil vapor extraction is best used for volatile organic compounds and fuels, it would have limited application in the tank farm area.

Monitored Natural Attenuation. Monitored natural attenuation relies on natural processes to lower contaminant concentrations through physical, chemical, or other biological processes that, "under favorable conditions, act without human intervention to reduce the mass, toxicity, mobility, volume, or concentration of contaminants" (EPA 1999) until cleanup levels are met. Although natural attenuation methods may be readily implemented, significant action or commitment of resources (e.g., personnel to conduct sampling and perform analytical work, construction activity, and loss of land use) may be required.

F.2.6.1.4. Ex Situ Treatment Technologies. Ex situ technologies would be used in conjunction with removal technologies as discussed in Section F.2.6.1.2. Ex situ treatment technologies would have potential application for near-surface spills and leaks but would not have application for tank leaks near tanks used for storage of high-level waste. Ex situ treatment of contaminated soils would likely require excavation by hand to remove contaminated soils within the tank farms. Worker exposures associated with hand excavation of soils contaminated from concentrated tank or transfer line leakage would be prohibitive. Additionally, an enclosure structure would also likely be required to reduce the potential for airborne contamination during excavation. Remote removal techniques are possible but would require research and development before being considered for deployment in the tank farms.

Biodegradation. Ex situ biodegradation is essentially the same as in situ biodegradation, except that the soil is excavated and placed in a system or pile where treatment is applied (DOE-RL 2000). Biodegradation is effective on organic contaminants but is not effective on radionuclides or inorganics; therefore, this technology would have limited application in the tank farm area.

Soil Washing. Soil washing is a process that applies to coarse-grained soils contaminated with a wide variety of metal, radionuclide, and organic contaminants. This process uses a wash solution (e.g., water) to remove soil contaminants by dissolving or suspending the contaminants in solution or concentrating them through particle size separation, gravity separation, and attrition scrubbing. The wash solution requires treatment to remove the contaminants that have been washed and desorbed from the soil. Although soil washing could be applicable at WMA B-BX-BY, there are significant safety and contamination control issues associated with excavation of the more contaminated soils beneath the tanks.

Solidification and Stabilization. Solidification and stabilization uses admixtures to encapsulate excavated soil and render inert various hazardous substances. This process is targeted at metals, radionuclides, and organics. Stabilizing agents include cement, asphalt, and polymeric materials. Solidification and stabilization is applicable at WMA B-BX-BY.

Thermal Desorption. Thermal desorption uses relatively low temperature heat of 150 to 425 °C (302 to 842 °F) to volatilize organic contaminants from soil. A carrier gas or vacuum is used to collect and transport the volatilized organics to a gas treatment system. Thermal desorption is only effective on organics, and it would have limited applicability at WMA B-BX-BY.

Encapsulation. Encapsulation is accomplished by fixing individual particles in a solid matrix as discussed above for solidification and stabilization or by enclosing a quantity of waste in an inert jacket or container. Encapsulation of contaminated soils is potentially applicable at WMA B-BX-BY excluding the issues associated with excavation of the contaminated soils.

F.2.6.2 Interim Corrective Measure Technologies for Groundwater Contamination

This section describes the ICMs for groundwater contamination that are defined in the Phase 1 RFI/CMS work plan (DOE-RL 2000) and in Treat et al. (1995).

F.2.6.2.1. Hydraulic Containment: Extraction Wells. Hydraulic containment involves placement of extraction wells close along a line or surrounding an area and pumping the groundwater to form depression zones thereby creating a barrier to the passage of groundwater and contaminants contained in the groundwater. The extracted groundwater may require treatment to remove the contaminants.

Hydraulic containment using extraction wells is applicable at WMA B-BX-BY. However, this may not be practical within the context of other waste sites in the 200 Areas, and a high potential exists for extracting contamination from nearby cribs and environmental restoration disposal sites. The application of this alternative is further reduced by the limited thickness of the aquifer beneath the WMA.

F.2.6.2.2. Impermeable Barriers. Impermeable barriers are solid walls that are placed into the subsurface to retard the movement of groundwater. Groundwater flowing toward a barrier will divert away from and eventually flow around the barrier. A barrier could be supplemented with extraction wells at the ends of the barrier to prevent mobile contaminants from migrating around the barrier. The great depth to the aquifer, >250 ft, limits the implementability of this alternative.

Sheet-Pile Barrier. Sheet-pile barriers are constructed by driving interlocking sheet piles into the ground with either vibratory or impact pile drivers. This barrier would need to be coupled with a horizontal barrier to form a complete barrier envelope. Sheet-pile barriers were tested in the Hanford Site 100-N Area and were unsuccessful. The piling was destroyed after penetrating to a depth of 9.2 m (30 ft). Based on the depth to groundwater, installation of a sheet-pile barrier at WMA B-BX-BY would not be possible.

Cryogenic (Freeze-Wall) Barrier. A cryogenic (or freeze-wall) barrier is formed using two methods. A closed-loop system recirculates chilled brine or other refrigerants through an array of closely spaced wells or pipes, freezing and expanding the water in the soil voids surrounding the freeze pipes. An open loop system involves the injection of liquid nitrogen into the ground through perforated well casings. Cryogenic barriers may be applicable at WMA B-BX-BY. Maintenance of a cryogenic barrier requires a long-term commitment of resources. However, the great depth to the aquifer, >250 ft, limits the implementability of this alternative.

Chemical Jet Grout Encapsulation. Chemical jet grout encapsulation uses primarily high-pressure jet grouting to form columns of grouted soil via directionally drilled wells. Standard grouts such as portland cements or bentonite clays are used. More exotic grouts could be used for enhanced set times and better compatibility with Hanford soils. Chemical jet grout encapsulation is applicable at WMA B-BX-BY. However, the great depth to the aquifer, >250 ft, limits the implementability of this alternative.

Jet Grout Curtains. Jet grout curtain placement is similar to chemical jet grout encapsulation discussed above except that both vertical and horizontal wells, rather than directionally drilled wells, are used for injection. Jet grout curtain technology is applicable to WMA B-BX-BY. However, the great depth to the aquifer, >250 ft, limits the implementability of this alternative.

Permeation Chemical Grouting. Permeation chemical grouting is similar to jet grouting except that lower pressures are used for injection. Permeation chemical grouts could be injected using

both vertical and horizontal wells. Permeation chemical grouting is applicable at WMA B-BX-BY, although performance is highly dependent upon the properties of the grouting material used and the properties of the soil. The great depth to the aquifer, >250 ft, limits the implementability of this alternative.

Wax Emulsion Permeation Grouting. A mineral wax-bentonite emulsion has been developed for grouting applications. This wax grout consists of a stable emulsion of wax, water, and a surfactant. Once inside the soil matrix, the wax particles begin to aggregate and move through void spaces until they bridge an opening and become fixed. Bridging the openings between pores reduces the permeability of the soil. Wax emulsion permeation tests have been conducted at the Hanford Site and have shown that soil hydraulic conductivity can be reduced by two to three orders of magnitude. Wax emulsions are more applicable as surface barriers.

Silicate Permeation Grouting and Colloidal Silica. Sodium silicate permeation grouting uses a silicate-based chemical grout with favorable characteristics that can be controlled by altering the formulation of the grout. By altering the proportions of the components of sodium silicate grout, the set time and grout viscosity can be controlled. Colloidal silica is also being explored for use in forming subsurface barriers at the Hanford Site. Colloidal silica is a colloidal suspension with gelling properties. Tests using Hanford soils have been performed on sodium silicate grouts and colloidal silica and have shown that soil hydraulic conductivity can be reduced by three to four orders of magnitude. This technology is potentially applicable at WMA B-BX-BY, but is limited due to the great depth to the groundwater.

Polymer Permeation Grouting. Polymer permeation grouting employs an injected liquid monomer or resin that converts to a polymer in place to form a concrete-like monolithic barrier. Polymer-forming chemicals could be injected into the ground using the same methods for emplacing cement slurry walls. Although some polymer grouts (e.g., furfuryl alcohol) are chemically incompatible with Hanford Site soils, polymer permeation grouting is applicable at WMA B-BX-BY, but is limited due to the great depth to the groundwater.

Formed-in-Place Horizontal Grout Barriers. Placement of formed-in-place horizontal grout barriers involves the use of a proprietary technology to generate a barrier slab of uniform thickness between guide wires placed by horizontal drilling methods. The technology uses high-pressure jets mounted on a reciprocation machine tool. The grout slurry sprayed through the jets disrupts and mixes soils to a mortar-like consistency between the guide pipes. The machine tool passes through this semi-liquid material as the hardware is pulled along the guide wires, forming a uniform barrier behind it. Adjacent panels would be placed at the edge of the previous panel (before it hardens totally), overlapping the previous panel to some extent to form an extended slab. Formed-in-place horizontal grout barriers may be applicable at WMA B-BX-BY although the technology has never been incorporated at full scale. This alternative would be limited to the vadose zone immediately beneath the tank farm excavations.

Concepts Not Considered Feasible for the Hanford Site. The following concepts are not considered feasible for Hanford Site underground storage tank applications and are listed here for completeness only:

- Soil fracturing
- Longwall mining

- Modified sulfur cement
- Sequestering agents
- Reactive barriers
- Impermeable coatings
- Microtunneling
- In situ vitrification barriers
- Soil saw
- Deep soil mixing
- Slurry walls
- Soil-mixed walls.

F.2.6.2.3. In Situ Treatment Technologies. In situ treatment technologies are oriented at treating the contamination in place to either selectively extract contaminants or to stabilize and isolate contaminants from migrating in the groundwater.

Adsorption-Type Treatment Barrier. Permeable treatment beds and barriers are constructed by excavating a trench and backfilling it with a mixture of soil and adsorbents. The bed is placed downgradient of the contaminated plume. As the natural groundwater flow carries the contaminants through the bed, the contaminants that the barrier is designed to remove are adsorbed onto the bed. Adsorption-type treatment barriers would have limited applicability to WMA B-BX-BY due to the depth of soil that would have to be excavated to reach groundwater.

Phosphate Precipitation Barrier. Phosphate compounds are used in these barriers to precipitate heavy metals (e.g., strontium-90) in the soil matrix. This technology is in the developmental stages and its applicability to WMA B-BX-BY is not known.

Monitored Natural Attenuation. Monitored natural attenuation relies on natural processes to lower contaminant concentrations through physical, chemical, and other biological processes that, "under favorable conditions, act without human intervention to reduce the mass, toxicity, mobility, volume, or concentration of contaminants" (EPA 1999) until cleanup levels are met. Although natural attenuation methods may be readily implemented, significant action or commitment of resources (e.g., personnel to conduct sampling and perform analytical work, construction activity, and loss of land use) may be required. Monitored natural attenuation would have limited applicability at WMA B-BX-BY for the long-lived mobile radionuclides.

F.2.6.2.4. Ex Situ Treatment Technologies. Ex situ treatment technologies are used to remove contaminants from groundwater after the groundwater has been pumped to the surface. Ex situ treatment technologies that are potentially applicable at WMA B-BX-BY are noted below.

Precipitation Technology. Precipitation technology is used to remove metals and radionuclides from water by precipitation.

Membrane Technology. Membranes can be considered for the treatment of radionuclides (e.g., strontium-90). The membrane adsorbs the contaminant. This technology is in the developmental stage.

Ion-Exchange Technology. Ion-exchange technology removes ions from solution by adsorption on a solid medium, typically an ion-exchange resin bed or column. As the groundwater is passed through the resin, ionic species in the groundwater exchange with ions on the resin and are adsorbed onto the surface of the resin.

Wet Air Oxidation. Wet air oxidation is based on a liquid-phase reaction between organics in the wastewater and compressed air. This process is used for treatment of organics and may have limited applicability at WMA B-BX-BY.

Activated Carbon. When contaminated wastewater is passed over activated carbon beds, organic hydrocarbon contaminants are absorbed onto the carbon. This process is used for treatment of organics and may have limited applicability at WMA B-BX-BY.

Tritium Treatment Technologies. The most successful treatment systems for tritium treatment and separation are gaseous phase applications as used in commercial nuclear power operations. Technologies being considered or being used for tritium are a combination of electrolysis and catalytic exchange, bithermal catalytic exchange, and membrane separation.

F.3.0 REFERENCES

Anderson, F. J., 2001, *Engineering Report, Single-Shell Tank Farms Interim Measures to Limit Infiltration Through the Vadose Zone*, RPP-5002, Rev. 1, CH2M HILL Hanford Group, Inc., Richland Washington.

Anderson, F. J., 2002, *White Paper on Interim Surface Barriers*, CH2M-13838, Draft, CH2M HILL Hanford Group, Inc., Richland Washington.

DOE-RL, 2000, *Phase 1 RCRA Facility Investigation/Corrective Measures Study Work Plan for Single-Shell Tank Waste Management Areas*, DOE/RL-99-36, Rev. 1, U.S. Department of Energy, Richland Operations Office, Richland, Washington.

EPA, 1999, *Use of Monitored Natural Attenuation at Superfund, RCRA Corrective Action, and Underground Storage Tank Sites*, OSWER Directive Number 9200.4-17P, U.S. Environmental Protection Agency, Washington, D.C.

Molton, P. M., 1999, "Reducing Water Infiltration Around Hanford Tanks," Forum Proceedings Volume 1, May 4-6,1999, TechCon Program, Pacific Northwest National Laboratory, Richland, Washington.

Norman, N. A., 1999, *Hanford Tanks Initiative Engineering Study Refinements Report*, HNF-4195, Rev. 0, Parsons Infrastructure and Technology Group, Inc., Richland, Washington.

Treat, R. L., B. B. Peters, R. J. Cameron, M. A. Dippre, A. Hossain, W. D. McCormack, T. L. Trenkler, M. B. Walter, M. F. Walters, J. K. Rouse, T. J. McLaughlin, and J. M. Cruse, 1995, *Feasibility Study of Tank Leakage Mitigation Using Subsurface Barriers*, WHC-SD-WM-ES-300, Rev. 1, Westinghouse Hanford Company, Richland, Washington.

Schroeder, B. K. and J. E. Carvo, 1992, *Single-Shell Tank Interim Cover Engineering Study*, WHC-SD-WM-ES-165, Rev. 0, Westinghouse Hanford Company, Richland, Washington.

This page intentionally left blank.

APPENDIX G

REGULATORY ANALYSIS

This page intentionally left blank.

CONTENTS

G.1.0 INTRODUCTION G-1

G.2.0 REGULATORY PERFORMANCE MEASURES G-3

G.3.0 REGULATORY COMPLIANCE FROM FIELD DATA G-5
G.3.1 SOILS DATA G-5
G.3.2 GROUNDWATER DATA G-6

G.4.0 HUMAN HEALTH RISK AND DOSE RESULTS COMPARISON TO REGULATIONS G-9

G.5.0 REFERENCES G-10

TABLES

G.1. Regulatory Performance Measures G-4
G.2. Case Descriptions for the Two-Dimensional Simulations G-6
G.3. Modeled Groundwater Concentrations (Average Weighted) at Specified Boundaries G-7
G.4. Groundwater Monitoring Results Exceeding Maximum Contaminant Levels or Drinking Water Standards at Waste Management Area B-BX-BY G-8
G.5. Comparison of Peak Incremental Lifetime Cancer Risk, Hazard Index, and Dose for the Industrial Worker Scenario G-9

LIST OF TERMS

HFFACO	*Hanford Federal Facility Agreement and Consent Order*
ILCR	incremental lifetime cancer risk
Kd	distribution coefficient
RCRA	*Resource Conservation and Recovery Act of 1976*
WAC	*Washington Administrative Code*
WMA	waste management area

G.1.0 INTRODUCTION

Phase 1 RCRA Facility Investigation/Corrective Measures Study Work Plan for Single-Shell Tank Waste Management Areas (DOE-RL 2000) provides the regulatory framework for the *Resource Conservation and Recovery Act of 1976* (RCRA) Corrective Action Program. This regulatory framework is based on federal statutes and regulations, Washington State statutes and regulations, the *Hanford Federal Facility Agreement and Consent Order* (HFFACO) (Ecology et al. 1989); and the Hanford Site RCRA Permit (Ecology 2001). Applicable or relevant and appropriate requirements are provided in Appendix F of DOE-RL (2000).

The purpose of a field investigation report is to summarize data from a waste management area (WMA) investigation and evaluate the data to the extent necessary to determine the need for immediate action through interim measures or accelerated interim corrective measures at the WMA. At a minimum, the data is evaluated to determine the potential risk associated with hypothetical exposure to soil and groundwater at the WMA boundary (i.e., BX tank farm east fence line boundary) as described in Section 4.0 of DOE-RL (2000). If the potential near-term risk to human health is excessive, the U.S. Department of Energy and Washington State Department of Ecology may propose one or more interim measures to mitigate the risk or may initiate an accelerated corrective measures study to evaluate and compare more complex interim corrective measures.

The evaluation of the risks associated with existing contamination serves several purposes. Some of these purposes include the following:

- Establish the need for additional interim measures or interim corrective measures
- Provide necessary input to Hanford Site-wide cumulative risk assessments
- Serve as a basis to begin identifying cleanup standards for closure.

Cleanup standards are based on both regulatory requirements and the potential risk to human health and the environment. The potential risk depends in part on the hypothetical exposure scenario, which in turn depends on the assumed land use (including surface water and groundwater). Exposure and land use scenarios are also important in identifying the appropriate regulatory requirements for cleanup. For example, the determination of cleanup standards under the "The Model Toxics Control Act Cleanup Regulation" (*Washington Administrative Code* [WAC] 173-340) depends on whether an unrestricted (residential) or industrial scenario is applied, and the use of alternate concentration limits under "Concentration Limits" (WAC 173-303-645(5)) depends in part on future groundwater uses. In 1999, the U.S. Department of Energy issued *Final Hanford Comprehensive Land-Use Plan Environmental Impact Statement* (DOE 1999), which used the *National Environmental Policy Act of 1969* process to evaluate several land uses for the Hanford Site planned over the next 50 years. That environmental impact statement and associated record of decision "Record of Decision: Hanford Comprehensive Land-Use Plan Environmental Impact Statement (HCP EIS)" (64 FR 61615), identify 'industrial-exclusive use' as the planned use for the 200 Areas Central Plateau, an area that encompasses the 200 East and 200 West Areas. The Washington State Department of Ecology is evaluating how the U.S. Department of Energy land use planning efforts fit within the Washington State Department of Ecology cleanup framework; the agency has not agreed at this time to an industrial use scenario. Therefore, potential risk and the regulatory requirements for

establishing media cleanup standards for the RCRA Corrective Action Program cannot be finalized. Section 4 and Appendix E of this report present the risk assessment and evaluation approach and results that consider several potential exposure scenarios identified in DOE-RL (2000).

G.2.0 REGULATORY PERFORMANCE MEASURES

Table G.1 identifies quantitative performance measures for various constituents, including hazardous and radiological contaminants. The level of protection established by the standards is expressed in terms of the maximum dose or contaminant concentration under various exposure scenarios. Each standard, therefore, reflects the determination by the regulatory agency of an appropriate level of protection that should be provided to protect human health. Generally, the spectrum of regulations reflected in Table G.1 demonstrates that the level of protection provided by regulatory agencies is consistent among the regulations whether they apply to dangerous contaminants (e.g., chemicals and metals) or radiological contaminants. The level of protection provided under the regulations ranges from between 1 incremental lifetime cancer risk (ILCR) in 10,000 (1.0×10^{-4}) and 1 in 1,000,000 (1.0×10^{-6}) on an annual basis.

The most important regulations related to this WMA B-BX-BY field investigation report are those addressing cleanup of soils and groundwater and the associated risk or dose to human health through the groundwater exposure pathway. The following sections discuss compliance with the applicable regulations.

Table G.1. Regulatory Performance Measures

Regulation	Requirement	Performance Measure	Point of Compliance	Notes
DOE Order 5400.5	***Protection of the general public and environment.***			
Protection of the Public	All pathways for LLW except air (mrem/yr)	25	100 m downgradient for groundwater, at waste site for direct exposure	100 years of institutional control.
	All pathways including other Hanford sources per 10 CFR 20, DOE Order 5400.5 and DNFSB 94-2 (mrem/yr)	100	100 m downgradient for groundwater, at waste site for direct exposure	
Protection of Groundwater (40 CFR 141)	Beta/proton emitters (mrem/yr)	4	100 m downgradient	100 years of institutional control. 500 years of passive control. 10,000 years for impacts analysis. Assumes water ingestion of 2 L/day. Alpha emitters: 15 pCi/L = 40 mrem/yr Radon: 3 pCi/L = 20 mrem/yr
	Alpha emitters (pCi/L)	15		
40 CFR 141 and DOE Order 5400.5	***Drinking water standards for select constituents with the potential for release to groundwater during operations, retrieval actions, or post closure***			
MCLs and derived concentration guide for select constituents Source: 40 CFR 141	H-3 C-14 I-129 U Tc-99 Cs-137 NO_3 Cr U-238 U-235	20,000 pCi/L 2,000 pCi/L 1 pCi/L 0.03 mg/L (Total) 900 pCi/L 200 pCi/L 45 mg/L 0.5 mg/L 20 pCi/L 20 pCi/L	Drinking water source	1,000 yr for compliance analysis. Alpha Emitters: 15 pCi/L = 40 mrem/yr

LLW = low-level waste
MCL = maximum contaminant level

G.3.0 REGULATORY COMPLIANCE FROM FIELD DATA

Regulatory compliance data for soils and groundwater collected during the field investigation activities are presented with comparison to regulatory requirements in Appendices B and C. The following sections discuss WAC 173-340 related to assessing derived soil concentrations for groundwater protection, "Deriving Soil Concentrations for Ground Water Protection" (WAC 173-340-747), and groundwater contamination present in WMA B-BX-BY groundwater monitoring.

G.3.1 SOILS DATA

Under WAC 173-340-747, the term 'soil concentration' means the concentration in the soil that will not cause an exceedance of the groundwater cleanup level established under "Ground Water Cleanup Standards" (WAC 173-340-720). Six different methodologies can be used to determine if the criterion has been met. This WMA B-BX-BY field investigation report uses the alternative fate and transport model (WAC 173-340-747(8)). The values used in the fate and transport modeling are based on best estimates and do not comply with the default values in WAC 173-340-747. The values used provide an estimate of groundwater impacts from the soil inventory estimate (Sections 3.3 and 4.2 and Appendix E). Numerical simulation results are obtained on long-term transient contaminant concentrations at the water table and for calculation at the BX tank farm east fence line boundary, 200 Area exclusion boundary, and the shoreline at the Columbia River. These calculation points are based on DOE-RL (2000).

Table G.2 provides the case numbers and descriptions for the numerical simulations as discussed in Section 4.0 of the main text and Appendix E. Numerical results are obtained on long-term transient contaminant concentrations and at calculation locations at the BX tank farm east fence line boundary, 200 Area exclusion boundary; and the Columbia River shoreline (DOE-RL 2000).

The groundwater concentration values based on inventory show that, for the BX tank farm east fence line boundary, drinking water standards (40 CFR 141) will be exceeded. Table G.3 lists the predicted technetium-99, uranium-238, and nitrate levels and the associated 40 CFR 141 limits. Table G.3 lists the groundwater concentration values for the BX tank farm east fence line boundary (cases 1 through 11), B-38 trench boundary (cases 12, 13, and 14), 200 Area exclusion boundary, and the Columbia River shoreline.

The predicted groundwater concentrations exceed the regulatory standards at the BX tank farm east fence line boundary. Exceedances of the groundwater maximum contaminant levels for technetium-99 occur at the BX tank farm east fence line boundary except for case 9 (Table G.3). Exceedances of the groundwater maximum contaminant levels for uranium-238 occur in cases 3 and 10 and for nitrate in cases 3, 4, 12, 13, and 14 at the BX tank farm east fence line boundary (Table G.3). At the 200 Area exclusion boundary (i.e., the rest of the Central Plateau including 200 North Area extending north to the base of Gable Butte), uranium-238, nitrate, and technetium-99 did not exceed the groundwater maximum contaminant levels for any of the cases (Table G.3). At the Columbia River shoreline, no constituent exceeded the groundwater maximum contaminant levels for any of the cases (Table G.3).

Table G.2, Case Descriptions for the Two-Dimensional Simulations

Case Number	Description[a]	Interim Barrier	Inventory Distribution	Meteoric Recharge (mm/yr)
1	Base case (no action alternative)	No	Uniform	100
2	Barrier alternative	Yes	Uniform	100
3	Water-line leak (1 gal/min for 20 years)	No	Uniform	100
4	Water line leak (200,000 gal)	No	Uniform	100
5	Alternative inventory distribution with no barrier	No	Alternative	100
6	Alternative inventory with barrier	Yes	Alternative	100
7	Base case with 50% recharge	No	Uniform	50
8	Base case with 30% recharge	No	Uniform	30
9	Base case with 10% recharge	No	Uniform	10
10	Base case with Kd = 0.1ml/g for U-238	No	Uniform	100
11	Base case with Kd = 1.0 ml/g for U-238	No	Uniform	100
12	B-38 trench with 55.4 mm/year recharge	No	Uniform	55.4
13	B-38 trench with 100 mm/year recharge	No	Uniform	100
14	B-38 trench with delayed closure barrier	No	Uniform	100

[a] See Appendix E, Section E.2.1 for details on each case.
Kd = distribution coefficient

G.3.2 GROUNDWATER DATA

Based on *Hanford Site Groundwater Monitoring for Fiscal Year 2001* (Hartman et al. 2002), groundwater monitoring well data for the RCRA groundwater wells associated with WMA B-BX-BY indicate the following constituents have exceeded the 40 CFR 141 drinking water standards during fiscal year 2001:

- Antimony
- Cyanide
- Gross alpha
- Gross beta
- Iodine-129
- Nitrate
- Technetium-99
- Tritium
- Uranium.

However, these exceedances are not correlated solely to release events in the WMA. Some of these exceedances can be attributed to cribs and trenches (Section 3.0 and Appendix C). Table G.4 provides the RCRA groundwater monitoring well exceedances for the various constituents and the number of exceedances that have occurred for fiscal year 2001.

Table G.3. Modeled Groundwater Concentrations (Average Weighted) at Specified Boundaries

Case	BX Tank Farm Boundary[a]			200 Area Exclusion Boundary			Columbia River Shoreline		
	Technetium-99 (pCi/L)	Uranium-238 (pCi/L)	Nitrate (µg/L)	Technetium-99 (pCi/L)	Uranium-238 (pCi/L)	Nitrate (µg/L)	Technetium-99 (pCi/L)	Uranium-238 (pCi/L)	Nitrate (µg/L)
Case 1	6,650	0.85	36,900	53.1	0.0349	254	22.7	—	71.4
Case 2	6,580	0.0996	36,900	46.7	0.0038	253	14.9	—	66.3
Case 3	172,000	27,600	565,000	308	19.8	901	46.6	—	137
Case 4	16,700	2.99	105,000	78.4	0.11	388	26.2	—	84.2
Case 5	5,790	0.422	34,600	44.6	0.174	232	19.5	—	67.6
Case 6	5,780	0.06	34,600	42.1	0.00223	231	13.4	—	63.2
Case 7	3,590	0.11	20,100	28	0.00409	156	11.5	—	54.4
Case 8	2,270	0.025	12,600	18.2	0.00078	101	8.01	—	42.3
Case 9	833	0.0037	4,650	6.78	0.0000059	38.1	3.39	—	19.1
Case 10	6,650	544	36,900	53.1	7.43	254	22.7	2.91	71.4
Case 11	6,650	0.044	36,900	53.1	0.0024	254	22.7	—	71.4
Case 12	24.1	—	173,000	0.0269	—	193	0.674	—	89.0
Case 13	80.8	—	579,000	0.0874	—	627	1.98	—	261
Case 14	149	—	1,070,000	0.164	—	1,170	3.76	—	496
Regulatory Standard	**900 pCi/L**	**20 pCi/L**	**45,000 µg/L**	**900 pCi/L**	**20 pCi/L[b]**	**45,000 µg/L**	**900 pCi/L**	**20 pCi/L**	**45,000 µg/L**

[a]Groundwater concentrations given are the breakthrough values for the cross-sections. See Appendix E.
[b]Based on a limit of 30 µg/L and a conversion factor of 6.93×10^{-7} Ci/g
Dash (—) indicates value is insignificant.

Table G.4. Groundwater Monitoring Results Exceeding Maximum Contaminant Levels or Drinking Water Standards at Waste Management Area B-BX-BY

Well Number	Antimony (µg/L)	Cyanide (µg/L)	Gross Alpha (pCi/L)	Gross Beta (pCi/L)	Nitrate (µg/L)	Iodine-129 (pCi/L)	Technetium-99 (pCi/L)	Tritium (pCi/L)	Uranium (µg/L)
299-E32-9	NA	NA	NA	58 (1)	NA	3 (1)	NA	NA	NA
299-E32-10	17 (1)	NA	NA	1,200 (2)	178,000 (4)	NA	3,490 (4)	NA	NA
299-E33-7	NA	423 (3)	NA	4,210 (3)	748,000 (4)	NA	11,600 (4)	NA	NA
299-E33-9	NA	NA	357 (2)	3,090 (3)	212,000 (4)	NA	7,660 (4)	NA	678 (4)
299-E33-13	NA	NA	16 (1)	975 (2)	425,000 (2)	NA	3,290 (2)	NA	NA
299-E33-15	NA	NA	NA	80 (1)	441,000 (2)	NA	NA	NA	NA
299-E33-16	NA	NA	NA	1,400 (3)	695,000 (4)	NA	5,780 (4)	NA	NA
299-E33-17	NA	NA	NA	NA	267,000 (1)	NA	NA	NA	NA
299-E33-18	NA	NA	108 (2)	1,200 (3)	205,000 (4)	NA	3,810 (4)	NA	193 (4)
299-E33-20	NA	NA	NA	103 (1)	460,000 (3)	NA	NA	NA	NA
299-E33-26	NA	NA	53 (2)	2,720 (3)	441,000 (4)	NA	7,510 (4)	NA	137 (4)
299-E33-28	NA	NA	NA	55 (1)	NA	NA	NA	NA	NA
299-E33-31	NA	NA	33 (1)	1,310 (3)	259,000 (3)	NA	3,800 (4)	NA	79 (4)
299-E33-32	NA	NA	NA	739 (4)	98,700 (4)	NA	2,090 (5)	NA	NA
299-E33-34	NA	333 (3)	21 (1)	3,060 (4)	456,000 (4)	NA	8,170 (4)	NA	46 (2)
299-E33-35	NA	NA	NA	658 (3)	120,000 (4)	4 (1)	2,420 (4)	NA	NA
299-E33-38	NA	383 (3)	84 (2)	4,600 (3)	531,000 (4)	NA	13,000 (4)	NA	165 (4)
299-E33-41	NA	NA	70 (2)	1,140 (2)	52,700 (1)	NA	3,290 (4)	NA	118 (2)
299-E33-42	NA	NA	NA	1,190 (3)	136,000 (4)	NA	3,380 (4)	NA	31 (1)
299- E33-43	NA	NA	NA	229 (3)	77,500 (1)	NA	915 (1)	NA	NA
299-E33-44	NA	NA	245 (2)	3,320 (3)	224,000 (4)	NA	8,230 (4)	NA	567 (4)
299-E33-339	NA	NA	NA	NA	NA	NA	NA	21,400 (1)	NA
DWS or MCL	6	200	15	50	45,000	1	900	20,000	30

Bold indicates an upgradient groundwater monitoring well. Number indicates the maximum result for that well during the monitoring period from October 1, 2000 to September 30, 2001. Parenthesis indicates the number of exceedances in the particular well.

DWS = drinking water standard (40 CFR 141)
MCL = maximum contaminant level
NA = well did not exceed MCLs for the constituent

G.4.0 HUMAN HEALTH RISK AND DOSE RESULTS COMPARISON TO REGULATIONS

As presented in Section 4.0 and in Appendix E, the peak ILCR, hazard index, and dose for the industrial worker scenario is used as the baseline for comparison purposes. The results indicate that at the BX tank farm east fence line boundary, the ILCR exceeds regulatory standard of 1.0×10^{-5} (Table G.5). Based on current groundwater concentrations of technetium-99 (2,461.6 pCi/L) in RCRA groundwater well 299-E33-45, the ILCR would be 1.75×10^{-5} for the industrial worker scenario. The hazard index does not exceed the regulatory standard of 1.0 at the BX tank farm east fence line boundary (Table G.5). Dose does not exceed the regulatory standard of 4 mrem/yr for beta/photon emitters for all cases at the BX tank farm east fence line boundary (Table G.5).

Table G.5. Comparison of Peak Incremental Lifetime Cancer Risk, Hazard Index, and Dose for the Industrial Worker Scenario

Case	BX Tank Farm East Fence Line Boundary	200 Area Exclusion Boundary	Columbia River Shoreline
Industrial Worker Peak Incremental Lifetime Cancer Risk			
1	5.39E-05	5.48E-07	2.34E-07
2	5.34E-05	4.82E-07	1.54E-07
7	4.85E-05	2.89E-07	1.19E-07
8	4.83E-05	1.88E-07	8.27E-08
Industrial Worker Peak Hazard Index			
1	1.98E-01	1.74E-03	4.88E-04
2	1.98E-01	1.73E-03	4.54E-04
7	1.77E-01	1.07E-03	3.72E-04
8	1.97E-01	1.88E-04	2.89E-04
Industrial Worker Peak Dose (mrem/yr)			
1	3.18E+00	3.23E-02	1.38E-02
2	3.15E+00	2.84E-02	9.07E-03
7	2.86E+00	1.71E-02	7.00E-03
8	2.85E+00	1.11E-02	4.88E-03

G.5.0 REFERENCES

10 CFR 20, "Standards for Protection Against Radiation," *Code of Federal Regulations*, as amended.

40 CFR 141, "National Primary Drinking Water Regulations," *Code of Federal Regulations*, as amended.

64 FR 61615, 1999, "Record of Decision: Hanford Comprehensive Land-Use Plan Environmental Impact Statement (HCP EIS)," *Federal Register*, Vol. 64, No. 218, pp. 61615, November 12.

DNFSB 94-2, 1994, *Recommendation 94-2 to the Secretary of Energy*, Defense Nuclear Facilities Safety Board, Washington, D.C.

DOE Order 5400.5, 1993, *Radiation Protection of the Public and Environment*, U.S. Department of Energy, Washington, D.C.

DOE, 1999, *Final Hanford Comprehensive Land-Use Plan Environmental Impact Statement*, DOE/EIS-0222F, U.S. Department of Energy, Richland Operations Office, Richland, Washington.

DOE-RL, 2000, *Phase 1 RCRA Facility Investigation/Corrective Measures Study Work Plan for Single-Shell Tank Waste Management Areas*, DOE/RL-99-36, Rev. 1, U.S. Department of Energy, Richland Operations Office, Richland, Washington.

Ecology, EPA, and DOE, 1989, *Hanford Federal Facility Agreement and Consent Order*, as amended, Washington State Department of Ecology, Olympia, Washington, U.S. Environmental Protection Agency, Washington, D.C., and U.S. Department of Energy, Washington, D.C.

Ecology, 2001, *Dangerous Waste Portion of the Resource Conservation and Recovery Act Permit for the Treatment, Storage, and Disposal of Dangerous Waste*, Permit Number WA7890008967, Rev. 7, Washington State Department of Ecology, Olympia, Washington.

Hartman, M. J., L. F. Morasch, and W. D Webber, editors, 2002, *Hanford Site Groundwater Monitoring for Fiscal Year 2001*, PNNL-13788, Pacific Northwest National Laboratory, Richland, Washington.

National Environmental Policy Act of 1969, 42 USC 4321 et seq.

Resource Conservation and Recovery Act of 1976, Public Law 94-580, 90 Stat. 2795, 42 USC 901 et seq.

WAC 173-303, "Dangerous Waste Regulations," *Washington Administrative Code*, as amended.

WAC 173-340, "Model Toxics Control Act - Cleanup," *Washington Administrative Code*, as amended.

APPENDIX H

QUALITY ASSURANCE AND QUALITY CONTROL REQUIREMENTS

This page intentionally left blank.

CONTENTS

H.1.0 QUALITY ASSURANCE AND QUALITY CONTROL REQUIREMENTS H-1

H.2.0 REFERENCES H-2

This page intentionally left blank.

H.1.0 QUALITY ASSURANCE AND QUALITY CONTROL REQUIREMENTS

Quality assurance and quality control requirements for conducting the *Resource Conservation and Recovery Act of 1976* field investigations are addressed in Appendix A of the *Phase 1 RCRA Facility Investigation/Corrective Measures Study Work Plan for Single-Shell Tank Waste Management Areas* (DOE-RL 2000), which is known as the master work plan. The major areas covered in the master work plan are as follows:

- Project management
- Measurement/data acquisition
- Assessment/oversight
- Data validation and usability
- Data quality assessment.

The project management described in the master work plan is still valid, although the company responsible for the effort has shifted to CH2M HILL Hanford Group, Inc., because of contract changes. The Office of River Protection is now the U.S. Department of Energy office responsible for the tasks.

The general requirements established in the master work plan for sampling methods, sample handling and custody, analytical methods, and field and laboratory quality control have been followed in the activities described in this document. As noted in the main text to this document, there were few deviations from the work plans on sampling and these were due to operational concerns. Other requirements had no deviations.

CH2M HILL Hanford Group, Inc. management and tank farm staffs have routinely conducted safety assessments of the waste management area B-BX-BY *Resource Conservation and Recovery Act of 1976* field investigation. There is, at this time, no separate formal quality assurance assessment by the Tank Farm Vadose Zone Project.

Informal reviews of data validity and usability have been held, mainly as part of the determination of second and third tier analyses and in the preparation of this waste management area B-BX-BY field investigation report. Similarly, only informal data quality assessments have been performed, primarily because a systematic sampling approach was used rather than a random sampling design.

H.2.0 REFERENCES

DOE-RL, 2000, *Phase 1 RCRA Facility Investigation/Corrective Measures Study Work Plan for Single-Shell Tank Waste Management Areas*, DOE/RL-99-36, Rev. 1, U.S. Department of Energy, Richland Operations Office, Richland, Washington.

Resource Conservation and Recovery Act of 1976, Public Law 94-580, 90 Stat. 2795, 42 USC 901 et seq.

APPENDIX I

PREPARERS

This page intentionally left blank.

CONTENTS

I.1.0 PREPARERS I-1
I.1.1 OFFICE OF RIVER PROTECTION I-1
I.1.2 CORE TEAM I-1
I.1.3 PEER REVIEW TEAM I-6
I.1.4 SUPPORT TEAM I-6
I.1.4.1 Field Work I-6
I.1.4.2 Computer Modeling and Risk Calculations I-6
I.1.4.3 Laboratory Measurements and Analysis I-7
I.1.4.4 Science and Technology Participants I-7

This page intentionally left blank.

I.1.0 PREPARERS

I.1.1 OFFICE OF RIVER PROTECTION

Robert M. Yasek, Physical Scientist

B.S.	Geophysics, New Mexico Institute of Mining and Technology	1984

Mr. Yasek has over 16 years of experience in leadership and management of government projects, both military and civilian. He currently serves as the Department of Energy project manager for the Hanford Tank Farms Vadose Zone Project. Prior to working at Hanford, he was the Department of Energy Lead for Thermal Testing for the DOE Yucca Mountain Project. Additional duties at the Yucca Mountain Project included project management of borehole geophysics for the high-level waste repository program. Mr. Yasek's military experience includes project management for flight testing of advanced weapons systems for the U.S. Air Force and operations of radar and command, control and communications (C^3) systems. Between military and civilian government service, Mr. Yasek worked as a field geophysicist for a privately owned company, specializing in borehole geophysics.

I.1.2 CORE TEAM

Frank J. Anderson, Scientist, CH2M HILL Hanford Group, Inc.

B.S.	Geological Engineering, Colorado School of Mines	1964
M.S.	Geological Engineering, University of Arizona	1968

Mr. Anderson has over 31 years of experience as a geological engineer, environmental consultant, government manager, and professor involving environmental characterization, compliance and remediation, mining, geology, water resources development, and program and project management. He has worked as a consultant at five Department of Energy sites during the past decade: Hanford and Oak Ridge reservations, Portsmouth and Paducah Gaseous Diffusion Plants, and Idaho National Engineering and Environmental Laboratory. He has also been a manager for the U.S. Geological Survey and the U.S. Office of Surface Mining, and an assistant professor of geology. Mr. Anderson was responsible for fiscal year 2001 interim measures engineering design and construction activities for the Tank Farm Vadose Zone Project and prepared Section 3.5 and Appendix F in this document.

Dwayne Crumpler, Senior Hydrogeologist, Columbia Engineering and Environmental Services

B.S.	Geology, Lamar University	1985
M.S.	Geology, Baylor University	1989

Mr. Crumpler has over 15 years of experience in groundwater field investigations related to RCRA facility investigations and CERCLA remedial investigations at municipal landfills, Department of Defense, and Department of Energy facilities. He serves as a Senior Geologist and Regulatory Specialist for the preparation of various RCRA and NEPA documents related to the Hanford Site. He has conducted and analyzed seismic field studies, aquifer pumping tests and slug tests, installed monitoring wells and soil borings, and conducted groundwater and

surface-water sampling programs at Department of Energy and Department of Defense facilities. He has prepared the site-specific work plans associated with the single-shell tanks RCRA corrective action program and has been involved in the single-shell tank retrieval program. He was the coordinator for the document and preparation of the human health risk analyses, regulatory analyses, introduction, approach, conclusions, and recommendations for this document.

Sonia Enloe, Senior Administrative Secretary, Pacific Northwest National Laboratory

Ms. Enloe currently provides direct administrative support to Dr. John Zachara within the Environmental Dynamics and Simulations Directorate at the W.R. Wiley Environmental Molecular Sciences Laboratory. Ms. Enloe has 13 years of administrative experience, 12 of which have been working with Dr. Zachara. In her position, she performs full secretarial, administrative, and general office duties of a responsible and confidential nature. Ms. Enloe formatted and edited Appendix D for the WMA B-BX-BY field investigation report.

Vernon G. Johnson, Staff Scientist V, Pacific Northwest National Laboratory

B.S.	Geology and Chemistry, Oregon State University	1964
M.S.	Oceanography and Chemistry, Oregon State University	1966
Ph.D.	Oceanography and Water Resources, Oregon State University	1979

Dr. Johnson has over 30 years experience in surface and groundwater environmental aspects of nuclear and hazardous waste and is a licensed hydrogeologist in the state of Washington. He has been involved in groundwater and site characterization activities at the Hanford Site since 1983. He conducted RCRA groundwater assessments at Hanford single-shell tank farm waste management areas from 1996 until April 2002. Prior to coming to Hanford, he was a health physicist at Grand Junction, Colorado and at several nuclear facilities at the Idaho National Engineering and Environmental Laboratory where he was involved in nuclear safety assessments, effluent monitoring, and radionuclide transport studies. In his earlier career, he conducted radioecological research in the Columbia River and estuary while at Oregon State University and transport and fate studies of hazardous chemicals in soils while employed at the Environmental Protection Agency Environmental Research Laboratory in Corvallis, Oregon. He was responsible for preparation of the groundwater contamination and related sections of the B-BX-BY field investigation report.

Thomas E. Jones, Principal Scientist, CH2M HILL Hanford Group, Inc.

B.S.	Chemistry, College of Great Falls	1970
Ph.D.	Chemistry, Washington State University	1974

Tom Jones holds a Ph.D. in Inorganic/Analytical Chemistry from Washington State University and has over 20 years experience at the Hanford Site in the areas of tank waste characterization, development of tank waste inventory estimates, and tank farm vadose zone investigations. Over the past four years, Dr. Jones has led the task developing tank leak inventory estimates.

Raziuddin Khaleel, Consulting Engineer, Environmental and Nuclear Initiatives, Fluor Federal Services

B.S.	Civil Engineering, Bangladesh University of Engineering and Technology	1966
M.S.	Water Science and Engineering, Asian University of Technology	1970
Ph.D.	Soil and Water Engineering, Texas A&M University	1977

Dr. Khaleel has over 30 years of experience in groundwater hydrology and numerical simulations of subsurface flow and transport. He was a key contributor to the Hanford Site solid waste performance assessments and the immobilized low-activity waste performance assessment, particularly in the area of conceptual model development, direction of modeling, and in writing the document. For this document, he was responsible for creating the modeling data package, coordinating the modeling work, and writing of several sections.

Anthony J. Knepp, Manager, CH2M HILL Hanford Group, Inc.

B.S.	Engineering, Johns Hopkins University	1971
M.S.	Environmental Systems Engineering, Clemson University	1973

Anthony Knepp was responsible for the management and direction of the field investigation report including its conclusions and recommendations. Mr. Knepp has over 25 years of experience in environmental cleanup and has worked as a consulting engineer, project engineer, government manager, and project manager. His experience includes water resources planning, development of water supply systems, construction of industrial treatment facilities, and environmental characterization and cleanup. For the last 10 years, he has concentrated on remediation of radiologically contaminated groundwater and soils.

Karrol D. Lehman, Senior Technical Writer/Editor, Mid-Columbia Engineering, Inc.

B.A.	Biology, Central Washington University	1975
J.D.	University of Puget Sound School of Law	1987

Ms. Lehman has over 29 years of experience in regulatory programs, environmental compliance, safety analysis and authorization basis documentation, and laboratory analyses. She has provided technical and administrative expertise on regulatory compliance issues, authorization basis management, regulatory inspections and audits, commitment tracking, and other topics related to environmental compliance and radiological, nuclear, and process safety. She has coordinated the production and assisted in the development and drafting of formal safety documentation for Department of Energy facilities and has provided legal support, litigation preparation, and case management support for a corporate legal department. She has conducted training courses in various settings and is a Certified Hazardous Materials Manager.
Ms. Lehman was the technical information coordinator for this field investigation report and maintained and coordinated the document production schedule in addition to providing technical editing support.

Clark W. Lindenmeier, Senior Research Scientist, Pacific Northwest National Laboratory, Applied Geology and Geochemistry Group

B.S.	Biology/Genetics option and Psychology minor, Washington State University	1984
M.S.	Psychology (clinical emphasis), Eastern Washington University	1986
M.S.	Environmental Sciences (Earth Sciences option), Washington State University	1996

Mr. Lindenmeier currently is the Pacific Northwest National Laboratory (PNNL) project manager under the direction of the Tank Farm Vadose Zone Project supporting the Office of River Protection. Mr. Lindenmeier is responsible for supervising the PNNL laboratory and data management activities associated with the Tank Farm Vadose Zone Project and coordinating the laboratory investigation activities to meet the project objectives of senior PNNL and CH2M HILL Hanford Group, Inc. technical staff. Mr. Lindenmeier has 18 years of laboratory experience with areas of emphasis in experimental design, analytical measurements, data management, data quality objectives, and project planning.

Frederick M. Mann, Scientist, CH2M HILL Hanford Group, Inc.

B.S.	Physics, Stanford University	1970
Ph.D.	Physics, California Institute of Technology	1975

Dr. Mann is the team leader for the immobilized low-activity waste performance assessment activity, which is charged with preparing this document. He was the main author of the 1998 and 2001 versions of the Hanford *Immobilized Low-Activity Tank Waste Performance Assessment*. He has worked for over 25 years in the field of nuclear data and the application of those data to large energy facilities. He has advised the Department of Energy and the International Atomic Energy Agency. He was the chief internal reviewer of the document.

David A. Myers, Scientist, CH2M HILL Hanford Group, Inc.

B.S.	Geology, University of Puget Sound	1965
M.S.	Geology and Hydrology, University of Idaho	1967

David Myers is a registered professional geologist in Idaho and Oregon. His work has focused on water resources, as well as environmental monitoring and remediation of groundwater contamination. Since arriving at the Hanford Site in 1974, Mr. Myers has provided technical support for the Site-Wide Groundwater Monitoring Program, as well as early development of the *Resource Conservation and Recovery Act of 1976* monitoring program for the low-level waste burial grounds. He served as a senior hydrogeologist within the environmental restoration program, actively participating in the design and implementation of groundwater remediation projects. He supports the Tank Farm Vadose Zone Project as a technical coordinator, ensuring that multiple aspects of this complex problem are integrated and coordinated. For this document, he was responsible for preparing the geology sections and field investigation activities sections in Sections 2.0 and 3.0 and Appendices B and C.

R. Jeffrey Serne, Staff Scientist, Pacific Northwest National Laboratory, Applied Geology and Geochemistry Group

B.S.	Chemistry, University of Washington	1969
B.S.	Oceanography, University of Washington	1969

Mr. Serne currently is leading the Pacific Northwest National Laboratory applied geochemical research and characterization efforts supporting the Office of River Protection Vadose Zone and Immobilization Low-Activity Waste Projects. The goal of the Vadose Zone Project is to determine the distribution of contaminants that have leaked from SSTs and their future fate. Mr. Serne is also lead geochemist for the near-field and the far-field geochemical studies for the proposed immobilized low-activity waste repository. Mr. Serne is a co-investigator/collaborator on four Environmental Management Science Program basic science projects pertaining to the vadose zone. He was lead author on the two borehole characterization reports in support of the field investigation report. Mr. Serne was co-author of Appendix B.

Harold A. Sydnor, Scientist, CH2M HILL Hanford Group, Inc.

B.S.	Geology, Western Kentucky University	1979
M.S.	Environmental Resource Management, University of Findlay	1998

Mr. Sydnor is the team leader for characterization activities inside the single-shell tank farms. He has over 20 years of experience performing geologic and hydrogeologic investigations and evaluations in the private and public sectors. He was the field team leader for characterization activities associated with the work plan addendum.

Marcus I. Wood, Principal Scientist, Fluor Hanford, Inc.

B.S.	Geology, University of North Carolina	1973
Ph.D.	Geology, Brown University	1980

Dr. Wood currently is responsible for developing the performance assessment analyses for the disposal of solid low-level waste at the Hanford Site. He is the coordinating author of the Hanford Site solid waste performance assessments and has been largely responsible for the integration and the interpretation of the analytical results in those documents. He has coordinated similar analyses for the Environmental Restoration Disposal Facility (ERDF), at which wastes generated in the remediation of Hanford Site waste sites that are regulated under the *Comprehensive Environmental Resource Conservation and Recovery Act of 1981* and the 200 West Area low-level burial grounds are disposed. He has directed numerous projects to quantify the geochemical properties of radionuclides in the Hanford Site geohydrologic environment. He also was responsible for developing a multifunctional waste package backfill material for isolating spent fuel and high-level waste. He was responsible for the conceptual model and for writing portions of Sections 3 and 5, and Appendix B.

John M. Zachara, Chief Scientist VI, Pacific Northwest National Laboratory

B.S.	Chemistry and Geology, Bucknell University	1973
M.S.	Soil/Watershed Chemistry, University of Washington	1979
Ph.D.	Soil Chemistry, Washington State University	1986

Dr. Zachara is chief scientist and one of four associate scientific directors of the William R. Wiley Environmental Molecular Sciences Laboratory (EMSL) at Battelle, Pacific Northwest National Laboratory. The EMSL is a state-of-science U.S. Department of Energy user facility focused on environmental molecular science. Dr. Zachara employs various molecular spectroscopies, electron and scanning probe microscopies, and modeling techniques in the study of contaminant geochemistry. He has performed research on these subjects for over 25 years and is the author of over 120 scientific publications. Dr. Zachara coordinates EMSL research focused on the Hanford Site vadose zone, and he functioned as chief scientist for the Science and Technology portion of the B-BX-BY tank farms study that is summarized in Appendix D.

I.1.3 PEER REVIEW TEAM

Charles R. Cole	Pacific Northwest National Laboratory
Karl R. Fecht	Bechtel Hanford, Inc.
Bruce H. Ford	Fluor Hanford, Inc.

I.1.4 SUPPORT TEAM

I.1.4.1 Field Work

Kevin Hartelius (Health Physics Technician)	CH2M HILL Hanford Group, Inc.
Lisa Hartley (Nuclear Chemical Operator)	CH2M HILL Hanford Group, Inc.
Klint Johnson(Field Work Supervisor)	CH2M HILL Hanford Group, Inc.
Kelly Olson	Resonant Sonics International
Steve Olson	Resonant Sonics International
Loyd Petty (Field Work Supervisor)	CH2M HILL Hanford Group, Inc.
Kent Reynolds	Duratek Federal Services
Rick Sharp (Nuclear Chemical Operator)	CH2M HILL Hanford Group, Inc.
Dave Skoglie (Site Safety Designer)	Duratek Federal Services
Scott Snook (Nuclear Chemical Operator)	CH2M HILL Hanford Group, Inc.
Greg Sullivan (Nuclear Chemical Operator)	CH2M HILL Hanford Group, Inc.

I.1.4.2 Computer Modeling and Risk Calculations

Robert Emmel	Jacobs Engineering Group, Inc.
R. Douglas Evans	Jacobs Engineering Group, Inc.
Vicky Freedman	Pacific Northwest National Laboratory
Mark D. White	Pacific Northwest National Laboratory
Mark D. Williams	Pacific Northwest National Laboratory

I.1.4.3 Laboratory Measurements and Analysis

Steven R. Baum	Pacific Northwest National Laboratory
Bruce N. Bjornstad	Pacific Northwest National Laboratory
Christopher F. Brown	Pacific Northwest National Laboratory
Ray E. Clayton	Pacific Northwest National Laboratory
Glendon W. Gee	Pacific Northwest National Laboratory
Keith N. Geisler	Pacific Northwest National Laboratory
Duane G. Horton	Pacific Northwest National Laboratory
Igor V. Kutnyakov	Pacific Northwest National Laboratory
David C. Lanigan	Pacific Northwest National Laboratory
George V. Last	Pacific Northwest National Laboratory
Virginia L. LeGore	Pacific Northwest National Laboratory
Michael J. Lindberg	Pacific Northwest National Laboratory
Kevin A. Lindsey	Kennedy / Jenks Consultants
Clark W. Lindenmeier	Pacific Northwest National Laboratory
Robert D. Orr	Pacific Northwest National Laboratory
Herbert T. Schaef	Pacific Northwest National Laboratory
Steven. C. Smith	Pacific Northwest National Laboratory
Michelle M. Valenta	Pacific Northwest National Laboratory
Tanya S. Vickerman	Pacific Northwest National Laboratory
Bruce A. Williams	Pacific Northwest National Laboratory
Teresa C. Wilson	Pacific Northwest National Laboratory

I.1.4.4 Science and Technology Participants

Karsten Pruess	Lawrence Berkeley National Laboratory
Odeta S. Qafoku	Pacific Northwest National Laboratory
Charles T. Resch	Pacific Northwest National Laboratory
Sarah Roberts	Lawrence Livermore National Laboratory
Steven C. Smith	Pacific Northwest National Laboratory
Carl I. Steefel	Lawrence Livermore National Laboratory Calvin C. Ainsworth Pacific Northwest National Laboratory
Gordon E. Brown, Jr.	Stanford University
Susan Carroll	Lawrence Livermore National Laboratory
Jeffrey G. Catalano	Stanford University
Paul L. Gassman	Pacific Northwest National Laboratory
Glendon W. Gee	Pacific Northwest National Laboratory
Steven M. Heald	Argonne National Laboratory; Pacific Northwest National Laboratory
Peter C. Lichtner	Los Alamos National Laboratory
Chongxuan Liu	Pacific Northwest National Laboratory
James P. McKinley	Pacific Northwest National Laboratory
Zheming Wang	Pacific Northwest National Laboratory
Anderson L. Ward	Pacific Northwest National Laboratory
Steve B. Yabusaki	Pacific Northwest National Laboratory
Zhuanfang L. Zhang	Pacific Northwest National Laboratory

This page intentionally left blank.